

University of Alberta

**PERFORMANCE EVALUATION, OPTIMAL POWER ALLOCATION, AND
PHYSICAL LAYER DESIGNS FOR WIRELESS RELAYING SYSTEMS**

by

Golnaz Farhadi

A thesis submitted to the Faculty of Graduate Studies and Research
in partial fulfillment of the requirements for the degree of

Doctor of Philosophy

Department of Electrical and Computer Engineering

©Golnaz Farhadi
Fall 2009
Edmonton, Alberta

Permission is hereby granted to the University of Alberta Libraries to reproduce single copies of this thesis and to lend or sell such copies for private, scholarly or scientific research purposes only. Where the thesis is converted to, or otherwise made available in digital form, the University of Alberta will advise potential users of the thesis of these terms.

The author reserves all other publication and other rights in association with the copyright in the thesis, and except as herein before provided, neither the thesis nor any substantial portion thereof may be printed or otherwise reproduced in any material form whatever without the author's prior written permission.

Examining Committee

Norman C. Beaulieu, Electrical and Computer Engineering

Behnaam Aazhang, Electrical and Computer Engineering, Rice University

Ehab S. Elmallah, Computing Science

Sergiy Vorobyov, Electrical and Computer Engineering

Hai Jiang, Electrical and Computer Engineering

Masoud Ardakani, Electrical and Computer Engineering

Abstract

Cooperative communication is a promising way to improve wireless network performance by exploiting spatial diversity in fading channels in a distributed manner. Performance of various wireless cooperative configurations are investigated. Theoretical expressions for outage and error probabilities in general fading of amplify-and-forward multi-hop systems are derived using the characteristic function or moment generating function of the inverse of the instantaneous received signal-to-noise ratio.

In addition, ergodic capacity of different multi-hop systems is evaluated assuming the channel state information is only available at the receiving terminals. It is shown that decode-and-forward multi-hop systems achieve higher ergodic capacities than amplify-and-forward multi-hop systems. Furthermore, theoretical expressions in the form of single finite integrals for the capacity of different source-adaptive amplify-and-forward multi-hop systems are obtained.

New optimal power allocation schemes that maximize the instantaneous received signal-to-noise ratio in an amplify-and-forward multi-hop transmission system are also obtained for short-term and long-term power constraints. The optimal power allocation strategy under short-term power constraint requires a centralized implementation, whereas the optimal power solutions to the long-term power constraints can be implemented in a decentralized manner. Outage probabilities of the proposed power-optimized systems are derived and the performance gains of the optimal power allocation schemes are examined.

Previous studies have been primarily focused on cooperative systems in which the functionality of the receivers relies on availability of channel information. Low complexity receivers for coherent amplify-and-forward multi-relay systems requiring no instantaneous fading amplitude information are proposed. Analytical expressions for evaluation of the average output signal-to-noise ratio and symbol error probability are derived and it is demonstrated that these schemes achieve full diversity. Furthermore, upper and lower bounds on

the ergodic capacity are obtained. In addition, a maximum energy selection scheme in a noncoherent amplify-and-forward multi-relay system is investigated. An expression for the symbol error probability of this system is derived. It is shown that this scheme achieves full diversity whereas it requires neither instantaneous nor statistical channel gain information at the destination.

Finally, performance of different multi-hop diversity transmission systems are studied and expressions for evaluation of their outages and bit error probabilities are derived in Rayleigh fading.

Acknowledgements

Many people has helped me to continue my studies and to accomplish my goals. First ad foremost, I would like to thank my supervisor, Professor Norman C. Beaulieu, for his continuous support, encouragement and patience during my Ph.D. program. This research would not have been fulfilled without his vast knowledge, experience, and brilliant comments.

I would also like to thank the members of my defense committee, Behnaam Aazhang, Ehab S. Elmallah, Sergiy Vorobyov, Hai Jiang, and Masoud Ardakani for reviewing my thesis.

Funding supports from the Alberta Ingenuity and the Informatics Circle of Research and Excellence (*iCORE*) are greatly appreciated.

The *iCORE* Wireless Communications Laboratory (*iWCL*) has been a truly vibrant environment and has greatly enriched my graduate experience. I enjoyed many discussions with my lab-mates on many academic and non-academic topics. Many thanks also go to Sharon Walker, Linda Abraham, and Suzanne Cunningham for their kindness and helpfulness during my Ph.D. program.

Last, my sincere thanks goes to my family and especially my beloved husband, Alireza, for their tremendous support, care, encouragement and love.

Table of Contents

1	Introduction	1
1.1	Thesis Motivations and Contributions	2
1.2	Thesis Outline	8
2	Background and Related Works	9
2.1	Elements of Cooperative Communications	9
2.1.1	Processing Methods at Relays	9
2.1.2	Relaying Protocols	10
2.1.3	Channel Allocation and Relays Modes of Operation	12
2.2	General System Configurations and Features	13
2.3	Related Works	14
2.3.1	Multi-Relay Cooperative Systems	16
2.3.1.1	Performance Analysis	16
2.3.1.2	Detection Schemes at the Destination	18
2.3.2	Multi-Hop and Multi-Hop Diversity Transmission Systems	21
2.3.3	Optimal Power Allocation for Cooperative Wireless Systems	22
3	Multi-Hop Relaying Systems	26
3.1	System Models	27
3.2	Outage and Error Probabilities of AF Multi-Hop Systems	28
3.2.1	Statistical Properties of AF Multi-Hop Systems	28
3.2.1.1	Systems With Variable-Gain Relays	28
3.2.1.2	Systems With Fixed-Gain Relays	29
3.2.2	Outage Probability Analysis	30
3.2.3	Error Probability Analysis	31

3.2.3.1	Error Probabilities Involving the Incomplete Gamma Function	31
3.2.3.2	Error Probabilities Involving the Gaussian Q-Function	32
3.2.3.3	Error Probabilities Involving the Marcum Q-Function	34
3.2.4	Numerical Results	35
3.2.5	Asymptotic Behavior	38
3.2.5.1	Numerical Examples	42
3.3	Capacity Analysis	45
3.3.1	Ergodic Capacity Without Transmitter CSI	46
3.3.1.1	AF Multi-Hop Transmission Systems	46
3.3.1.2	DF Multi-Hop Transmission Systems	49
3.3.1.3	Comparison Between AF and DF Multi-hop Transmission Systems	49
3.3.1.4	Results and Discussion	50
3.3.2	Capacity of AF Relaying Systems Under Adaptive Transmission	53
3.3.2.1	Optimal Power and Rate Adaptation	54
3.3.2.2	Optimal Rate Adaptation With Constant Transmit Power	56
3.3.2.3	Channel Inversion With Fixed Rate	57
3.3.2.4	Numerical Results and Discussion	58
4	Optimal Power Allocation for AF Multi-Hop Relaying Systems	62
4.1	System Model and Problem Formulation	62
4.2	Optimal Power Allocation Under ST Power Constraint	63
4.2.1	Mechanism	63
4.2.2	Outage Probability Analysis	64
4.2.3	Asymptotic Outage Probability Behavior	66
4.2.4	Average Optimal Per-Hop Power Portion	67
4.2.5	Impact of Individual Per-Hop Power Constraints	68
4.3	Optimal Power Allocation Under LT Power Constraint	70
4.3.1	Mechanism	70
4.3.2	Outage Probability Analysis	73
4.3.3	Asymptotic Outage Probability Behavior	73
4.4	Numerical Results	74

5	AF Multi-Relay Cooperative Systems	79
5.1	Systems Employing MRC at Destination	79
5.1.1	System Model	79
5.1.2	Performance Analysis	81
5.1.2.1	Error Probability Analysis	81
5.1.2.2	Capacity Analysis	82
5.2	Low Complexity Coherent Receivers	85
5.2.1	System Models	85
5.2.1.1	Immediate Preceding Channel Phase Information Available	86
5.2.1.2	Distributed Phase Information at the Relays	87
5.2.2	Performance Analysis of DEGC Schemes	88
5.2.2.1	Error Probability Analysis	88
5.2.2.2	Achievable Diversity Gain	90
5.2.2.3	Average Output SNR	92
5.2.2.4	Ergodic Capacity Analysis	94
5.2.3	Numerical Results and Discussion	95
5.2.3.1	Performance Analysis Results	95
5.2.3.2	Impact of Combining Loss	100
5.3	Low Complexity Noncoherent Receiver	103
5.3.1	System Model	103
5.3.2	Performance Analysis of Noncoherent MES Scheme	104
5.3.2.1	Error Probability Analysis	104
5.3.2.2	Achievable Diversity Gain	106
5.3.3	Numerical Results	107
6	Multi-Hop Diversity Systems	110
6.1	System Models	111
6.1.1	Systems With Fixed Relaying	111
6.1.2	Systems With Selective Relaying	112
6.2	Outage Probability Analysis	113
6.2.1	Systems With Fixed Relaying	113
6.2.1.1	DF Relaying	113
6.2.1.2	AF Relaying	114

6.2.2	Systems With Selective Relaying	116
6.2.2.1	DF Relaying	116
6.2.2.2	AF Relaying	118
6.3	Bit Error Probability Analysis	120
6.3.1	Systems With Fixed Relaying	120
6.3.1.1	DF relaying	120
6.3.1.2	AF Relaying	121
6.3.2	Systems With Selective Relaying	122
6.3.2.1	DF Relaying	122
6.3.2.2	AF Relaying	123
6.4	Results and Discussions	124
7	Conclusions and Future Work	129
7.1	Concluding Remarks	129
7.2	Directions for Future Research	132
	Bibliography	134
A	Proof of Lemmas	144
A.1	Proof of Lemma 3.1	144
A.2	Proof of Lemma 3.2	145
A.3	Proof of Lemma 3.3	146
A.4	Proof of Lemma 3.4	147
A.5	Proof of Lemma 3.5	147
A.6	Proof of Lemma 4.1	148
A.7	Proof of Lemma 6.1	149
A.8	Proof of Lemma 6.2	150

List of Tables

3.1	Parameters a and b for different modulation/detection schemes from [89] . . .	32
3.2	Average bit and symbol error probabilities of different modulation schemes involving the Gaussian Q-function	33
3.3	Average bit error probabilities of different modulation schemes involving the Marcum Q-function	34
3.4	Values of r for different types of fading from [89]	41
3.5	Values of γ_c and β_c for different multi-hop systems with i.i.d. links where $\Gamma_{k-1,k} = \Gamma_{0,1}$ and $m_k = 1, k = 1, \dots, K$	59
3.6	Values of γ_c and β_c for different multi-hop systems with non i.d. links where $\Gamma_{k-1,k} = \frac{1}{k}\Gamma_{0,1}$ and $m_k = \frac{k}{2}, k = 1, \dots, K$	59
5.1	Optimum number of relays for different AF multi-relay systems employing the proposed R-DEGC and S-DEGC schemes	103

List of Figures

2.1	A K -hop transmission system where the source, T_0 , communicates with the destination, T_K , via $K - 1$ relays, T_1, \dots, T_{K-1}	14
2.2	An N -relay cooperative system where the source, T_0 , communicates with the destination, T_{N+1} , via N relays, T_1, \dots, T_N	15
2.3	A K -hop diversity transmission system where the source, T_0 , communicates with the destination, T_K , via $K - 1$ relays, T_1, \dots, T_{K-1}	15
3.1	Outage probabilities for different AF multi-hop relaying systems with variable-gain relays ($\gamma_{th} = 1$).	36
3.2	Outage probabilities for different AF multi-hop relaying systems with fixed-gain relays ($\gamma_{th} = 1$).	37
3.3	Bit error probabilities for different BPSK and 16-QAM AF multi-hop relaying systems with variable-gain relays.	37
3.4	Bit error probabilities for different BPSK and 16-QAM AF multi-hop relaying systems with fixed-gain relays.	38
3.5	Comparison between the exact bit error probability and the lower bound given in [24] for different BPSK AF multi-hop relaying systems with fixed-gain relays.	39
3.6	Bit error probabilities for different 4-DPSK AF multi-hop relaying systems with variable-gain relays.	39
3.7	Outage probabilities for different multi-hop transmission systems with fixed-gain relays and balanced links ($\gamma_{th} = 1$).	43
3.8	Bit error probabilities for different multi-hop transmission systems with fixed-gain relays and balanced links.	43
3.9	Outage probabilities for different multi-hop transmission systems with fixed-gain relays and unbalanced links ($\gamma_{th} = 1$).	44

3.10	Bit error probabilities for different multi-hop transmission systems with fixed-gain relays and unbalanced links.	45
3.11	The ergodic capacities of K -hop transmission systems with balanced links employing an AF relaying scheme. M denotes the number of terms used to evaluate the series given in (3.41).	51
3.12	The ergodic capacities of K -hop transmission systems with unbalanced links employing an AF relaying scheme. M denotes the number of terms used to evaluate the series given in (3.41).	51
3.13	Comparison between ergodic capacities of K -hop transmission systems employing either DF relaying or AF relaying.	52
3.14	Ergodic capacities versus relay location of dual-hop transmission systems employing either DF relaying or AF relaying.	53
3.15	The source-adaptive multi-hop relaying system.	54
3.16	Channel capacity versus β_c of different multi-hop transmission systems employing the truncated channel inversion adaptive technique.	58
3.17	Channel capacity of various multi-hop transmission systems employing different adaptation policies.	60
3.18	Outage probability of different multi-hop transmission systems employing either optimal power and rate adaptation or the truncated channel inversion adaptive scheme.	61
4.1	Outage probabilities for different AF dual-hop transmission systems. The acronyms ST, LT1, and LT2, respectively, stand for power-optimized systems under ST power constraint, total LT power constraint, and individual LT power constraints.	75
4.2	Outage probabilities for different AF triple-hop transmission systems. The acronyms ST, LT1, and LT2, respectively, stand for power-optimized systems under ST power constraint, total LT power constraint, and individual LT power constraints.	75
4.3	Average power portions utilized per hop in different AF dual-hop transmission systems. The acronyms ST and LT1, respectively, stand for power-optimized systems under ST power constraint and total LT power constraint.	77

4.4	Average power portions utilized per hop in different AF triple-hop transmission systems. The acronyms ST and LT1, respectively, stand for power-optimized systems under ST power constraint and total LT power constraint.	77
5.1	Bit error probabilities for different multi-relay systems with fixed-gain relays employing R-MRC.	82
5.2	Ergodic capacities of different AF systems employing R-MRC with variable-gain relays chosen according to (5.2b).	84
5.3	Ergodic capacities of different AF systems employing R-MRC with fixed-gain relays chosen according to (5.2c).	85
5.4	Bit error probabilities of different BPSK AF multi-relay systems in Rayleigh fading with different power decay factors.	96
5.5	Average output SNRs of AF double-relay systems in Rayleigh fading with different power decay factors.	96
5.6	Ergodic capacities of AF double-relay systems in Rayleigh fading with i.i.d. links ($\delta = 0$).	97
5.7	Ergodic capacities of AF double-relay systems in Rayleigh fading with non i.i.d. links ($\delta = 1$).	98
5.8	Ergodic capacities versus number of relays of different AF multi-relay systems operating over Rayleigh fading channels with $\delta = 0$.	99
5.9	Bit error probabilities versus number of relays of different BPSK AF multi-relay systems operating over Rayleigh fading channels with $\delta = 0.5$.	101
5.10	Average output SNRs versus number of relays of different AF multi-relay systems operating over Rayleigh fading channels with $\delta = 0.5$.	101
5.11	Ergodic capacities versus number of relays of different AF multi-relay systems operating over Rayleigh fading channels with $\delta = 0.5$.	102
5.12	Bit error probabilities for different coherent and noncoherent BFSK AF single-relay systems.	108
5.13	Bit error probabilities for different coherent and noncoherent BFSK AF double-relay systems.	108
6.1	Tree diagram for a triple-hop diversity transmission system employing selective DF relaying.	118
6.2	Tree diagram for a triple-hop diversity transmission system employing selective AF relaying.	120

6.3	Outage probabilities for different multi-hop diversity transmission systems employing DF relaying.	124
6.4	Bit error probabilities for different multi-hop diversity transmission systems employing DF relaying.	125
6.5	Outage probabilities for different multi-hop diversity transmission systems employing AF relaying.	126
6.6	Bit error probabilities for different multi-hop diversity transmission systems employing AF relaying.	126
6.7	Comparison of outage probabilities among different multi-hop diversity transmission systems employing either DF relaying or AF relaying.	127
6.8	Comparison of bit error probabilities among different multi-hop diversity transmission systems employing either DF relaying or AF relaying.	128

List of Symbols

T_i	Terminal i in the system	14
$\alpha_{i,j}$	Fading gain of the channel between terminals T_i and T_j	14
n_i	Received noise at the I^{th} terminal i	14
N_0	Noise power	14
$\gamma_{i,j}$	Instantaneous SNR of the channel between terminals T_i and T_j	14
P_i	Transmitter power from terminal T_i	14
$\Gamma_{i,j}$	Average SNR of the channel between terminals T_i and T_j	14
$\Omega_{i,j}$	Fading power of the channel between terminals T_i and T_j	14
K	Number of hops	27
y_k	Received signal at the k^{th} terminal	27
x_k	Transmitted signal from the k^{th} terminal	27
A_k^V	Amplification gain at the k^{th} relay in an AF multi-hop system with variable-gain relays	27
A_k^F	Amplification gain at the k^{th} relay in an AF multi-hop system with fixed-gain relays	27
$\mathbb{E}(\cdot)$	Expectation operator	28
γ_t	Instantaneous end-to-end received SNR	29
X	Inverse of the instantaneous end-to-end received SNR	29
$M(\cdot)$	MGF of a random variable	29
m_i	Nakagami- m fading parameter over the link between terminals T_{i-1} and T_i	29
$\Gamma(\cdot)$	Gamma function	29

$K_m(\cdot)$	Modified Bessel function of the second kind of order m	29
$f_\gamma(\cdot)$	PDF of the random variable γ	30
ξ_n	The n^{th} weight of the Laguerre polynomial	30
ζ_n	The n^{th} zero of the Laguerre polynomial	30
N_p	Order of the Laguerre polynomial	30
P_{out}	Outage probability	30
$\mathcal{F}^{-1}(\cdot)$	Inverse Fourier transform operator	31
$\Psi(w)$	CHF of a random variable	31
$\delta(\cdot)$	Delta function	31
P_b	Bit error probability	31
$\Gamma(\cdot, \cdot)$	Incomplete gamma function	31
$J_b(\cdot)$	Bessel function of the first kind of order b	32
$Q(\cdot)$	Gaussian Q-function	32
P_s	Symbol error probability	32
$[\cdot]$	Integer part (floor) operator	32
$erf(\cdot)$	Error function	33
$Q_l(\cdot, \cdot)$	Marcum Q-function of integer order l	34
Γ_0	Average link SNR in a single-hop system	41
$\mu_H(\cdot)$	Harmonic mean	42
ϵ	Path loss exponent	42
d_0	Distance between source and destination	44
P_T	Total available transmitter power	46
\mathcal{E}	Ergodic capacity	46
Γ_t	Expected value of the end-to-end instantaneous received SNR	47
$G(\cdot)$	Meijer G-function	47
$E_1(\cdot)$	Exponential integral function	49
ν	Euler's constant	56
β_k	Optimal power coefficient at terminal T_k in a multi-hop system	63

L	Lagrangean function	64
λ	Lagrange multiplier	64
$F_Y(\cdot)$	CDF of random variable Y	66
$\Im(\cdot)$	Imaginary part of a complex number	66
\hat{A}_i^V	Amplification gain at the i^{th} relay in a multi-relay system with variable-gain relays	80
\hat{A}_i^F	Amplification gain at the i^{th} relay in a multi-relay system with fixed-gain relays	80
$\Gamma_{s,d}$	Average SNR over the source-destination link	82
$\tilde{\alpha}_{i,j}$	Fading amplitude of the channel between terminal T_i and T_j	85
$\theta_{i,j}$	Fading phase of the channel between terminal T_i and T_j	85
$E_n(\cdot)$	Generalized exponential integral function	92
δ	Power decay factor	95
E_s	Symbol energy	104
\mathcal{L}^{-1}	Inverse Laplace transform operator	114
$\gamma(\cdot, \cdot)$	Lower incomplete gamma function	114

List of Abbreviations

DF	Decode-and-forward	2
AF	Amplify-and-forward	2
SNR	Signal-to-noise ratio	2
MGF	Moment generating function	2
CHF	Characteristic function	2
CSI	Channel state information	3
ST	Short-term	4
LT	Long-term	4
MRC	Maximal ratio combining	5
ML	Maximum likelihood	5
SC	Selection combining	5
DEGC	Distributed equal gain combining	6
MES	Maximum Energy Selection	7
<i>M</i> -FSK	<i>M</i> -ary frequency shift keying	7
EF	Estimate-and-forward	10
MMSE	Minimum mean square error	10
DSSC	Distributed switch-and-stay combining	12
MAC	Medium access control	12
TDMA	Time-division multiple-access	12
FDMA	Frequency-division multiple-access	12
CDMA	Code-division multiple-access	12
ADC	Analog-to-digital converter	13
DAC	Digital-to-analog converter	13

<i>M</i> -PSK	<i>M</i> -ary phase shift keying	16
<i>M</i> -QAM	<i>M</i> -ary quadrature amplitude modulation	17
PDF	Probability density function	17
CDF	Cumulative density function	17
C-MRC	Cooperative-MRC	18
OOK	On-off keying	20
BFSK	Binary frequency shift keying	20
ASK	Amplitude shift keying	20
BPSK	Binary phase-shift keying	32
DPSK	Differential phase-shift keying	32
QPSK	Quadrature phase-shift keying	34
i.i.d.	Independent identically distributed	46
CTS	Clear-to-send	71
R-MRC	Repetition-based maximal ratio combining	80
RTS	Request-to-send	86
R-DEGC	Repetition-based distributed equal gain combining	86
S-DEGC	Spectral-efficient distributed equal gain combining	87
S-MRC	Spectral-efficient maximal ratio combining	90

Chapter 1

Introduction

The tremendous growth of wireless technologies in the wireless industry is expanding opportunities for economic growth, enhanced security and a better quality of life. Yet, the industry is also facing many demands for providing services (especially with a multimedia content) with higher data rates, improved quality, greater mobility, and lower cost. The conventional technique to mitigate channel impairments (such as noise, fading, and interference from other users) and to increase data rates is the deployment of multiple antennas at the transmitters and/or the receivers. However, due to size, cost, and hardware limitations, multiple antennas may not be a feasible solution for some practical wireless networks.

Cooperative communications has emerged as a new communication paradigm promising significant capacity and coverage increase as well as enhanced performance in current and future wireless networks. Different from conventional point-to-point communications, individual mobile users throughout a cooperative wireless network cooperate with the nearby transmitting users to send data to a receiver, which is otherwise too far away to be directly accessed reliably. In fact, in a cooperative communications network, a virtual multiple antenna system can be created by using antennas belonging to multiple users within the network. Thus, cooperative communications benefits in the same way as promised by the multiple antenna techniques. On the other hand, it eliminates the need for physical deployment of antennas at the transmitters and/or receivers within the network. This significantly reduces the system cost, complexity, and especially the size of the receivers. Cooperative wireless networks exhibit applications in many scenarios including crisis management services (such as disaster recovery, or rescue operations), home networking, environment control, vehicle-to-vehicle communications, medical monitoring, and low-cost Internet access in remote residential areas.

1.1 Thesis Motivations and Contributions

Since introduction of cooperative communications [1]–[3], a great deal of research has been devoted to performance evaluation [4]–[29], developing new relaying protocols [4], [30]–[32], designing more efficient receivers [33]–[43], and obtaining optimal power allocation schemes [31], [44]–[58]. However, there are still a number of challenging problems and issues that should be addressed to make cooperative communications more attractive for practical applications. Motivations for this thesis followed by our contributions are outlined in the following.

- **Performance analysis of multi-hop relaying systems**

Multi-hop transmission is a promising technique for application in multi-hop cellular or ad hoc networks due to its low complexity, performance improvement as well as providing broader coverage. Outage and error probabilities of a multi-hop system employing a decode-and-forward (DF) relaying can be readily obtained [19], [26]. On the other hand, amplify-and-forward (AF) relaying is a less complex scheme since the relays do not involve any sort of decoding or encoding and simply amplify what they receive. However, performance of AF multi-hop relaying systems either has been evaluated in terms of lower bounds [24] that are not tight, especially for moderate to large values of signal-to-noise ratio (SNR) and larger number of hops, or requires evaluation of double integrals [25] that not only have no closed-form solution but also are numerically involved due to the mathematical forms of their integrands. Thus, it is important to find simple, accurate closed-form expressions for evaluation of the outage and error probabilities of AF multi-hop systems. In Chapter 3 of this thesis, we develop a new general framework for evaluation of the error probabilities in fading of a variety of modulation schemes in terms of the moment generating function (MGF) of the reciprocal of the instantaneous received SNR. The solutions obtained are in the form of single integrals that can be readily evaluated using standard mathematical software. A single integral expression for evaluation of the outage probability is also given in terms of the characteristic function (CHF) of the inverse of the received SNR. Furthermore, we study the asymptotic behavior of the outage and error probabilities to determine the achievable diversity gains as well as to gain more insights to the performances of the systems under study.

In addition, the performance of various wireless cooperative systems in fading channels has been mainly evaluated in terms of outage probability or error rate. On the

other hand, another important performance metric of a wireless communication system in a fading environment is its ergodic capacity which represents a measure of the maximum average number of information bits that can be reliably transmitted. There have been many papers investigating the capacity of a variety of Gaussian relay channels [59]–[69]. However, relayed transmission is particularly attractive in fading environments for enabling reliable communication between a source-destination pair when the direct link is subject to a deep fade. But, there have been only a few studies on the ergodic capacity analysis of a single-relay cooperative system employing DF relaying or AF relaying [70] over Rayleigh fading channels. In [70], the ergodic capacities were obtained through Monte Carlo simulations and no analytical expressions for their calculation were given. Therefore, another aim of this work is to develop a framework for evaluation of ergodic capacity¹ of a variety of wireless cooperative systems. Thus, continuing our performance evaluation of multi-hop relaying systems in Chapter 3, we investigate the ergodic capacity in Rayleigh fading of these systems employing either AF relaying or DF relaying, assuming channel state information (CSI) is only known at the receiving terminals. We derive upper bounds on the ergodic capacity of an AF multi-hop relaying system based on Jensen’s inequality and the harmonic-geometric means inequality. We also obtain a precise expression for the ergodic capacity of an AF multi-hop relaying system in the form of an infinite series. In addition, the ergodic capacity of a DF multi-hop transmission system is obtained. It is shown that multi-hop transmission systems employing a DF relaying scheme achieve higher ergodic capacities than multi-hop transmission systems with AF relaying schemes.

In addition, all papers on multi-hop relaying systems consider fixed rate and fixed power transmission. On the other hand, employment of an adaptive technique in a wireless system can lead to better utilization of the channel [72], [73]. Thus, in Chapter 3, we also investigate capacity in general fading of an AF multi-hop relaying system employing different source-adaptive transmission techniques introduced in [72], namely, optimal power and rate adaptation, optimal rate adaptation with constant power, and channel inversion with fixed rate. In such systems the source adapts

¹In this thesis, the maximum achievable rate in the Shannon sense is referred to as “capacity”. Note that, as shown later in Chapters 3 and 5, the effective input-output relation in an AF relaying system can be written in a vector format. Hence, according to [71, Theorem 1], the capacity in fading of an AF relaying system is the expected value of the maximum achievable rate. However, as shown in [68] and [70] as well as Section 3.3.1.2, this statement is not valid for DF relaying systems.

its rate and/or power according to the channel variations utilizing only a feedback of the effective received SNR from the destination to the source. We derive exact expressions for the capacity for each source-adaptive multi-hop transmission system in terms of the CHF of the reciprocal of the instantaneous received SNR. It is shown that a system with optimal power and rate adaptation outperforms the system with truncated channel inversion adaptive technique. Systems employing optimal rate adaptation with constant power achieve almost the same capacity as those with optimal rate and power adaptation at large values of SNR. However, the capacity performance of a system with the truncated channel inversion adaptive technique is better than the corresponding system employing optimal rate adaptation with constant power for small values of SNR.

- **Optimal power allocation for AF multi-hop relaying systems**

Power efficiency is an important factor for a cooperative wireless system. Thus, choosing the optimal power coefficients for the source and the relays is an important design issue. Optimal power allocation schemes for several cooperative wireless systems under different optimization objectives and assumptions have been obtained [31], [44]–[58]. However, there is no optimal power allocation scheme developed for AF multi-hop transmission systems with arbitrary number of hops. Thus, in Chapter 4 of this thesis, we obtain optimal power allocation schemes that maximize the instantaneous received SNR in an AF multi-hop transmission system under short-term (ST) and long-term (LT) power constraints. Theoretical expressions for evaluation of the outage probability in Rayleigh fading of the proposed power-optimized AF multi-hop transmission systems are evaluated using the infinite series approach introduced by Beaulieu [74]. Furthermore, we examine large SNR behavior of the outage probability of these systems. It is shown that at sufficiently large values of SNR, the gap in the outage performance between a power-optimized AF multi-hop transmission system under ST power constraint and that with uniform power allocation linearly increases with the number of hops. In contrast with the optimal power allocation scheme under ST power constraint that requires a centralized implementation architecture, the optimal power allocation strategies for the LT power constraints can be implemented in a decentralized manner. In addition, it is shown that a system employing such optimal power allocation schemes can achieve a significant performance gain by achieving diversity order 2.

- **Low complexity receivers for AF multi-relay cooperative systems**

Many studies on multi-relay cooperative systems consider employment of a maximal ratio combining (MRC) receiver at the destination assuming that the relays retransmit in orthogonal subchannels (i.e. repetition-based scheduling protocol [4]) [3], [4], [14]. It is shown in [33], [34] that MRC is not the maximum likelihood (ML) detector for DF multi-relay systems. ML and near-ML detection schemes for both coherent and noncoherent DF multi-relay systems were then developed in [34]. On the other hand, MRC of the signals received at the destination in an AF multi-relay cooperative system is an ML scheme [33], [40]. However, it requires global knowledge at the destination of CSI of all links. Other combining schemes such as selection combining (SC) [15] and switch-and-stay diversity combining [39] also require knowledge of fading amplitude information for the source-relay channels as well as the relay-destination channels at the receiver. In addition, an optimal scheme for an AF cooperative system where all relays forward their received signals simultaneously (i.e. a spectral-efficient scheduling protocol) was developed in [75]. However, this optimal scheme requires that global CSI knowledge of all links be available at all relays. This requirement imposes a very large system overhead that makes it almost impractical. Another alternate spectral efficient protocol for AF multi-relay cooperative systems has been recently proposed in [31] in which only the best relay is selected for cooperation. The selection algorithm is implemented at the destination assuming that fading amplitude information of all channels is known. The relay selected as the best relay at the destination is then activated through a feedback channel.

In Chapter 5, we investigate low complexity receivers for AF multi-relay cooperative systems assuming that no instantaneous fading channel amplitudes are known (or exploited) at the relays and the destination. We consider the following scenarios where the channels' phase information either can be acquired in a distributed manner or is not required otherwise.

1. The phase information of the channels between source-destination and all relay-destination links is known to the destination. Each relay also has knowledge of the phase of the channel between the source and itself. In other words, each relay terminal and the destination have phase information of their (immediate) preceding channel(s).
2. Each relay has channel phase information of its backward (source-relay) and

forward (relay-destination) links. Only the destination has (or exploits) phase information of the source-destination channel.

3. No fading channel phase information is available at the relays and the destination.

Our goal is to develop detection schemes under these scenarios that achieve full spatial diversity gain.

Coherent detection at the destination in an AF cooperative system assuming phase information is known according to either the first or second scenarios is possible as long as the fading channel phases are properly incorporated into the relay amplification gains² and an appropriate scheduling protocol is employed. In the first scenario, a repetition-based scheduling should be employed. However, the relays in the second scenario can simultaneously forward their signals to the destination. We propose low complexity combining schemes for these two scenarios which simply add (coherently) the signals received at the destination. Since the required channel phase information can be acquired in a distributed manner, these detectors are referred to as *distributed equal gain combining* (DEGC) schemes. Note that the employment of a DEGC scheme for a repetition-based AF cooperative system has been proposed in [77]. However, the instantaneous received SNR expression given in [77, eq. (4)] is only valid if the noise powers of the signals received at the destination are equal. This is clearly not the case for an AF cooperative system because the noise powers of the signals received at the destination through the relays depend on the instantaneous fading amplitude of the relay-destination channels. Therefore, the performance analysis given in [77] is not valid and a new analysis is given here. As a benchmark for performance evaluation of the proposed schemes, in the first part of Chapter 5, we examine the performance of systems employing MRC in terms of achievable diversity gain and the ergodic capacity.

The third scenario requires employment of a noncoherent detection scheme at the destination. It is shown in [40] that the general noncoherent ML detection for AF multi-relay cooperative systems is too complex for employment in practice. On the other hand, suboptimal receivers for noncoherent AF cooperative systems have been

²While the simplest form of AF relaying ignores the phase of the signal received at the relay, [76] has shown that using phase information at the relay can enhance the performance of AF systems. The effect of phase adjustment by the relay can be represented by a complex-valued relay gain.

proposed in a few recent works [41]–[43]. However, they either have high implementation complexity or do not achieve full spatial diversity. In Chapter 5, we propose employment of a *maximum energy selection* (MES) receiver scheme for noncoherent AF cooperative diversity systems. A feature of this scheme is that the destination does not require any instantaneous or statistical information of the fading channel gains. An expression for the symbol error probability of this system with M -ary frequency shift keying (FSK) modulation is derived. It is shown that a noncoherent AF system employing the proposed MES scheme achieves full spatial diversity. This is an important result regarding noncoherent AF cooperative systems. Note that the corresponding noncoherent DF cooperative system (with more than one relay) employing an ML detection scheme loses about half of the potential spatial diversity gain [34].

- **Performance analysis of multi-hop diversity transmission systems**

A multi-hop diversity transmission system is a generalization of multi-hop transmission systems in which relays collaborate with each other in order to exploit diversity [26]. Although, the results presented in [26] show that the performance of multi-hop diversity schemes must be superior to that of multi-hop systems without diversity, an accurate analysis for outage probabilities of multi-hop diversity transmission systems with fixed DF or fixed AF relaying in Rayleigh fading was not given explicitly. Furthermore, the bit error probability analysis given in [26] for a multi-hop diversity transmission system with fixed AF relaying overestimates the bit error probability performance. In addition, no discussion on the achievable diversity gains was presented in [26].

In Chapter 6 of this thesis, we focus on the performance analysis of multi-hop diversity schemes in which either a DF relaying or an AF relaying is employed at the relays. Simple, accurate, closed-form approximations for the calculation of the outage and bit error probabilities of multi-hop diversity transmission systems employing fixed AF relaying are derived. An exact expression for the calculation of the outage probability of multi-hop diversity transmission systems employing fixed DF relaying is also obtained. As is expected intuitively, the analysis shows that a multi-hop diversity transmission system with fixed DF relaying does not achieve diversity gain. A selective relaying scheme for multi-hop diversity transmission, which adapts transmissions based on threshold tests on the received SNR at each relay, is proposed. The

proposed scheme is an extension of the selective relaying protocol proposed in [3]³ to multi-hop scenarios in which relay nodes collaborate with each other. It is shown that a multi-hop diversity transmission system employing the proposed selective DF relaying protocol achieves diversity gain equal to the number of hops without the need for additional resources (i.e. power and bandwidth). The proposed selective DF relaying scheme is especially applicable to multi-hop cellular, or ad hoc networks that already involve regenerative relay terminals along a multi-hop path relaying (by decoding, re-encoding, and forwarding) data from a source to a destination. On the other hand, the results show that multi-hop diversity transmission systems employing selective AF relaying do not perform as well as those employing the fixed AF relaying protocol. However, the relay terminals in multi-hop diversity transmission systems employing selective AF relaying use less, or at most equal power as those in the corresponding systems with fixed AF relaying. Thus, the application of selective AF relaying protocol is more suitable for multi-hop transmission systems having power limitations at the relays.

1.2 Thesis Outline

This thesis is organized as follows. In Chapter 2, we first describe the basic concepts of cooperative communications. We then review the related works on the performance analysis, design of efficient receivers and development of optimal power allocation schemes for a variety of wireless cooperative communications systems. Chapter 3 focuses on performance analysis of multi-hop relaying systems in terms of outage probability, error probability, and capacity. In Chapter 4, optimal power allocation schemes for AF multi-hop relaying systems are developed. In Chapter 5, AF multi-relay cooperative systems are examined and low complexity coherent and noncoherent detection schemes are proposed for employment at the destination of these systems. Chapter 6 evaluates performance of multi-hop diversity transmission systems employing different relaying protocols. Chapter 7 concludes the thesis and gives ideas for future research.

³Note that in this thesis, the “selection relaying” scheme of [3] is re-named as “selective relaying” in order to avoid any confusion with selection combining diversity schemes.

Chapter 2

Background and Related Works

In this chapter, key ingredients of cooperative communications are first described. General system configurations and assumptions considered in this thesis are also presented. In addition, a detailed review of the research works related to the problems studied here is given.

2.1 Elements of Cooperative Communications

2.1.1 Processing Methods at Relays

The relays can be classified in two main categories, regenerative and nonregenerative relays. In systems with regenerative relays, the relay decodes its received signal, re-encodes it and re-transmits. This signaling scheme at the relay is called *decode-and-forward* (DF) [3]. On the other hand, in systems with nonregenerative relays, the relay amplifies its received signal and then forwards. This signaling scheme is referred to as *amplify-and-forward* (AF) [3]. The choice of the amplification gain affects the overall system performance [3], [20]. In fact, nonregenerative relays can be further classified into two subcategories, variable-gain relays and fixed-gain relays. In systems with nonregenerative variable-gain relays, the amplification gain is adapted in such a way to provide a constant power at the relay output for retransmission using the receiver CSI at the relays¹ [3]. In contrast, in systems with nonregenerative fixed-gain relays, the amplification gain is fixed and does not require knowledge of the instantaneous received CSI at the relay [20]. Although systems with nonregenerative fixed-gain relays may not perform as well as those with nonregenerative

¹The required CSI at the relay can be obtained by employing a conventional practical channel estimation technique [78, Ch. 6].

variable-gain relays [20], their easy deployment and low complexity make them attractive from a practical point of view.

Another processing scheme that does not involve decoding at the relays is *estimate-and-forward* (EF) relaying. In this scheme, the relay forwards an analog estimate of its received signal [60]. In [60], the maximum achievable rate of an EF Gaussian single-relay channel has been obtained. It is shown that when the relay is positioned close to the source, DF performs better than EF in terms of the maximum achievable rate [79]. However, EF achieves a higher rate than DF when the relay is close to the destination [79]. Both EF and DF protocols outperform AF in terms of the maximum achievable rates [79]².

In the EF protocol, an important question is how is the estimation performed at the relays? A few methods have been proposed in the literature for forming an estimate of the signal received at the relay [80], [81]. For example, estimation at the relay may be done by entropy constrained scalar quantization of its received signal [80]. Although employment of this estimation technique does not offer the theoretical maximum achievable rate of an EF system, it achieves a higher rate than the DF system when the relay-destination link is strong [80].

An estimate of the signal received at the relay may also be obtained by an unconstrained minimum mean square error (MMSE) scheme [81]. In this scheme, the relay estimate is a function of the hyperbolic tangent of its received signal [81, eq. (2)]. Note that in this context, AF relaying can be viewed as a linear MMSE scheme with a normalization in order to maintain the power constraint at the relay [81]. It has been shown that an EF system employing the unconstrained MMSE scheme achieves a higher rate than the corresponding AF system [81].

2.1.2 Relaying Protocols

Basically, there are three main classes for relaying protocols, namely, fixed relaying, selective relaying, and incremental relaying. In systems employing *fixed relaying*, relays process what they receive (e.g. by amplifying or decoding) and then re-transmit. However, as intuitively expected and as analysis shows [3], the performance of a system employing fixed DF relaying is limited by the direct transmission between the source and relays. Thus, another class of relaying, *selective relaying*, is proposed in [3] and [4] to achieve diversity gain. According to the selective relaying protocols, particular relays are selected to participate

²Note that, as shown in [3] as well as Chapters 5 and 6, AF relaying provides better diversity order than DF relaying for specific system configurations.

in the transmission. For instance, the selective relaying protocol in [3] suggests that if the received SNR at the relay is above a certain threshold, the relay is allowed for cooperation; otherwise the source repeats its message. In another selective relaying protocol, only the relay that achieves the best end-to-end performance is chosen for cooperation [30]–[32]. Different policies have been proposed in the literature for selecting the best relays based on the instantaneous amplitudes of source-relay and relay-destination links. The best relay selection relaying algorithms usually require centralized implementations and impose overhead to the system. *Incremental relaying* is another relaying method in which limited feedback from the destination is utilized in order to determine relayed transmission versus direct transmission [3]. In this scheme, upon receipt of the signal at the destination, a single bit is broadcast from the destination indicating the success or failure of the direct transmission. If the received signal-to-noise ratio (SNR) over the source-destination channel was above a certain threshold, the feedback indicates success and the relay does not cooperate. Otherwise, the feedback requests the relay to process its signal and forward it to the destination. Although incremental relaying achieves better performance, it adds system complexity and requires more overhead.

Different combinations of the relaying protocols mentioned earlier and the processing methods described in Section 2.1.1 have been investigated in the literature [3], [4], [14], [79]. Recall that the basic premise of cooperative communication is to achieve spatial diversity without physical deployment of antenna arrays at the source and/or destination [3]. From this point of view, the diversity benefit of cooperative communication depends on specific channel conditions, system resources and hardware constraints at the relays, which dictate employment of a particular relaying/processing combination at the relays [82]. For instance, AF and EF cooperative systems with fixed relaying employing MRC at the destination achieve full diversity gain [3], [14], [79]. However, the corresponding DF system does not offer full diversity gain due to the propagation of the decoding errors at the relays [3]. DF cooperative systems with selective relaying, on the other hand, have been shown to achieve diversity gain by suppressing the error causing relays from the cooperation [3], [4]. Furthermore, a hybrid EF/DF relaying scheme aiming to increase the maximum achievable rate has been investigated in [79]. In this hybrid scheme, the relay chooses the relaying protocol resulting in a higher rate at the destination for a specific channel condition in each time slot. Thus, the achievable rate of this hybrid scheme is the maximum of the achievable rates of individual EF and DF relaying protocols [79]. It is shown that this hybrid scheme offers superior outage performance over individual EF and DF relaying

protocols for all channel conditions and achieves full diversity gain. Cooperative systems employing AF selective relaying, AF incremental relaying and DF incremental relaying have also been shown to achieve full diversity gain [3]. An EF cooperative system employing incremental relaying has not been investigated in the literature yet. However, note that the incremental relaying protocol can be viewed as a distributed switch-and-stay combining (DSSC) followed by MRC when the relay-destination link is active [38]. In addition, it is shown that EF relaying always achieves a higher rate than direct transmission [79]. Hence, the achievable rate at the destination when the relay is active is higher than that of the case where the relay is not cooperating. Therefore, it is expected that an EF cooperative system with incremental relaying achieves full diversity. Rigorous diversity order analysis of this system is beyond the scope of this thesis.

2.1.3 Channel Allocation and Relays Modes of Operation

Another key element of a wireless cooperative system is how the channel is allocated to the source and the relays for their transmissions. A medium access control (MAC) protocol provides addressing and channel access mechanisms for several terminals to transmit over a shared physical medium. Time-division multiple-access (TDMA), frequency-division multiple-access (FDMA) and code-division multiple-access (CDMA) have been widely used MAC protocols in cellular communications systems. The basic idea is to assign orthogonal channels (across time, frequency, or space) to terminals in order to avoid interference among them. For instance, the MAC protocol considered in [4] divides the available bandwidth into orthogonal channels and allocates them to source terminals within the network.

The relays in a cooperative communication system should also process their received signals and then re-transmit. Basically, relay operations can be categorized into two modes, full-duplex operation in which the relay can receive and transmit simultaneously and half-duplex operation in which the relay cannot simultaneously transmit and receive in the same time slot over the same frequency band. Due to the severe attenuations over the wireless channels, and limitations of the current radio technology to provide sufficient electrical isolation between the transmit and receive circuitry, the relay's transmitted signal drowns out the signal at its receiver input. This makes full-duplex operation of relays too difficult for implementation. In order to satisfy a half-duplex operation constraint, each channel is further divided into orthogonal sub channel(s) (e.g. across time using a time-division scheme [3] and [4]) allocated to the relays cooperating in the transmission. Note that to

achieve this time division multiplexing operation, the relays store their received signals by either digital or analog delay circuits [83]. For instance, in an AF relaying system, a digital delay can be implemented by a bandpass sampling scheme using an analog-to-digital converter (ADC) and storing the digital samples [83]. The bandpass signal can then be reconstructed using a digital-to-analog converter (DAC). Note that the baseband processing, such as demodulating and decoding, is not required after ADC in AF relaying systems as opposed to the DF relaying systems.

2.2 General System Configurations and Features

A wireless cooperative system configuration employing a relaying protocol imposes different requirements on the wireless terminal hardware capabilities, channel availability, and system resources. A framework was developed in [82] that determines a relationship between the constraints on the available system resources and the achievable combinations of communication links among cooperating terminals within the system. In this thesis, we focus on the three common system configurations, namely, multi-hop systems, multi-relay cooperative systems, and multi-hop diversity systems.

Multi-hop relaying is a simple form of a wireless cooperative system in which a source communicates with the destination via a number of relays. Multi-hop transmission has become a promising technique for application in current and future cellular or ad hoc wireless networks for saving transmitter power, extending coverage and enhancing performance. Figure 2.1 shows a multi-hop transmission system. In Chapter 3, we focus on the performance evaluation of multi-hop relaying systems in terms of outage probability, error rate and capacity. In Chapter 4, optimal power allocation schemes for AF multi-hop systems under different power constraints are developed.

Another common scenario for a wireless cooperative system is the case where a source communicates with a destination with the help of a number of relays in order to achieve spatial diversity. This form of a cooperative system, referred to as multi-relay cooperative system in this thesis, is shown in Figure 2.2. In Chapter 5, we introduce coherent and noncoherent receiver structures for AF multi-relay systems requiring partial or no CSI. The performances of the proposed schemes are evaluated and, in particular, it is shown that full diversity gain is achieved. In addition, the partial CSI required can be obtained in a disturbed manner making the proposed schemes attractive for application in ad hoc wireless networks.

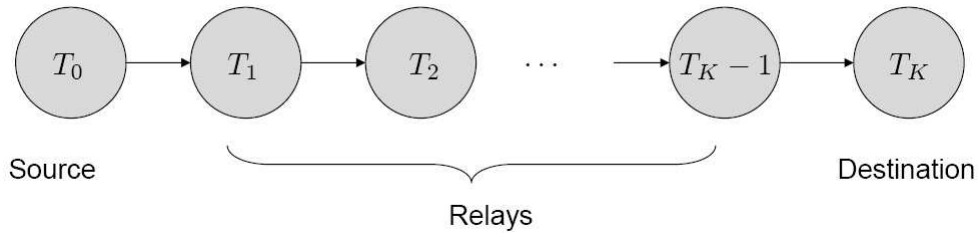


Figure 2.1. A K -hop transmission system where the source, T_0 , communicates with the destination, T_K , via $K - 1$ relays, T_1, \dots, T_{K-1} .

In a conventional multi-hop transmission system, each relay receives the signal transmitted from its immediately preceding terminal. Due to the broadcast nature of wireless media, each relay can receive the signals from all preceding transmitting terminals as well as the signal of the immediately preceding terminal, combine them appropriately, process the combiner output (either by decoding or by amplifying) and then re-transmit it. This concept forms the basis of multi-hop diversity schemes introduced in [26]. Figure 2.3 shows a multi-hop diversity transmission system. In Chapter 6, we evaluate the outage and bit error probabilities of different AF and DF multi-hop diversity transmission systems. In addition, a selective relaying scheme is proposed that achieves full diversity gain.

In all systems considered in this thesis, it is assumed that the relays operate in the half-duplex mode. The MAC scheme allocates a frequency band to the source for its transmission, which is further divided into orthogonal subchannels across time using a time-division scheme to permit half-duplex operation at the relays. In addition, we denote the fading gain of the channel between terminals T_i and T_j by $\alpha_{i,j}$. The noise at the i^{th} terminal, n_i , is modeled as a zero-mean complex Gaussian random variable with power N_0 . The instantaneous SNR of the channel between terminals T_i and T_j is then defined as $\gamma_{i,j} \triangleq \frac{P_i}{N_0} |\alpha_{i,j}|^2$ where P_i denotes the transmitter power from terminal T_i . The average SNR over the channel between T_i and T_j is denoted by $\Gamma_{i,j} \triangleq \frac{P_i}{N_0} \Omega_{i,j}$ where $\Omega_{i,j}$ is the fading power over the link.

2.3 Related Works

The basic idea behind cooperative communications returns back to the information-theoretic analysis of a three-terminal Gaussian relay channel by van der Meulen [59] and Cover and El Gamal [60]. While this past work considers the capacity improvements in Gaussian

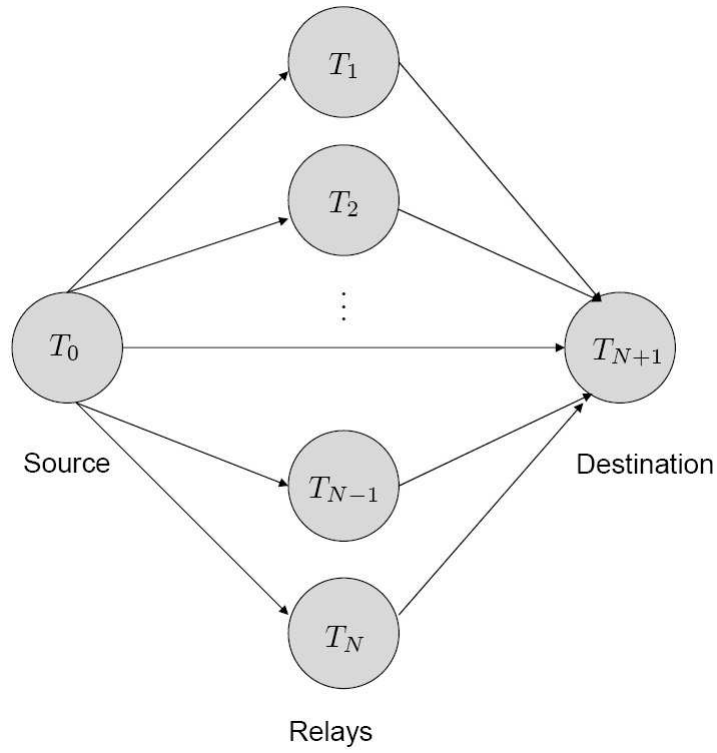


Figure 2.2. An N -relay cooperative system where the source, T_0 , communicates with the destination, T_{N+1} , via N relays, T_1, \dots, T_N .

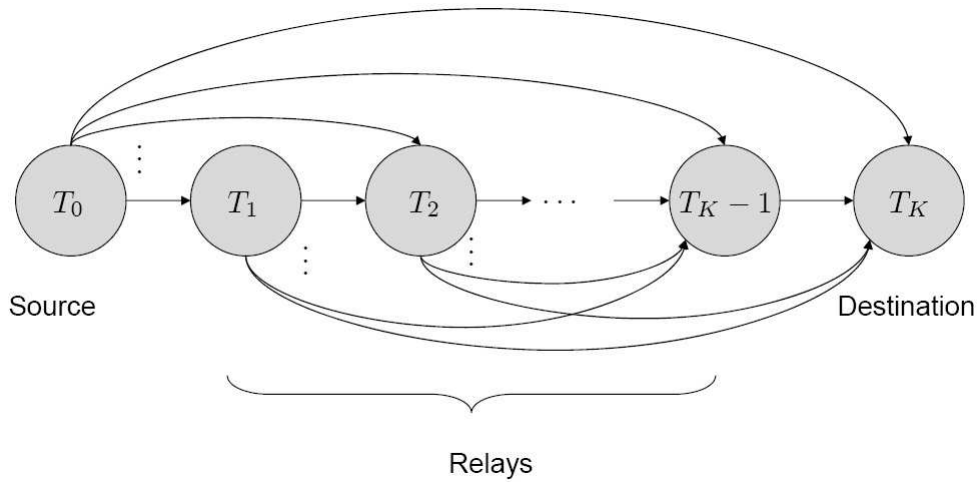


Figure 2.3. A K -hop diversity transmission system where the source, T_0 , communicates with the destination, T_K , via $K - 1$ relays, T_1, \dots, T_{K-1} .

relay channels, cooperative communications exploits the broadcast nature of the wireless medium aiming to provide spatial diversity in a fading environment through relaying by forming a virtual antenna array. Cooperative diversity for wireless networks was first introduced in [1], [2]. In [1], the implementation of user cooperation in a three-terminal (single-relay) CDMA system was considered and analyzed in terms of achievable rate region and outage probability. However, some assumptions made in [1], such as the availability of CSI at the transmitters and the ability of full-duplex operation, make implementation of the proposed protocol difficult from a practical point of view.

The next important work in the context of cooperative communications was by Laneman *et al.* [3]. In [3], a three-terminal system was considered in which the MAC protocol not only allocates orthogonal channels to each terminal but also achieves orthogonal relaying (by dividing each channel into orthogonal sub-channels across time) to ensure half-duplex operation. It was also assumed that CSI is only available at the receivers. Various cooperative protocols were then developed and evaluated in terms of asymptotic outage probability in Rayleigh fading.

Since then, a variety of wireless cooperative systems with different numbers of relays and types of processing and detection at the relays and destination have been considered and analyzed in terms of different performance metrics, such as outage and error probabilities. In the following, a literature review of the research works in the area cooperative communications related to the systems considered in this thesis is given.

2.3.1 Multi-Relay Cooperative Systems

2.3.1.1 Performance Analysis

Performance evaluation of multi-relay cooperative communication systems employing different relaying protocols has gained a lot of attention in the recent years. The asymptotic outage performance of a multi-relay cooperative system employing either repetition-based selective DF relaying or space-time coded selective DF relaying was studied in [4]. The exact outage probability and bit error rate of multi-relay systems employing selective DF relaying over Rayleigh fading channels were obtained in [5] and [6], respectively. The outage probability of DF multi-relay systems over Nakagami- m fading channels was investigated in [7] and [8]. Symbol and bit error probabilities in Nakagami- m fading of M -ary phase shift keying (PSK) DF multi-relay systems were evaluated in [9] and [10], respectively. Recently, symbol error probability in Nakagami- m fading of a DF single-relay system was

evaluated in [11]. Exact expressions for M -PSK and M -ary quadrature amplitude modulation (QAM) were derived. Asymptotic approximations were also obtained. An optimal power allocation scheme was investigated using the approximate error rate obtained. Furthermore, a criterion for choosing a *good* relay was given in terms of fading channel and system parameters.

The majority of works concerning error probability evaluations of DF cooperative communication systems assume uncoded relaying protocols, due to the simplicity in both analysis and implementation. In particular, uncoded DF relaying can perform symbol-by-symbol demodulation and re-transmission. However, DF relaying protocols can be extended to combine with coding techniques yielding an impressive gain [84]–[86]. However, since these coded cooperation methods impose an increased system complexity and overhead, we do not consider them in this thesis.

The relative simplicity of AF relaying has encouraged the design and/or performance evaluation of cooperative systems employing this protocol.

In [12], an upper bound on the instantaneous received SNR in an AF multi-relay system with variable-gain relays was obtained using the inequality between harmonic and geometric means and it was then used for error probability analysis. The lower bound on the error probability obtained in [12] needs a numerical integration which is rather involved due to the mathematical form of the MGF and it also loses its tightness as the numbers of relays increases and in particular in large-SNR regimes. In [13], the error probability of an AF multi-relay system with variable-gain relays was studied over Rayleigh fading channels. An exact analytical expression for calculation of the error probability was given in [13]. However, it is numerically complex. Hence, upper and lower bounds on the error probability were derived in [13]. An approximate asymptotic expression for the symbol error rate calculation of a multi-relay system with nonregenerative variable-gain relays employing fixed AF relaying was given in [14], using the methodology developed in [87]. The approximate expressions obtained in [14] are accurate for moderate to large values of SNR and are valid for Rayleigh, Ricean and Hoyt fading channels. In [15], closed-form expressions for the probability density function (PDF) and cumulative density function (CDF) of the end-to-end SNR of a cooperative system with a single nonregenerative relay (either variable-gain or fixed-gain) in Nakagami- m fading were derived. The results in [15] were then utilized for performance evaluation of a single-relay system employing SC diversity at the destination. In [16], an upper bound on the outage probability of a multi-relay system with variable-gain relays was derived by approximating the harmonic mean of two

exponential random variables as another exponential random variable. Although the obtained bound on the outage probability is tight for large values of SNR, it diverges in the small-SNR regime. The outage and error probabilities in Nakagami- m of an AF multi-relay system were evaluated in [17] by upper bounding the instantaneous received SNR at the destination through each relay by the minimum of the instantaneous SNR over source-relay and relay-destination links. The lower bounds obtained become tighter with increasing SNR. Error probability in Nakagami- m of an AF cooperative system with a single fixed-gain relay was evaluated in [88] using the MGF of the instantaneous received SNR. Performance of an AF multi-relay system with variable-gain relays was evaluated in [18] over Nakagami- m fading channels. In [18], an expression for the PDF of the instantaneous received SNR at the destination through a relay was first derived in Nakagami- m fading. Then, accurate single integral expressions for evaluation of symbol error probability of a variety of modulation schemes were obtained.

2.3.1.2 Detection Schemes at the Destination

Most of works on cooperative communications assume CSI is available and employ MRC at the destinations. Although MRC of the received signal in an AF cooperative communication system is an ML detector [33], this is not true for cooperative systems employing DF relaying [33]. In [1], an ML detector was presented for a single-relay DF system with binary phase shift keying (BPSK). However, as shown in [1], performance analysis of such detector is too complicated. A suboptimal combiner, referred to as λ -MRC, was then developed in [1]. Numerical results showed that this scheme performs very closely to the optimal detector. In [34], a general framework for ML detection of coherent and noncoherent DF multi-relay cooperative systems was given. However, the ML detectors obtained for both coherent and noncoherent cases are nonlinear and hard to implement. Thus, near-optimal detectors with piecewise-linear (PL) combiners, which closely approximate the non-linear ML detectors, were developed for both coherent and noncoherent demodulation of binary modulations. In a more recent work [35], a new weighted combiner, termed as cooperative-MRC (C-MRC), was proposed for general coherent cooperative systems employing fixed DF relaying. It was shown that this scheme can achieve full potential diversity gain regardless of the underlying constellation. It was also shown that the error performance of the C-MRC scheme provides a tight lower bound on that of ML detection. Furthermore, the performance of a DF cooperative system employing a C-MRC scheme was compared to that of the corresponding systems offering the same diversity gain, namely a coopera-

tive system with either AF relaying or selective DF relaying employing MRC scheme at the destination. Although the DF cooperative system with C-MRC offers slightly inferior performance than that of the corresponding system with AF relaying, it outperforms the system employing selective relaying.

However, note that employments of both MRC diversity in AF multi-relay systems and C-MRC combiner in DF multi-relay systems require global knowledge at the destination of CSI of all links. Thus, employment of other conventional diversity schemes that require partial knowledge of CSI at the destination was proposed for application in cooperative systems. Performance of multi-relay system with fixed DF relaying employing SC at the destinations was evaluated in [36] and [37]. Employment of a DSSC for a DF single-relay system was studied in [38]. In the proposed scheme, the destination compares the received SNR with a predetermined fixed switching threshold. If the received SNR is lower than this threshold, then a branch-switching occurs. This scheme requires a feedback to both the source and the relay, indicating a switching on the transmission path (from the direct to the relayed one and vice versa) during the next time slot. This scheme operates similarly to the incremental relaying protocol described in [3]. However, the destination does not employ an MRC in cases where the relayed branch is active. Outage and bit error probabilities of this system were obtained in [38] and it was shown that employment of the proposed DSSC in a DF single-relay system achieves full diversity. DSSC scheme in [38] was then extend for AF and DF systems with two relays in [39]. Expressions for evaluation of the outage and error probabilities were obtained over Rayleigh fading channels. Numerical results presented in [39] showed that the dual-relay systems employing the proposed DSSC achieve the same diversity gain and outage performance as if the best relay is selected for each transmission slot, with less complexity.

As we have seen so far, multi-relay cooperative systems mostly involve receiver structures that require either global or partial knowledge of CSI at the destination. CSI in slow fading of the source- and relay-destination links can be accurately obtained at the destination using the conventional practical channel estimation schemes [78, Ch. 6]. However, due to the noise amplification at the relays, CSI of source-relay links required to be available at the destination in many detection schemes employed in systems with AF relaying [3], [39] may not be accurately estimated at the destination. In addition, obtaining CSI requires channel monitoring in each coherence time. Thus, estimation of channel coefficients reduces the effective transmission rate in a situation where the channel parameters change within the period of one transmission block. Therefore, noncoherent modulation and de-

modulation seem more practical. In contrast with the noncoherent cooperative systems employing fixed DF relaying for which a PL near-ML detector can be obtained [34], there are few results for non-coherent cooperative systems with AF relaying [40]. In fact, ML detection for a non-coherent AF cooperative system is too complex for analysis and implementation [40]. Suboptimal receivers for noncoherent AF cooperative systems have been studied in a few recent works [41]–[43]. It was observed in [40] that a noncoherent combining scheme inspired by MRC performs worse than direct transmission. In [41], ML and suboptimal detection schemes for noncoherent AF cooperative systems with on-off keying (OOK) and binary frequency shift keying (BFSK) signalings were obtained. Both ML and suboptimal detection schemes require knowledge of the average fading channel gains of all links at the destination. The numerical results presented in [41] show that the performances of the suboptimal receivers are close to those of the ML schemes for the cases considered. However, there was no rigorous analysis given for performance evaluation of the suboptimal receivers and their achievable diversity gains. Closed-form lower bounds on the bit error probabilities of OOK and BFSK AF systems employing the corresponding ML detectors were derived in [41] assuming unfaded relay-destination links. Upper bounds on the bit error probabilities of these systems were also obtained by numerical evaluation of the Bhattacharyya distance between the likelihood functions. It was shown that an OOK system with ML achieves at least half of the potential diversity gain, whereas a BFSK system with ML achieves full diversity gain. However, the ML detectors in [41] involve integrals that have no closed-form solutions and hence are very complex for implementation. It was further shown in [42] that there is no closed-form ML detector for a noncoherent AF cooperative system where the relay outputs are under a long-term power constraint. Near-ML as well as a simple diversity combining scheme for OOK or amplitude shift keying (ASK) signalings were derived in [42] that can be expressed in closed-form and require the second-order statistics of the fading channel gains. Although these schemes outperform direct transmission (noncooperative system), there is no rigorous analysis given for the achievable diversity gain. In particular, it is clearly seen from the simulation results that the diversity combining scheme in [42] does not achieve full spatial diversity. In addition, it was shown in [42] that an ML detector for a noncoherent AF cooperative system where the relay outputs are under short-term power constraints does not depend on the signals received at the destination through the relays and thus performs the same as the noncooperative system. A noncoherent detection scheme using the generalized likelihood ratio test method was proposed in [43] that only requires knowledge of the local noise energy for its

operation. Closed-form upper and lower bounds on the error probability of this detector for the case of binary signaling and single-relay transmission were obtained. It was shown that near full spatial diversity is achieved in this case. There was no analysis presented in [43] for the general case of multiple relays and only a few simulation results showed performance improvement (implying higher diversity orders, but not necessarily full diversity) by adding more relays.

2.3.2 Multi-Hop and Multi-Hop Diversity Transmission Systems

A multi-hop transmission system is another class of cooperative communication systems that has attracted a lot of attention in the recent years. In a serial multi-hop transmission scheme without diversity, each relay terminal simply processes the received signal from the immediately preceding transmitting terminal and then forwards it to the next terminal. The outage probability and bit error rate of dual-hop transmission systems with regenerative relays employing DF relaying, nonregenerative variable-gain relays, and nonregenerative fixed-gain relays, both employing AF relaying, over Rayleigh fading channels were studied in [19] and [20]. A dual-hop transmission system in which the relay gain is adopted based on the CSI of both hops was proposed in [21] and closed-form expressions for its outage probability and error rate were derived over Rayleigh fading channels. This system offers better end-to-end performance compared to dual-hop systems with variable-gain and fixed-gain relays, however, at the expense of an increase in the average power consumption. Closed-form expression for evaluation of bit error probability in Nakagami- m fading of an AF dual-hop system with a fixed-gain relay was derived in [22]. A closed-form asymptotic expression for the bit error probability in large SNR regions was also obtained.

A numerical method was proposed in [28] to evaluate the outage probability of a multi-hop transmission system with nonregenerative variable-gain relays over Nakagami- m fading channels. In [23], performance bounds on the outage probability and bit error rate of a multi-hop transmission system with nonregenerative fixed-gain relays were obtained over generalized fading channels based on Pade approximation. New performance bounds on the outages and bit error probabilities of multi-hop transmission systems with nonregenerative relays (both variable-gain relays and fixed-gain relays) were obtained in Nakagami- m fading in [24] using the statistics of the geometric mean of individual hop SNRs. However, the performance bounds given in [23] and [24] are not tight for the case of non-identical hop SNRs, particularly in large SNR regions. In [25], a single integral expression for evaluation of the MGF of the instantaneous received SNR in an AF multi-hop system was obtained

using the MGF of the inverse of instantaneous received SNR. The bit error probability was then evaluated using the MGF-based approach described in [89, Ch. 9]. Therefore, exact evaluation of error probability using the method in [25] requires numerical computation of double integrals.

Note that each relay in a single primary route between the source and the destination could employ diversity to improve the system performance. The outage probability and bit error rate performances of this multi-hop diversity transmission system employing either fixed DF relaying or a fixed AF relaying protocol have been studied in [26]. Performance of AF multi-hop diversity systems with fixed-gain relays was evaluated in [27] over Rayleigh fading channels and theoretical expressions for evaluation of the average received SNR and symbol error probability were derived. The superior performance of a multi-hop diversity system over that of the corresponding system without diversity was demonstrated in [26] and [27].

2.3.3 Optimal Power Allocation for Cooperative Wireless Systems

Another issue in the context of cooperative communications is the development of power allocation schemes. Generally, most of the works assume a uniform power allocation among transmitting terminals. However, employing an optimal power allocation scheme can improve the system performance. Optimal power allocation schemes for various cooperative structures were investigated in the literature considering different relaying schemes, optimization criteria, and assumptions on the availability of CSI [31], [44]–[58]. For example, optimal power allocation schemes which maximize the instantaneous maximum mutual information subject to total and individual power constraints, were given in [45] for dual-hop systems equipped with a single regenerative relays, and in [46] for dual-hop systems equipped with a single variable-gain relay. In [47], optimal power allocation schemes were obtained for dual-hop transmission systems with and without diversity employing either DF or AF relaying, and a multi-hop transmission system with DF relaying. The optimization problem in [47] aimed to minimize the outage probability of each system in Rayleigh fading subject to a given power budget. In [48], the total power consumption in a DF multi-hop transmission system is minimized subject to achieving a target bit error rate. The optimal power allocation obtained requires having a global knowledge of location of each terminal at the relays, which in turn implies a centralized implementation.

On the other hand, there have been a number of studies on obtaining optimal power allocation schemes for multi-relay cooperative systems. Optimal power allocation schemes for

both AF and DF Gaussian multi-relay systems were obtained in [49] aiming to maximize the achievable rate under a total power constraint. In [50], optimal power allocation for a DF single-relay system was investigated. Assuming CSI is known at both the transmitter and the receiver, the achievable data rate was derived and optimized subject to different power constraints at the source and the relay. In [51], optimal power allocations for an AF single-relay system were obtained for minimizing the outage probability subject to total and individual average power constraints and under different assumptions for availability of CSI at the transmitter. For the case where the perfect CSI is available at the source and the relay, the optimal power allocation strategy provides significant performance gain. For a more practical case where limited feedback is used, a low complexity suboptimal power allocation scheme is developed in [51] that achieves most of the gain offered by the optimal scheme. In addition, [51] considers the case where there is no CSI known at the transmitter and derives the optimal power allocation that minimizes the outage probability subject to a total average power constraint. It was shown in [51] that there is a minimal performance gain achieved in this scheme and in fact equal power allocation between the source and the relay is nearly optimal. An optimal power allocation for a DF single-relay system was derived in [52] that maximizes the achievable data rate subject to an average power constraint. It was again shown that an impressive performance gain can be achieved by incorporating a finite rate feedback in a cooperative system. In [53], a tight bound on the outage probability in Rayleigh fading of an AF multi-relay system was first derived. Then, an optimal power allocation scheme that minimizes the obtained outage probability bound under a total power constraint was given using the knowledge of average link SNRs. It was shown that the optimal power allocation scheme achieves performance gains of about 1-2 dB in large SNR regions. An optimal power allocation scheme for AF multi-relay systems was obtained in [31] that maximizes the mutual information subject to both total and individual power constraints. The optimal power coefficients obtained depend on the global knowledge of the CSI of all links and hence requires a centralized implementation. An optimal power allocation scheme was proposed in [54] for maximizing the instantaneous received SNR in an AF multi-relay system where the relays transmit simultaneously in the second time slot. Since the obtained optimal power allocation scheme is too complex for practical implementation, a closed-form suboptimal power allocation solution was obtained in [54]. Although the suboptimal scheme performs as well the optimal scheme, it requires global knowledge of CSI and hence, similar to [31], should be implemented in a centralized manner. In [55], optimal power allocation schemes for different multi-relay systems were

studied assuming that the statistical channel knowledge (in the form of fading distribution and the path loss information across all nodes) and perfect CSI are, respectively, available at the transmitters and the receivers. Optimal power allocation strategies that minimize large SNR approximation of the outage probability in systems with AF and DF relaying subject to a ST power constraint were then obtained. The optimal power coefficients at the relays in both AF and DF systems depend only on the ratio of the average source-relay channel gain to the average relay-destination channel gain. Numerical results in [55] show that optimal power allocation scheme achieve a significant gain, especially as the number of relays increases. However, the optimal power allocation strategies obtained in [55], require a centralized implementation. Distributed power allocation policies for both AF and DF multi-relay systems that maximize the instantaneous received SNR at the destination were derived in [56]. For the special case of a single-relay system, closed-form optimal power coefficients were obtained. For the general case, derivation of a closed-form power allocation solution based on the exact SNR expression is very involved. Hence, a sub-optimal power allocation scheme was obtained in [56] based on an upper bound on the instantaneous received SNR. Numerical results in this paper also indicate the importance of the optimal power allocation scheme with increasing number of relays. In [57], an optimal power allocation scheme for a multi-relay system employing selective DF relaying was studied assuming that only the average channel gains are known at the transmitters. The optimal power allocation scheme obtained that minimizes the outage probability subject to a ST power constraint. However, due to the complex implementation of the optimal scheme, a suboptimal power allocation policy was developed in [57]. In the suboptimal scheme a fixed fraction of the total power is assigned to the source in the first stage of the transmission and the remaining power is equally allocated to the set of relays selected for the cooperation. Note that if this set is empty, the power is allocated to the source in the second stage of the transmission. In this scheme, each terminal only need to have the average gain of the channel between itself and the destination as well as the number of selected relays. Numerical results given in [57] show that the suboptimal scheme offers significant performance gain. In addition, it achieves an outage probability close to that achieved in the optimal scheme. In [58], a distributed power allocation strategy for multi-relay systems employing selective DF relaying that minimizes the total transmit power subject to a target SNR at the destination with a target outage probability was presented. In this scheme, each relay that is able to decode the signal received from the source compares the gain of the channel between itself and the destination with a given threshold value and then decides

to cooperate with the source or not. The optimum strategy determines the source transmit power as well as the threshold values at the relays. This optimal strategy requires CSI of source-relay links and source-destination link available at the source. Two simpler distributed power allocation methods were also proposed in [58] having less computational complexity with a little performance loss comparing to the optimal strategy.

Chapter 3

Multi-Hop Relaying Systems

In this chapter, we focus on the performance evaluation of multi-hop relaying systems in terms of outage probability, error rate and ergodic capacity. As mentioned earlier, exact expressions for evaluation of the outage and error probabilities of DF multi-hop systems can be readily obtained [19], [26]. Although, closed-form expressions for the outage and error probabilities for dual-hop systems with variable-gain relays and fixed-gain relays are derived in [29] and [20], respectively, there are no such expressions for AF multi-hop systems with arbitrary number of relays. In fact, the numerical method proposed in [28] for evaluation of the outage probability of an AF multi-hop system with variable-gain relays needs a large number of terms for convergence, especially for moderate to large values of SNR, to get a required accuracy. Error probability analysis presented in [25] for AF multi-hop systems with variable-gain relays requires evaluation of double integrals. In addition, lower bounds on the outage and error probabilities in Nakagami- m fading of AF multi-hop systems with fixed-gain relays obtained in [24] are not tight, especially in larger values of SNR and for larger number of hops. In Section 3.2, outage and error probabilities in general fading of AF multi-hop systems both with variable-gain relays and fixed-gain relays are evaluated and closed-form single integral expressions are derived. The asymptotic outages and error probabilities for large values of SNR are also obtained. In addition, another important performance measure of a wireless system in fading is its capacity. However, capacity in fading of multi-hop relaying systems has not been examined in the literature. Section 3.3 evaluates the ergodic capacity of different multi-hop relaying systems.

A version of this chapter has been submitted in part to IEEE Transactions on Communications and IEEE Transactions on Vehicular Technology, and has been published in part in IEEE Transactions on Wireless Communications, 7:1851-1856 (2008) and 8:2286-2291 (2009), Proceedings of IEEE International Conference on Communications (ICC), 1:4300-4305 (2008), and Proceedings of IEEE Global Communications Conference (GLOBECOM), 1:1-6 (2008).

3.1 System Models

Consider a K -hop wireless transmission system as shown in Figure (2.1) in which a source terminal, T_0 , communicates with a destination terminal, T_K , via $K - 1$ half-duplex relay terminals, T_1, T_2, \dots, T_{K-1} . In general, the k^{th} relay terminal, T_k , receives the signal from the immediately preceding transmitting terminal, T_{k-1} , in the k^{th} time slot, processes it by either decoding or amplifying and then forwards it to the next terminal, T_{k+1} , in the next time slot. The received signal at the k^{th} terminal, y_k , is given by

$$y_k = \alpha_{k-1,k}x_{k-1} + n_k, \quad k = 1, \dots, K \quad (3.1)$$

where x_{k-1} denotes the transmitted signal from the $(k - 1)^{th}$ terminal. In a multi-hop transmission system employing a DF relaying scheme, the transmitted signal from the k^{th} relay terminal, x_k , $k = 1, \dots, K - 1$, is an estimate of the transmitted source signal, x_0 , obtained by decoding of the received signal at the k^{th} terminal, y_k .

In a multi-hop transmission system employing AF relaying, the k^{th} relay terminal amplifies its received signal by a gain A_k , i.e. $x_k = A_k y_k$, and then forwards it to the next terminal. In systems with variable-gain relays, the amplification factor at the k^{th} relay is chosen as [3]

$$A_k^V = \sqrt{\frac{P_k}{P_{k-1} |\alpha_{k-1,k}|^2 + N_0}}, \quad k = 1, \dots, K - 1 \quad (3.2)$$

in order to ensure that the relay output power is P_k ¹. In contrast, in systems with fixed-gain relays, the amplification gain at the k^{th} relay, A_k^F , is a constant. The relay amplification gain in this case can have an arbitrary value, in general. However, the relay output power can take any value for an arbitrary choice of the relay gain. This requires that the relay have access to an unconstrained source of power. In practice, the relay amplification gain is chosen such that an average power constraint at the relay output is satisfied [41]- [43], i.e.

$$A_k^F = \sqrt{\frac{P_k}{P_{k-1} \mathbb{E}(|\alpha_{k-1,k}|^2) + N_0}}$$

¹It can be shown using [3, Appendix II] that this choice for the relay amplification gain maximizes the instantaneous received SNR in an AF dual-hop system. Note that, as shown in Sections 3.2.3 and 3.3.1.1, the error probability and the achievable rate in systems with AF relaying are, respectively, decreasing and increasing functions of the instantaneous received SNR at the destination. Thus, the amplification gain in (3.2) maximizes the achievable rate and minimizes the error probability of this system. In addition, using [28, eqs. (13) and (14)], it can be readily shown that the instantaneous received SNR in an AF multi-hop relaying system with an arbitrary number of hops is an increasing function with respect to the relay amplification gains. Thus, the relay amplification factor in (3.2) which meets the power constraints at the relays with equality [3] maximizes the instantaneous received SNR in AF multi-hop relaying systems, and hence maximizes the achievable rate and minimizes the error probability in these systems.

$$= \sqrt{\frac{\frac{P_k}{N_0}}{\Gamma_{k-1,k} + 1}} \quad (3.3)$$

where $\mathbb{E}(\cdot)$ denotes the expectation operator.

3.2 Outage and Error Probabilities of AF Multi-Hop Systems

Theoretical evaluation of outage and error probabilities of a wireless communication system in fading is generally done using the PDF, MGF, or CHF of the instantaneous received SNR [89]. However, closed-form expressions for the PDF, MGF, or CHF of the instantaneous received SNR of an AF multi-hop system with variable-gain relays and fixed-gain relays are still unknown for an arbitrary number of hops. On the other hand, as shown in Section 3.2.1, the MGF or CHF of the reciprocal of the instantaneous received SNR can be obtained in closed-form for a variety of fading channel models. We then evaluate the outage probability using the CHF of the inverse of the instantaneous received SNR. In addition, we develop a new general framework for evaluation of the error probabilities in fading of a variety of modulation schemes in terms of the MGF of the reciprocal of the instantaneous received SNR. The solutions obtained are in the form of single integrals that can be readily evaluated using standard mathematical software. Furthermore, simple closed-form expressions for the outage and error probabilities of AF multi-hop systems with fixed-gain relays are obtained for sufficiently large values of SNR. The analysis and methods are applicable for all fading models having the property that the value of the signal power PDF at the origin is nonzero; this includes, e.g., the important cases of Rayleigh, Ricean, and Hoyt fading but excludes Nakagami- m fading with $m \neq 1$. A simple design criterion is then presented which guarantees better outage and error performances for a multi-hop system compared to direct transmission.

3.2.1 Statistical Properties of AF Multi-Hop Systems

3.2.1.1 Systems With Variable-Gain Relays

The instantaneous received SNR in an AF multi-hop system with an arbitrary number of variable-gain relays is given by [28, eq. (2)]

$$\gamma_t^V = \left(\prod_{i=0}^{K-1} \left(1 + \frac{1}{\gamma_{i,i+1}} \right) - 1 \right)^{-1} \quad (3.4a)$$

which can be well approximated as [28, eq. (4)]

$$\gamma_t^V \approx \left(\sum_{i=0}^{K-1} \frac{1}{\gamma_{i,i+1}} \right)^{-1} \quad (3.4b)$$

especially for sufficiently large values of SNR. The expression given in (3.4b) for γ_t^V is more mathematically tractable than the one given in (3.4a). However, closed-form expressions for the PDF and CDF of γ_t^V in (3.4b) are unknown for an arbitrary number of hops². On the other hand, as seen in eq. (3.4b), the inverse of the end-to-end instantaneous received SNR, $X^V = \frac{1}{\gamma_t^V}$, is the sum of the inverse of individual per-hop SNRs. Then, the MGF of X^V is given by

$$M_{X^V}(s) = \prod_{i=1}^K M_{\frac{1}{\gamma_{i-1,i}}}(s) \quad (3.5)$$

where $M_{\frac{1}{\gamma_{i-1,i}}}(s)$ can be obtained in closed-form for a variety of fading channel models [25, eqs. (6)-(12), (16)]. For example, it is given by [28]

$$M_{\frac{1}{\gamma_{i-1,i}}}(s) = \frac{2}{\Gamma(m_i)} \left(\frac{m_i s}{\Gamma_{i-1,i}} \right)^{\frac{m_i}{2}} K_{m_i} \left(2 \sqrt{\frac{m_i s}{\Gamma_{i-1,i}}} \right) \quad (3.6)$$

in Nakagami- m fading where $m_i \geq \frac{1}{2}$ is the Nakagami- m fading parameter over the link between terminals T_{i-1} and T_i , $\Gamma(\cdot)$ denotes the gamma function [90, eq. (8.310.1)], and $K_{m_i}(\cdot)$ denotes the modified Bessel function of the second kind of order m_i [90, eq. (8.432.1)].

3.2.1.2 Systems With Fixed-Gain Relays

The instantaneous received SNR in an AF multi-hop system with fixed-gain relays is given by [23, eq. (3)]

$$\gamma_t^F = \left(\sum_{k=0}^{K-1} Y_k \right)^{-1} \quad (3.7a)$$

where

$$Y_k \triangleq \prod_{i=0}^k \frac{C_i}{\gamma_{i,i+1}} \quad (3.7b)$$

where $C_0 \triangleq 1$ and $C_i \triangleq \frac{P_i}{N_0(A_i^F)^2}$ is a constant for the fixed gain A_i^F . Closed-form expressions for the PDF and CDF of γ_t^F for the special case of dual-hop systems are known and given in [20]. However, such expressions for the PDF and CDF of a general system with arbitrary number of fixed-gain relays have not been obtained yet. Similar to the systems

²Note that closed-form expressions for the PDF and CDF of γ_t^V are given in [19, eqs. (19) and (27)] for the special case of an AF dual-hop system in Rayleigh fading.

with variable-gain relays, we obtain an expression for the MGF of the reciprocal of the instantaneous received SNR, $X^F = \frac{1}{\gamma_t^F}$. Note that the random variables Y_k , $k = 0, \dots, K-1$, are correlated and hence the MGF of the reciprocal of the instantaneous received SNR, X^F , is not the product of individual MGFs of Y_k . Let $\boldsymbol{\gamma}$ denote the vector of the instantaneous received SNRs over the first $K-1$ hops, i.e. $\boldsymbol{\gamma} = [\gamma_{0,1}, \gamma_{1,2}, \dots, \gamma_{k,k+1}, \dots, \gamma_{K-2,K-1}]$. The MGF of X^F conditioned on $\boldsymbol{\gamma}$ is obtained as

$$M_{X^F|\boldsymbol{\gamma}}(s) = \exp\left(-s \sum_{k=0}^{K-2} Y_k\right) M_{\frac{1}{\gamma_{K-1,K}}} \left(\frac{\prod_{i=1}^{K-1} C_i}{\prod_{i=0}^{K-2} \gamma_{i,i+1}} s \right) \quad (3.8)$$

where $M_{\frac{1}{\gamma_{K-1,K}}}(s)$ is given in (3.6) for the case of Nakagami- m fading. Recall that the MGF of the inverse of individual per-hop SNR can be found in [25] for different types of fading. The MGF of X^F is then given by

$$M_{X^F}(s) = \underbrace{\int_0^\infty \dots \int_0^\infty}_{(K-1)\text{-fold}} M_{X^F|\boldsymbol{\gamma}}(s) \prod_{i=0}^{K-1} f_{\gamma_{i,i+1}}(\gamma_{i,i+1}) d\gamma_{i,i+1} \quad (3.9)$$

where $f_\gamma(\cdot)$ denote the PDF of the random variable γ . The multi-fold integral in (3.9) can be evaluated using the numerical integration method given in [91, eq. (25.4.45)] for a variety of fading channel models. For instance,

$$M_{X^F}(s) \approx \sum_{n_0=1}^{N_p} \dots \sum_{n_{K-2}=1}^{N_p} \left(\prod_{i=0}^{K-2} \frac{\xi_{n_i} \zeta_{n_i}^{m_i-1}}{\Gamma(m_i+1)} \right) M_{X^F|\boldsymbol{\gamma}}(s) \Big|_{\gamma_{i,i+1} = \frac{\zeta_{n_i} \Gamma_{i,i+1}}{m_i}} \quad (3.10)$$

in Nakagami- m fading where ξ_n and ζ_n , $n = 1, \dots, N_p$, are the weights and zeros of the Laguerre polynomial of order N_p [91, Table 25.9], respectively.

3.2.2 Outage Probability Analysis

The outage probability in an AF multi-hop system is defined as the probability that the end-to-end instantaneous received SNR falls below a certain threshold, γ_{th} , i.e.

$$P_{out} = Pr(\gamma_t < \gamma_{th}) = Pr\left(X > \frac{1}{\gamma_{th}}\right) \quad (3.11)$$

where $X = \frac{1}{\gamma_t}$ and γ_t is given in (3.4) and (3.7) for systems with variable-gain relays and fixed-gain relays, respectively. The outage probability, in general, can be obtained using the CHF of X as

$$\begin{aligned} P_{out} &= 1 - Pr\left(X > \frac{1}{\gamma_{th}}\right) \\ &= 1 - \mathcal{F}^{-1}\left(\frac{1}{j\omega} \Psi_X(-\omega) + \pi\delta(\omega)\right) \Big|_{x=\frac{1}{\gamma_{th}}} \end{aligned} \quad (3.12a)$$

$$= \frac{1}{2} + \int_{-\infty}^{\infty} \frac{\exp(-jwx) \Psi_X(w)}{2\pi jw} dw \Big|_{x=\frac{1}{\gamma_{th}}} \quad (3.12b)$$

$$= \frac{1}{2} + 2 \int_0^{\frac{\pi}{2}} \Re \left(\frac{\exp(-jx \tan(\theta)) \Psi_X(\tan(\theta))}{2\pi j \tan(\theta)} \right) \sec^2(\theta) d\theta \Big|_{x=\frac{1}{\gamma_{th}}} \quad (3.12c)$$

where $\mathcal{F}^{-1}(\cdot)$ denotes the inverse Fourier transform operator, $\Psi_X(w)$ is the CHF of X , $\delta(\cdot)$ denotes the delta function, (3.12a) is written using the integration property of the Fourier transform, and (3.12c) is obtained using the change of variable $w = \tan(\theta)$. Note that $\Psi_X(\cdot)$ for systems with variable-gain relays and fixed-gain relays are given by (3.5) and (3.9), respectively, with s replaced by $-jw$.

3.2.3 Error Probability Analysis

In this section, new solutions for the average symbol error probability are derived for different modulation formats. It will be convenient to organize different modulation formats according to the mathematical form of the error rate expressions for the respective modulation types. We consider modulation formats resulting in analyses involving the incomplete gamma function, the Gaussian Q-function, and the Marcum Q-function, each in turn.

3.2.3.1 Error Probabilities Involving the Incomplete Gamma Function

The bit error probability conditioned on the instantaneous received SNR, γ_t , of different binary modulation schemes can be generally written as [89, eq. (8.100)]

$$P_b = \frac{\Gamma(b, a\gamma_t)}{2\Gamma(b)} \quad (3.13)$$

where the parameters a and b depend on the type of modulation/detection scheme given in [89, Table 8.1] reproduced here as Table 3.1 for completeness, and $\Gamma(\cdot, \cdot)$ is the incomplete gamma function [90, eq. (8.350.2)]. The bit error probability in the presence of fading is then obtained by taking the expectation of (3.13) with respect to γ_t as

$$P_b = \mathbb{E} \left(\frac{\Gamma(b, a\gamma_t)}{2\Gamma(b)} \right). \quad (3.14a)$$

Using the McLaurin series of $\Gamma(\cdot, \cdot)$ given in [90, eq. (8.354.2)], one obtains

$$P_b = \frac{1}{2} - \sum_{n=0}^{\infty} \frac{(-1)^n a^{b+n} \mathbb{E}(\gamma_t^{b+n})}{2\Gamma(b)n!(b+n)}. \quad (3.14b)$$

Note that the moments of the instantaneous received SNR, i.e. $\mathbb{E}(\gamma_t^m)$, $\forall m \in \mathbb{N}$, can be written in terms of the MGF of the reciprocal of the instantaneous received SNR, $X \triangleq \frac{1}{\gamma_t}$, as

$$\mathbb{E}(\gamma_t^m) = \frac{1}{\Gamma(m)} \int_0^{\infty} M_X(s) s^{m-1} ds \quad (3.15)$$

Table 3.1. Parameters a and b for different modulation/detection schemes from [89]

Type of modulation/detection	a	b
Orthogonal coherent BFSK	$\frac{1}{2}$	$\frac{1}{2}$
Orthogonal noncoherent BFSK	$\frac{1}{2}$	1
Binary phase-shift keying (BPSK)	1	$\frac{1}{2}$
Differentially coherent binary phase shift keying (DPSK)	1	1

using [90, eq. (3.381.4)] where $M_X(s)$ denotes the MGF of X . Then, the bit error probability in (3.14b) is evaluated as

$$P_b = \frac{1}{2} - \frac{1}{2\Gamma(b)} \int_0^\infty M_X(s) \sum_{n=0}^{\infty} \frac{(-1)^n s^{b+n-1} a^{b+n}}{n!(b+n)\Gamma(b+n)} ds \quad (3.16a)$$

$$= \frac{1}{2} - \frac{1}{2\Gamma(b)} \int_0^\infty M_X(s) s^{\frac{b}{2}-1} a^{\frac{b}{2}} J_b(2\sqrt{sa}) ds \quad (3.16b)$$

$$= \frac{1}{2} - \frac{a^{\frac{b}{2}}}{2\Gamma(b)} \int_0^{\frac{\pi}{2}} \frac{M_X(\tan(u)) J_b(2\sqrt{a \tan(u)})}{\tan^{1-\frac{b}{2}}(u) \cos^2(u)} du \quad (3.16c)$$

where $J_b(\cdot)$ is the Bessel function of the first kind of order b , (3.16b) is written using the McLaurin series of $J_b(\cdot)$ given in [90, eq. (8.402)], and (3.16c) is obtained using the change of variable $s = \tan(u)$. Note that $M_X(\cdot)$ for systems with variable-gain relays and fixed-gain relays are given by (3.5) and (3.9), respectively. Note that (3.16c) is an exact expression for P_b and the single integral is over a closed, finite interval. It can be readily evaluated in MATLAB or MAPLE.

3.2.3.2 Error Probabilities Involving the Gaussian Q-Function

Evaluation of symbol or bit error probabilities of many coherent modulation schemes involves taking the expectation of $Q(\tau\sqrt{\gamma_t})$ with respect to γ_t where $Q(\cdot)$ is the Gaussian Q-function [89, eq. (4.1)] and τ is a parameter depending on the type of modulation [89]. This is the case, for instance, for evaluation of the bit error probability of M -ASK with Gray encoding [92, eqs. (9) and (10)], the symbol error probability of M -ASK [89, eq. (8.3)], the bit error probability of M -QAM with Gray encoding [92, eqs. (14) and (16)], and the symbol error probability of M -QAM [89, eq. (8.9)]. Table 3.2, reproduced from [89] and [92], gives expressions for bit error probabilities, P_b , and symbol error probabilities, P_s , of these modulation schemes. In Table 3.2, $[\cdot]$ denotes the integer part (floor) of its argument.

Table 3.2. Average bit and symbol error probabilities of different modulation schemes involving the Gaussian Q-function

Modulation	Average bit error probability	Average symbol error probability
M -ASK	$\frac{2}{M \log_2 M} \sum_{k=1}^{\log_2 M} \sum_{i=0}^{(1-2^{-k})M-1}$ $\left\{ (-1)^{\lfloor \frac{i2^{k-1}}{M} \rfloor} \left(2^{k-1} - \left\lfloor \frac{i2^{k-1}}{M} + \frac{1}{2} \right\rfloor \right) \right.$ $\left. \mathbb{E} \left(Q \left(\sqrt{\frac{6(2i+1)^2 \gamma_t \log_2 M}{M^2-1}} \right) \right) \right\}$ <p>[92, eqs. (9) and (10)]</p>	$2 \left(\frac{M-1}{M} \right) \mathbb{E} \left(Q \left(\sqrt{\frac{6\gamma_t}{M^2-1}} \right) \right)$ <p>[89, eq. (8.3)]</p>
M -QAM	$P_{bit} \Big _{\substack{\sqrt{M}\text{-ASK} \\ \gamma_t \rightarrow \frac{\gamma_t}{2}}} \text{ [92, eqs. (14) and (16)]}$	$1 - \left(1 - P_s \Big _{\substack{\sqrt{M}\text{-ASK} \\ \gamma_t \rightarrow \frac{\gamma_t}{2}}} \right)^2$ <p>[89, eq. (8.9)]</p>

The expected value of $Q(\tau\sqrt{\gamma_t})$ can be evaluated as

$$\mathbb{E} (Q (\tau\sqrt{\gamma_t})) = \frac{1}{2} \mathbb{E} \left(1 - \text{erf} \left(\tau \sqrt{\frac{\gamma_t}{2}} \right) \right) \quad (3.17)$$

where $\text{erf}(\cdot)$ denotes the error function [90, eq. (8.250.1)]. The expectation in (3.17) cannot be evaluated in closed-form using the MGF-based method of [89, Ch. 9] because the MGF of the SNR in general multi-hop transmission systems is not known in closed-form. We can, however, proceed by using the McLaurin series of $\text{erf}(\cdot)$ and $\sin(\cdot)$ given in [90, eq. (8.253.1)] and [90, eq. (1.411.1)], respectively. One obtains

$$\mathbb{E} (Q (\tau\sqrt{\gamma_t})) = \frac{1}{2} - \frac{1}{\sqrt{\pi}} \sum_{n=0}^{\infty} \frac{(-1)^n \tau^{2n+1} \mathbb{E} \left(\gamma_t^{n+\frac{1}{2}} \right)}{n!(2n+1)2^{n+\frac{1}{2}}} \quad (3.18a)$$

$$= \frac{1}{2} - \frac{1}{\sqrt{\pi}} \int_0^{\infty} M_X(s) \sum_{n=0}^{\infty} \frac{(-1)^n \tau^{2n+1} s^{n-\frac{1}{2}}}{n!(2n+1)2^{n+\frac{1}{2}} \Gamma(n+\frac{1}{2})} ds \quad (3.18b)$$

where we have used (3.15) to obtain (3.18b). Then, using the McLaurin series of $\sin(\cdot)$ given in [90, eq. (1.411.1)], eq. (3.18b) is evaluated as

$$\begin{aligned} \mathbb{E} (Q (\tau\sqrt{\gamma_t})) &= \frac{1}{2} - \frac{1}{\pi} \int_0^{\infty} M_X(s) \frac{\sin(\tau\sqrt{2s})}{s} ds \\ &= \frac{1}{2} - \frac{1}{\pi} \int_0^{\frac{\pi}{2}} \frac{M_X(\tan(u)) \sin(\tau\sqrt{2 \tan(u)})}{\cos^2(u) \tan(u)} du. \end{aligned} \quad (3.18c)$$

Eq. (3.18c) provides a new solution for evaluation of the average bit and symbol error probabilities in general fading of different modulation schemes involving the Gaussian Q-function using the MGF of the reciprocal of the instantaneous received SNR.

Table 3.3. Average bit error probabilities of different modulation schemes involving the Marcum Q-function

Modulation	Average bit error probability
Offset BPSK	$\frac{1}{2} - \frac{1}{2} \mathbb{E} \left(Q_1 \left((\sqrt{G} + 1) \sqrt{\frac{\gamma_t}{2}}, (\sqrt{G} - 1) \sqrt{\frac{\gamma_t}{2}} \right) \right)$ $+ \frac{1}{2} \mathbb{E} \left(Q_1 \left((\sqrt{G} - 1) \sqrt{\frac{\gamma_t}{2}}, (\sqrt{G} + 1) \sqrt{\frac{\gamma_t}{2}} \right) \right)$ [89, eqs. (8.61), (8.62)]
Offset QPSK	$\frac{1}{4} - \frac{1}{4} \mathbb{E} \left(Q_1 \left((\sqrt{2G} + 1) \sqrt{\frac{\gamma_t}{2}}, (\sqrt{2G} - 1) \sqrt{\frac{\gamma_t}{2}} \right) \right)$ $+ \frac{1}{4} \mathbb{E} \left(Q_1 \left((\sqrt{2G} - 1) \sqrt{\frac{\gamma_t}{2}}, (\sqrt{2G} + 1) \sqrt{\frac{\gamma_t}{2}} \right) \right)$ $+ \frac{1}{4} - \frac{1}{4} \mathbb{E} \left(Q_1 \left(\sqrt{\gamma_t (G + 1 + \sqrt{2G})}, \sqrt{\gamma_t (G + 1 - \sqrt{2G})} \right) \right)$ $+ \frac{1}{4} \mathbb{E} \left(Q_1 \left(\sqrt{\gamma_t (G + 1 - \sqrt{2G})}, \sqrt{\gamma_t (G + 1 + \sqrt{2G})} \right) \right)$ <p style="text-align: right;">[89, eqs. (8.64), (8.65)]</p>
4-DPSK	$\frac{1}{2} - \frac{1}{2} \mathbb{E} \left(Q_1 \left(\sqrt{(2 + \sqrt{2})\gamma_t}, \sqrt{(2 - \sqrt{2})\gamma_t} \right) \right)$ $+ \frac{1}{2} \mathbb{E} \left(Q_1 \left(\sqrt{(2 - \sqrt{2})\gamma_t}, \sqrt{(2 + \sqrt{2})\gamma_t} \right) \right)$ [89, eqs. (8.61), (8.88)]

3.2.3.3 Error Probabilities Involving the Marcum Q-Function

Evaluation of error probability of some differentially coherent and noncoherent modulation schemes requires taking the expectation of $Q_l(\sqrt{\tau_1\gamma_t}, \sqrt{\tau_2\gamma_t})$ with respect to γ_t where $Q_l(\cdot, \cdot)$ denotes the Marcum Q-function [89, eq. (4.60)] of integer order l , and τ_1 and τ_2 depend on the type of modulation. This is the case, for instance, for evaluation of the bit error probabilities of offset BPSK [89, eqs. (8.61), (8.62)], offset quadrature phase-shift keying (QPSK) [89, eqs. (8.64)-(8.66)], and 4-ary DPSK (4-DPSK) [89, eqs. (8.61), (8.88)], as summarized in Table 3.3, compiled from [89, Ch. 8]. In Table 3.3, the parameter G denotes the SNR gain of the carrier synchronization technique used to produce an estimate of the received carrier phase [89].

The expected value of $Q_l(\sqrt{\tau_1\gamma_t}, \sqrt{\tau_2\gamma_t})$ can be evaluated as

$$\begin{aligned} & \mathbb{E} \left(Q_l \left(\sqrt{\tau_1\gamma_t}, \sqrt{\tau_2\gamma_t} \right) \right) \\ &= \sum_{n=0}^{\infty} \frac{\tau_1^n}{2^n n!} \sum_{k=0}^{n+l-1} \frac{\tau_2^k}{2^k k!} \mathbb{E} \left(\gamma_t^{n+k} \exp \left(-\frac{\tau_1 + \tau_2}{2} \gamma \right) \right) \end{aligned} \quad (3.19a)$$

using the series representation for the Marcum Q-function of integer order [93, eq. (4)] where

$$\mathbb{E} \left(\gamma_t^{n+k} \exp \left(-\frac{\tau_1 + \tau_2}{2} \gamma \right) \right) \quad (3.19b)$$

$$= \sum_{m=0}^{\infty} \frac{(-1)^m \left(\frac{\tau_1+\tau_2}{2}\right)^m}{m!} \mathbb{E} \left(\gamma_t^{n+k+m} \right) \quad (3.19c)$$

$$= \int_0^{\infty} M_X(s) \sum_{m=0}^{\infty} \frac{(-1)^m \left(\frac{\tau_1+\tau_2}{2}\right)^m s^{n+k+m-1}}{m!(n+k+m-1)!} ds \quad (3.19d)$$

$$= \int_0^{\infty} M_X(s) \frac{s^{n+k-1} J_{n+k-1} \left(2\sqrt{\frac{\tau_1+\tau_2}{2}} s \right)}{\left(\frac{\tau_1+\tau_2}{2}\right)^{\frac{n+k-1}{2}}} ds \quad (3.19e)$$

where (3.19c) and (3.19e) are written using the McLaurin series for $\exp(\cdot)$ and $J_{n+k-1}(\cdot)$ functions given in [90, eq. (1.211.1)] and [90, eq. (8.402)], respectively. Note that the number of terms needed in (3.19a) to get a required accuracy in evaluation of the expected value of $Q_l(\sqrt{\tau_1\gamma_t}, \sqrt{\tau_2\gamma_t})$ (and consequently the error probability) depends on system and channel parameters, in general. However, since the series in (3.19a) contains a product of two factorial terms in its denominator, it converges rapidly. The expression (3.19) provides a new solution for evaluation of the average error probabilities in fading of modulation schemes involving the Marcum Q-function.

Note that for the special case of $\tau_1 = 0$, $Q_l(0, \sqrt{\tau_2\gamma_t})$ can be written in terms of incomplete gamma function as [89, eq. (4.71)]

$$Q_l(0, \sqrt{\tau_2\gamma_t}) = \frac{\Gamma\left(l, \frac{\tau_2\gamma_t}{2}\right)}{\Gamma(l)} \quad (3.20)$$

and hence the result obtained in Section 3.2.3.1 can be used to evaluate the expected value of $Q_l(0, \sqrt{\tau_2\gamma_t})$.

3.2.4 Numerical Results

In this section, several numerical examples are presented to test the accuracy of the analytical expressions obtained in Sections 3.2.2 and 3.2.3 for evaluation of the outage and error probabilities of AF multi-hop systems with variable-gain and fixed-gain relays. In the numerical examples, we assume multi-hop systems for which the average SNR over the k^{th} hop is $\Gamma_{k-1,k} = \frac{1}{k}\Gamma_{0,1}$. We consider BPSK, 16-QAM and 4-DPSK systems both in Rayleigh fading ($m_k = 1$, $k = 1, \dots, K$) and in Nakagami- m fading with $m_k = 2$, $k = 1, \dots, K$. The bit error probabilities of these modulation schemes can be obtained using Tables 3.1-3.3. The MGF expression presented in Section 3.2.1.2 for systems with fixed-gain relays is valid for any arbitrary fixed gain. In addition, for evaluation of the MGF, we take $N_p = 15$ in small SNR regions and $N_p = 60^3$ for large values of SNR. In numerical examples, $C_i = 1.7$ for all relay terminals, as assumed in [24].

³Note that the weights and zeros of the Laguerre polynomial are given in [91, Table 25.9] up to the order $N_p = 15$. However, the weights and zeros can be readily obtained in MAPLE for higher orders of Laguerre polynomials.

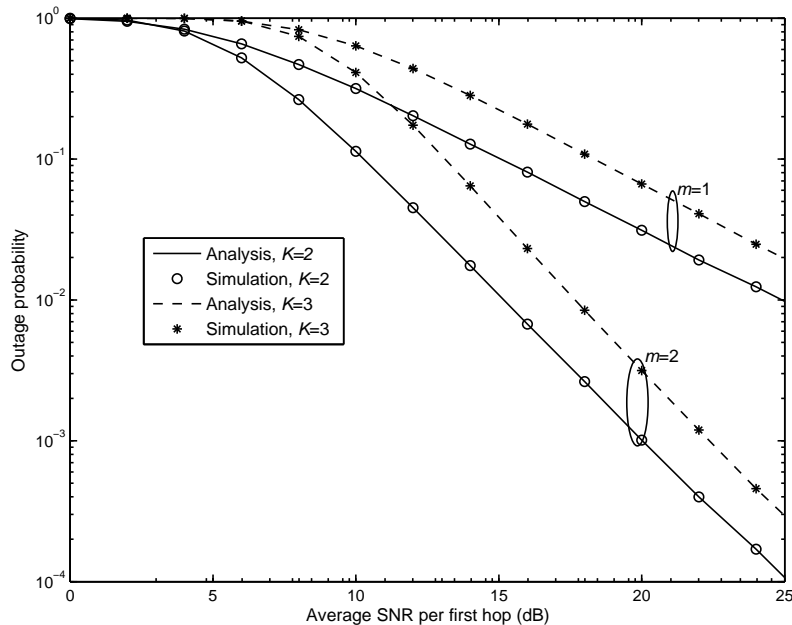


Figure 3.1. Outage probabilities for different AF multi-hop relaying systems with variable-gain relays ($\gamma_{th} = 1$).

Figures 3.1 and 3.2 show the outage probabilities for different AF multi-hop systems with variable-gain and fixed-gain relays, respectively. It is seen in these figures that the theoretical results obtained using (3.12) exactly match the Monte Carlo simulation results. For comparison purposes, in Figure 3.2, we have also included the lower bound on the outage probability obtained in [24]. It is clearly seen that the lower bound loses its tightness with increasing SNR and especially for larger numbers of hops.

Figures 3.3 and 3.4 show bit error probabilities for different BPSK and 16-QAM multi-hop transmission systems with variable-gain relays and fixed-gain relays, respectively, computed using (3.16) and (3.18). Simulation results are also shown in Figures 3.3 and 3.4 to validate the theoretical results. It is clearly seen that the analytical results are in exact agreement with the simulation results. It is also seen that systems with different numbers of hops follow the same error rate performance behavior for sufficiently large values of SNR. For instance, double-hop and triple-hop systems in Rayleigh fading achieve diversity gain one, as also shown later in Section 3.2.5. However, note that the amount of fading in a Nakagami- m channel is given by $\frac{1}{m}$ [89, eq. (2.24)]. This indicates that the severity of fading decreases with increasing Nakagami parameter m . Thus, as seen in Figures 3.3 and 3.4, systems operating in Nakagami fading with $m = 2$ perform better (have curves with

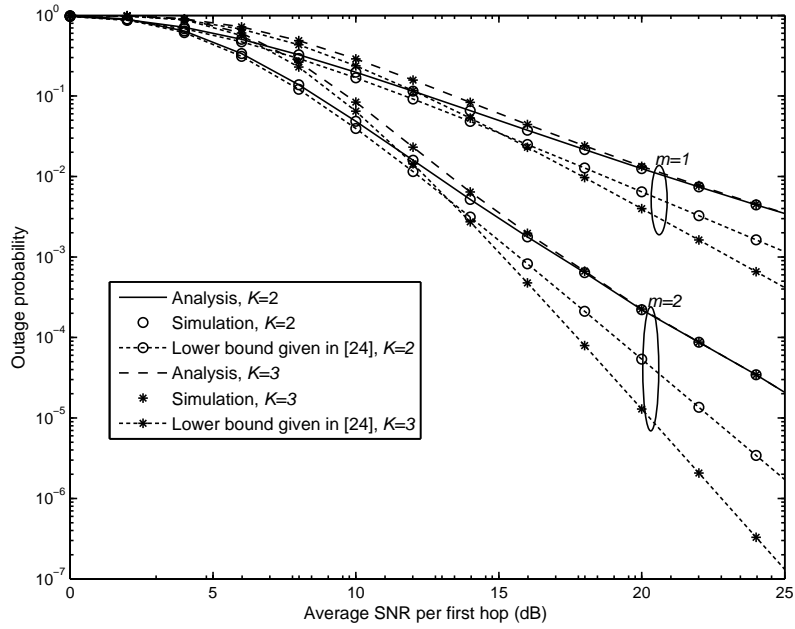


Figure 3.2. Outage probabilities for different AF multi-hop relaying systems with fixed-gain relays ($\gamma_{th} = 1$).

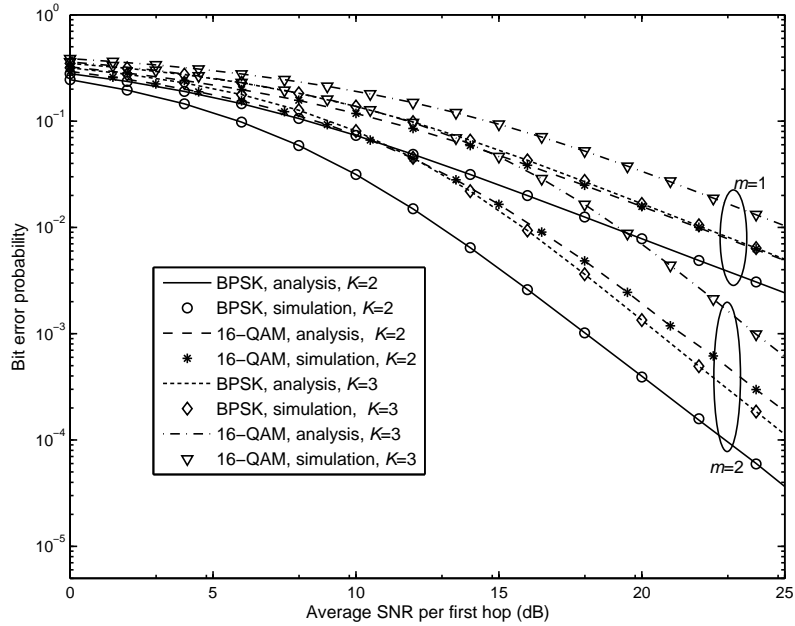


Figure 3.3. Bit error probabilities for different BPSK and 16-QAM AF multi-hop relaying systems with variable-gain relays.

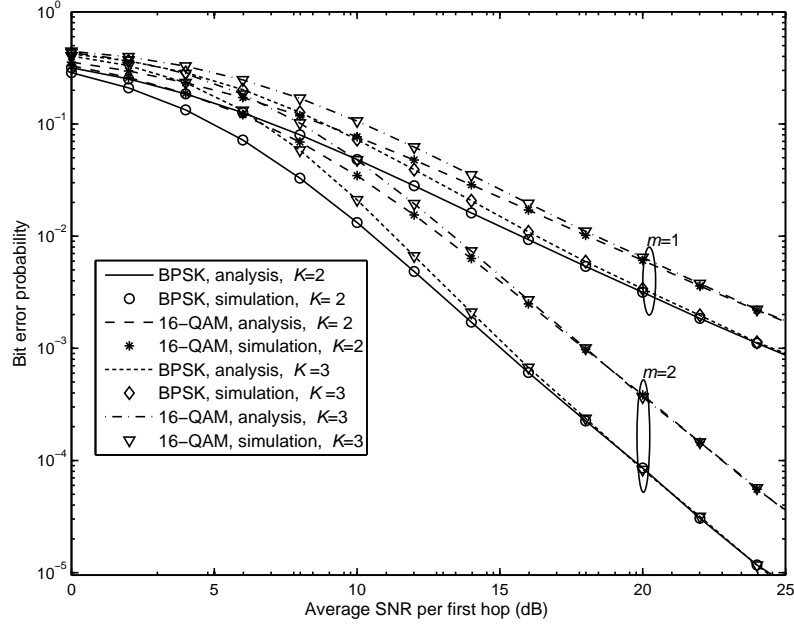


Figure 3.4. Bit error probabilities for different BPSK and 16-QAM AF multi-hop relaying systems with fixed-gain relays.

higher slopes) than the corresponding systems in Rayleigh fading (i.e. Nakagami fading with $m = 1$). Figure 3.5 compares exact bit error probabilities of BPSK multi-hop systems with fixed-gain relays with the lower bound given in [24, eq. (25)]. It is again seen that the lower bound significantly overestimates the system performance for moderate to large values of SNR. Figure 3.6 illustrates bit error probabilities for different 4-DPSK multi-hop transmission systems with variable-gain relays. The number of terms used in (3.19a) to evaluate the bit error probabilities was as few as 50 for small to moderate values of SNR. As the SNR increases, more terms in (3.19a) were required to get high accuracy (e. g. as many as 150 terms for large values of SNR). Again, it is seen from this figure that the theoretical results precisely match the simulation results.

3.2.5 Asymptotic Behavior

The large SNR behavior of outage and error probabilities in AF multi-hop systems is examined in this section. Although, accurate theoretical expressions for evaluation of the outage and error probabilities for AF multi-hop relaying systems with variable-gain and fixed-gain relays were obtained in Sections 3.2.2 and 3.2.3, studying the asymptotic behavior of the outage and error probabilities for sufficiently large values of SNR provides valuable insights into the system performance as well as simple system design criteria, as we will see

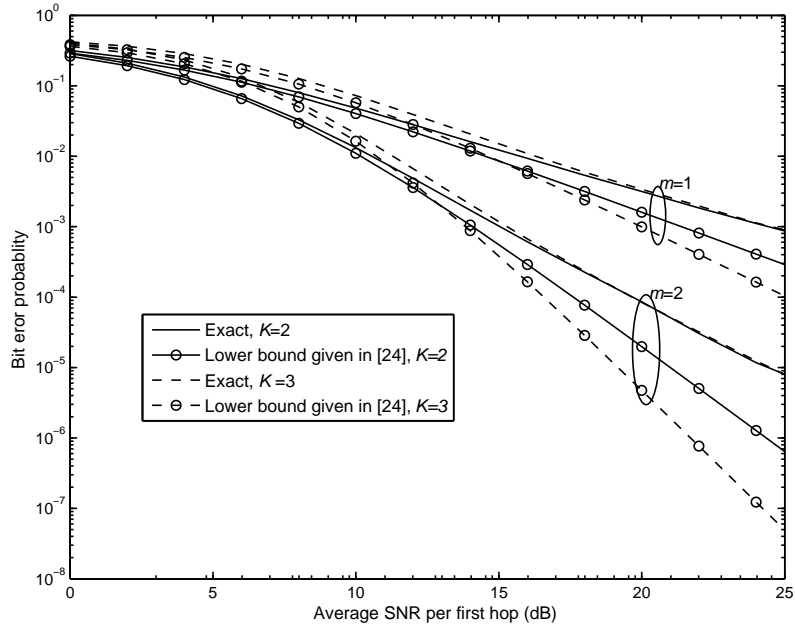


Figure 3.5. Comparison between the exact bit error probability and the lower bound given in [24] for different BPSK AF multi-hop relay systems with fixed-gain relays.

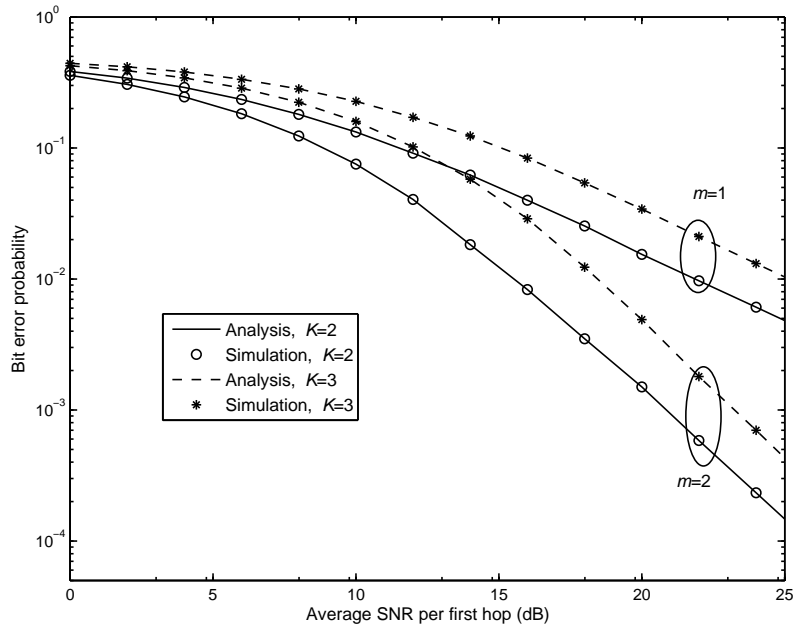


Figure 3.6. Bit error probabilities for different 4-DPSK AF multi-hop relay systems with variable-gain relays.

later.

The following Lemma states that the outage and error probabilities for sufficiently large values of SNR can be determined by the behavior of the PDF of the received SNR at the origin.

Lemma 3.1: The outage and error probabilities for sufficiently large values of SNR are given by

$$P_{out} \rightarrow \frac{\gamma_{th}^{t+1}}{(t+1)!} \frac{\partial^t f_{\gamma_t}}{\partial \gamma^t}(0) \quad (3.21)$$

$$P_b \rightarrow \frac{\Gamma(b+t+1)}{2\Gamma(b)a^{t+1}(t+1)!} \frac{\partial^t f_{\gamma_t}}{\partial \gamma^t}(0) \quad (3.22)$$

and

$$P_s = \mathbb{E}(Q(\tau_0\sqrt{\gamma_t})) \rightarrow \frac{\prod_{i=1}^{t+1}(2i-1)}{2(t+1)\tau_0^{2(t+1)}} \frac{\partial^t f_{\gamma_t}}{\partial \gamma^t}(0) \quad (3.23)$$

where τ_0 depends on the type of modulation (e.g. $\tau_0 = \sqrt{2}$ for BPSK) [89] and $f_{\gamma_t}(\cdot)$ denotes the PDF of γ_t and t is the order of the first nonzero derivative of $f_{\gamma_t}(\gamma)$ at $\gamma = 0$.

Proof: A proof for eq. (3.21) as well as a proof for eq. (3.23) are given in [87] and [14], respectively. A proof for eq. (3.22) and an alternate proof for eq. (3.21) are given in Appendix A.1.

Thus, the calculation of outages or error probabilities reduces to the evaluation of the derivatives of $f_{\gamma_t}(\gamma)$ at the origin. In a multi-hop system with variable-gain relays, one has

$$f_{\gamma_t^v}(0) = \sum_{k=1}^K f_{\gamma_{k-1,k}}(0) \quad (3.24a)$$

using [14, Proposition 3] where $f_{\gamma_{k-1,k}}(0)$ denotes the value of the PDF of the k^{th} hop SNR at the origin and is given by

$$f_{\gamma_{k-1,k}}(0) = \frac{r}{\Gamma_{k-1,k}} \quad (3.24b)$$

where r is a constant parameter given in Table 3.4 for different types of fading. In Table 3.4, K_r and q respectively denote the Ricean and Hoyt fading parameters. The outage and error probabilities for sufficiently large values of SNR are then obtained by (3.21)-(3.23) with $t = 0$ and $f_{\gamma_t}(0)$ replaced by (3.24).

In systems with fixed-gain relays, a lower bound on the value of the pdf of γ_t^F at zero, $f_{\gamma_t^F}(0)$, can be calculated using the following lemma.

Lemma 3.2: Consider \mathcal{M} nonnegative independent random variables, $X_1, \dots, X_{\mathcal{M}}$, whose PDFs at zero, $f_{X_m}(0)$, and expected values, $\mathbb{E}(X_m)$, are known and nonzero for

Table 3.4. Values of r for different types of fading from [89]

Type of Fading	r
Rayleigh	1
Ricean	$(K_r + 1) \exp(-K_r)$
Hoyt	$\frac{1+q^2}{2q}$

$m = 1, \dots, \mathcal{M}$. If the random variable V is defined as

$$V = g(X_1, \dots, X_{\mathcal{M}}) = \left(\sum_{m=1}^{\mathcal{M}} \prod_{h=1}^m \frac{\Psi_{h-1}}{X_h} \right)^{-1} \quad (3.25)$$

where Ψ_m , $m = 0, \dots, \mathcal{M} - 1$, is an arbitrary constant, then the PDF of V at zero is bounded by

$$f_V(0) \geq \sum_{m=1}^{\mathcal{M}} f_{X_m}(0) \left(\sum_{j=m-1}^{\mathcal{M}-1} \frac{\prod_{h=0}^j \Psi_h}{\prod_{\substack{h=1 \\ h \neq m}}^{j+1} \mathbb{E}(X_h)} \right). \quad (3.26)$$

Proof: A proof of Lemma 3.2 is given in Appendix A.2.

Thus, using Lemma 3.2 the value of the PDF of γ_t^F at zero is bounded by

$$f_{\gamma_t^F}(0) \geq \sum_{k=1}^K \frac{r}{\Gamma_{k-1,k}} \sum_{j=k-1}^{K-1} \frac{\prod_{h=0}^j C_h}{\prod_{\substack{h=1 \\ h \neq m}}^{j+1} \Gamma_{h-1,h}}. \quad (3.27)$$

Lower bounds on the asymptotic outages and error probabilities for AF multi-hop systems with fixed-gain relays are then obtained by (3.21)-(3.23) with $t = 0$ and $f_{\gamma_t}(0)$ replaced by (3.27).

The asymptotic error probabilities obtained using (3.24) and (3.27) show that a multi-hop transmission system either with variable-gain relays or fixed gain relays has diversity order one. However, a multi-hop system with variable-gain relays can perform better than a single-hop system if [14, eq. (41)]

$$\sum_{k=1}^K \frac{1}{\Gamma_{k-1,k}} < \frac{1}{\Gamma_0} \quad (3.28)$$

where Γ_0 denotes the single-hop average SNR. Similarly, using Lemmas 3.1 and 3.2, a multi-hop system with fixed-gain relays outperforms a single hop system in terms of outage and error probabilities for sufficiently large values of SNR if

$$\sum_{k=1}^K (K - k + 1) \mu_H \left(\tilde{\Gamma}_k, \tilde{\Gamma}_{k+1}, \dots, \tilde{\Gamma}_K \right)^{-1} < \frac{1}{\Gamma_0} \quad (3.29)$$

where $\tilde{\Gamma}_k = \frac{\prod_{h=1}^k \Gamma_{h-1,h}}{\prod_{h=1}^{k-1} C_h}$ and $\mu_H(\tilde{\Gamma}_k, \tilde{\Gamma}_{k+1}, \dots, \tilde{\Gamma}_K)$ denotes the harmonic mean of $\tilde{\Gamma}_k, \dots, \tilde{\Gamma}_K$ ⁴. Generally, one can conclude that a K_1 -hop transmission system performs better than a K_2 -hop transmission system (where we assume without loss of generality that $K_2 < K_1$) if

$$\sum_{k=1}^{K_1} \frac{1}{\Gamma_{k-1,k}} < \sum_{k=1}^{K_2} \frac{1}{\Gamma_{k-1,k}} \quad (3.30)$$

in systems with variable gain relays, and

$$\sum_{k=1}^{K_1} (K_1 - k + 1) \mu_H(\tilde{\Gamma}_k, \tilde{\Gamma}_{k+1}, \dots, \tilde{\Gamma}_{K_1})^{-1} < \sum_{k=1}^{K_2} (K_2 - k + 1) \mu_H(\tilde{\Gamma}_k, \tilde{\Gamma}_{k+1}, \dots, \tilde{\Gamma}_{K_2})^{-1} \quad (3.31)$$

in systems with fixed-gain relays.

3.2.5.1 Numerical Examples

The accuracy of the asymptotic results for AF multi-hop systems with variable-gain relays has been shown in [14]. In this section, several numerical examples are presented to investigate the performances of different AF multi-hop systems with fixed-gain relays for sufficiently large values of SNR. In the numerical examples, we consider systems with BPSK operating over Rayleigh fading channels. We also take $C_i = 1.7$ for all relay terminals.

Example 1: Multi-hop transmission systems with balanced links

In this example, we consider the outage and bit error rate performances of different multi-hop transmission systems in which each terminal is located an equal distant from the preceding transmitting terminal. To have a fair performance comparison between systems with different numbers of hops, it is assumed that all systems use the same total transmission power. Each terminal in a K -hop transmission system then uses $\frac{1}{K}$ of the total transmission power according to a uniform power allocation policy⁵. Thus, using the Friis propagation formula [94], the average link SNRs in a K -hop system are given by, $\Gamma_{k-1,k} = K^{\epsilon-1} \Gamma_0$, $k = 1, \dots, K$ where ϵ is the path loss exponent.

Figures 3.7 and 3.8, respectively, show the outages and the bit error probabilities versus Γ_0 for this system configuration for different numbers of hops and $\epsilon = 3$. These figures clearly indicate the high accuracy of the analytically obtained outage and bit error probabilities for multi-hop transmission systems with balanced links in moderate to large SNR

⁴The harmonic mean of X_1, X_2, \dots, X_N is defined as $N \left(\sum_{i=1}^N 1/X_i \right)^{-1}$ [91, eq. (3.1.13)].

⁵This implies that the peak power per terminal in a multi-hop relaying system employing uniform power allocation policy linearly decreases with the number of hops which in turn increases lifetime of the individual terminals within the system compared to that of the source terminal in the single-hop system.

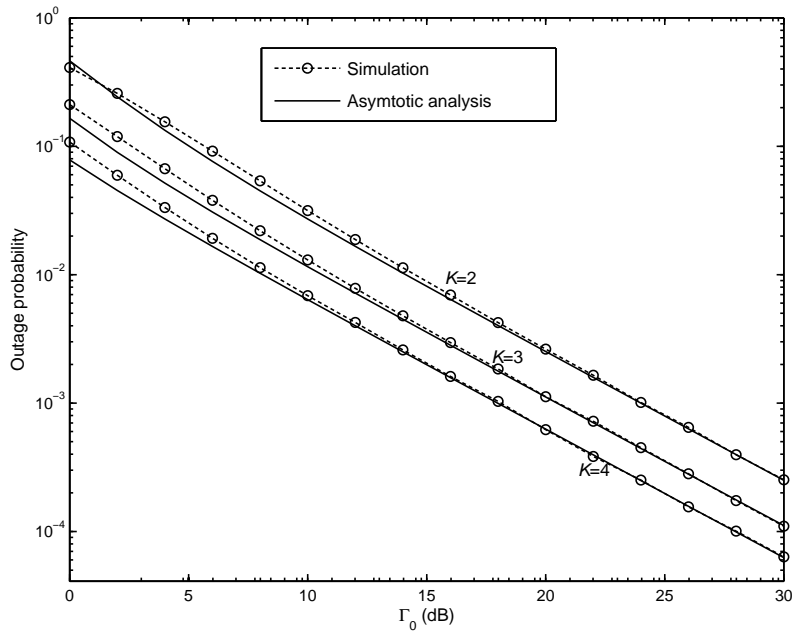


Figure 3.7. Outage probabilities for different multi-hop transmission systems with fixed-gain relays and balanced links ($\gamma_{th} = 1$).

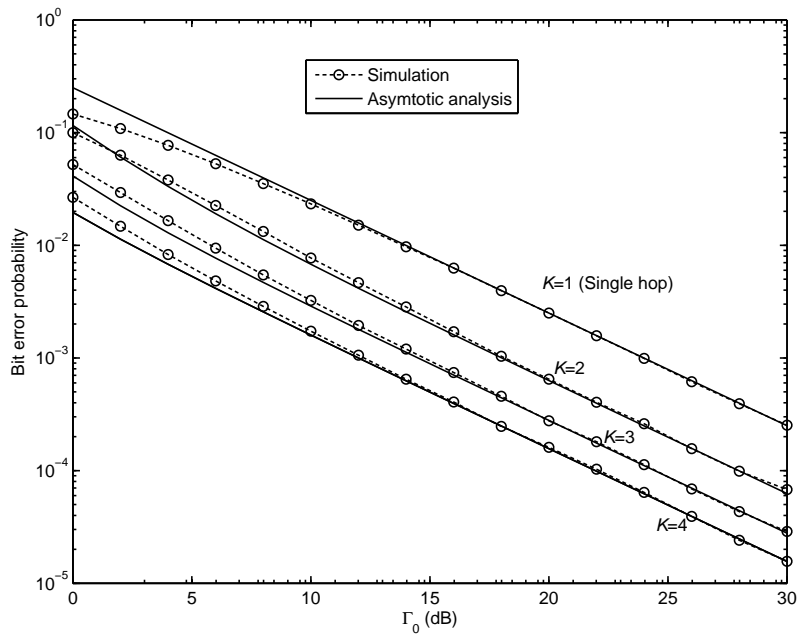


Figure 3.8. Bit error probabilities for different multi-hop transmission systems with fixed-gain relays and balanced links.

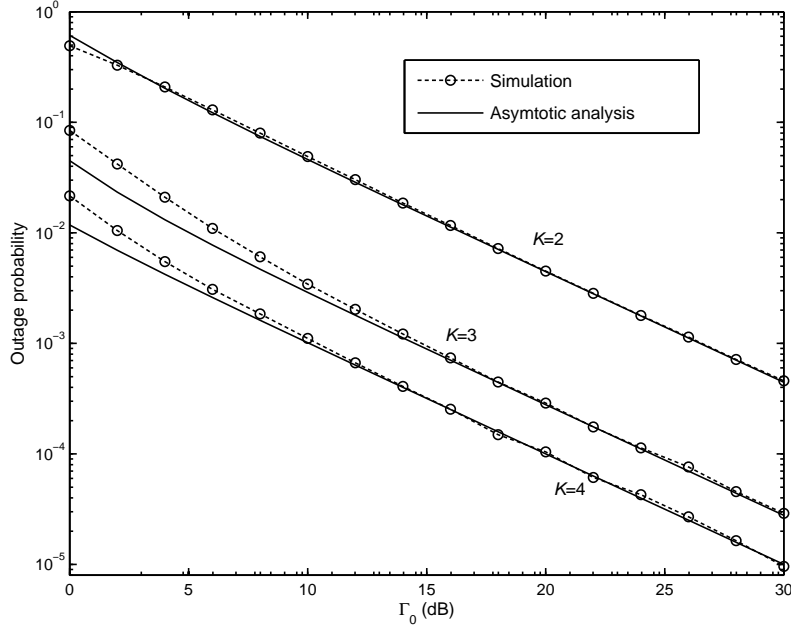


Figure 3.9. Outage probabilities for different multi-hop transmission systems with fixed-gain relays and unbalanced links ($\gamma_{th} = 1$).

regions. It is also seen that by increasing the number of hops, the outage and bit error rate performances improve (and the corresponding conditions (3.29) and (3.31) are satisfied). This result further reveals the importance of multi-hopping in wireless communication systems because, not only, can it save transmitter power at the individual terminals in the system, but can improve the outage and error rate performances, as well.

Example 2: Multi-hop transmission systems with unbalanced links

Consider a K -hop transmission system in which the k^{th} relay, $k = 1, \dots, K - 1$ is located at a distance $\frac{2k}{K(K+1)}d_0$ from its previous terminal where d_0 denotes the distance between source and destination. All systems use equal transmission power. Each terminal in a K -hop transmission system is allocated $\frac{1}{K}$ of the total transmission power. Thus, using the Friis propagation formula [94], the average link SNRs in a K -hop system are given by, $\Gamma_{k-1,k} = \frac{1}{K} \left(\frac{K(K+1)}{2k} \right)^\epsilon \Gamma_0$. Figures 3.9 and 3.10, respectively, show the outages and the bit error probabilities of this system configuration for different numbers of hops and $\epsilon = 3$. These figures again show close agreement between analytical and simulation results for multi-hop transmission systems with unbalanced links in moderate to large SNR regions. The average individual link SNRs assumed for this example also satisfy the conditions (3.29) and (3.31). Thus, as seen in Figures 3.9 and 3.10, the outage and bit error rate performances improve as the number of hops increases.

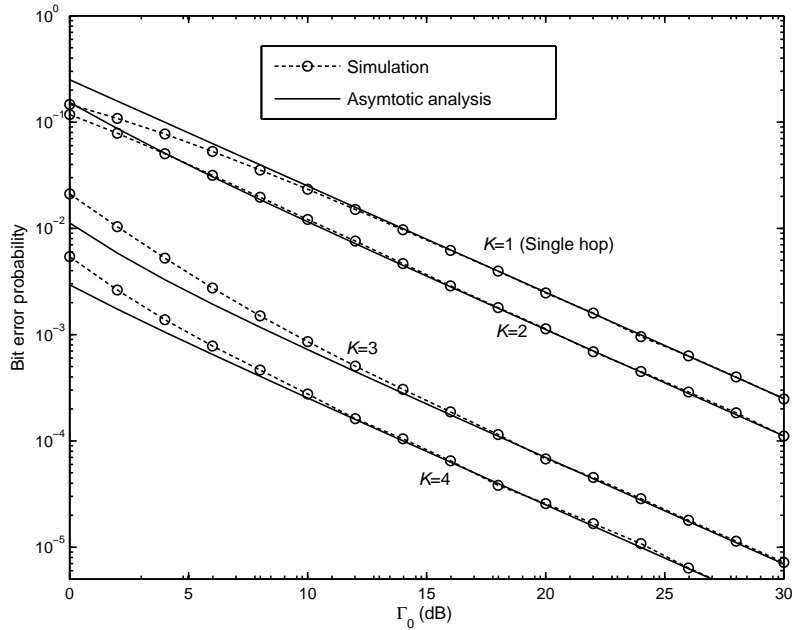


Figure 3.10. Bit error probabilities for different multi-hop transmission systems with fixed-gain relays and unbalanced links.

3.3 Capacity Analysis

Another fundamental performance metric of any wireless communication system in a fading environment is its capacity. Most previous works have examined the capacity of wireless relay networks in Gaussian channels assuming no fading. However, relayed transmission is particularly attractive in fading environments for enabling reliable communications between a source-destination pair when the direct link is subject to a deep fade. In Section 3.3.1, we evaluate the ergodic capacity in Rayleigh fading of a multi-hop transmission system with an arbitrary number of half-duplex relays employing either AF or DF relaying, assuming CSI is only known at the receiving terminals. In Section 3.3.2, we consider capacity in general fading of an AF multi-hop relaying system employing different source-adaptive transmission techniques introduced in [72], namely, optimal power and rate adaptation, optimal rate adaptation with constant power, and channel inversion with fixed rate. In such systems the source adapts its rate and/or power according to the channel variations utilizing only a feedback of the effective received SNR from the destination to the source.

3.3.1 Ergodic Capacity Without Transmitter CSI

Consider a K -hop wireless relaying system described in Section 3.1. It is assumed that CSI is only known at the receiving terminals. Thus, the total available transmitter power, P_T , is equally allocated to the transmitting terminals according to a uniform power allocation policy, i.e. $P_k = \frac{1}{K}P_T$. In addition, equal portions of the total transmission time are allocated to each transmitting terminal along the multi-hop path. Furthermore, it is assumed that only one terminal transmits in each time slot.

3.3.1.1 AF Multi-Hop Transmission Systems

The input-output relation in a K -hop transmission system with AF relaying is given by [28]

$$y_K = \alpha_{K-1,K} \prod_{i=1}^{K-1} A_i^V \alpha_{i-1,i} x_0 + \sum_{i=1}^{K-1} \prod_{k=i}^{K-1} A_k^V \alpha_{k-1,k} n_k + n_K \quad (3.32)$$

where A_i^V , $i = 1, \dots, K-1$, is given by (3.2) to ensure that the instantaneous power constraint at the i^{th} relay output is satisfied. Suppose that the transmitted signal from the source is chosen from an independent identically distributed (i.i.d.) Gaussian codebook⁶. Then, according to [71, Theorem 1], the ergodic capacity of an AF multi-hop relaying system is obtained as⁷

$$\mathcal{E}_{AF} = \frac{1}{K} \mathbb{E} \left(\log \left(1 + \gamma_t^V \right) \right) \quad (3.33)$$

where γ_t^V denotes the end-to-end received instantaneous SNR at the destination given by (3.4). Recall that a closed-form expression for the PDF of γ_t^V given in (3.4b), which facilitates the ergodic capacity analysis of an AF multi-hop relaying system, is unknown for an arbitrary number of hops. In the sequel, we first derive two upper bounds on the ergodic capacity of an AF multi-hop transmission system using Jensen's inequality and an inequality between harmonic and geometric means. Then, we obtain a precise infinite series representation for the ergodic capacity. An integral expression for the ergodic capacity in general fading of AF multi-hop systems is obtained later in Section 3.3.2.2.

- **Upper Bound Based on Jensen's Inequality:** Using Jensen's inequality [96], an upper bound on the ergodic capacity in (3.33) is obtained as

$$\mathcal{E}_{AF} \leq \frac{1}{K} \log \left(1 + \Gamma_t^V \right) \quad (3.34a)$$

⁶Note that the codeword should be long enough to capture the ergodic nature of the fading channels. This indicates that the transmission length over each time slot should be much larger than the channel coherence time [95]. This requirement implies that the ergodic capacity can be achieved for delay-tolerant applications, such as transmission of a long text document.

⁷Note that the factor $\frac{1}{K}$ is due to transmission of information over K orthogonal time slots in a K -hop system.

where $\Gamma_t^V = \mathbb{E}(\gamma_t^V)$ is the expected value of the end-to-end received SNR at the destination given by

$$\Gamma_t^V = \int_0^\infty M_{X^V}(s) ds \quad (3.34b)$$

using eq. (3.15) for an AF multi-hop system with an arbitrary number of hops where $M_{X^V}(s)$ is given by (3.5) with the individual product terms replaced by (3.6). Note that, in general, the integral in (3.34b) has no closed-form solution and it is numerically evaluated.

- **Upper Bound Based on Harmonic-Geometric Means Inequality:** According to an inequality between the harmonic mean and the geometric mean [91, eq. (3.2.1)], the received end-to-end instantaneous SNR, γ_t^V , is upper bounded as

$$\gamma_t^V \leq \gamma_g = \frac{1}{K} \prod_{k=1}^K \gamma_i^{1/K}. \quad (3.35)$$

The pdf of γ_g is given by [24]

$$f_{\gamma_g}(\gamma) = \frac{K}{\gamma} G_{0,K}^{K,0} \left((\gamma K)^K \prod_{k=1}^K \frac{1}{\Gamma_{k-1,k}} \left| \begin{array}{c} - \\ \underbrace{1, 1, \dots, 1}_K \end{array} \right. \right) \quad (3.36)$$

for independent non-identical Rayleigh fading channels where $G(\cdot)$ denotes the Meijer G-function [90, eq. (9.301)]. Since $\gamma_t^V \leq \gamma_g$, $\log(1 + \gamma_t^V) \leq \log(1 + \gamma_g)$, and therefore, the ergodic capacity of an AF multi-hop transmission system is upper bounded as

$$\begin{aligned} \mathcal{E}_{AF} &\leq \frac{1}{K} \mathbb{E}(\log(1 + \gamma_g)) \\ &= \frac{G_{K,2K}^{2K,K} \left(K^K \prod_{k=1}^K \frac{1}{\Gamma_{k-1,k}} \left| \begin{array}{c} 0, \frac{1}{K}, \frac{2}{K}, \dots, \frac{K-1}{K} \\ \underbrace{1, 1, \dots, 1}_{K-1}, \frac{K-1}{K}, \frac{K-2}{K}, \dots, \frac{1}{K}, 0, 0 \end{array} \right. \right)}{K (2\pi)^{K-1} \ln 2} \end{aligned} \quad (3.37)$$

which can be simply evaluated in MAPLE.

- **Infinite Series Representation:** A precise approach for evaluating the ergodic capacity of an AF multi-hop transmission system can be based on using the series representation of the function $\ln(1 + x)$ given by

$$\ln(1 + x) = 2 \sum_{n=1}^{\infty} \frac{1}{2n-1} \left(\frac{x}{x+2} \right)^{2n-1}, \quad \forall x > -1 \quad (3.38)$$

or

$$\ln(1+x) = \sum_{n=1}^{\infty} \frac{1}{n} \left(\frac{x}{x+1} \right)^n, \quad \forall x > -1/2 \quad (3.39)$$

from [90, eq. (1.512.2)] and [90, eq. (1.512.3)], respectively. The well known series for $\ln(1+x)$ given by [90, eq. (1.511.1)]

$$\ln(1+x) = \sum_{n=1}^{\infty} (-1)^{n+1} \frac{x^n}{n} \quad (3.40)$$

cannot be used here because its radius of convergence is not sufficiently large; in fact (3.40) requires $-1 < x < 1$ for convergence. Since the expectation in (3.33) is over values of SNR from 0 to infinity, we require an infinite series representation that converges on 0 to infinity. The series in (3.38) and (3.39) satisfy this requirement. The following Lemma establishes that the series in (3.38) converges (almost) twice as fast as the series in (3.39) to the value of the function $\ln(1+x)$.

Lemma 3.3: The series in (3.38) truncated at $n = M$ gives more accurate estimation of the function $\ln(1+x)$ than the series in (3.39) truncated at $n = 2M - 1$.

Proof: A proof of Lemma 3.3 is given in Appendix A.3.

In addition, it is shown in the following Lemma that the series in (3.38) converges uniformly over $x \geq 0$.

Lemma 3.4: The series in (3.38) is uniformly convergent for $x \geq 0$.

Proof: A proof of Lemma 3.4 is given in Appendix A.4.

This property ensures that the series whose n^{th} term is the expected value of the n^{th} term of (3.38) is convergent to $\mathbb{E}(\ln(1+x))$. Thus, utilizing the series representation of $\ln(1+\gamma_t)$ given in (3.38) and its uniform convergence property, the ergodic capacity of an AF multi-hop transmission system is obtained as

$$\mathcal{E}_{AF} = \frac{2}{K \ln 2} \sum_{n=1}^{\infty} \frac{1}{2n-1} \mathbb{E}(Z^{2n-1}) \quad (3.41a)$$

where $Z = \frac{\gamma_t^v}{\gamma_t^v + 2} = \frac{1}{2X^v + 1}$ and it can be shown that the m^{th} moment of Z is given by

$$\mathbb{E}(Z^m) = \frac{1}{(m-1)!} \int_0^{\infty} s^{m-1} \exp(-s) M_{X^v}(2s) ds \quad (3.41b)$$

where $M_{X^v}(s)$ is given by (3.5) with the individual product terms replaced by (3.6). Note that the ergodic capacity expression in (3.41a) requires only calculation of the odd moments of Z . In addition, truncating the series in (3.41a) at a certain moment of Z gives a lower bound on the ergodic capacity since all the terms in the series (3.41a) are positive.

3.3.1.2 DF Multi-Hop Transmission Systems

In a DF multi-hop transmission system, the received signal at each relay is fully decoded, re-encoded and then re-transmitted to the next terminal. Suppose that the transmitted codewords from the source and the relays are chosen from an i.i.d. Gaussian codebook. The k^{th} terminal, $k = 1, 2, \dots, K$, can then decode the codeword transmitted from the $(k - 1)^{\text{th}}$ terminal with rate R_k if

$$\begin{aligned} R_k \leq \mathcal{E}_k &= \frac{1}{K} \mathbb{E} (\log(1 + \gamma_{k-1,k})) \\ &= \frac{1}{K \ln 2} \exp\left(\frac{1}{\Gamma_{k-1,k}}\right) E_1\left(\frac{1}{\Gamma_{k-1,k}}\right) \end{aligned} \quad (3.42)$$

where \mathcal{E}_k denotes the capacity of the k^{th} link [71] in Rayleigh fading, and $E_1(\cdot)$ denotes the exponential integral function [91, eq. (5.1.1)]. Thus, the overall system achievable rate should be the minimum of the achievable rates over each individual link. On the other hand, according to the min-cut max-flow theorem [60], the overall system capacity cannot be larger than the capacity of each individual link. Therefore, the ergodic capacity in a DF multi-hop transmission system is given by

$$\mathcal{E}_{DF} = \min \{\mathcal{E}_1, \mathcal{E}_2, \dots, \mathcal{E}_K\}. \quad (3.43)$$

Note that according to Jensen's inequality [96], one has

$$\mathcal{E}_{DF} > \mathbb{E} \left(\min \left\{ \frac{1}{K} \log(1 + \gamma_{0,1}), \dots, \frac{1}{K} \log(1 + \gamma_{k-1,k}) \right\} \right) \quad (3.44)$$

which indicates that the ergodic capacity in fading of a DF multi-hop relaying system is not the average of the maximum achievable rate (mutual information) over the random fading.

3.3.1.3 Comparison Between AF and DF Multi-hop Transmission Systems

According to Jensen's inequality [96], one has

$$\begin{aligned} \mathcal{E}_{DF} &> \frac{1}{K} \mathbb{E} (\min \{\log(1 + \gamma_{0,1}), \dots, \log(1 + \gamma_{K-1,K})\}) \\ &= \frac{1}{K} \mathbb{E} (\log(1 + \min \{\gamma_{0,1}, \dots, \gamma_{K-1,K}\})). \end{aligned} \quad (3.45)$$

On the other hand, it can be readily shown that

$$X^V \geq \max \left\{ \frac{1}{\gamma_{0,1}}, \frac{1}{\gamma_{1,2}}, \dots, \frac{1}{\gamma_{K-1,K}} \right\} \quad (3.46)$$

and thus

$$\gamma_t^V \leq \min \{\gamma_{0,1}, \gamma_{1,2}, \dots, \gamma_{K-1,K}\}. \quad (3.47)$$

Therefore, combining (3.45) and (3.47), one obtains

$$\mathcal{E}_{DF} > \frac{1}{K} \mathbb{E} \left(\log(1 + \gamma_t^Y) \right) = \mathcal{E}_{AF} \quad (3.48)$$

which proves that a DF multi-hop transmission system achieves higher ergodic capacity than the corresponding AF multi-hop transmission system, regardless of the type of fading.

3.3.1.4 Results and Discussion

In this section, numerical results are presented for different multi-hop transmission operating over Rayleigh fading channels. In the numerical examples, we consider multi-hop systems with both balanced and unbalanced links, as described, respectively, in examples 1 and 2 of Section 3.2.5.1. Recall that all systems use equal total power and employ uniform power allocation policy to distribute the total available power to the source and the relays. Then, the average link SNRs in K -hop transmission systems with balanced links and unbalanced links are, respectively, given by $\Gamma_{k-1,k} = K^{\epsilon-1} \Gamma_0$ and $\Gamma_{k-1,k} = \frac{1}{K} \left(\frac{K(K+1)}{2k} \right)^\epsilon \Gamma_0$, $k = 1, \dots, K$. In the following numerical examples, we assume that $\epsilon = 4$.

Figures 3.11 and 3.12 show the ergodic capacities versus Γ_0 for different AF multi-hop transmission systems with balanced links and unbalanced links, respectively. Figures 3.11 and 3.12 indicate the tightness of the upper bound based on Jensen's inequality. For instance, the inaccuracies of this upper bound in the 4-hop transmission systems with i.i.d. (balanced) and non i.i.d. (unbalanced) links are, respectively, around 6% and 8% at 20 dB. It is also seen that the upper bound based on Jensen's inequality gets tighter than the upper bound based on the inequality between harmonic and geometric means, as the number of hops increases and especially in the non i.i.d. case. For example, the gap between these upper bounds in a 4-hop transmission system at 20 dB increases from 0.06 in the i.i.d. case to 0.43 in the non i.i.d. case. Note that the inequality in (3.35) is an equality when $\gamma_1 = \gamma_2 = \dots = \gamma_K$ [91], and thus it is expected that the upper bound given in (3.37) will be less tight in systems with unbalanced links, as seen in Figure 3.12. In addition, Figures 3.11 and 3.12 show the high accuracy of the infinite series approach for evaluation of the ergodic capacity in systems both with i.i.d. and non i.i.d. links. As shown in Figures 3.11 and 3.12, in small SNR regimes, the series in (3.41) converges fast and a small number of terms (e.g. as few as 10 terms) are enough to get high accuracy. However, by increasing SNR and the number of hops, the series in (3.41) converges more slowly, and then more terms (e.g. as many as 1000 terms for moderate values of SNR and 3500 terms for large values of SNR) are required to get acceptable accuracy.

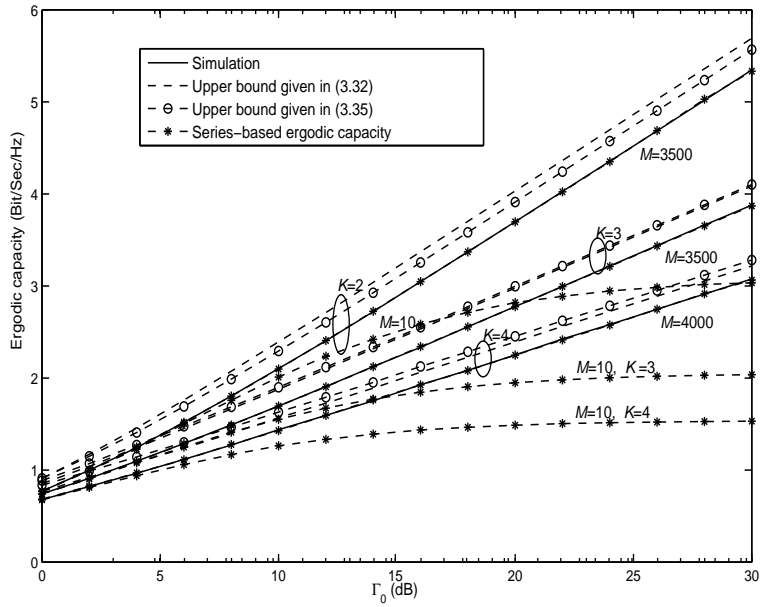


Figure 3.11. The ergodic capacities of K -hop transmission systems with balanced links employing an AF relaying scheme. M denotes the number of terms used to evaluate the series given in (3.41).

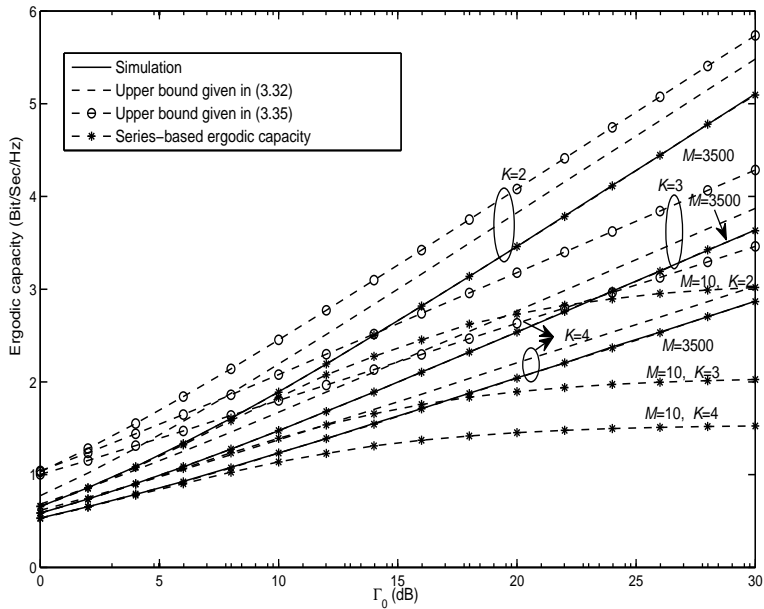


Figure 3.12. The ergodic capacities of K -hop transmission systems with unbalanced links employing an AF relaying scheme. M denotes the number of terms used to evaluate the series given in (3.41).

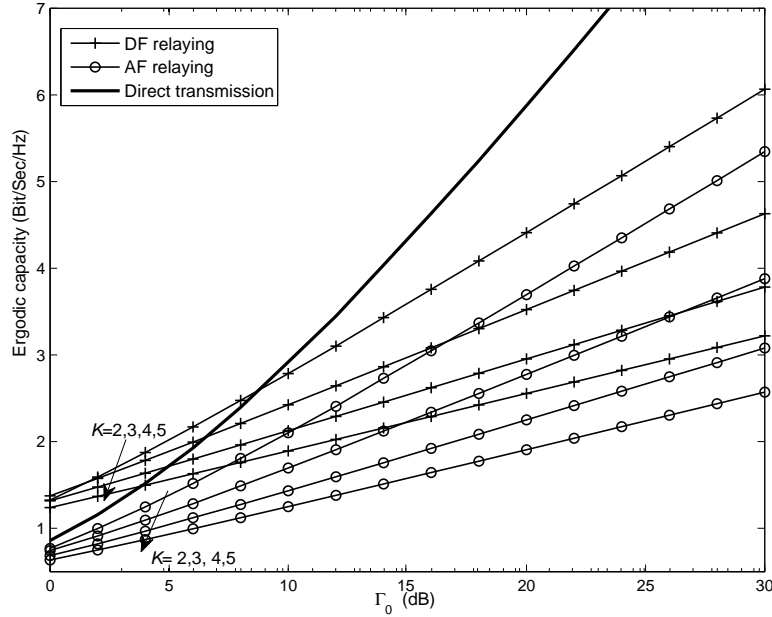


Figure 3.13. Comparison between ergodic capacities of K -hop transmission systems employing either DF relaying or AF relaying.

Figure 3.13 compares the ergodic capacities of DF and AF multi-hop transmission systems with balanced links. As shown in Section 3.3.1.3, it is seen from this figure that a DF multi-hop transmission system achieves higher ergodic capacities than the corresponding system with AF relaying. In addition, as seen in Figure 3.13, increasing the number of hops may improve ergodic capacity in small-SNR regimes, but degrades the performance for larger values of SNR. The degradation of the ergodic capacity resulting from increasing the number of hops is mainly due to the time-division channel allocation scheme considered in this thesis. However, ergodic capacity also depends on the average link SNRs and consequently the location of the relay terminals. A particular configuration of the relay terminals may outweigh the impact of the time-division channel allocation scheme and consequently contribute to the ergodic capacity. For example, Figure 3.14 shows the impact of relay location on the ergodic capacities of DF and AF dual-hop transmission systems where the relay is located at a distance d_r from the source on a straight line between the source and destination. Two cases are considered in Figure 3.14. In the first case, it is assumed that the noise powers at the relay and destination are equal and the total transmitter power is P_T , and thus, the average link SNRs over the first and the second hops are, respectively, given by $\Gamma_{0,1} = \frac{\Gamma_0}{2d_r^\alpha}$ and $\Gamma_{1,2} = \frac{\Gamma_0}{2(d_0-d_r)^\alpha}$. In the second case, it is assumed that the noise

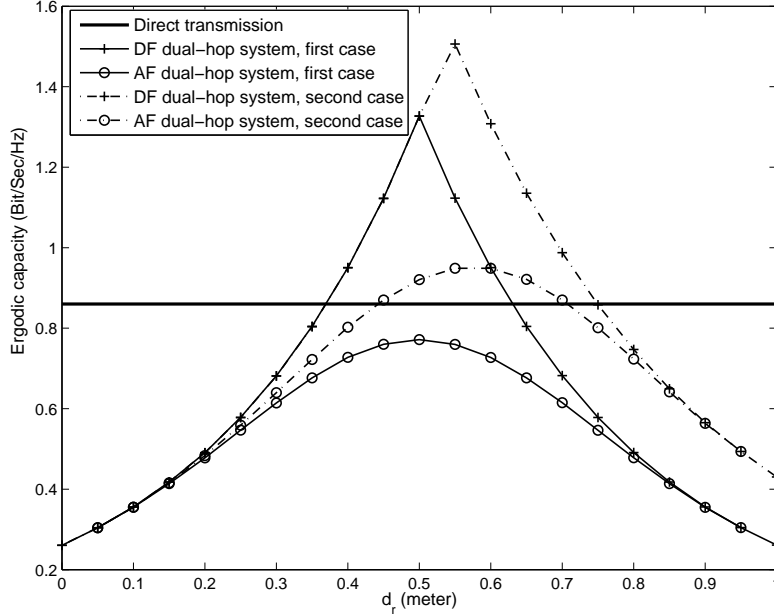


Figure 3.14. Ergodic capacities versus relay location of dual-hop transmission systems employing either DF relaying or AF relaying.

power at the destination is twice the noise power at the relay and again the total transmitter power is P_T . Thus, in this case, $\Gamma_{0,1} = \frac{\Gamma_0}{d_r^\alpha}$ and $\Gamma_{1,2} = \frac{\Gamma_0}{2(d_0 - d_r)^\alpha}$. In Figure 3.14, it is also assumed that $d_0 = 1$ meter, and $\Gamma_0 = 1$ dB. It is seen that the DF dual-hop system performs better than direct transmission when the relay is located over the range $[0.369, 0.631]$ in the first case and over the range $[0.369, 0.749]$ in second case. The AF dual-hop system performs worse than direct transmission over the entire range of d_r in the first case, but its performance is better than direct transmission in the second case when the relay is located over the range $[0.442, 0.707]$. In addition, in the first case, the optimal relay location that maximizes the ergodic capacity is at the midpoint between source and destination in both DF and AF systems. However, the optimal relay location is shifted closer to the destination in the second case, at $d_r = 0.55$ meter in the DF dual-hop system and at $d_r = 0.6$ meter in the AF dual-hop system.

3.3.2 Capacity of AF Relaying Systems Under Adaptive Transmission

In this section, we study capacity in general fading of an AF multi-hop relaying system employing different source-adaptive transmission techniques introduced in [72], namely, optimal power and rate adaptation, optimal rate adaptation with constant power, and channel inversion with fixed rate. In such systems the source adapts its rate and/or power according

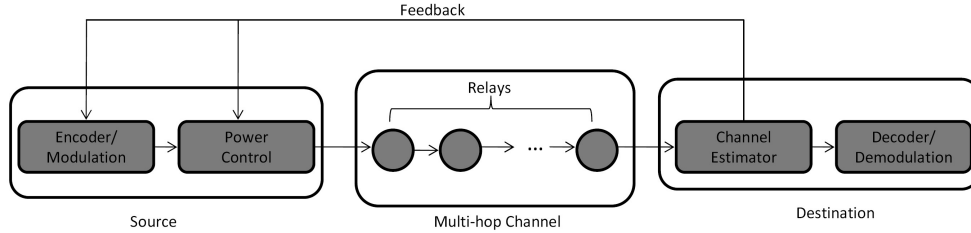


Figure 3.15. The source-adaptive multi-hop relaying system.

to the channel variations utilizing only a feedback of the effective received SNR from the destination to the source. Note that rate adaptation at the source is typically done by fixing the symbol rate and using multiple modulation schemes or changing the constellation size [73] based on the the instantaneous end-to-end received SNR that is measured at the destination and is fed back to the source.

Figure 3.15 shows a K -hop wireless system employing a source-adaptive transmission technique. All transmissions are over orthogonal time slots to ensure half-duplex operation at the relay terminals. The amplification at each relay is chosen as (3.2) to satisfy an instantaneous power constraint at the relay output.

Note that capacity analysis of a wireless communication system in fading under adaptive transmission generally involves evaluating integrals that require a closed-form expression for the PDF of the instantaneous received SNR [72]. However, as mentioned earlier, a closed-form expression for the PDF of the instantaneous received SNR for an AF multi-hop relaying system with an arbitrary number of hops is still unknown. In the following, we derive expressions for the evaluation of the capacity of an AF multi-hop relaying system under different source-adaptive transmission techniques in terms of the CHF of the reciprocal of the instantaneous received SNR.

3.3.2.1 Optimal Power and Rate Adaptation

The channel capacity given an average power constraint under optimal power and rate adaptation is given by [72, eq. (7)]

$$C_{OPR} = \frac{1}{K} \int_{\gamma_c}^{\infty} \log_2 \left(\frac{\gamma}{\gamma_c} \right) f_{\gamma_t^V}(\gamma) d\gamma \quad (3.49a)$$

where γ_c is the optimal cutoff SNR below which no data is transmitted that must satisfy [72, eq. (8)]

$$\int_{\gamma_c}^{\infty} \left(\frac{1}{\gamma_c} - \frac{1}{\gamma} \right) f_{\gamma_t^V}(\gamma) d\gamma = 1 \quad (3.49b)$$

according to the average power constraint. Since data transmission is suspended when $\gamma_t^V < \gamma_c$, there is a probability of outage (corresponding to the event of no transmission) given by

$$P_{out} = Pr(\gamma_t^V < \gamma_c) \quad (3.49c)$$

which is evaluated using (3.12) where $\gamma_{th} = \gamma_c$ and $\Psi_X(\cdot)$ is given by (3.5) with s replaced by $-jw$. Note that the capacity \mathcal{C}_{OPR} is achieved when the source adapts both its power and rate according to channel condition [72]. In this scheme, the power at the source is adapted as [73, eq. (4.12)]

$$P_{0_{OPR}} = \begin{cases} \left(\frac{1}{\gamma_c} - \frac{1}{\gamma_t^V}\right) P_0, & \gamma_t^V \geq \gamma_c \\ 0, & \gamma_t^V < \gamma_c. \end{cases} \quad (3.50)$$

In order to evaluate (3.49a) and (3.49b) for an AF multi-hop transmission system, we use the change of variable $\gamma = \frac{1}{x}$, and the Fourier-transform relation between the CHF of X , $\Psi_X(w)$, and the PDF of X , $f_X(x)$, given by [73, eq. (B.11)]

$$f_X(x) = \frac{1}{2\pi} \int_{-\infty}^{\infty} \Psi_X(w) \exp(-jwx) dw. \quad (3.51)$$

In addition, the following Lemma gives an expression for evaluation of the infinite-range integrals involved in our capacity analysis.

Lemma 3.5: Let $U(w)$ denote an arbitrary complex function having the form

$$U(w) = \Psi_X(w) \int_{a_1}^{a_2} g(x) \exp(-jwx) dx \quad (3.52)$$

where $g(x)$ denotes an arbitrary real function and the integral limits, a_1 and a_2 , can be any real numbers. Then, one has

$$\int_{-\infty}^{\infty} U(w) dw = 2 \int_0^{\infty} \Re(U(w)) dw = 2 \int_0^{\frac{\pi}{2}} \Re(U(\tan(\theta))) \sec^2(\theta) d\theta \quad (3.53)$$

where $\Re(\cdot)$ denotes the real part of its argument.

Proof: A proof of Lemma 3.5 is given in Appendix A.5.

Then, we have

$$\begin{aligned} \mathcal{C}_{OPR} &= \frac{1}{K} \int_0^{\frac{1}{\gamma_c}} \log_2 \left(\frac{1}{\gamma_c x} \right) f_{X^V}(x) dx \\ &= \frac{1}{2\pi K} \int_{-\infty}^{\infty} \Psi_{X^V}(w) \left[\int_0^{\frac{1}{\gamma_c}} \log_2 \left(\frac{1}{\gamma_c x} \right) \exp(-jwx) dx \right] dw \\ &= \frac{1}{2\pi K \ln 2} \int_{-\infty}^{\infty} \Psi_{X^V}(w) \frac{\nu + \ln(jw) - \ln(\gamma_c) + E_1 \left(\frac{jw}{\gamma_c} \right)}{jw} dw \\ &= \frac{1}{\pi K \ln 2} \int_0^{\frac{\pi}{2}} \Re \left(\frac{\Psi_{X^V}(\tan(\theta)) \frac{\nu + \ln(j \tan(\theta)) - \ln(\gamma_c) + E_1 \left(\frac{j \tan(\theta)}{\gamma_c} \right)}{j \tan(\theta)}}{\cos^2(\theta)} \right) d\theta \end{aligned} \quad (3.54a)$$

where ν is the Euler's constant [90, p. xxxii]. The average power condition in (3.49b) can be rewritten as

$$\begin{aligned}
& \int_0^{\frac{1}{\gamma_c}} \left(\frac{1}{\gamma_c} - x \right) f_{X^v}(x) dx \\
&= \frac{1}{2\pi} \int_{-\infty}^{\infty} \Psi_{X^v}(w) \left[\int_0^{\frac{1}{\gamma_c}} \left(\frac{1}{\gamma_c} - x \right) \exp(-jwx) dx \right] dw \\
&= \frac{1}{2\pi} \int_{-\infty}^{\infty} \Psi_{X^v}(w) \frac{\gamma_c - jw - \gamma_c \exp\left(-\frac{jw}{\gamma_c}\right)}{w^2 \gamma_c} dw \\
&= \frac{1}{\pi} \int_0^{\frac{\pi}{2}} \Re \left(\Psi_{X^v}(\tan(\theta)) \frac{\gamma_c - j \tan(\theta) - \gamma_c \exp\left(-\frac{j \tan(\theta)}{\gamma_c}\right)}{\tan^2(\theta) \gamma_c} \right) \sec^2(\theta) d\theta = 1 \quad (3.54b)
\end{aligned}$$

that can be numerically solved to obtain γ_c .

3.3.2.2 Optimal Rate Adaptation With Constant Transmit Power

The channel capacity under optimal rate adaptation with constant transmit power is given by [72, eq. (29)]

$$C_{ORA} = \frac{1}{K} \int_0^{\infty} \log_2(1 + \gamma) f_{\gamma_i^v}(\gamma) d\gamma \quad (3.55)$$

that, in fact, represents the capacity of the channel without adaptation [72]. Recall that this capacity was previously evaluated using upper bounds as well as an infinite-series expression in Section 3.3.1. In addition, while the transmitter in a system with a rate-adaptive technique is more complex compared to that in a fixed-rate system, the receiver has a relatively simple structure [73]. Thus, in this case, the hardware constraints in the system determine whether employment of adaptive technique is preferred or not.

For an AF multi-hop transmission system, C_{ORA} is obtained as

$$\begin{aligned}
C_{ORA} &= \frac{1}{K} \int_0^{\infty} \log_2 \left(1 + \frac{1}{x} \right) f_{X^v}(x) dx \\
&= \frac{1}{2\pi K} \int_{-\infty}^{\infty} \Psi_{X^v}(w) \left[\int_0^{\infty} \log_2 \left(1 + \frac{1}{x} \right) \exp(-jwx) dx \right] dw \\
&= \frac{1}{2\pi K \ln 2} \int_{-\infty}^{\infty} \Psi_{X^v}(w) \frac{\ln(jw) + \exp(jw)E_1(jw) + \nu}{jw} dw \\
&= \frac{1}{\pi K \ln 2} \int_0^{\frac{\pi}{2}} \Re \left(\frac{\Psi_{X^v}(\tan(\theta)) (\ln(j \tan(\theta)) + \exp(j \tan(\theta))E_1(j \tan(\theta)) + \nu)}{j \cos^2(\theta) \tan(\theta)} \right) d\theta \quad (3.56)
\end{aligned}$$

using the change of variable $\gamma = \frac{1}{x}$, and eqs. (3.51) and (3.53).

3.3.2.3 Channel Inversion With Fixed Rate

In channel inversion with the fixed rate adaptive technique, the source only adapts its power to keep a constant SNR at the destination. The channel capacity of a multi-hop relaying system employing this adaptive technique is given by [72, eq. (46)]

$$\mathcal{C}_{CIFR} = \frac{1}{K} \log_2 \left(1 + \frac{1}{\int_0^\infty \frac{1}{\gamma} f_{\gamma_t^V}(\gamma) d\gamma} \right). \quad (3.57a)$$

For example, \mathcal{C}_{CIFR} in Nakagami- m fading of an AF multi-hop transmission system is obtained as

$$\mathcal{C}_{CIFR} = \begin{cases} 0, & \text{any } m_k \leq 1 \\ \frac{1}{K} \log_2 \left(1 + \left(\sum_{k=1}^K \frac{m_k}{(m_k-1)\Gamma_{k-1,k}} \right)^{-1} \right), & \text{all } m_k > 1. \end{cases} \quad (3.57b)$$

However, since the transmitter power must compensate deep channel fades, this adaptive technique results in a large capacity loss. A modified approach, termed truncated channel inversion is proposed in [72] that halts data transmission when the received SNR is below a cutoff level β_c . The channel capacity with this modified adaptive technique is given by [72, eq. (47)]

$$\mathcal{C}_{TCIFR} = \frac{1}{K} \log_2 \left(1 + \frac{1}{\int_{\beta_c}^\infty \frac{1}{\gamma} f_{\gamma_t^V}(\gamma) d\gamma} \right) Pr(\gamma_t^V \geq \beta_c) \quad (3.58a)$$

where $Pr(\gamma_t^V \geq \beta_c)$ and $\int_{\beta_c}^\infty \frac{1}{\gamma} f_{\gamma_t^V}(\gamma) d\gamma$ for an AF multi-hop transmission system are obtained as

$$Pr(\gamma_t^V \geq \beta_c) = \frac{1}{\pi} \int_0^{\frac{\pi}{2}} \Re \left(\Psi_{X^V}(\tan(\theta)) \frac{1 - \exp\left(-\frac{j \tan(\theta)}{\beta_c}\right)}{j \tan(\theta)} \right) \sec^2(\theta) d\theta \quad (3.58b)$$

using (3.12), and

$$\begin{aligned} \int_{\beta_c}^\infty \frac{1}{\gamma} f_{\gamma_t^V}(\gamma) d\gamma &= \int_0^{\frac{1}{\beta_c}} x f_{X^V}(x) dx \\ &= \frac{1}{2\pi} \int_{-\infty}^\infty \Psi_{X^V}(w) \left[\int_0^{\frac{1}{\beta_c}} x \exp(-jwx) dx \right] dw \\ &= \frac{1}{2\pi} \int_{-\infty}^\infty \Psi_{X^V}(w) \frac{(jw + \beta_c) \exp\left(-\frac{jw}{\beta_c}\right) - \beta_c}{\beta_c w^2} dw \\ &= \frac{1}{\pi} \int_0^{\frac{\pi}{2}} \Re \left(\Psi_{X^V}(\tan(\theta)) \frac{(j \tan(\theta) + \beta_c) \exp\left(-\frac{j \tan(\theta)}{\beta_c}\right) - \beta_c}{\beta_c \sin^2(\theta)} \right) d\theta \end{aligned} \quad (3.58c)$$

in which we have used the change of variable $\gamma = \frac{1}{x}$, and eqs. (3.51) and (3.53). The cutoff level β_c can be chosen such that either a certain probability of outage is achieved

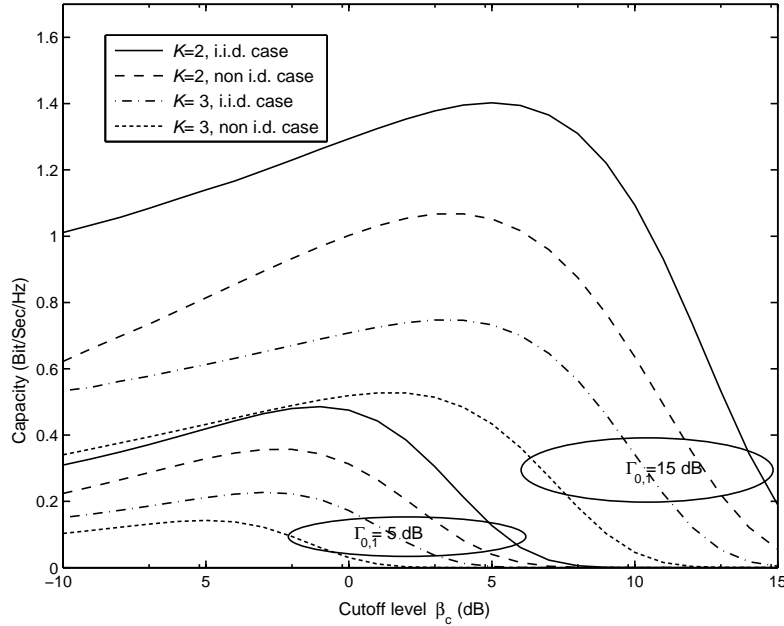


Figure 3.16. Channel capacity versus β_c of different multi-hop transmission systems employing the truncated channel inversion adaptive technique.

or the channel capacity (3.58a) is maximized. Figure 3.16 shows the channel capacities, \mathcal{C}_{TCIFR} , versus β_c of different multi-hop transmission systems. In Figure 3.16, we assume Nakagami- m fading where $m_k = 1$ and $\Gamma_{k-1,k} = \Gamma_{0,1}$ for the case of i.i.d. links, and $m_k = \frac{k}{2}$ and $\Gamma_{k-1,k} = \frac{1}{k}\Gamma_{0,1}$, $k = 1, \dots, K$ for the case of non i.i.d. links. It is seen that there is a cutoff level at which \mathcal{C}_{TCIFR} is maximized. This maximizing cutoff level can be numerically obtained by solving $\partial\mathcal{C}_{TCIFR}/\partial\beta_c = 0$, which is equivalent to solving

$$\frac{Pr(\gamma_t^V \geq \beta_c)}{\beta_c \int_{\beta_c}^{\infty} \frac{1}{\gamma} f_{\gamma_t^V}(\gamma) d\gamma \left(1 + \int_{\beta_c}^{\infty} \frac{1}{\gamma} f_{\gamma_t^V}(\gamma) d\gamma\right)} - \ln \left(1 + \left(\int_{\beta_c}^{\infty} \frac{1}{\gamma} f_{\gamma_t^V}(\gamma) d\gamma\right)^{-1}\right) = 0 \quad (3.59)$$

where $Pr(\gamma_t^V \geq \beta_c)$ and $\int_{\beta_c}^{\infty} \frac{1}{\gamma} f_{\gamma_t^V}(\gamma) d\gamma$ are, respectively, replaced by (3.12) and (3.58c).

Note that the power at the source employing this technique is adapted as [73, eq. (4.19)]

$$P_{0TCIFR} = \begin{cases} \frac{P_0}{\gamma_t^V \int_{\beta_c}^{\infty} \frac{1}{\gamma} f_{\gamma_t^V}(\gamma) d\gamma}, & \gamma_t^V \geq \beta_c \\ 0, & \gamma_t^V < \beta_c \end{cases} \quad (3.60)$$

where $\int_{\beta_c}^{\infty} \frac{1}{\gamma} f_{\gamma_t^V}(\gamma) d\gamma$ is given in (3.58c).

3.3.2.4 Numerical Results and Discussion

In this section, we present some numerical examples for the capacity and outage probability of AF multi-hop relaying systems employing source-adaptive transmission techniques. We

Table 3.5. Values of γ_c and β_c for different multi-hop systems with i.i.d. links where $\Gamma_{k-1,k} = \Gamma_{0,1}$ and $m_k = 1, k = 1, \dots, K$

$\Gamma_{0,1}$ (dB)	$\gamma_c _{K=2}$	$\beta_c _{K=2}$	$\gamma_c _{K=3}$	$\beta_c _{K=3}$
0	0.23705	0.3667	0.16648	0.23500
5	0.41485	0.7779	0.31743	0.5196
10	0.62161	1.5825	0.52144	1.0885
15	0.7975	3.182	0.72395	2.2101
20	0.90775	6.59	0.8677	4.526

Table 3.6. Values of γ_c and β_c for different multi-hop systems with non i.d. links where $\Gamma_{k-1,k} = \frac{1}{k}\Gamma_{0,1}$ and $m_k = \frac{k}{2}, k = 1, \dots, K$

$\Gamma_{0,1}$ (dB)	$\gamma_c _{K=2}$	$\beta_c _{K=2}$	$\gamma_c _{K=3}$	$\beta_c _{K=3}$
0	0.17486	0.2699	0.104276	0.13947
5	0.31162	0.5701	0.21224	0.31799
10	0.48615	1.1505	0.37947	0.6847
15	0.66105	2.271	0.57865	1.4068
20	0.79885	4.525	0.75285	2.8443

consider dual-hop and triple-hop transmission systems in Nakagami- m fading both with i.i.d. links where $m_k = 1$ and $\Gamma_{k-1,k} = \Gamma_{0,1}$, and with non i.d. links where $m_k = \frac{k}{2}$ and $\Gamma_{k-1,k} = \frac{1}{k}\Gamma_{0,1}, k = 1, \dots, K$. Recall that the data transmission in systems under optimal rate and power adaptation and truncated channel inversion with fixed rate is suspended when the received SNR is below the cut-off levels γ_c and β_c , respectively. The optimal cutoff level γ_c and the maximizing cutoff level β_c are numerically obtained using (3.54b) and (3.59), respectively. Tables 3.5 and 3.6 show values for the cutoff levels γ_c and β_c for different multi-hop systems with i.i.d. and non i.d. links, respectively.

Figures 3.17 and 3.18 show channel capacities and of outage probabilities of different source-adaptive multi-hop relaying systems, respectively. In Figure 3.17, the exact expressions for the channel capacity derived in (3.54), (3.56), and (3.58) are plotted as well as Monte Carlo simulation results. The outage probabilities shown in Figure 3.18 denote the probabilities of no data transmissions in systems under optimal rate and power adaptation and truncated channel inversion techniques given by $Pr(\gamma_t^V < \gamma_c)$ and $Pr(\gamma_t^V < \beta_c)$, respectively. In Figure 3.18, we have plotted theoretical outage probabilities obtained using

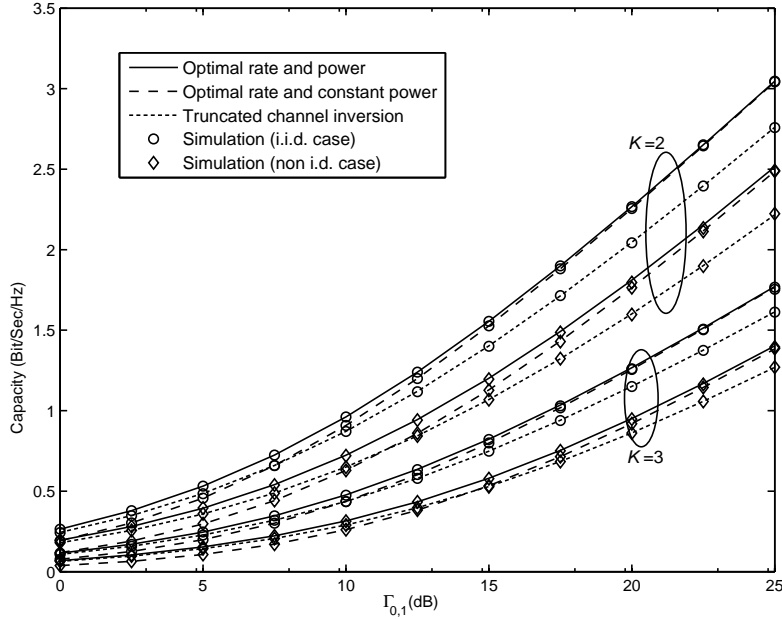


Figure 3.17. Channel capacity of various multi-hop transmission systems employing different adaptation policies.

(3.12) along with results obtained from Monte Carlo simulation. It is clearly seen from Figures 3.17 and 3.18 that the theoretical results exactly match the simulation results.

It is seen from Figure 3.17 that the optimal power and rate adaptation technique achieves the best performance compared to the other adaptive techniques, as expected. However, as seen from Figure 3.17, the gap between the capacities of optimal rate and power adaptive technique, and rate adaptation with constant power diminishes with increasing SNR. This is due to the fact the optimal rate and power adaptive technique allocates more power to the source for good channel conditions (see eq. (3.50)). That is, the source is very likely to transmit with a constant power (almost P_0) in large SNR regimes. Thus, at large values of SNR, the optimal rate and power adaptation yields a slightly small increase in capacity over the rate adaptation technique with constant power, as seen in Figure 3.17. In addition, note that since the optimal rate adaptation with constant power only adapts its rate, it has less complexity than the optimal rate and power adaptive technique.

In addition, as seen in Tables 3.5 and 3.6, γ_c is within the range $[0, 1]$, whereas $\beta_c > \gamma_c$ and can be greater than 1 (also see Figure 3.16). This implies that a system with the optimal rate and power adaptation achieves higher capacity and better probability of outage than a system with the truncated channel inversion, as seen in Figures 3.17 and 3.18. It is

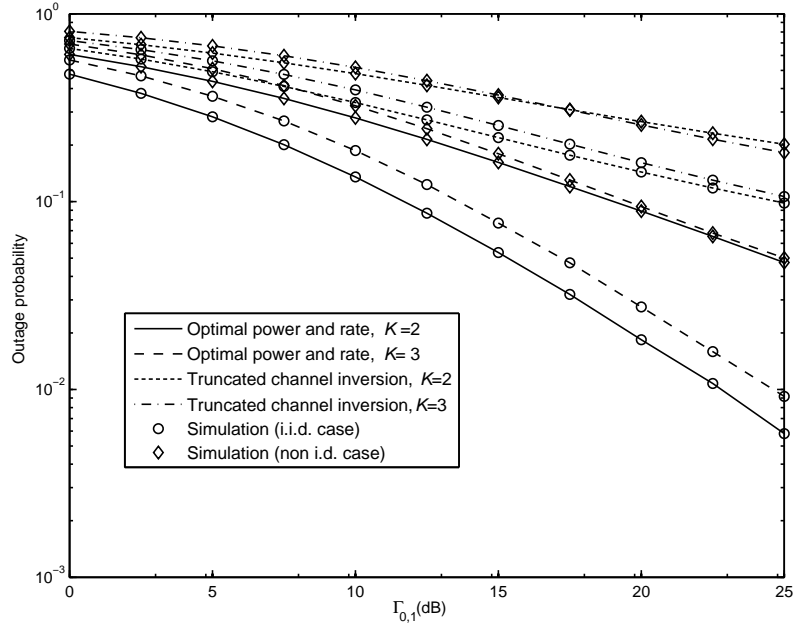


Figure 3.18. Outage probability of different multi-hop transmission systems employing either optimal power and rate adaptation or the truncated channel inversion adaptive scheme.

also seen from Figure 3.17 that the truncated channel inversion with fixed rate adaptive technique outperforms the rate adaptation technique with constant power at small values of SNR. In addition, the channel inversion with fixed rate adaptive technique is the least complex scheme because the source only adjusts its power. However, recall that the data transmission is suspended in the truncated channel inversion with fixed rate technique when the received SNR is below a cut-off level, β_c . This cut-off level is determined such that the capacity in eq. (3.58a) is maximized (e.g. see Figure 3.16). However, this maximization in the capacity is at the cost of increased probability of outage, as seen in Figure 3.18.

Chapter 4

Optimal Power Allocation for AF Multi-Hop Relaying Systems

Relayed transmission has been proposed as a viable option to improve reliability and to extend wireless network coverage. On the other hand, emerging wireless applications, e.g. sensor networks, give an increasing demand for small devices having limited battery lifetimes. As mentioned in Section 2.3.3, optimal power allocation schemes have been developed for a variety of cooperative system configurations (e.g. see [31], [44]–[53], [55]–[58]). However, there is no optimal power allocation scheme obtained for AF multi-hop relaying systems with an arbitrary number of hops. In this section, we obtain optimal power allocation schemes that maximize the instantaneous received SNR in an AF multi-hop transmission system for two kinds of power constraints, namely, the short-term (ST) and long-term (LT) power constraints. We then derive expressions for evaluation of the outage probabilities in Rayleigh fading of AF multi-hop transmission systems employing the proposed optimal power allocation schemes. The asymptotic outage probabilities of the power-optimized AF multi-hop transmission systems are also obtained.

4.1 System Model and Problem Formulation

Consider an AF K -hop wireless transmission system in which a source terminal communicates with a destination terminal via $K - 1$ relay terminals over orthogonal time slots. Each relay amplifies the signal received from its immediate preceding terminal and then forwards to the next terminal in the next time slot. The amplification gain at the k^{th} relay

A version of this chapter has been accepted for publication in IEEE Transactions on Wireless Communications.

is adapted based on the instantaneous fading amplitude over the channel between terminals T_{k-1} and T_k , α_k , to result in a power P_k at the relay output and hence is given by (3.2).

It is assumed that the total available power is P_T . In a K -hop transmission system with uniform power allocation scheme, equal portions of the total power P_T are assigned to each transmitting terminal, i.e. $P_k = P = \frac{1}{K}P_T$, $k = 0, \dots, K-1$. In general, the allocated power to the k^{th} terminal, P_k , in a K -hop transmission system can be written as

$$P_k = \beta_k P \quad (4.1a)$$

where $\beta_k \geq 0$, and either

$$\sum_{k=0}^{K-1} \beta_k = K, \text{ Short-term power constraint} \quad (4.1b)$$

or

$$\mathbb{E} \left(\sum_{k=0}^{K-1} \beta_k \right) = K, \text{ Long-term power constraint} \quad (4.1c)$$

where the expectation is taken over fading gains. Our goal is to find coefficients β_k such that the instantaneous received SNR, γ_t^V , in an AF multi-hop transmission system is maximized.

4.2 Optimal Power Allocation Under ST Power Constraint

4.2.1 Mechanism

The optimal power allocation problem under ST power constraint can be formulated as

$$\begin{aligned} \max \quad & \gamma_t^V \\ \text{subject to} \quad & \sum_{k=0}^{K-1} \beta_k = K \end{aligned} \quad (4.2a)$$

where γ_t^V is given in (3.4a) and can be rewritten as

$$\gamma_t^V = \left(\prod_{k=1}^K \left(1 + \frac{1}{\beta_{k-1} \gamma_k} \right) - 1 \right)^{-1} \quad (4.2b)$$

where $\gamma_k \triangleq \frac{P}{N_0} |\alpha_{k-1,k}|^2$. Note that since the objective function in (4.2a) is concave and the constraint is linear, the optimization problem in (4.2a) is a convex problem and hence has a unique optimal solution [97].

Using the Lagrange multiplier method [97], one has

$$L = \left(\prod_{k=1}^K \left(1 + \frac{1}{\beta_{k-1} \gamma_k} \right) - 1 \right)^{-1} - \lambda \left(\sum_{k=0}^{K-1} \beta_k - K \right) \quad (4.3)$$

where L is the Lagrangean function and λ is a Lagrange multiplier. Then, taking the derivative of L with respect to β_k , $k = 0, 1, \dots, K - 1$, yields a relation between β_k and β_j , $k \neq j$, as

$$\beta_k^2 \gamma_{k+1} \left(1 + \frac{1}{\beta_k \gamma_{k+1}} \right) = \beta_j^2 \gamma_{j+1} \left(1 + \frac{1}{\beta_j \gamma_{j+1}} \right) \quad (4.4)$$

and thus

$$\beta_j = \frac{-1 + \sqrt{1 + 4\gamma_{j+1}\beta_k(\beta_k\gamma_{k+1} + 1)}}{2\gamma_{j+1}}. \quad (4.5)$$

Using the equity constraint in (4.2a), β_k , $k = 0, \dots, K - 1$, is the real positive solution (less than K) of

$$\beta_k \left(1 + \sum_{\substack{j=0 \\ j \neq k}}^{K-1} \frac{-1 + \sqrt{1 + 4\gamma_{j+1}\beta_k(\beta_k\gamma_{k+1} + 1)}}{2\gamma_{j+1}} \right) = K. \quad (4.6)$$

In principle, (4.6) can be solved numerically. Note that the obtained coefficients, β_k , $k = 0, \dots, K - 1$, depend on the global knowledge of the instantaneous SNR over each hop and thus can be implemented in a centralized manner. The destination collects the channel amplitudes over each link and consequently γ_k , solves the corresponding equation according to (4.6) to obtain the optimal coefficients β_k , calculates the optimal power values $P_k = \beta_k P$, and then assigns them to the corresponding terminals along the multi-hop path through feedback channels. Thus, the proposed power-optimized multi-hop transmission system is especially applicable for the uplink of a cellular network.

It should be mentioned that the ST power constraint in (4.1b) imposes a maximum power constraint P_T for each individual terminal [98]. In this thesis, we assume that each transmitting terminal along the multi-hop path is able to provide the maximum power P_T . Since $\beta_k \geq 0$, $k = 0, \dots, K - 1$, and their sum is equal to K , the obtained optimal power coefficients β_k are less than (at most equal to) K . This ensures that the optimum allocated power to each terminal does not exceed the maximum allowed power P_T .

4.2.2 Outage Probability Analysis

In this section, the outage probability in Rayleigh fading of the proposed power-optimized AF multi-hop transmission system under ST power constraint is evaluated. As mentioned earlier, the outage probability is defined as the probability that the instantaneous received SNR falls below a certain threshold, γ_{th} . However, note that the coefficients β_k , $k = 0, \dots, K - 1$, for K -hop transmission systems that are the solution of eq. (4.6) may not

be known in closed-form in general. Hence, finding a closed-form expression for the instantaneous received SNR in a power-optimized multi-hop transmission system under ST power constraint becomes mathematically very involved, if not impossible, even for the simple case of $K = 2$. This makes the evaluation of the outage probability theoretically intractable. On the other hand, as shown in [28], the instantaneous received SNR in (4.2b) can be well approximated as

$$\gamma_t^V \cong \left(\sum_{k=1}^K \frac{1}{\beta_{k-1}\gamma_k} \right)^{-1} \quad (4.7)$$

especially for sufficiently large values of SNR. In this case, the Lagrangean function is given by

$$L = \left(\sum_{k=0}^{K-1} \frac{1}{\beta_k \gamma_{k+1}} \right)^{-1} - \lambda \left(\sum_{k=0}^{K-1} \beta_k - K \right). \quad (4.8)$$

Then, taking the derivative of L with respect to β_k , $k = 0, 1, \dots, K-1$, and solving the obtained set of equations as well as eq. (4.1b) yields a closed-form solution for the power coefficients under ST power constraint, β_k^{ST} , as

$$\beta_k^{ST} = \frac{K}{\sqrt{\gamma_{k+1}} \sum_{j=0}^{K-1} \frac{1}{\sqrt{\gamma_{j+1}}}}. \quad (4.9)$$

Therefore, the instantaneous received SNR in a power-optimized AF multi-hop relaying system under ST power constraint is obtained as

$$\gamma_t^{ST} \cong K \left(\sum_{k=1}^K \frac{1}{\sqrt{\gamma_k}} \right)^{-2} \quad (4.10)$$

where γ_k has an exponential distribution with average $\Gamma_k = \frac{P}{N_0} \Omega_{k-1,k}$ in Rayleigh fading.

For the special case of a power-optimized AF dual-hop transmission system, the outage probability is obtained as

$$\begin{aligned} P_{out_{2-hop}}^{ST} &= Pr \left(2 \left(\frac{1}{\sqrt{\gamma_1}} + \frac{1}{\sqrt{\gamma_2}} \right)^{-2} \leq \gamma_{th} \right) \\ &= \int_0^\infty Pr \left(\frac{1}{\sqrt{\gamma_1}} + \frac{1}{\sqrt{\gamma_2}} \geq \sqrt{\frac{2}{\gamma_{th}}} \mid \gamma_2 \right) f(\gamma_2) d\gamma_2 \\ &= \int_0^\infty Pr \left(\gamma_1 \leq \left(\sqrt{\frac{2}{\gamma_{th}}} - \sqrt{\frac{1}{\gamma_2}} \right)^{-2} \mid \gamma_2 \right) f(\gamma_2) d\gamma_2 \\ &= 1 - \int_{\frac{\gamma_{th}}{2}}^\infty \frac{1}{\Gamma_2} \exp \left(-\frac{\gamma_2}{\Gamma_2} - \frac{1}{\Gamma_1 \left(\sqrt{\frac{2}{\gamma_{th}}} - \sqrt{\frac{1}{\gamma_2}} \right)^2} \right) d\gamma_2 \end{aligned} \quad (4.11)$$

that can be simply evaluated in MAPLE. In general, the outage probability of a power-optimized AF multi-hop transmission system under ST power constraint with an arbitrary number of hops is obtained as

$$\begin{aligned} P_{out}^{ST} &= Pr\left(\gamma_t^{ST} \leq \gamma_{th}\right) = Pr\left(Y \geq \sqrt{\frac{K}{\gamma_{th}}}\right) \\ &= 1 - F_Y\left(\sqrt{\frac{K}{\gamma_{th}}}\right) \end{aligned} \quad (4.12a)$$

where $Y \triangleq \sum_{k=1}^K \frac{1}{\sqrt{\gamma_k}}$ and $F_Y(\cdot)$ denotes the CDF of Y . Since Y is the sum of K independent random variables, the CDF of Y can be found using the PDF or CHF of Y . The PDF of Y is the convolution of the PDF of its summands and sometimes finding a closed-form expression for the PDF is very involved or intractable. On the other hand, the CHF of Y , $\Psi_Y(\omega)$, is obtained as

$$\Psi_Y(w) = \prod_{k=1}^K \Psi_{\frac{1}{\sqrt{\gamma_k}}}(w) = \prod_{k=1}^K \frac{1}{\sqrt{\pi}} G_{0,3}^{3,0} \left(\frac{-w^2}{4\Gamma_k} \middle| \begin{matrix} - \\ 1, \frac{1}{2}, 0 \end{matrix} \right). \quad (4.12b)$$

Then, the CDF of Y is given by

$$F_Y(y) = \frac{1}{2} + 2 \int_0^{\frac{\pi}{2}} \Re \left(\frac{\exp(-jy \tan(\theta)) \Psi_Y(\tan(\theta))}{2\pi j \tan(\theta)} \right) \sec^2(\theta) d\theta \quad (4.12c)$$

using (3.12). However, a closed-form solution for the integral in (4.12c) is unknown. In addition, numerical evaluation of an integral involving the product of a number of Meijer G-functions (K product terms in a K -hop system) is very involved, if not impossible. Thus, we utilize the infinite series approach presented in [74] for evaluating the CDF of Y . Then, we have

$$F_Y(y) \Big|_{y=\sqrt{\frac{K}{\gamma_{th}}}} = \frac{1}{2} - \sum_{\substack{n=1 \\ n \text{ odd}}}^{\infty} \frac{2\Im \left(\exp\left(-\frac{jn\omega_0\sqrt{K}}{\sqrt{\gamma_{th}}}\right) \Psi_Y(n\omega_0) \right)}{n\pi} \quad (4.12d)$$

where $\Im(\cdot)$ denotes the imaginary part of its argument and ω_0 is a parameter that controls accuracy [74].

4.2.3 Asymptotic Outage Probability Behavior

The following Lemma gives an expression for the asymptotic outage probability of a power-optimized AF multi-hop transmission system under ST power constraint for large values of SNR.

Lemma 4.1: The asymptotic outage probability for sufficiently large values of SNR in Rayleigh fading of a power-optimized AF K -hop transmission system under ST power

constraint is given by

$$P_{out}^{ST} \rightarrow \frac{\gamma_{th}}{K} \sum_{k=1}^K \frac{1}{\Gamma_k}. \quad (4.13)$$

Proof: A proof of Lemma 4.1 is given in Appendix A.6.

Note that the asymptotic outage probability of an AF K -hop transmission system employing uniform power allocation scheme is given by

$$P_{out_{uniform}} \rightarrow \gamma_{th} \sum_{k=1}^K \frac{1}{\Gamma_k} \quad (4.14)$$

using eqs. (3.21) and (3.24) in Rayleigh fading. Comparing (4.14) with (4.13) shows that for sufficiently large values of SNR, a power-optimized AF K -hop transmission system under ST power constraint offers K times better outage performance than the corresponding system employing uniform power allocation.

4.2.4 Average Optimal Per-Hop Power Portion

In a multi-hop transmission system with i.i.d. links, the average per-hop power portions are the same (due to symmetry). Since the total power portions is K (see eq. (4.1b)), the average power portions per hop is equal to 1, i.e. $\mathbb{E}(P_k) = P$. In the sequel, we obtain the average power portions utilized at each hop, $\mathbb{E}(\beta_k)$, $k = 0, 1, \dots, K-1$, in multi-hop transmission systems with non i.i.d. links. For the special case of a dual-hop system, the average power portions utilized per hop is obtained as

$$\mathbb{E}(\beta_k) = \mathbb{E} \left(\frac{2}{1 + \sqrt{\frac{\gamma_{k+1}}{\gamma_{j+1}}}} \right) = \frac{2}{\pi} G_{3,3}^{3,3} \left(\frac{\Gamma_{j+1}}{\Gamma_{k+1}} \middle| \begin{matrix} 0, \frac{1}{2}, 1 \\ 1, 1, \frac{1}{2} \end{matrix} \right) \quad j, k \in \{0, 1\}, j \neq k. \quad (4.15)$$

In general, the average power portions per hop in a multi-hop transmission system with K number of hops can be obtained as

$$\mathbb{E}(\beta_k) = \int_0^\infty M_{\frac{1}{\beta_k}}(s) ds \quad (4.16a)$$

using eq. (3.15) where $M_{\frac{1}{\beta_k}}(s)$ denotes the MGF of $\frac{1}{\beta_k}$. Let $Z_k \triangleq \sqrt{\gamma_{k+1}} \sum_{j=0}^{K-1} \frac{1}{\sqrt{\gamma_{j+1}}}$. Then, $\frac{1}{\beta_k} = \frac{1}{K} (Z_k + 1)$ and its MGF, $M_{\frac{1}{\beta_k}}(s)$, is given by

$$M_{\frac{1}{\beta_k}}(s) = \exp \left(-\frac{s}{K} \right) M_{Z_k} \left(\frac{s}{K} \right) \quad (4.16b)$$

where

$$M_{Z_k}(s) = \int_0^\infty \prod_{j=0}^{K-1} \frac{1}{\sqrt{\pi}} G_{0,3}^{3,0} \left(\frac{\gamma_{k+1} s^2}{4\Gamma_{j+1}} \middle| \begin{matrix} - \\ 1, \frac{1}{2}, 0 \end{matrix} \right) \frac{\exp \left(-\frac{\gamma_{k+1}}{\Gamma_{k+1}} \right)}{\Gamma_{k+1}} d\gamma_{k+1} \quad (4.16c)$$

using (4.12b). Note that (4.16c) has no closed-form solution, and hence exact calculation of the average power portion given in (4.16a) requires numerical evaluation of a double integral. However, as mentioned earlier, numerical evaluation of an integral involving the product of a number of Meijer G-function ($K - 1$ product terms in a K -hop system) is very involved, if not impossible. On the other hand, the integral in (4.16c) can be efficiently computed using numerical integration method given in [91] as

$$M_{Z_k}(s) \approx \sum_{m=1}^{N_p} \xi_m \prod_{j=0}^{K-1} \frac{1}{\sqrt{\pi}} G_{0,3}^{3,0} \left(\frac{\zeta_m \Gamma_{k+1} s^2}{4\Gamma_{j+1}} \middle| \begin{matrix} - \\ 1, \frac{1}{2}, 0 \end{matrix} \right) \quad (4.17)$$

where ξ_n and ζ_n , $n = 1, \dots, N_p$, are the weights and zeros of the Laguerre polynomial of order N_p [91, Table 25.9], respectively. Then, the average power portion per each hop can be similarly evaluated as

$$\begin{aligned} \mathbb{E}(\beta_k) &= K \int_0^\infty \exp(-s) M_{Z_k}(s) ds \\ &\approx K \sum_{n=1}^{N_p} \xi_n M_{Z_k}(\zeta_n) \end{aligned} \quad (4.18)$$

where $M_{Z_k}(\cdot)$ is calculated using (4.17).

4.2.5 Impact of Individual Per-Hop Power Constraints

In this thesis, we assume that each terminal is able to provide the maximum power P_T in order to determine the best possible performance achievable in AF multi-hop systems under the total ST power constraint (4.1b). However, each terminal may be subject to a maximum power constraint as $P_k \leq P_{\max} = \tilde{\beta}_{\max} P$, where $P < P_{\max} < P_T$ [47]. Since these individual per-hop power constraints are linear, they do not change the convex property of the optimization problem in (4.2a). Therefore, the optimal power coefficients can be first obtained by solving (4.6) neglecting the individual per-hop power constraints. Let set \mathbb{C}_v denote a set of terminals whose optimal power coefficients obtained from (4.6) violate the maximum per terminal power constraint, i.e. $\beta_k > \tilde{\beta}_{\max}$, $\forall T_k \in \mathbb{C}_v$. The allocated power for these violating terminals can be clipped to the maximum allowed power, i.e. $P_k = P_{\max}$, $\forall T_k \in \mathbb{C}_v$. Clipping the power means that the individual power constraints corresponding to the violating terminals are satisfied with equity. Then re-optimization will be done over the set of remaining terminals $T_k \notin \mathbb{C}_v$ with the modified ST constraint as $\sum_{T_k \notin \mathbb{C}_v} \beta_k = K - N_{\mathbb{C}_v} \tilde{\beta}_{\max}$ where $N_{\mathbb{C}_v}$ denotes the cardinality of set \mathbb{C}_v .

Since \mathbb{C}_v is a random set, the outage probability can be evaluated using the theorem of total probability by averaging the conditional outage probability given \mathbb{C}_v over all possible

cases for \mathbb{C}_v . For instance, for an AF dual-hop system, there are three different cases for the set \mathbb{C}_v as

$$\begin{aligned}\mathbb{C}_{v_1} &= \{\}, \beta_0 \leq \tilde{\beta}_{\max}, \beta_1 \leq \tilde{\beta}_{\max} \\ \mathbb{C}_{v_2} &= \{T_0\}, \beta_0 > \tilde{\beta}_{\max}, \beta_1 \leq \tilde{\beta}_{\max} \\ \mathbb{C}_{v_3} &= \{T_1\}, \beta_0 \leq \tilde{\beta}_{\max}, \beta_1 > \tilde{\beta}_{\max}\end{aligned}\quad (4.19)$$

where β_0 and β_1 are given by using (4.9) with $K = 2$. Note that since $\beta_0 + \beta_1 = 2$ and $P_{\max} > P$ (i.e. $\tilde{\beta}_{\max} > 1$), β_0 and β_1 cannot be greater than $\tilde{\beta}_{\max}$ at the same time. The instantaneous received SNR at the destination corresponding to each set is given by

$$\begin{aligned}\gamma_{t_1} &= \gamma_t^{ST} \\ \gamma_{t_2} &= \left(\frac{1}{\tilde{\beta}_{\max}\gamma_1} + \frac{1}{(2 - \tilde{\beta}_{\max})\gamma_2} \right)^{-1} \\ \gamma_{t_3} &= \left(\frac{1}{(2 - \tilde{\beta}_{\max})\gamma_1} + \frac{1}{\tilde{\beta}_{\max}\gamma_2} \right)^{-1}.\end{aligned}\quad (4.20)$$

The outage probability is then obtained as

$$P_{out} = \sum_{i=1}^3 Pr(\gamma_{t_i} \leq \gamma_{th}) Pr(\mathbb{C}_{v_i}) \quad (4.21a)$$

where $Pr(\gamma_{t_1} \leq \gamma_{th})$ is given by (4.11), $Pr(\gamma_{t_2} \leq \gamma_{th})$ is given by [19, eq. (27)] where Γ_1 and Γ_2 are replaced by $\tilde{\beta}_{\max}\Gamma_1$ and $(2 - \tilde{\beta}_{\max})\Gamma_2$, and similarly $Pr(\gamma_{t_3} \leq \gamma_{th})$ is given by [19, eq. (27)] where Γ_1 and Γ_2 are replaced by $(2 - \tilde{\beta}_{\max})\Gamma_1$ and $\tilde{\beta}_{\max}\Gamma_2$, respectively. The probability of each case for set \mathbb{C}_v is given by

$$\begin{aligned}Pr(\mathbb{C}_{v_1}) &= Pr(\beta_0 \leq \tilde{\beta}_{\max}, \beta_1 \leq \tilde{\beta}_{\max}) \\ &= Pr(2 - \tilde{\beta}_{\max} \leq \beta_0 \leq \tilde{\beta}_{\max}) = F_{\beta_0}(\tilde{\beta}_{\max}) - F_{\beta_0}(2 - \tilde{\beta}_{\max})\end{aligned}\quad (4.21b)$$

$$\begin{aligned}Pr(\mathbb{C}_{v_2}) &= Pr(\beta_0 > \tilde{\beta}_{\max}, \beta_1 \leq \tilde{\beta}_{\max}) \\ &= Pr(\beta_0 > \tilde{\beta}_{\max}) = 1 - F_{\beta_0}(\tilde{\beta}_{\max})\end{aligned}\quad (4.21c)$$

$$\begin{aligned}Pr(\mathbb{C}_{v_3}) &= Pr(\beta_0 \leq \tilde{\beta}_{\max}, \beta_1 > \tilde{\beta}_{\max}) \\ &= Pr(\beta_0 < 2 - \tilde{\beta}_{\max}) = F_{\beta_0}(2 - \tilde{\beta}_{\max})\end{aligned}\quad (4.21d)$$

where $F_{\beta_0}(\beta)$ denotes the CDF of β_0 and for $0 \leq \beta \leq 2$ is given by

$$F_{\beta_0}(\beta) = Pr\left(\frac{2}{1 + \sqrt{\frac{\gamma_1}{\gamma_2}}} \leq \beta\right)$$

$$= \int_0^\infty \frac{1}{\Gamma_2} \exp\left(-\frac{\gamma_2 \left(\frac{2}{\beta} - 1\right)^2}{\Gamma_1} - \frac{\gamma_2}{\Gamma_2}\right) d\gamma_2 = \frac{1}{\Gamma_2} \left(\frac{\left(\frac{2}{\beta} - 1\right)^2}{\Gamma_1} + \frac{1}{\Gamma_2}\right)^{-1}. \quad (4.21e)$$

Note that the number of possible cases for the random set \mathbb{C}_v increases dramatically as the number of hops increases. In addition, depending on the maximum allowed power per terminal, clipping of the power for the violating terminals and re-optimization may be required more than once. Furthermore, the instantaneous received SNR at the destination corresponding to each case will not be a well-defined function of the individual per-hop instantaneous SNRs, in general, making calculation of the conditional outage probabilities almost intractable. Thus, evaluation of the outage probability of a general multi-hop transmission system employing the optimal power allocation policy subject to both total and individual ST power constraints is very involved, especially when the number of hops increases. The outage probability expression in (4.12) is basically a lower bound on the performance of a power-optimized multi-hop transmission system under both total and individual ST power constraints. This lower bound gets very tight for the cases where the maximum allowed power per each hop is close to P_T . However, if the maximum allowed power per terminal is very close to P , employment of the uniform power allocation makes more sense due to its ease of implementation. Clipping the power at the violating terminals severely limits the performance of the optimal power allocation scheme in this case resulting in almost the same (slightly better) outage probability as a system with uniform power allocation policy.

4.3 Optimal Power Allocation Under LT Power Constraint

4.3.1 Mechanism

The optimal power allocation problem under LT power constraint is formulated as

$$\begin{aligned} \max \quad & \gamma_t^V \\ \text{subject to} \quad & \mathbb{E}\left(\sum_{k=0}^{K-1} \beta_k\right) = K. \end{aligned} \quad (4.22)$$

The optimization problem in (4.22) is a convex problem and hence has a unique optimal solution. Using the Lagrange multiplier method, one gets a relation between power coefficients, β_k and β_j , $k, j = 0, 1, \dots, K - 1$, $j \neq k$, as given in (A.19). Now, suppose

that each power coefficient is a function of the instantaneous received SNR of its next immediate hop, i.e. $\beta_k = \mathcal{U}(\gamma_{k+1})$ where $\mathcal{U}(\cdot)$ is an arbitrary function. Then according to (A.19),

$$\beta_k^2 \gamma_{k+1} \left(1 + \frac{1}{\beta_k \gamma_{k+1}} \right) = \eta \quad (4.23)$$

where η is a constant. Therefore, β_k is obtained as

$$\beta_k = \frac{-1 + \sqrt{1 + 4\eta\gamma_{k+1}}}{2\gamma_{k+1}} \quad (4.24a)$$

where the constant η is determined such that the LT power constraint in (4.22) is satisfied. Thus, η is obtained by numerical solving of

$$\mathbb{E} \left(\sum_{k=0}^{K-1} \frac{-1 + \sqrt{1 + 4\eta\gamma_{k+1}}}{2\gamma_{k+1}} \right) = K. \quad (4.24b)$$

In principle, the constant η is a function of all average SNRs, Γ_k , $k = 1, \dots, K$. Therefore, the obtained power coefficient β_k in (4.24a) depends on the instantaneous SNR of the immediate following terminal, γ_{k+1} , as well as the average SNRs of all links. Note that each terminal, T_k , can acquire the instantaneous channel information of its next immediate hop, γ_{k+1} , utilizing the clear to send (CTS) frame send from terminal T_{k+1} to T_k . Furthermore, the destination can compute the constant η at the initialization stage before the communication begins and then feed it back to the terminals. Note that η remains almost constant during the entire communication. Thus, the optimal power allocation scheme under LT power constraint in (4.22) can be implemented in a decentralized manner.

Similar to Section 4.2.2, one can get a closed-form solution for the power coefficients β_k , $k = 0, 1, \dots, K - 1$, by maximizing the approximate expression for γ_t^Y given in (4.7). In addition, maximizing γ_t^Y is equivalent to minimizing its inverse. Thus, in this case the Lagrangean function is given by

$$L = \left(\sum_{k=0}^{K-1} \frac{1}{\beta_k \gamma_{k+1}} \right) + \lambda^{LT1} \left(\mathbb{E} \left(\sum_{k=0}^{K-1} \beta_k \right) - K \right) \quad (4.25)$$

where λ^{LT1} is the Lagrange multiplier. Taking the derivative of L with respect to β_k yields a closed-form solution for power coefficients under total LT power constraint in (4.22) as

$$\beta_k^{LT1} = \frac{1}{\sqrt{\lambda^{LT1} \gamma_{k+1}}}, \quad k = 0, 1, \dots, K - 1 \quad (4.26a)$$

where λ^{LT1} is obtained using the LT power constraint in (4.22) as

$$\lambda^{LT1} = \frac{\pi}{K^2} \left(\sum_{k=1}^K \frac{1}{\sqrt{\Gamma_k}} \right)^2. \quad (4.26b)$$

It can be readily shown that for sufficiently large values of SNR, β_k in (4.24a) tends to β_k^{LT1} where η is replaced by $\frac{1}{\lambda^{LT1}}$.

The average per-hop power portion in a power-optimized system under total LT power constraint in (4.22) is given by

$$\mathbb{E}(\beta_k^{LT1}) = \mathbb{E}\left(\frac{1}{\sqrt{\lambda^{LT1}\gamma_{k+1}}}\right) = \sqrt{\frac{\pi}{\lambda^{LT1}\Gamma_{k+1}}} = \frac{K}{\sum_{j=0}^{K-1} \sqrt{\frac{\Gamma_{k+1}}{\Gamma_{j+1}}}}. \quad (4.27)$$

Note that since $\sum_{k=0}^{K-1} \mathbb{E}(\beta_k) = K$, the average power portions per each hop, β_k^{LT1} , $k = 0, 1, \dots, K-1$, has a real value between 0 and K . This implies that each terminal should be able to provide the maximum average power P_T . It is more practical, however, to limit the individual per-hop average powers as $\mathbb{E}(P_k) = P$ which is equivalent to $\mathbb{E}(\beta_k) = 1$. These individual LT power constraints also ensure that the average total power is equal to P_T . The optimization problem under individual LT power constraints can be written as

$$\begin{aligned} \min \quad & \frac{1}{\gamma_t} \cong \sum_{k=0}^{K-1} \frac{1}{\beta_k \gamma_{k+1}} \\ \text{subject to} \quad & \mathbb{E}(\beta_k) = 1, \quad k = 0, 1, \dots, K-1. \end{aligned} \quad (4.28)$$

Then, using the Lagrange multiplier method [97], one has

$$L = \frac{1}{\gamma_t} + \sum_{k=0}^{K-1} \lambda_k^{LT2} (\mathbb{E}(\beta_k) - 1). \quad (4.29)$$

Taking the derivative of L with respect to β_k , $k = 0, 1, \dots, K-1$, one obtains

$$\beta_k^{LT2} = \frac{1}{\sqrt{\lambda_k^{LT2}\gamma_{k+1}}} \quad (4.30a)$$

for power coefficients subject to individual LT power constraints where the Lagrange multiplier, λ_k^{LT2} , is obtained as

$$\lambda_k^{LT2} = \left(\mathbb{E}\left(\frac{1}{\sqrt{\gamma_{k+1}}}\right) \right)^2 = \frac{\pi}{\Gamma_{k+1}} \quad (4.30b)$$

using the individual LT power constraint in (4.28).

Note that the obtained power coefficients under individual LT power constraints, β_k^{LT2} , $k = 0, \dots, K-1$, only depend on the instantaneous and average SNR of immediate forward channel. Thus, this power allocation strategy can be implemented in a fully distributed manner, making it attractive for application in ad hoc wireless networks.

4.3.2 Outage Probability Analysis

The instantaneous received SNR in the power-optimized AF multi-hop transmission system under total LT power constraint is given by

$$\gamma_t^{LT1} = \left(\sum_{k=1}^K \sqrt{\frac{\lambda^{LT1}}{\gamma_k}} \right)^{-1} \quad (4.31a)$$

and can be written in terms of γ_t^{ST} given in (4.10) as

$$\gamma_t^{LT1} = \sqrt{\frac{\gamma_t^{ST}}{\lambda^{LT1} K}}. \quad (4.31b)$$

Therefore, the outage probability for a power-optimized AF multi-hop transmission system under total LT power constraint is obtained as

$$\begin{aligned} P_{out}^{LT1} &= Pr \left(\gamma_t^{LT1} < \gamma_{th} \right) = Pr \left(\gamma_t^{ST} < \lambda^{LT1} K \gamma_{th}^2 \right) \\ &= P_{out}^{ST} \Big|_{\gamma_{th} \rightarrow \lambda^{LT1} K \gamma_{th}^2} \end{aligned} \quad (4.32)$$

where P_{out}^{ST} is given in (4.11) for a dual-hop system and in (4.12) for a multi-hop system with an arbitrary number of hops.

The instantaneous received SNR in the power-optimized AF multi-hop transmission system under individual LT power constraints is given by

$$\gamma_t^{LT2} = \left(\sum_{k=1}^K \sqrt{\frac{\lambda_k}{\gamma_k}} \right)^{-1} \quad (4.33a)$$

and can be written in terms of γ_t^{ST} as

$$\gamma_t^{LT2} = \sqrt{\frac{\gamma_t^{ST}}{K}} \Big|_{\gamma_k \rightarrow \frac{\gamma_k}{\lambda_k^{LT2}}}. \quad (4.33b)$$

Therefore, the outage probability in this case is obtained as

$$\begin{aligned} P_{out}^{LT2} &= Pr \left(\gamma_t^{LT2} < \gamma_{th} \right) = Pr \left(\gamma_t^{ST} < K \gamma_{th}^2 \right) \Big|_{\gamma_k \rightarrow \frac{\gamma_k}{\lambda_k^{LT2}}} \\ &= P_{out}^{ST} \Big|_{\substack{\gamma_{th} \rightarrow K \gamma_{th}^2 \\ \Gamma_k \rightarrow \frac{\Gamma_k}{\lambda_k^{LT2}}}}. \end{aligned} \quad (4.34)$$

4.3.3 Asymptotic Outage Probability Behavior

The outage probabilities of power-optimized AF multi-hop transmission systems under total and individual LT power constraints can be evaluated in terms of the outage probability of the corresponding system under ST power constraint as given in (4.32) and (4.34),

respectively. Thus, the asymptotic outage behaviors for large values of SNR can be determined using Lemma 4.1 as

$$\begin{aligned} P_{out}^{LT1} &\rightarrow \lambda^{LT1} \gamma_{th}^2 \sum_{k=1}^K \frac{1}{\Gamma_k} \\ &= \frac{\gamma_{th}^2 \pi}{K} \left(\sum_{k=1}^K \frac{1}{\sqrt{\Gamma_k}} \right)^2 \sum_{k=1}^K \frac{1}{\Gamma_k} \end{aligned} \quad (4.35)$$

and

$$\begin{aligned} P_{out}^{LT2} &\rightarrow \gamma_{th}^2 \sum_{k=1}^K \frac{\lambda_k^{LT2}}{\Gamma_k} \\ &= \gamma_{th}^2 \pi \sum_{k=1}^K \frac{1}{\Gamma_k^2} \end{aligned} \quad (4.36)$$

for power-optimized AF multi-hop transmission systems under total and individual LT power constraints, respectively. Eqs. (4.35) and (4.36) show that the power-optimized AF multi-hop transmission systems under either total or individual LT power constraints can provide a substantial performance gain by achieving diversity gain 2.

4.4 Numerical Results

In the numerical examples, we consider different multi-hop transmission systems both with balanced and unbalanced links in which the terminals are located in a straight line of length d_0 meters between the source and destination, as described in examples 1 and 2 of Section 3.2.5.1. Recall that in systems with balanced links, terminals are located in equi-distant points from each other¹, while in systems with unbalanced links, it is assumed that the k^{th} terminal, $k = 1, \dots, K$ is located in distance $d_k = \frac{2k}{K(K+1)}d_0$ from its previous terminal, T_{k-1} . Assuming that a K -hop system uses a total power $P_T = KP$, using the Friss propagation formula [94], one has $\Gamma_k = K^{\epsilon-1}\Gamma_0$, $k = 1, \dots, K$ in K -hop systems with balanced links where Γ_0 denotes the average SNR in a single-hop system and $\Gamma_k = \frac{1}{K} \left(\frac{(K+1)K}{2k} \right)^\epsilon \Gamma_0$, $k = 1, \dots, K$ in K -hop systems with unbalanced links. In the numerical examples, we assume $\epsilon = 4$, and $\gamma_{th} = 1$.

Figures 4.1 and 4.2 show the outage probabilities for different dual-hop and triple-hop transmission systems, respectively. Simulation results in both figures were obtained using a Monte Carlo method with as many as 5×10^6 samples. The theoretical outage probabilities in Figure 4.1 were obtained using the closed-form expression given in [19, eq. (27)]

¹It is shown in [14] that this is the optimal relay configuration in the sense of minimizing the error probability when uniform power allocation is employed.

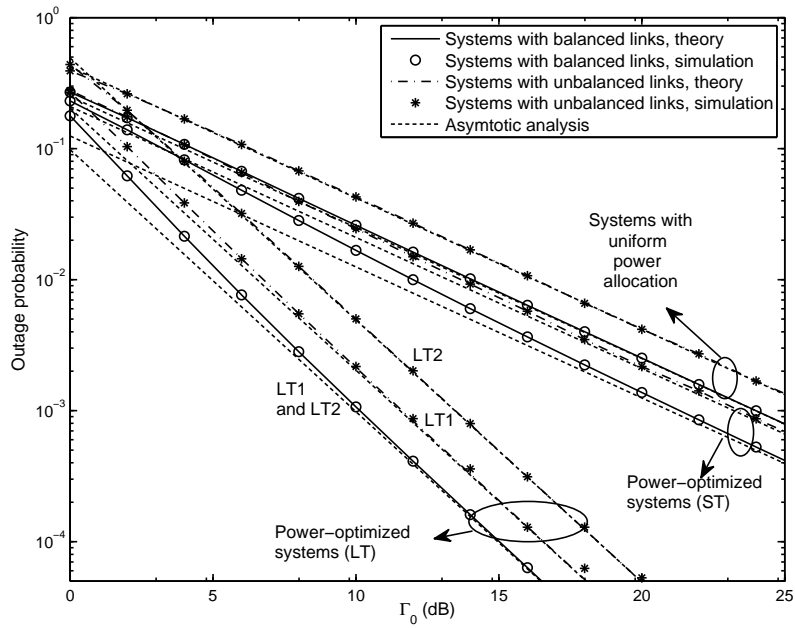


Figure 4.1. Outage probabilities for different AF dual-hop transmission systems. The acronyms ST, LT1, and LT2, respectively, stand for power-optimized systems under ST power constraint, total LT power constraint, and individual LT power constraints.

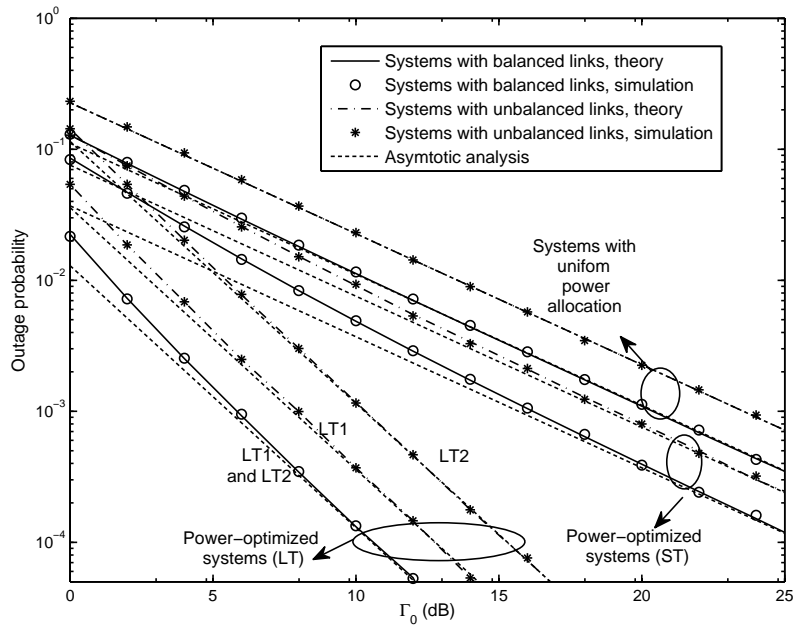


Figure 4.2. Outage probabilities for different AF triple-hop transmission systems. The acronyms ST, LT1, and LT2, respectively, stand for power-optimized systems under ST power constraint, total LT power constraint, and individual LT power constraints.

for systems with uniform power allocation, and using (4.11) for power-optimized systems under ST power constraint. The theoretical results in Figure 4.2 for power-optimized triple-hop systems under ST power constraints were obtained using (4.12) where we assumed $\omega_0 = 0.92$ and used as few as 50 terms for small values of SNR and as many as 300 terms for large values of SNR in evaluation of the series (4.12d). In Figures 4.1 and 4.2, we have also plotted the expressions obtained for the outage probabilities of the power-optimized systems under total and individual LT power constraints given in (4.32) and (4.34), respectively. The theoretical results in Figure 4.2 for systems with uniform power allocation were obtained using (3.12) where $\Psi_X(\cdot)$ is given by (3.5) with $s = -jw$ and the individual product terms replaced by (3.6) with $m_i = 1, i = 1, \dots, K$.

It is seen from Figures 4.1 and 4.2 that the theoretical results match precisely the simulation results. The asymptotic outage probabilities are also in good agreement with the simulation results for moderate to large values of SNR. It is seen that the power-optimized AF multi-hop transmission systems achieve better outage probabilities than those of systems with uniform power allocation. As shown in Section 4.2.3 and seen from Figures 4.1 and 4.2, at sufficiently large values of SNR, power-optimized dual-hop and triple-hop transmission systems under ST power constraint perform, respectively, two and three times better than the corresponding systems with uniform power allocation. For instance, at 20 dB, power-optimized dual-hop and triple-hop transmission systems with balanced links achieve outage probabilities 0.0013 and 3.9×10^{-4} , respectively, compared to the respective outage probabilities 0.0025 and 1.15×10^{-3} achieved in the corresponding systems with uniform power allocation. Furthermore, as seen in Figures 4.1 and 4.2, power-optimized systems under LT power constraints offer superior performance gain achieving diversity gain 2. For instance, an AF dual-hop system with balanced links employing the optimal power allocation scheme under either total or individual LT power constraint² achieves almost 14 dB gain comparing to the corresponding system with uniform power allocation at an outage probability of 10^{-3} . The total LT power constraint is a more relaxed constraint than the individual LT power constraints. Thus, as seen in Figures 4.1 and 4.2, a system (with unbalanced links) employing the optimal power allocation policy under total LT power constraint outperforms the system employing the one under individual LT power constraints.

Figures 4.3 and 4.4 show the average power portions utilized per hop in different dual-

²Note that in systems with balanced links, the optimal power coefficients under total and individual LT power constraints are the same.

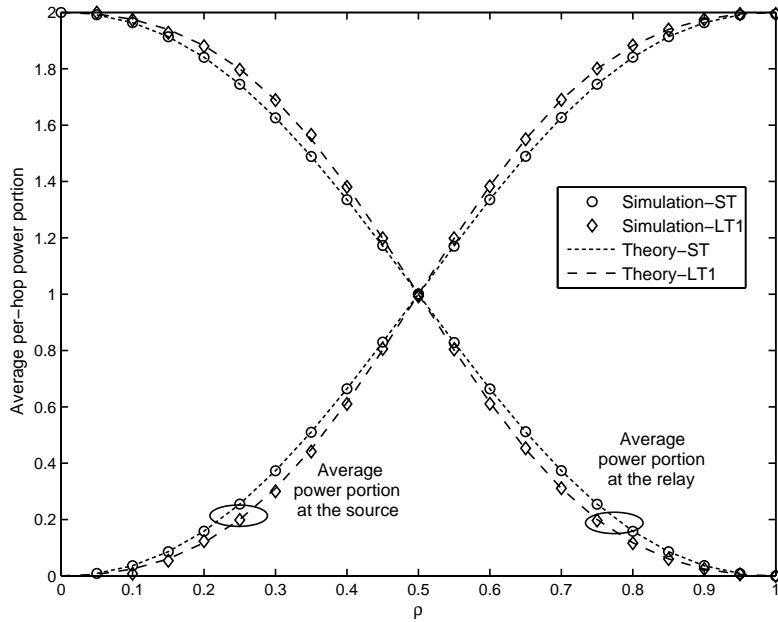


Figure 4.3. Average power portions utilized per hop in different AF dual-hop transmission systems. The acronyms ST and LT1, respectively, stand for power-optimized systems under ST power constraint and total LT power constraint.

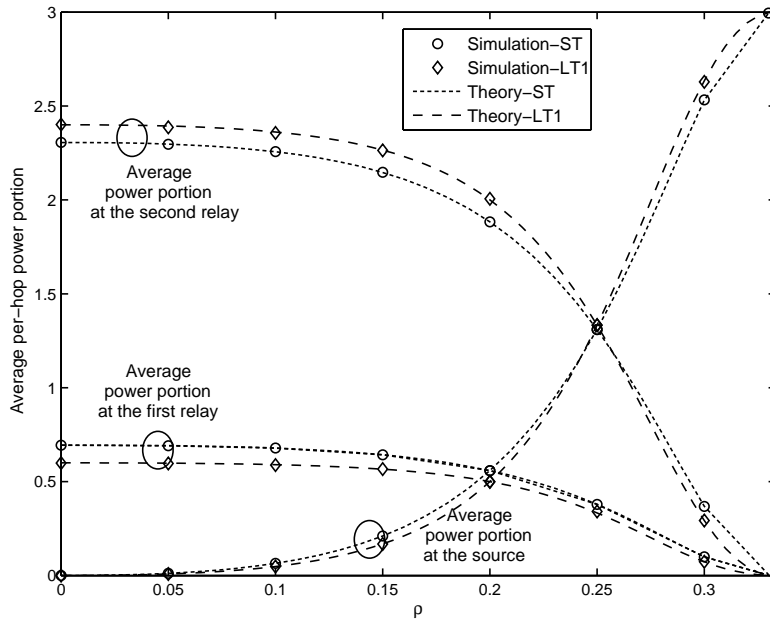


Figure 4.4. Average power portions utilized per hop in different AF triple-hop transmission systems. The acronyms ST and LT1, respectively, stand for power-optimized systems under ST power constraint and total LT power constraint.

hop and triple-hop systems, respectively. In Figures 4.3 and 4.4, we have considered systems where the k^{th} relay is located at distance $k\rho$ from its previous terminal in a straight line where $0 \leq \rho \leq 1$ in dual-hop systems and $0 \leq \rho \leq \frac{1}{3}$ in triple-hop systems. We have also assumed that all systems use equal total power. The noise powers at all terminals are assumed to be the same, as well. Therefore, according to the Friis propagation formula [94], one has $\Gamma_1 = \frac{1}{2\rho^\epsilon} \Gamma_0$, and $\Gamma_2 = \frac{1}{2(1-\rho)^\epsilon} \Gamma_0$ in dual-hop systems; and $\Gamma_1 = \frac{1}{3\rho^\epsilon} \Gamma_0$, $\Gamma_2 = \frac{1}{3(2\rho)^\epsilon} \Gamma_0$, and $\Gamma_3 = \frac{1}{3(1-3\rho)^\epsilon} \Gamma_0$ in triple-hop systems. Simulation results shown in Figures 4.3 and 4.4 were obtained using a Monte Carlo method with as many as 10^6 points. Any value assumed for Γ_0 in the simulation set-up results in the same average per-hop power portion as long as the link SNR ratios are kept constant. In fact, as seen in eqs. (4.15), (4.17) and (4.18), and (4.27), the average per-hop power portions in all power-optimized systems evaluated in Sections 4.2 and 4.3 depend on the ratio of the link SNRs and not on their absolute values. The theoretical average power portions utilized per hop in the power-optimized systems under ST power constraint were obtained using (4.15) in Figure 4.3, and using (4.17) and (4.18) in Figure 4.4 assuming $N_p = 15$. In Figures 4.3 and 4.4, we have also plotted the expression derived in (4.27) for the average per-hop power portions utilized in power-optimized systems under total LT power constraint. It is seen from both Figures 4.3 and 4.4 that the analytical results are in precise agreement with the simulation results. As discussed earlier in Sections 4.2 and 4.3, it is seen that the average optimal power portions per hop under ST and total LT power constraints swap the range of values between 0 and K depending on the location of the relays. In addition, as seen from eqs. (4.9) and (4.26a), the power allocated to the k^{th} terminal, $k = 0, \dots, K - 1$, is proportional to the inverse of the square root of the SNR over the next immediate hop, γ_{k+1} . Thus, as seen in Figures 4.3 and 4.4, power allocation policies both under ST and total LT power constraints distribute the total power relatively in the same fashion to the terminals (on the average) along the multi-hop path and devote larger average power portions to the weaker links. For instance, in the dual-hop systems shown in Figure 4.3, more power is allocated to the source as the relay gets closer to the destination.

Chapter 5

AF Multi-Relay Cooperative Systems

In this chapter, low complexity receivers for AF multi-relay cooperative systems are developed. An AF multi-relay system with repetition based scheduling employing MRC at the destination is first studied in Section 5.1. Recall that MRC of the signals received at the destination from the source and the relays is an ML detector, and hence its performance provides a benchmark for performance evaluation of other receivers developed here. In Section 5.2 low complexity coherent receivers that only require phase information in a distributed manner are introduced and evaluated. In Section 5.3 employment of a detection scheme in a noncoherent AF system based on square-law envelope (energy) detection [89] at the destination is proposed. The proposed scheme achieves full spatial diversity while requiring neither instantaneous nor statistics knowledge of the fading channel information.

5.1 Systems Employing MRC at Destination

5.1.1 System Model

Consider a multi-relay cooperative system as shown in Figure 2.2 where the source, T_0 , communicates with the destination, T_{N+1} , with the help of N half-duplex relays, T_1, \dots, T_N . The source transmits the signal x_0 in the first time slot. The signals received at the relays and the destination from the source, T_0 , are given by

$$y_i^{T_0} = \alpha_{0,i}x_0 + n_i, \quad i = 1, \dots, N + 1. \quad (5.1)$$

A version of this chapter has been submitted in part to IEEE Transactions on Communications, and has been published in part in IEEE Transactions on Wireless Communications, 7:1851-1856 (2008) and 7:4462-4467 (2008), and in Proceedings of IEEE International Conference on Communications (ICC), 1:3730-3735 (2008) and 1:4300-4305 (2008).

The signal at each relay is then amplified and forwarded to the destination in a predetermined time slot (i.e. repetition-based scheduling [4]). The signal received at the destination through the i^{th} relay, $i = 1, \dots, N$, is given by

$$y_{N+1}^{T_i} = \hat{A}_i y_i^{T_0} + n_{N+1}^{T_i} = \hat{A}_i \alpha_{0,i} \alpha_{i,N+1} x_0 + \hat{A}_i \alpha_{i,N+1} n_i^{T_0} + n_{N+1}^{T_i}. \quad (5.2a)$$

where $n_i^{T_j}$, $i = 1, \dots, N + 1$, $j \neq i = 0, 1, \dots, N + 1$ denotes the received noise at terminal T_i in the time slot corresponding to the transmission from terminal T_j and \hat{A}_i is the amplification gain at the i^{th} relay. The relay amplification gain at the i^{th} relay in a multi-relay system with variable-gain relays, \hat{A}_i^V , is chosen as [3]

$$\hat{A}_i^V = \sqrt{\frac{\frac{P_i}{N_0}}{\gamma_{0,i} + 1}}. \quad (5.2b)$$

The relay amplification gain at the i^{th} relay in a system with fixed-gain relays, \hat{A}_i^F , can take any arbitrary value, in general [20]. In practice, it is mostly chosen such that an average power constraint at the relay is satisfied [41]- [43], i.e.

$$\hat{A}_i^F = \sqrt{\frac{\frac{P_i}{N_0}}{\Gamma_{0,i} + 1}}. \quad (5.2c)$$

The signals received at the destination, $y_{N+1}^{T_i}$, $i = 0, \dots, N$, are combined using MRC diversity. Note that the combination of repetition-based scheduling at the relays and MRC diversity at the destination is referred to as R-MRC scheme in this thesis. Thus, the instantaneous total received SNR at the destination, γ_t^{R-MRC} , is given by [14]

$$\begin{aligned} \gamma_t^{R-MRC} &= \gamma_{0,N+1} + \sum_{i=1}^N \frac{P_0 \alpha_{0,i}^2 \alpha_{i,N+1}^2}{N_0 \left(\alpha_{i,N+1}^2 + \frac{1}{\hat{A}_i^2} \right)} \\ &= \gamma_{0,N+1} + \sum_{i=1}^N \gamma_{T_i} \end{aligned} \quad (5.3a)$$

where γ_{T_i} denotes the instantaneous received SNR at the destination through the i^{th} relay and is given by [29]

$$\gamma_{T_i}^V = \frac{\gamma_{0,i} \gamma_{i,N+1}}{\gamma_{i,N+1} + \gamma_{0,i} + 1} \quad (5.3b)$$

and [22]

$$\gamma_{T_i}^F = \frac{\gamma_{0,i} \gamma_{i,N+1}}{\gamma_{i,N+1} + \hat{C}_i} \quad (5.3c)$$

in systems with variable-gain relays and fixed-gain relays, respectively, where $\hat{C}_i \triangleq \frac{P_i}{N_0 (\hat{A}_i^F)^2}$.

5.1.2 Performance Analysis

5.1.2.1 Error Probability Analysis

Error probability of an AF cooperative system employing MRC at the destination can be evaluated using the MGF-based approach [89] for a variety of modulation schemes. Note that the MGF of γ_t^{R-MRC} given in (5.3) can be obtained as the product of the MGFs of its summands, which are known and given in [19] and [20] for systems with variable-gain relays and fixed-gain relays, respectively. Exact calculation of the error probabilities using the MGF-based method involves single integrals that generally have no closed-form solutions and should be numerically evaluated. However, one can obtain simple closed-form expression for the symbol error probability in an AF cooperative system for sufficiently large values of SNR using eq. (3.23). Note that according to [14, Proposition 2], the first $N - 1$ derivatives of the PDF of the instantaneous received SNR, γ_t^{R-MRC} given in (5.3) at the origin are zero and its N^{th} order derivative at zero is given by the product of the values of the PDF of its summands at the origin. In systems with variable-gain relays, one has [14, eq. (31)]

$$\begin{aligned} \frac{\partial^N}{\partial \gamma^N} f_{\gamma_t^{R-MRC}}(0) &= f_{\gamma_{0,N+1}}(0) \prod_{i=1}^N (f_{\gamma_{0,i}}(0) + f_{\gamma_{i,N+1}}(0)) \\ &= \frac{r^{N+1}}{\Gamma_{0,N+1}} \prod_{i=1}^N \left(\frac{1}{\Gamma_{0,i}} + \frac{1}{\Gamma_{i,N+1}} \right) \end{aligned} \quad (5.4)$$

where r is given in Table 3.4 for different types of fading. In systems with fixed-gain relays, the N^{th} order derivative of the PDF of instantaneous received SNR is bounded by

$$\begin{aligned} \frac{\partial^N}{\partial \gamma^N} f_{\gamma_t^{R-MRC}}(0) &> f_{\gamma_{0,N+1}}(0) \prod_{i=1}^N \left(f_{\gamma_{0,i}}(0) \left(1 + \frac{\hat{C}_i}{\Gamma_{i,N+1}} \right) + f_{\gamma_{i,N+1}}(0) \frac{\hat{C}_i}{\Gamma_{0,i}} \right) \\ &= \frac{r^2}{\Gamma_{0,N+1}} \prod_{i=1}^N \left(\frac{1}{\Gamma_{0,i}} + \frac{2\hat{C}_i}{\Gamma_{0,i}\Gamma_{i,N+1}} \right) \end{aligned} \quad (5.5)$$

using Lemma 3.2 with $\mathcal{M} = 2$. Asymptotic expressions for the symbol error probability are then obtained using (3.23) with $t = N$ and $\frac{\partial^N}{\partial \gamma^N} f_{\gamma_t}(0)$ replaced by (5.4) and (5.5) for systems with variable-gain relays and fixed-gain relays, respectively. Eqs. (5.4) and (5.5) indicate that AF cooperative systems with both variable-gain relays and fixed-gain relays employing MRC diversity at the destination achieve full spatial diversity.

The accuracy of the asymptotic symbol error probability of AF multi-relay cooperative systems with variable-gain relays has been shown in [14]. Figure 5.1 shows bit error probabilities for different BPSK multi-relay cooperative systems with fixed-gain relays with i.i.d.

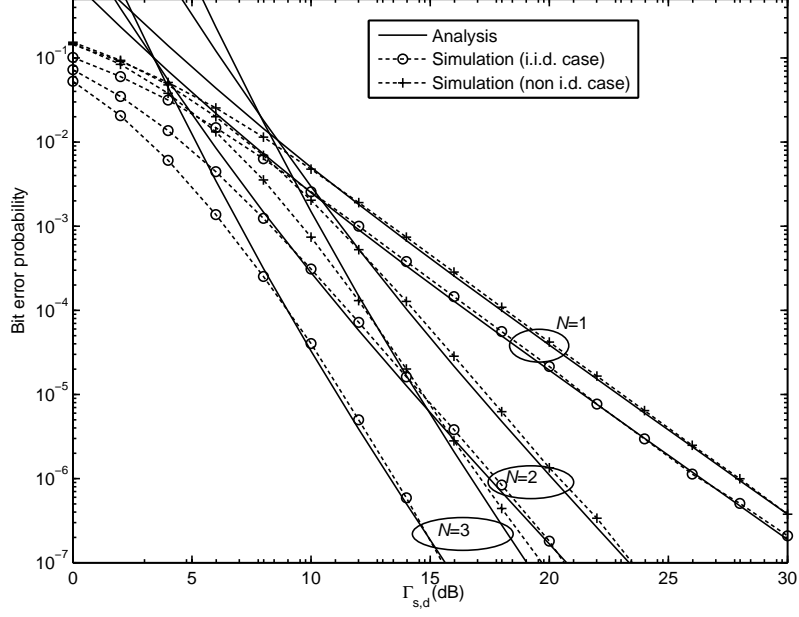


Figure 5.1. Bit error probabilities for different multi-relay systems with fixed-gain relays employing R-MRC.

links where $\Gamma_{0,i} = \Gamma_{i,N+1} = \Gamma_{s,d}$ and non i.d. links where $\Gamma_{0,i} = \Gamma_{i,N+1} = \frac{\Gamma_{s,d}}{i}$ where $\Gamma_{s,d}$ denotes the average SNR over the source-destination link. It is assumed that $\hat{C}_i = 1.7$ for all relay terminals. It is seen that the analytically obtained error probabilities are in good agreement with the simulation results for sufficiently large values of SNR in both cases of i.i.d. and non i.d. average link SNRs. It is also seen that increasing the number of relays improves the performance by achieving diversity gain equal to $N + 1$, as expected.

5.1.2.2 Capacity Analysis

In this section, the ergodic capacity of AF multi-relay systems employing R-MRC scheme is evaluated assuming that CSI is only known to the receivers. The signals received at the destination in an AF cooperative system can be written in a vector format as

$$\mathbf{y}_{N+1} = \tilde{\mathbf{h}}x_0 + \tilde{\mathbf{n}} \quad (5.6a)$$

where

$$\mathbf{y}_d = \left[\frac{y_{N+1}^{T_0}}{\sqrt{N_0}} \quad \frac{y_{N+1}^{T_1}}{\sqrt{\hat{A}_1^2 \alpha_{1,N+1}^2 N_0 + N_0}} \quad \dots \quad \frac{y_{N+1}^{T_N}}{\sqrt{\hat{A}_N^2 \alpha_{N,N+1}^2 N_0 + N_0}} \right]^T \quad (5.6b)$$

and

$$\tilde{\mathbf{h}} = \left[\frac{\alpha_{0,N+1}}{\sqrt{N_0}} \frac{\hat{A}_1 \alpha_{0,1} \alpha_{1,N+1}}{\sqrt{\hat{A}_1^2 \alpha_{1,N+1}^2 N_0 + N_0}} \cdots \frac{\hat{A}_N \alpha_{0,N} \alpha_{N,N+1}}{\sqrt{\hat{A}_N^2 \alpha_{N,N+1}^2 N_0 + N_0}} \right]^T \quad (5.6c)$$

and $\tilde{\mathbf{n}}$ is a vector of $N + 1$ zero-mean complex Gaussian random variables with unit variances. The ergodic capacity is then obtained as [71]

$$\begin{aligned} \mathcal{E}^{R-MRC} &= \frac{1}{N+1} \mathbb{E} \left(\log \left(1 + P_0 \tilde{\mathbf{h}}^H \tilde{\mathbf{h}} \right) \right) \\ &= \frac{1}{N+1} \mathbb{E} \left(\log \left(1 + \gamma_t^{R-MRC} \right) \right). \end{aligned} \quad (5.7)$$

Analytical evaluation of this expectation is facilitated by having a closed-form expression for the PDF of the total received SNR at the destination, γ_t^{R-MRC} . However, such expression for the PDF of γ_t^{R-MRC} in systems both with variable-gain relays and fixed-gain relays is still unknown. A closed-form upper bound on the ergodic capacity can be obtained utilizing Jensen's inequality [96] as

$$\mathcal{E}^{R-MRC} < \mathcal{E}_{UB}^{R-MRC} = \frac{1}{N+1} \log \left(1 + \Gamma_t^{R-MRC} \right) \quad (5.8a)$$

where Γ_t^{R-MRC} is the the expected value of the instantaneous total received SNR at the destination given by

$$\Gamma_t^{R-MRC} = \Gamma_{0,N+1} + \begin{cases} \sum_{i=1}^N \Gamma_{T_i}^V, & \text{Variable-gain relays} \\ \sum_{i=1}^N \Gamma_{T_i}^F, & \text{Fixed-gain relays} \end{cases} \quad (5.8b)$$

where $\Gamma_{T_i}^V$ and $\Gamma_{T_i}^F$ denote the average received SNR at the destination through the i^{th} relay in systems with variable-gain and fixed-gain relays, respectively, and are given by

$$\begin{aligned} \Gamma_{T_i}^V &= \frac{16\sqrt{\pi}}{3.3233\Gamma_{0,i}\Gamma_{i,N+1} \left(\frac{1}{\sqrt{\Gamma_{0,i}}} + \frac{1}{\sqrt{\Gamma_{i,N+1}}} \right)^6} \left[{}_2F_1 \left(3, 0.5; 3.5; \frac{\left(\frac{1}{\sqrt{\Gamma_{0,i}}} - \frac{1}{\sqrt{\Gamma_{i,N+1}}} \right)^2}{\left(\frac{1}{\sqrt{\Gamma_{0,i}}} + \frac{1}{\sqrt{\Gamma_{i,N+1}}} \right)^2} \right) \right. \\ &\quad \left. + \frac{3 \left(\frac{1}{\Gamma_{0,i}} + \frac{1}{\Gamma_{i,N+1}} \right)}{\left(\frac{1}{\sqrt{\Gamma_{0,i}}} + \frac{1}{\sqrt{\Gamma_{i,N+1}}} \right)^2} {}_2F_1 \left(4, 1.5; 3.5; \frac{\left(\frac{1}{\sqrt{\Gamma_{0,i}}} - \frac{1}{\sqrt{\Gamma_{i,N+1}}} \right)^2}{\left(\frac{1}{\sqrt{\Gamma_{0,i}}} + \frac{1}{\sqrt{\Gamma_{i,N+1}}} \right)^2} \right) \right] \end{aligned} \quad (5.8c)$$

in Rayleigh fading using the PDF of $\gamma_{T_i}^V$ given in [19, eq. (19)] and [90, eq. (6.621.3)] where ${}_2F_1(\cdot, \cdot; \cdot; \cdot)$ denotes the Gauss hypergeometric function [90, eq. (9.100)]; and

$$\begin{aligned} \Gamma_{T_i}^F &= \Gamma_{0,i} \mathbb{E} \left(\frac{\gamma_{i,N+1}}{\gamma_{i,N+1} + \hat{C}_i} \right) \\ &= \Gamma_{0,i} \left(1 - \frac{\hat{C}_i}{\Gamma_{i,N+1}} \exp \left(\frac{\hat{C}_i}{\Gamma_{i,N+1}} \right) E_1 \left(\frac{\hat{C}_i}{\Gamma_{i,N+1}} \right) \right) \end{aligned} \quad (5.8d)$$

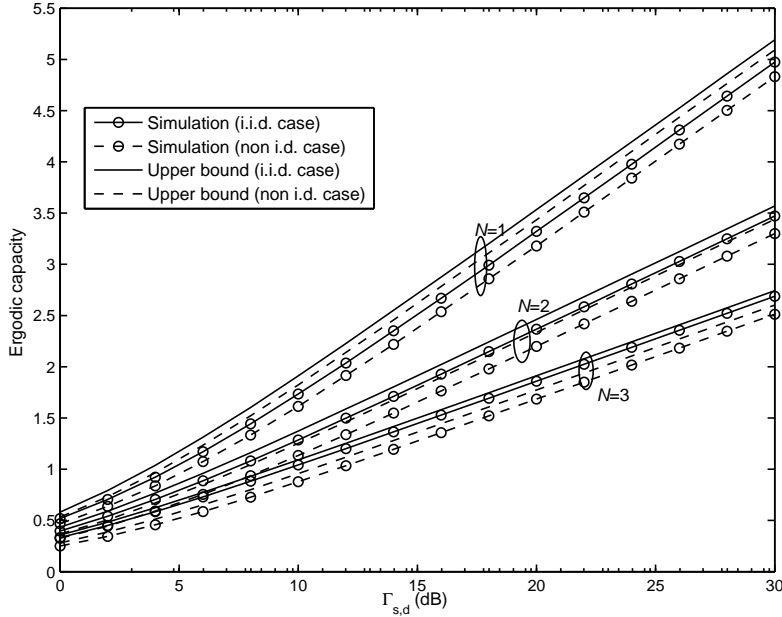


Figure 5.2. Ergodic capacities of different AF systems employing R-MRC with variable-gain relays chosen according to (5.2b).

in Rayleigh fading using [90, eq. (3.353.5)].

Figures 5.2 and 5.3, respectively, show ergodic capacities of different AF cooperative systems employing R-MRC with variable-gain relays and fixed-gain relays. In these figures, it is assumed that $\Gamma_{0,i} = \Gamma_{i,N+1} = \Gamma_{s,d}$ in systems with i.i.d. links and $\Gamma_{0,i} = \Gamma_{i,N+1} = \frac{\Gamma_{s,d}}{i+1}$ in systems with non i.d. links. Note that the amplification gain in systems with fixed-gain relays is chosen according to (5.2c) to ensure the average power constraint at the i^{th} relay is satisfied. Thus, $\hat{C}_i = \Gamma_{0,i} + 1$, $i = 1, \dots, N$ in Figure 5.3. These figures clearly indicate the tightness of the upper bound obtained for the ergodic capacities in Rayleigh fading of different AF cooperative systems with variable-gain relays and fixed-gain relays for both i.i.d. and non i.d. cases. For example, the inaccuracies of the upper bound in the double-relay system with variable-gain relays for the i.i.d. and the non i.d. cases are about 6% and 10% at 5 dB, respectively. It is also seen in Figures 5.2 and 5.3 that systems with fixed-gain relays with the amplification gain chosen as (5.2c) perform almost the same as systems with variable-gain relays.

In addition, since the relays transmit in orthogonal time slots (repetition-based scheduling), increasing the number of relays degrades the ergodic capacity, as seen in Figures 5.2 and 5.3.

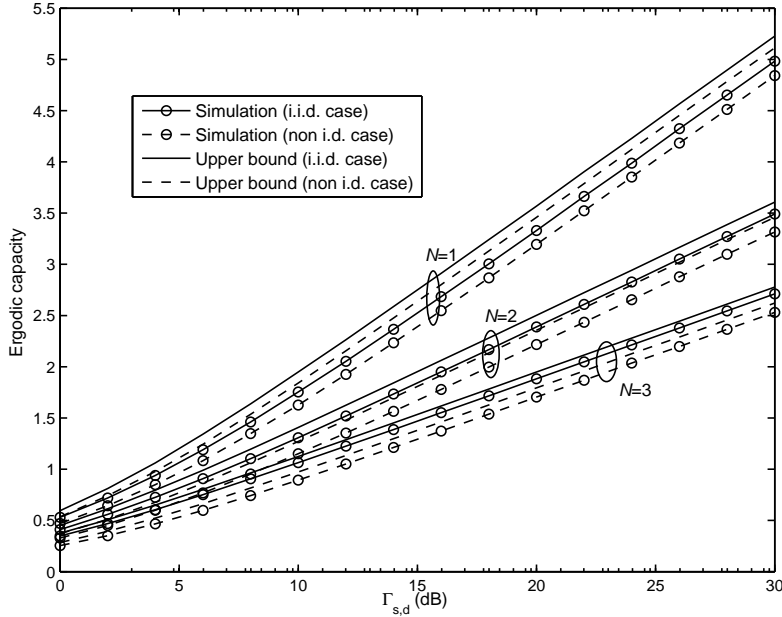


Figure 5.3. Ergodic capacities of different AF systems employing R-MRC with fixed-gain relays chosen according to (5.2c).

5.2 Low Complexity Coherent Receivers

In this section, we develop low complexity coherent receivers for AF multi-relay cooperative systems that, first, do not require any instantaneous channel amplitude information for their operations and, second, can acquire the required channel phase information in a distributed manner. System models are described in Section 5.2.1. Performance of the proposed schemes is evaluated in Section 5.2.2 in terms of error probability, average output SNR, and ergodic capacity. Numerical results are given in Section 5.2.3.

5.2.1 System Models

Consider a multi-relay cooperative system as shown in Figure 2.2 where the source, T_0 , communicates with the destination, T_{N+1} , with the help of N half-duplex relays, T_1, \dots, T_N . The fading gain of the channel between terminals T_i and T_j , $\alpha_{i,j}$, is modeled as a zero-mean complex Gaussian random variable with variance $\sigma_{i,j}^2$. Thus, the fading channel amplitude, $\tilde{\alpha}_{i,j} = |\alpha_{i,j}|$, has a Rayleigh distribution with power $\sigma_{i,j}^2$ and the fading channel phase, $\theta_{i,j}$, has a uniform distribution over the range 0 to 2π . The instantaneous SNR of the channel between terminals T_i and T_j defined as $\gamma_{i,j} \triangleq \frac{P_i}{N_0} \tilde{\alpha}_{i,j}^2$ is an exponential random

variable with average $\Gamma_{i,j} = \frac{P_i}{N_0} \sigma_{i,j}^2$.

It is assumed that the channel amplitudes are not known at the relays and the destination. In the sequel, we consider different scenarios for the availability of fading channel phase information in the system and develop low complexity detection schemes for each case.

5.2.1.1 Immediate Preceding Channel Phase Information Available

In this case, it is assumed that the n^{th} relay, $n = 1, \dots, N$, has knowledge of $\theta_{0,n}$ and the destination has knowledge of $\theta_{n,N+1}$, $n = 0, 1, \dots, N$. This channel phase information can be acquired using the request-to-send (RTS) packet received at the relays and destination transmitted from their preceding terminals, or by conventional methods¹.

The source transmits the signal x_0 in the first time slot. The signals received at the relays and the destination from the source, T_0 , are given by (5.1). The signal at each relay is then amplified and forwarded to the destination in a predetermined time slot (i.e. repetition-based scheduling). It is assumed that the total transmit power allocated for relay transmissions is $P_R = \sum_{i=1}^N P_i$. Then, each relay utilizes $\frac{1}{N}$ of the total power P_R for its transmission, $P_i = \frac{P_R}{N}$, $i = 1, \dots, N$. Thus, the amplification gain at the i^{th} relay is given by

$$\hat{\beta}_i = \hat{A}_i^F \exp(-j\theta_{0,i}) \quad (5.9)$$

where \hat{A}_i^F is given by (5.2c) ensuring that the long-term power constraint at the relay is satisfied [41]- [43]. The signal received at the destination through the i^{th} relay, $i = 1, \dots, N$, is then given by

$$y_{N+1}^{T_i} = \hat{\beta}_i y_i^{T_0} + n_{N+1}^{T_i} = \hat{A}_i^F \tilde{\alpha}_{0,i} \alpha_{i,N+1} x_0 + \hat{\beta}_i \alpha_{i,N+1} n_i^{T_0} + n_{N+1}^{T_i}. \quad (5.10)$$

In the proposed scheme, the signals received at the destination, $y_{N+1}^{T_i}$, $i = 0, 1, \dots, N$, in $N + 1$ orthogonal time slots are co-phased² and then added together. Thus, it is referred to as repetition-based DEGC (R-DEGC) relaying. The combiner output is then given by

$$\begin{aligned} y_o^{R-DEGC} &= \sum_{i=0}^N \exp(-j\theta_{i,N+1}) y_{N+1}^{T_i} \\ &= \left(\tilde{\alpha}_{0,N+1} + \sum_{i=1}^N \hat{A}_i^F \tilde{\alpha}_{0,i} \tilde{\alpha}_{i,N+1} \right) x_0 \end{aligned}$$

¹Note that the assumption being made in this case is that the receiver recovers the channel phase. This is done by any single channel coherent receiver, and techniques for phase estimation are well known [78, Ch. 6].

²Recall that the phases of the fading channels between the source and each relay are compensated by using complex relay amplification gains.

$$+ \sum_{i=1}^N \hat{\beta}_i \tilde{\alpha}_{i,N+1} n_i^{T_0} + \sum_{i=0}^N \exp(-j\theta_{i,N+1}) n_{N+1}^{T_i}. \quad (5.11)$$

The instantaneous received SNR is given by

$$\begin{aligned} \gamma_t^{R-DEGC} &= \frac{\left(\tilde{\alpha}_{0,N+1} + \sum_{i=1}^N \hat{A}_i \tilde{\alpha}_{0,i} \tilde{\alpha}_{i,N+1}\right)^2 P_0}{(N+1) N_0 + \sum_{i=1}^N \hat{A}_i^2 \tilde{\alpha}_{i,N+1}^2 N_0} \\ &= \frac{\left(\sqrt{\gamma_{0,N+1}} + \sum_{i=1}^N \sqrt{\frac{\gamma_{0,i} \gamma_{i,N+1}}{\hat{C}_i}}\right)^2}{N+1 + \sum_{i=1}^N \frac{\gamma_{i,N+1}}{\hat{C}_i}}. \end{aligned} \quad (5.12)$$

It is seen from eq. (5.12) that the instantaneous received SNR of an N -relay AF cooperative system employing the R-DEGC scheme is not equivalent to the result given in [77, eq. (4)].

5.2.1.2 Distributed Phase Information at the Relays

In this case, it is assumed that the n^{th} relay, $n = 1, \dots, N$, has phase information of the fading channel between itself and the destination, $\theta_{n,N+1}$, as well as phase information $\theta_{0,n}$. Note that the n^{th} relay can acquire the phase information of its forward channel, $\theta_{n,N+1}$, using the CTS packet received from the destination. It is also assumed that only the destination has (or exploits) phase information $\theta_{0,N+1}$.

The source initiates the transmission by sending the signal x_0 . The signals received at the destination and the relays in the first time slot are given in (5.1). In the second time slot, all relays forward their signals to the destination (i.e. a spectral-efficient scheduling). Note that the total available power for relay transmissions in the second time slot is P_R and each relay utilizes $P_i = \frac{1}{N} P_R$ for its transmission. The i^{th} relay amplifies its signal by the gain

$$\tilde{\beta}_i = \hat{A}_i^F \exp(-j(\theta_{0,i} + \theta_{i,N+1})). \quad (5.13)$$

The signal received at the destination in the second time slot is given by

$$y_{N+1}^{T_1, \dots, T_N} = \left(\sum_{i=1}^N \hat{A}_i^F \tilde{\alpha}_{0,i} \tilde{\alpha}_{i,N+1} \right) x_0 + \sum_{i=1}^N \tilde{\beta}_i \alpha_{i,N+1} n_i^{T_0} + n_{N+1}^{T_1, \dots, T_N}. \quad (5.14)$$

The destination co-phases the signal received from the source and then adds it to the signal received in the second time slot, $y_{N+1}^{T_1, \dots, T_N}$. Hence, it is referred to as spectral-efficient DEGC (S-DEGC) relaying. The combiner output is given by

$$\begin{aligned} y_o^{S-DEGC} &= y_{N+1}^{T_0} \exp(-j\theta_{0,N+1}) + y_{N+1}^{T_1, \dots, T_N} \\ &= \left(\tilde{\alpha}_{0,N+1} + \sum_{i=1}^N \hat{A}_i^F \tilde{\alpha}_{0,i} \tilde{\alpha}_{i,N+1} \right) x_0 + \sum_{i=1}^N \tilde{\beta}_i \alpha_{i,N+1} n_i^{T_0} \\ &\quad + \exp(-j\theta_{0,N+1}) n_{N+1}^{T_0} + n_{N+1}^{T_1, \dots, T_N} \end{aligned} \quad (5.15)$$

and the instantaneous received SNR is given by

$$\begin{aligned}\gamma_t^{S-DEGC} &= \frac{\left(\tilde{\alpha}_{0,N+1} + \sum_{i=1}^N \hat{A}_i^F \tilde{\alpha}_{0,i} \tilde{\alpha}_{i,N+1}\right)^2 P_0}{2N_0 + \sum_{i=1}^N A_i^2 \tilde{\alpha}_{i,N+1}^2 N_0} \\ &= \frac{\left(\sqrt{\gamma_{0,N+1}} + \sum_{i=1}^N \sqrt{\frac{\gamma_{0,i} \gamma_{i,N+1}}{\tilde{C}_i}}\right)^2}{2 + \sum_{i=1}^N \frac{\gamma_{i,N+1}}{\tilde{C}_i}}.\end{aligned}\quad (5.16)$$

5.2.2 Performance Analysis of DEGC Schemes

The instantaneous received SNR in an AF system employing either the R-DEGC scheme or the S-DEGC scheme can be written as

$$\gamma_t^{DEGC} = \frac{\left(\sqrt{\gamma_{0,N+1}} + \sum_{i=1}^N \sqrt{\frac{\gamma_{0,i} \gamma_{i,N+1}}{\tilde{C}_i}}\right)^2}{\mathbb{L} + \sum_{i=1}^N \frac{\gamma_{i,N+1}}{\tilde{C}_i}} \quad (5.17a)$$

where

$$\mathbb{L} = \begin{cases} N + 1, & \text{R-DEGC scheme} \\ 2, & \text{S-DEGC scheme} . \end{cases} \quad (5.17b)$$

Note that the instantaneous received SNRs in single-relay AF systems employing R-DEGC and S-DEGC schemes are the same and hence they offer the same performance. However, it is clearly seen from (5.17) that the S-DEGC scheme achieves larger instantaneous SNR and hence performance superior to the R-DEGC scheme as the number of relays increases. This is due to the fact that the relays in the S-DEGC scheme transmit simultaneously in the second time slot which in turn reduces the total noise power corrupting the signal received at the destination.

5.2.2.1 Error Probability Analysis

The instantaneous received SNR expression in an AF cooperative system employing either the R-DEGC scheme or the S-DEGC scheme given in (5.17a) can be rewritten as

$$\gamma_t^{DEGC} = \left(\sum_{i=0}^N X_i\right)^2 \quad (5.18a)$$

where

$$X_i \triangleq \frac{1}{\sqrt{\mathbb{L} + \sum_{l=1}^N \frac{\gamma_{l,N+1}}{\tilde{C}_l}}} \begin{cases} \sqrt{\gamma_{0,N+1}}, & i = 0 \\ \sqrt{\frac{\gamma_{0,i} \gamma_{i,N+1}}{\tilde{C}_i}}, & i = 1, \dots, N. \end{cases} \quad (5.18b)$$

Let $\boldsymbol{\gamma}_{N+1}$ denote vector of instantaneous SNRs over the relay-destination links, i.e. $\boldsymbol{\gamma}_{N+1} = [\gamma_{1,N+1}, \dots, \gamma_{N,N+1}]$. Note that $X_i, i = 0, \dots, N$, conditioned on $\boldsymbol{\gamma}_{N+1}$ are independent

random variables. Hence, the CHF of $Z = \sum_{i=0}^N X_i$ given $\boldsymbol{\gamma}_{N+1}$ is obtained as

$$\Psi_{Z|\boldsymbol{\gamma}_{N+1}}(w) = \prod_{i=0}^N \Psi_{X_i|\boldsymbol{\gamma}_{N+1}}(w) \quad (5.19a)$$

where

$$\Psi_{X_0|\boldsymbol{\gamma}_{N+1}}(w) = \Psi_{\sqrt{\gamma_{0,N+1}}} \left(w \sqrt{\frac{1}{\mathbb{L} + \sum_{l=1}^N \frac{\gamma_{l,N+1}}{\tilde{C}_l}}} \right) \quad (5.19b)$$

$$\Psi_{X_i|\boldsymbol{\gamma}_{N+1}}(w) = \Psi_{\sqrt{\gamma_{0,i}}} \left(w \sqrt{\frac{\frac{\gamma_{i,N+1}}{\tilde{C}_i}}{\mathbb{L} + \sum_{l=1}^N \frac{\gamma_{l,N+1}}{\tilde{C}_l}}} \right), \quad i = 1, \dots, N \quad (5.19c)$$

where $\Psi_{\sqrt{\gamma_{0,i}}}(\cdot)$, $i = 0, 1, \dots, N$, denotes the CHF of $\sqrt{\gamma_{0,i}}$ which is obtained using [90, eqs. (3.462.1) and (9.254.2)] as

$$\Psi_{\sqrt{\gamma_{0,i}}}(w) = 1 + jw\sqrt{\pi\Gamma_{0,i}} \exp\left(-\frac{1}{4}w^2\Gamma_{0,i}\right) \left(1 - Q\left(\frac{1}{2}jw\sqrt{2\Gamma_{0,i}}\right)\right) \quad (5.19d)$$

in Rayleigh fading. Then, the CHF of Z is obtained as

$$\Psi_Z(w) = \underbrace{\int_0^\infty \dots \int_0^\infty}_{N\text{-fold}} \Psi_{Z|\boldsymbol{\gamma}_{N+1}}(w) \prod_{i=1}^N f_{\gamma_{i,N+1}}(\gamma_{i,N+1}) d\gamma_{i,N+1} \quad (5.20a)$$

where $f_{\gamma_{i,N+1}}(\cdot)$ denotes the PDF of an exponential random variable. Note that the N -fold integral in (5.20a) can be evaluated using the numerical integration method given in [91, eq. (25.4.45)] as

$$\Psi_Z(w) \approx \underbrace{\sum_{n_1=1}^{N_p} \dots \sum_{n_N=1}^{N_p}}_N \prod_{i=1}^N \xi_{n_i} \Psi_{Z|\boldsymbol{\gamma}_{N+1}}(w) \Bigg|_{\substack{\gamma_{i,N+1} = \zeta_{n_i} \Gamma_{i,N+1} \\ i=1, \dots, N}} \quad (5.20b)$$

where ξ_n and ζ_n , $n = 1, \dots, N_p$, are the weights and zeros of the Laguerre polynomial of order N_p [91, Table 25.9], respectively. The symbol error probability is then obtained as

$$\begin{aligned} P_s^{DEGC} &= \mathbb{E}(Q(\tau_0 Z)) \\ &= \frac{1}{\pi} \int_0^{\frac{\pi}{2}} \Re[G(\tan(\phi)) \Psi_Z(\tan(\phi))] \sec^2(\phi) d\phi \end{aligned} \quad (5.21a)$$

using [99, eq. (7)] where τ_0 depends on the type of modulation (e.g. $\tau_0 = \sqrt{2}$ for BPSK) [89] and $G(\cdot)$ is the Fourier transform of $Q(\tau_0 z)$ given by

$$G(w) = \frac{j}{2w} \left(\sqrt{\pi} \exp\left(-\frac{w^2}{2\tau_0^2}\right) \Gamma\left(\frac{1}{2}, -\frac{w^2}{2\tau_0^2}\right) - 1 \right) \quad (5.21b)$$

using [99, Table III]. The integral in (5.21a) is numerically evaluated.

5.2.2.2 Achievable Diversity Gain

The achievable diversity gain of a wireless communication system can be determined from the large SNR behavior of its error probability. Let the parameter $SNR \triangleq \frac{P_T}{N_0}$ denote the instantaneous SNR (without fading). Obtaining an asymptotic expression for the error probability given in (5.21) when $SNR \rightarrow \infty$ is very involved. On the other hand, the achievable diversity gain can be determined using lower and upper bounds on the error probability. Recall that the MRC of the signals received at the destination in a TDMA-based AF cooperative system maximizes the instantaneous received SNR and hence results in the minimal error probability. Thus, the error performance of an AF cooperative system employing the R-DEGC scheme is lower bounded by the error performance of the corresponding system with MRC (referred to here as R-MRC). In addition, it can be readily shown that (see [75]) the instantaneous received SNR in an AF cooperative system where all relays transmit simultaneously in the second time slot, is maximized if the i^{th} relay gain is chosen as

$$\tilde{\beta}_i = w_i \sqrt{\frac{P_R/N_0}{\Gamma_{0,i} + 1}} \quad (5.22a)$$

where

$$\mathbf{w}^* = \frac{(\mathbf{I} + \mathbf{H}\mathbf{H}^\dagger)^{-1} \mathbf{h}}{\|(\mathbf{I} + \mathbf{H}\mathbf{H}^\dagger)^{-1} \mathbf{h}\|_2} \quad (5.22b)$$

where \mathbf{w} and \mathbf{h} are column vectors whose i^{th} elements are w_i and $\sqrt{N} \hat{A}_i^F \alpha_{0,i} \alpha_{i,N+1}$, respectively, \mathbf{H} is a diagonal matrix whose i^{th} diagonal element is $\sqrt{N} \hat{A}_i^F \alpha_{i,N+1}$, and $(\cdot)^\dagger$ and $\|\cdot\|_2$ denote the Hermitian and the 2-norm operations, respectively. Note that $\sum_{i=1}^N w_i^2 = 1$ and the total power used by the relays is equal to P_R . It can be shown that the instantaneous received SNR in this case is obtained as (5.3a) where γ_{T_i} is given by (5.3c) with \hat{C}_i replaced by $\frac{\hat{C}_i}{N}$. This optimal spectral-efficient scheme is referred to as S-MRC in this thesis. Therefore, the error probability of an AF cooperative system with S-MRC is a lower bound on the error probability of the corresponding system employing the S-DEGC scheme. Recall that the error probability in an AF system with MRC with fixed-gain relays decays as $\frac{1}{SNR^{N+1}}$ when $SNR \rightarrow \infty$.

Now note that the instantaneous received SNR in (5.17a) can be lower-bounded as

$$\gamma_t^{DEGC} \geq \gamma_t^{LB} = \frac{\gamma_{0,N+1} + \sum_{i=1}^N \frac{\gamma_{0,i} \gamma_{i,N+1}}{\hat{C}_i}}{\mathbb{L} + \sum_{i=1}^N \frac{\gamma_{i,N+1}}{\hat{C}_i}}. \quad (5.23)$$

The MGF of γ_t^{LB} conditioned on γ_{N+1} is given by

$$M_{\gamma_t^{LB}|\gamma_{N+1}}(s) = \left(1 - s \frac{\Gamma_{0,N+1}}{\mathbb{L} + \sum_{i=1}^N \frac{\gamma_{i,N+1}}{\hat{C}_i}}\right)^{-1} \prod_{i=1}^N \left(1 - s \frac{\Gamma_{0,i} \frac{\gamma_{i,N+1}}{\hat{C}_i}}{\mathbb{L} + \sum_{l=1}^N \frac{\gamma_{l,N+1}}{\hat{C}_l}}\right)^{-1} \quad (5.24)$$

in Rayleigh fading. Then, the MGF of γ_t^{LB} is obtained as

$$\begin{aligned} M_{\gamma_t^{LB}}(s) &= \underbrace{\int_0^\infty \dots \int_0^\infty}_{N\text{-fold}} M_{\gamma_t^{LB}|\gamma_{N+1}}(s) \prod_{i=1}^N f_{\gamma_{i,N+1}}(\gamma_{i,N+1}) d\gamma_{i,N+1} \\ &\approx \underbrace{\sum_{n_1=1}^{N_p} \dots \sum_{n_N=1}^{N_p}}_N \prod_{i=1}^N \xi_{n_i} M_{\gamma_t^{LB}|\gamma_{N+1}}(s) \Big|_{\substack{\gamma_{i,N+1} = \zeta_{n_i} \Gamma_{i,N+1} \\ i=1, \dots, N}} \end{aligned} \quad (5.25)$$

An upper bound on the symbol error probability is given by

$$P_s^{DEGC} \leq P_s^{UB} = \mathbb{E} \left(Q \left(\tau_0 \sqrt{\gamma_t^{LB}} \right) \right) \quad (5.26a)$$

which can be evaluated using the MGF of γ_t^{LB} as [89, eq. (5.3)]

$$P_s^{UB} = \frac{1}{\pi} \int_0^{\frac{\pi}{2}} M_{\gamma_t^{LB}} \left(-\frac{\tau_0^2}{2 \sin^2 \phi} \right) d\phi. \quad (5.26b)$$

Let $\mathcal{S}^{DEGC}(n_1, \dots, n_N)$ denote the summand term in (5.25). Note that $\Gamma_{i,j}$ can be rewritten as $SNR \tilde{\sigma}_{i,j}^2$ where $\tilde{\sigma}_{i,j}^2 \triangleq \sigma_{i,j}^2 \frac{P_i}{P_T}$. Then, we have

$$\lim_{SNR \rightarrow \infty} \mathcal{S}^{DEGC}(n_1, \dots, n_N) \rightarrow \frac{1}{SNR^{N+1} s^{N+1}} \mathcal{K}^{DEGC}(n_1, \dots, n_N) \quad (5.27)$$

where $\mathcal{K}^{DEGC}(n_1, \dots, n_N)$ has a constant value for all channel and system parameters given by

$$\mathcal{K}^{DEGC}(n_1, \dots, n_N) = \frac{\mathbb{L} + \sum_{k=1}^N \frac{\zeta_{n_k} \tilde{\sigma}_{k,N+1}^2}{\tilde{\sigma}_{0,k}^2}}{\tilde{\sigma}_{0,N+1}^2} \prod_{i=1}^N \left\{ \frac{\xi_{n_i} \mathbb{L} + \sum_{l=1}^N \zeta_{n_l} \frac{\tilde{\sigma}_{l,N+1}^2}{\tilde{\sigma}_{0,l}^2}}{\zeta_{n_i} \tilde{\sigma}_{i,N+1}^2} \right\}. \quad (5.28)$$

Thus, using (5.26b), the upper bound on the error probability tends to

$$\begin{aligned} \lim_{SNR \rightarrow \infty} P_e^{UB} &\rightarrow \frac{1}{SNR^{N+1}} \left\{ \frac{1}{\pi} \int_0^{\frac{\pi}{2}} \left(\frac{2}{\tau_0^2} \sin^2 \phi \right)^{N+1} d\phi \sum_{n_1=1}^{N_p} \dots \sum_{n_N=1}^{N_p} \mathcal{K}^{DEGC}(n_1, \dots, n_N) \right\} \\ &= \frac{1}{SNR^{N+1}} \frac{2^N}{\sqrt{\pi} \tau_0^{2(N+1)}} \frac{\Gamma \left(N + \frac{3}{2} \right)}{\Gamma(N+2)} \sum_{n_1=1}^{N_p} \dots \sum_{n_N=1}^{N_p} \mathcal{K}^{DEGC}(n_1, \dots, n_N) \end{aligned} \quad (5.29)$$

using [90, eq. (3.621.3)].

Since both the lower and upper bounds on the error probability decay as $\frac{1}{SNR^{N+1}}$, an N -relay AF cooperative system employing either R-DEGC or S-DEGC achieves full diversity, $N+1$.

5.2.2.3 Average Output SNR

The average output SNR for the special case of a single-relay system is obtained in closed-form as

$$\begin{aligned} \Gamma_t^{DEGC}|_{N=1} &= \frac{\pi}{2\Gamma_{1,2}} \sqrt{\hat{C}_1 \Gamma_{0,1} \Gamma_{0,2}} \left(\sqrt{\pi \Gamma_{1,2}} - 2\pi \sqrt{\mathbb{L} \hat{C}_1} \exp\left(\frac{\mathbb{L} \hat{C}_1}{\Gamma_{1,2}}\right) Q\left(\sqrt{\frac{2\mathbb{L} \hat{C}_1}{\Gamma_{1,2}}}\right) \right) \\ &+ \frac{\hat{C}_1}{\Gamma_{1,2}} \mathcal{G}\left(1, \frac{\mathbb{L} \hat{C}_1}{\Gamma_{1,2}}\right) (\Gamma_{0,2} - \mathbb{L} \Gamma_{0,1}) + \Gamma_{0,1} \end{aligned} \quad (5.30)$$

where the function $\mathcal{G}(n, \cdot)$ is defined as $\mathcal{G}(\cdot) \triangleq \exp(\cdot) E_n(\cdot)$ where $E_n(\cdot)$ is the generalized exponential integral function defined as $E_n(x) = \int_1^\infty \frac{\exp(-xt)}{t^n} dt$ [91, eq. (5.1.4)].

The average output SNR in a general AF system with an arbitrary number of relays ($N > 1$) employing either R-DEGC or S-DEGC can be evaluated by expanding the instantaneous received SNR in (5.17a) as

$$\gamma_t^{DEGC} = \sum_{k=1}^4 \phi_k \quad (5.31a)$$

where

$$\phi_k = \frac{1}{\mathbb{L} + \sum_{i=1}^N \frac{\gamma_{i,N+1}}{\hat{C}_i}} \begin{cases} \gamma_{0,N+1}, & k = 1 \\ \sum_{l=1}^N \frac{\gamma_{0,l} \gamma_{l,N+1}}{\hat{C}_l}, & k = 2 \\ 2\sqrt{\gamma_{0,N+1}} \sum_{l=1}^N \sqrt{\frac{\gamma_{0,l} \gamma_{l,N+1}}{\hat{C}_l}}, & k = 3 \\ 2 \sum_{h=1}^N \sum_{l>h}^N \sqrt{\frac{\gamma_{0,h} \gamma_{0,l} \gamma_{h,N+1} \gamma_{l,N+1}}{\hat{C}_h \hat{C}_l}}, & k = 4. \end{cases} \quad (5.31b)$$

Note that the denominator of ϕ_k involves weighted sums of independent random variables. It can be shown that the PDF of such sums for the general case of non identical links can be written in terms of sums of weighted exponential functions using the MGF and partial fraction expansion. Note that a sum of i.i.d. exponential random variables is a gamma random variable. Then, utilizing $\int_0^\infty \frac{x^{n-1}}{A+x} \exp(-\mu x) = \frac{(n-1)!}{\mu^{n-1}} \mathcal{G}(n, \mu A)$ (obtained using [90, eq. (3.353.5)]), the average output SNR, Γ_t^{DEGC} , is obtained as

$$\Gamma_t^{DEGC} = \sum_{k=1}^4 \mathbb{E}(\phi_k) \quad (5.32a)$$

where $\mathbb{E}(\phi_k)$, $k = 1, \dots, 4$, for the non i.d. links and the i.i.d. links (where $\Gamma_{i,j} = \Gamma$, $\forall i, j$ and $\hat{C}_i = C = \Gamma + 1$), are given by

$$\begin{aligned} \mathbb{E}(\phi_1)|_{non \ i.d. \ case} &= \Gamma_{0,N+1} \sum_{i=1}^N a_i \mathcal{G}\left(1, \frac{\mathbb{L} \hat{C}_i}{\Gamma_{i,N+1}}\right) \\ \mathbb{E}(\phi_1)|_{i.i.d. \ case} &= \frac{CN}{\Gamma} \mathcal{G}\left(N, \frac{\mathbb{L} NC}{\Gamma}\right) \end{aligned} \quad (5.32b)$$

$$\begin{aligned}\mathbb{E}(\phi_2) |_{\text{non i.d. case}} &= \sum_{l=1}^N \sum_{\substack{i=1 \\ i \neq l}}^N b_{l,i} \Gamma_{0,l} \int_0^\infty \frac{\gamma_{l,N+1}}{\hat{C}_l} g(\gamma_{l,N+1}) f_{\gamma_{l,N+1}}(\gamma_{l,N+1}) d\gamma_{l,N+1} \\ \mathbb{E}(\phi_2) |_{\text{i.i.d. case}} &= N(N-1)^2 \int_0^\infty \gamma \frac{\exp(-\frac{\gamma}{\Gamma})}{\Gamma} \mathcal{G}\left(N-1, (N-1) \left(\frac{\mathbb{L}C}{\Gamma} + \frac{\gamma}{\Gamma}\right)\right) d\gamma\end{aligned}\quad (5.32c)$$

$$\begin{aligned}\mathbb{E}(\phi_3) |_{\text{non i.d. case}} &= \frac{\pi}{2} \sum_{l=1}^N \sum_{\substack{i=1 \\ i \neq l}}^N b_{l,i} \int_0^\infty \sqrt{\frac{\gamma_{l,N+1} g^2(\gamma_{l,N+1})}{\hat{C}_l (\Gamma_{0,l} \Gamma_{0,N+1})}} f_{\gamma_{l,N+1}}(\gamma_{l,N+1}) d\gamma_{l,N+1} \\ \mathbb{E}(\phi_3) |_{\text{i.i.d. case}} &= \frac{\pi}{2} N(N-1)^2 \int_0^\infty \frac{\sqrt{C\gamma} \mathcal{G}\left(N-1, (N-1) \left(\frac{\mathbb{L}C}{\Gamma} + \frac{\gamma}{\Gamma}\right)\right) \exp(-\frac{\gamma}{\Gamma})}{\Gamma} d\gamma\end{aligned}\quad (5.32d)$$

and

$$\begin{aligned}\mathbb{E}(\phi_4) |_{N=2} &= \frac{\pi}{2} \sqrt{\Gamma_{0,1} \Gamma_{0,2}} \int_0^\infty \left[-\pi \sqrt{\mathbb{L} + \frac{\gamma_{1,3}}{\hat{C}_1}} \exp\left(\frac{\hat{C}_2 \left(L + \frac{\gamma_{1,3}}{\hat{C}_1}\right)}{\Gamma_{2,3}}\right) \right. \\ &\quad \left. \left(Q \left(\sqrt{\frac{2\hat{C}_2 \left(\mathbb{L} + \frac{\gamma_{1,3}}{\hat{C}_1}\right)}{\Gamma_{2,3}}} \right) \right) + \sqrt{\pi \Gamma_{2,3}} \sqrt{\frac{\gamma_{1,3}}{\hat{C}_1 \hat{C}_2}} \frac{\hat{C}_2}{\Gamma_{2,3}} f_{\gamma_{1,3}}(\gamma_{1,3}) \right] d\gamma_{1,3} \\ \mathbb{E}(\phi_4) |_{\text{non } N>2 \text{ i.d. case}} &= \frac{\pi}{2} \sum_{m=1}^N \sum_{\substack{k>m \\ i \neq k \neq m}}^N \int_0^\infty \int_0^\infty \tilde{b}_{k,m,i} \sqrt{\frac{\Gamma_{0,m} \Gamma_{0,k} \gamma_{m,N+1} \gamma_{k,N+1}}{\hat{C}_k \hat{C}_m}} \\ &\quad \tilde{g}(\gamma_{m,N+1}, \gamma_{k,N+1}) f_{\gamma_{m,N+1}}(\gamma_{m,N+1}) f_{\gamma_{k,N+1}}(\gamma_{k,N+1}) d\gamma_{m,N+1} d\gamma_{k,N+1} \\ \mathbb{E}(\phi_4) |_{\text{i.i.d. case } N>2} &= \frac{\pi}{12\Gamma^2} N(N^2-1)(N-2) \int_0^\infty \int_0^\infty \sqrt{\gamma_1 \gamma_2} \\ &\quad \mathcal{G}\left(N-2, (N-2) \left(\frac{\mathbb{L}C}{\Gamma} + \frac{\gamma_1}{\Gamma} + \frac{\gamma_2}{\Gamma}\right)\right) \exp\left(-\frac{\gamma_1 + \gamma_2}{\Gamma}\right) d\gamma_1 d\gamma_2\end{aligned}\quad (5.32e)$$

where

$$g(\gamma_{l,N+1}) = \mathcal{G}\left(1, \frac{\hat{C}_i}{\Gamma_{i,N+1}} \left(\mathbb{L} + \frac{\gamma_{l,N+1}}{\hat{C}_l}\right)\right) \quad (5.32f)$$

$$\tilde{g}(\gamma_{m,N+1}, \gamma_{k,N+1}) = \mathcal{G}\left(1, \left(\mathbb{L} + \frac{\gamma_{m,N+1}}{\hat{C}_m} + \frac{\gamma_{k,N+1}}{\hat{C}_k}\right) \frac{\hat{C}_i}{\Gamma_{i,N+1}}\right) \quad (5.32g)$$

and

$$a_i = \frac{\left(\frac{\Gamma_{i,N+1}}{\hat{C}_i}\right)^{N-2}}{\prod_{\substack{i=1 \\ i \neq k}}^N \frac{\Gamma_{i,N+1}}{\hat{C}_i} - \frac{\Gamma_{k,N+1}}{\hat{C}_k}} \quad (5.32h)$$

$$b_{l,i} = \frac{a_i \hat{C}_i \left(\frac{\Gamma_{i,N+1}}{\hat{C}_i} - \frac{\Gamma_{l,N+1}}{\hat{C}_l}\right)}{\Gamma_{i,N+1}} \quad (5.32i)$$

$$\tilde{b}_{k,m,i} = \frac{a_i \hat{C}_i^2 \left(\frac{\Gamma_{i,N+1}}{\hat{C}_i} - \frac{\Gamma_{m,N+1}}{\hat{C}_m}\right) \left(\frac{\Gamma_{i,N+1}}{\hat{C}_i} - \frac{\Gamma_{k,N+1}}{\hat{C}_k}\right)}{\Gamma_{i,N+1}^2}. \quad (5.32j)$$

Similar to (5.20a), the single and double integrals in (5.32c)-(5.32e) can be readily evaluated using the numerical integration given in [91, eq. (25.4.45)].

5.2.2.4 Ergodic Capacity Analysis

The input-output relations in AF cooperative systems employing R-DEGC and S-DEGC relaying are given in (5.11) and (5.15), respectively. Suppose that the transmitted signal from the source is chosen from an i.i.d. Gaussian codebook in which the codewords are long enough to capture the ergodic nature of the fading channels. Then, using [71, Theorem 1], the ergodic capacity of AF systems employing DEGC schemes is obtained as

$$\mathcal{E}^{DEGC} = \frac{1}{\mathbb{L}} \mathbb{E} \left\{ \log \left(1 + \gamma_t^{DEGC} \right) \right\} = \frac{1}{\mathbb{L}} \mathbb{E} \left\{ \log \left(1 + Z^2 \right) \right\} \quad (5.33)$$

where γ_t^{DEGC} and \mathbb{L} are given in (5.17a) and (5.17b), respectively. The factor $\frac{1}{\mathbb{L}}$ reflects the fact that the information is transmitted over $N + 1$ orthogonal time slots in the R-DEGC scheme and over two time slots in the S-DEGC scheme. In addition, recall that the S-DEGC scheme achieves larger instantaneous received SNR than does the R-DEGC scheme. Thus, it is expected that a system employing S-DEGC offers higher ergodic capacity than the corresponding system with R-DEGC.

Note that although the CHF of Z is known and is given in (5.20), a closed-form expression for the PDF of Z which facilitates exact evaluation of the ergodic capacity in (5.33) cannot be obtained, even for the special case of a single-relay system. Hence, in the sequel, we derive upper and lower bounds on the ergodic capacity. An upper bound on the ergodic capacity is obtained using Jensen's inequality [96] as

$$\mathcal{E}^{DEGC} < \mathcal{E}_{UP}^{DEGC} = \frac{1}{\mathbb{L}} \log \left(1 + \Gamma_t^{DEGC} \right) \quad (5.34)$$

where Γ_t^{DEGC} is given in (5.30) for the single-relay system and in (5.32) for AF cooperative systems with an arbitrary number of relays.

Now note that $\log(1 + \gamma_t^{DEGC})$ can be lower-bounded as

$$\log \left(1 + \gamma_t^{DEGC} \right) \geq \log(\gamma_t^{DEGC}) = 2 \log(Z) \quad (5.35)$$

which is very tight for $\gamma_t^{DEGC} \gg 1$. Thus, a lower-bound on the ergodic capacity in (5.33) is obtained as

$$\mathcal{E}^{DEGC} > \mathcal{E}_{LB}^{DEGC} = \frac{2}{\mathbb{L}} \mathbb{E} (\log(Z)). \quad (5.36)$$

For evaluation of the lower bound given in (5.36), we will first find an integral representation for the logarithm function. Recall the infinite series representation of $\ln(z)$ given

by [90, eq. (1.512.2)]

$$\ln(z) = 2 \sum_{n=1}^{\infty} \frac{1}{2n-1} \left(\frac{z-1}{z+1} \right)^{2n-1}, \quad \forall z > 0. \quad (5.37a)$$

Note that other series for $\ln(z)$ given in [90, eqs. (1.512.1) and (1.512.3)] cannot be used here because in both cases the radius of convergence is not from 0 to infinity. The series in (5.37a) can be rewritten as

$$\ln(z) = 2 \sum_{n=1}^{\infty} \frac{1}{2n-1} \int_0^{\infty} \frac{t^{2n-2}}{\Gamma(2n-1)} \exp\left(-t \left(\frac{x+1}{x-1}\right)\right) dt \quad (5.37b)$$

$$= \int_0^{\infty} \frac{1}{t} (1 - \exp(-2t)) \exp\left(-\frac{2t}{x-1}\right) dt \quad (5.37c)$$

$$= \int_0^{\infty} \frac{1}{v} (\exp(-2v) - \exp(-2vz)) dv \quad (5.37d)$$

where we have used the integral $\int_0^{\infty} \frac{t^{n-1} \exp(-\frac{t}{\mu})}{\Gamma(n)} dt = \mu^n$ [90, eq. (3.381.4)], the MacLaurin series for the hyperbolic sine function given in [90, eq. (1.411.2)], and the change of variable $v = \frac{t}{z-1}$ in eqs. (5.37b)-(5.37d), respectively. The lower bound on the ergodic capacity is then obtained as

$$\begin{aligned} \mathcal{E}_{LB}^{DEGC} &= \frac{2}{\mathbb{L}} \int_0^{\infty} \frac{1}{v} (\exp(-2v) - \Psi_Z(2jv)) dv \\ &= \frac{4}{\mathbb{L}} \int_0^{\frac{\pi}{2}} \frac{1}{\sin(2\theta)} [\exp(-2 \tan(\theta)) - \Psi_Z(2j \tan(\theta))] d\theta \end{aligned} \quad (5.38)$$

where $\Psi_Z(\cdot)$ is given in (5.20).

5.2.3 Numerical Results and Discussion

In this section, we present numerical examples for the performance of AF cooperative systems employing the R-DEGC and S-DEGC schemes. In the numerical examples, it is assumed that the average link SNRs follow an exponentially decaying power delay profile, i.e. $\Gamma_{0,i} = \Gamma_{i,N+1} = \Gamma_{s,d} \exp(-\delta i)$, $i = 1, \dots, N$, where δ is the power decay factor. Theoretical results in all examples are obtained assuming $N_p = 15$.

5.2.3.1 Performance Analysis Results

Figures 5.4 and 5.5, respectively, show the bit error probabilities and the average output SNR versus $\Gamma_{s,d}$ of different AF cooperative systems. It is seen from both figures that the theoretical results are in precise agreement with the simulation results. It is seen from Figure 5.4 that the systems with R-DEGC or S-DEGC achieve full diversity. Figures 5.6 and 5.7 show the ergodic capacities of double-relay systems with i.i.d. links ($\delta = 0$) and

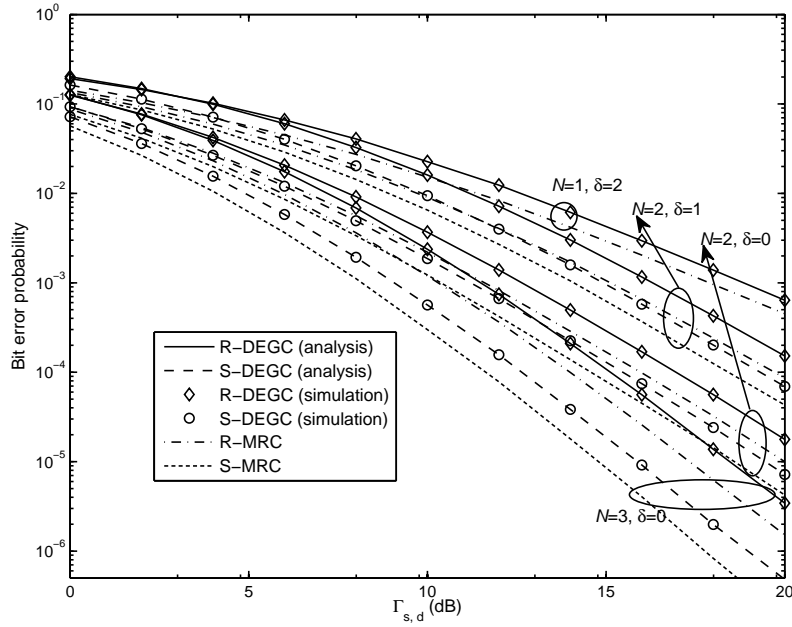


Figure 5.4. Bit error probabilities of different BPSK AF multi-relay systems in Rayleigh fading with different power decay factors.

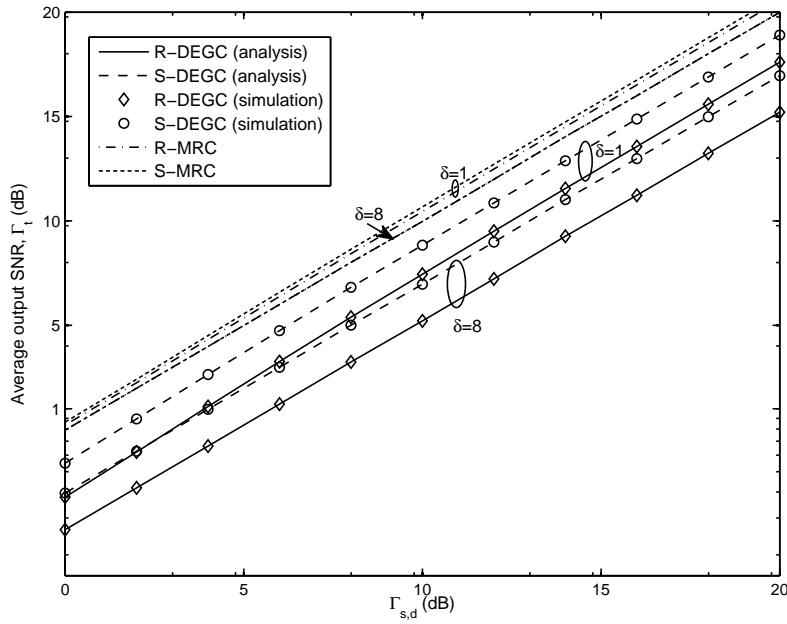


Figure 5.5. Average output SNRs of AF double-relay systems in Rayleigh fading with different power decay factors.

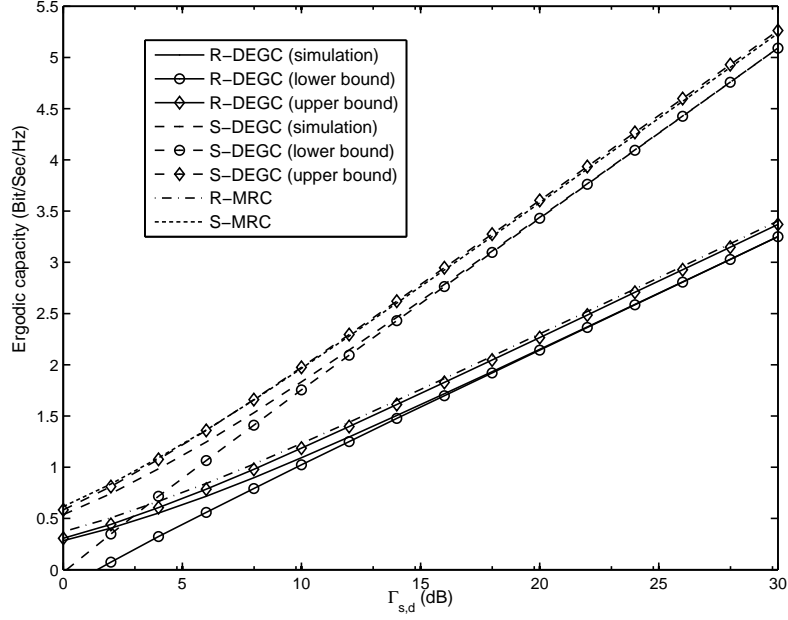


Figure 5.6. Ergodic capacities of AF double-relay systems in Rayleigh fading with i.i.d. links ($\delta = 0$).

non i.i.d. links ($\delta = 1$), respectively. It is seen from both Figures 5.6 and 5.7 that the upper bound on the ergodic capacity is tight in small SNR regions. For example, the inaccuracies of the upper bound in the system employing S-DEGC with i.i.d. and non i.i.d. links are about 9% and 12% at 5 dB, respectively. The lower bound on the ergodic capacity, on the other hand, gets very tight as SNR increases. This is because the inequality in (5.35) approaches equality with increasing SNR.

In Figures 5.4-5.7, we have also plotted the bit error probabilities, the average output SNRs, and ergodic capacities³ (obtained using Monte Carlo simulation) of AF systems with R-MRC and S-MRC. It is seen from these figures that the gap between performances of systems employing R-DEGC/S-DEGC and systems employing R-MRC/S-MRC increases as the parameter δ increases. For instance, the gap between the double-relay systems with R-DEGC and R-MRC at error probability 10^{-3} is about 1 dB and 1.2 dB for $\delta = 0$ and $\delta = 1$, respectively. Also, the SNR loss between the double-relay system with S-DEGC and the corresponding system with S-MRC at ergodic capacity 2 Bit/Sec/Hz is about 0.7 dB for the i.i.d. case ($\delta = 0$) and 1.5 dB for the non i.i.d. case ($\delta = 1$). This performance loss is a reasonable trade-off considering the low complexity and distributed implementation of

³The ergodic capacity of a system employing S-MRC can be obtained using (5.33) in which $\mathbb{L} = 2$ and γ_t^{DEGC} is replaced by the corresponding instantaneous received SNR in an S-MRC system.

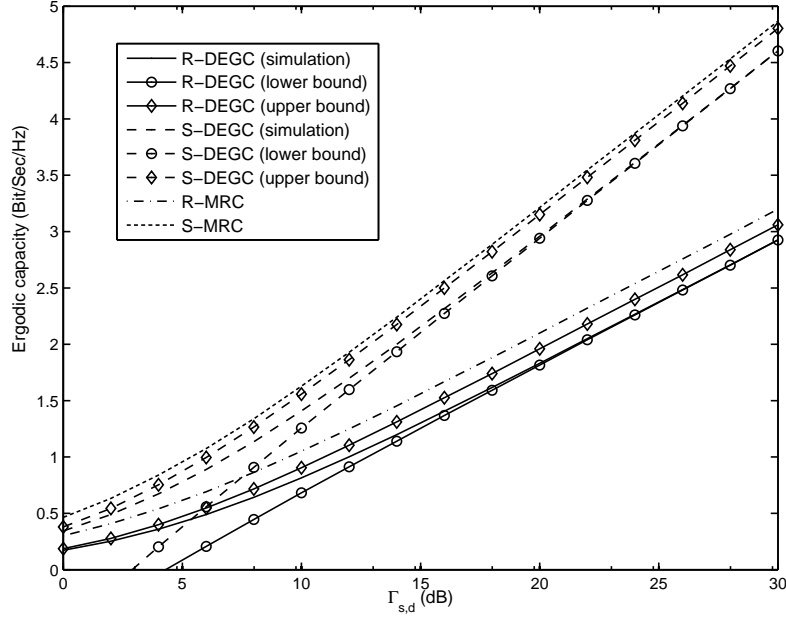


Figure 5.7. Ergodic capacities of AF double-relay systems in Rayleigh fading with non i.i.d. links ($\delta = 1$).

the DEGC schemes.

In addition, using eq. (5.3), it can be readily shown that the instantaneous received SNRs in systems with R-MRC and S-MRC get larger as the number of relays increases. Thus, as seen in Figure 5.4, these systems offer better performances with increasing the number of relays and achieve full diversity gains, as shown in Sections 5.1.2.1 and 5.2.2.2. Furthermore, note that in systems with R-MRC or R-DEGC, the destination should combine $N + 1$ signals received from the source and N relays in $N + 1$ orthogonal time slots. However, in systems with S-MRC or S-DEGC, the relays transmit simultaneously and hence the destination combines two signals, the one received from the source in the first time slot with the signals received from the relays in the second time slot. Combining more signals at the destination in systems with R-MRC or R-DEGC increases the total noise power at the combiner output (e.g. see eq. (5.17)). Thus, as seen from Figure 5.4, systems with S-MRC or S-DEGC achieve better performance gains than the corresponding systems with R-MRC or R-DEGC, especially by increasing the number of relays. For instance, the performance gaps between double-relay S-MRC and R-MRC systems with i.i.d. links ($\delta = 0$), and between double-relay S-DEGC and S-MRC systems with i.i.d. links are, respectively, about 1 dB and 1.7 dB at error probability 10^{-4} . These SNR gaps increase, respectively, about 1.3 dB and 0.8 dB in the corresponding triple-relay systems.

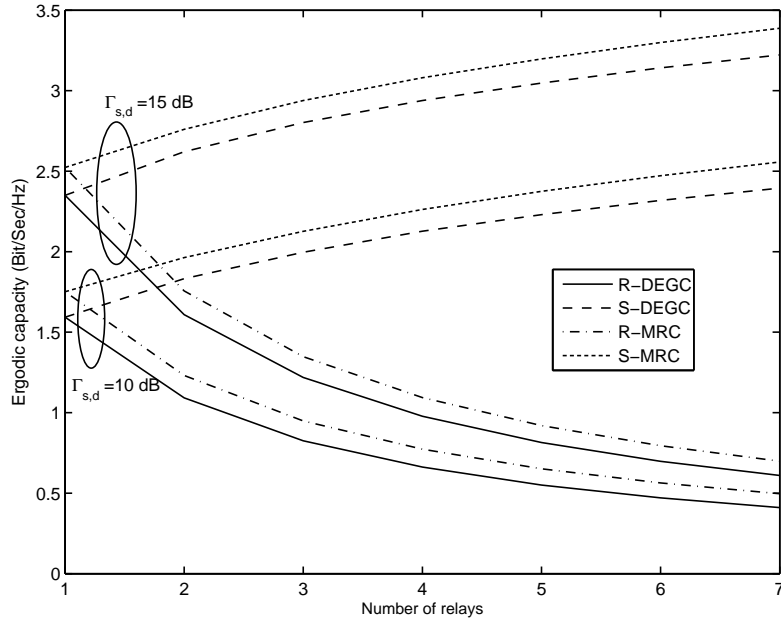


Figure 5.8. Ergodic capacities versus number of relays of different AF multi-relay systems operating over Rayleigh fading channels with $\delta = 0$.

Figure 5.8 compares the simulated ergodic capacities versus the number of relays of different AF multi-relay systems. Recall that the information in systems with R-MRC and R-DEGC is transmitted over $N + 1$ time slots. Thus, as seen from Figure 5.8, increasing the number of relays degrades the ergodic capacity of these systems. However, in systems with S-MRC and S-DEGC the relays transmit simultaneously in the second time slot. In addition, using eqs. (5.3) and (5.17), it can be readily shown that systems with S-MRC and S-DEGC achieve larger instantaneous received SNR at the destination than the corresponding systems with R-MRC and R-DEGC, especially with increasing the number of relays. Thus, as seen from Figure 5.8, systems with S-MRC and S-DEGC significantly outperform those with R-MRC and R-DEGC, especially for larger numbers of relays.

Furthermore, using eq. (5.3) with \hat{C}_i replaced by \hat{C}_i/N , it can be readily shown that the instantaneous received SNR in systems with S-MRC always become larger by increasing the number of relays. Thus, in contrast to the systems employing R-MRC, the ergodic capacity of systems with S-MRC improves by increasing the number of relays, as seen from Figure 5.8. It is also seen that S-DEGC systems considered in Figure 5.8 achieve higher ergodic capacities for larger numbers of relays. However, as discussed later in Section 5.2.3.2, increasing the number of relays does not necessarily improve the performance of a

system employing S-DEGC in small to moderate SNR regions.

5.2.3.2 Impact of Combining Loss

The proposed DEGC schemes achieve full diversity order while they are simpler to implement than MRC because they do not require channel amplitude estimation. However, adding more relays will not necessarily improve the performance for small to moderate values of SNR. This is because the signals received at the destination are added together with equal weights and hence those in a deep fade may degrade the performance. It is important to determine how much performance may be given up by adding relays in the low complexity AF cooperative systems employing R-DEGC and S-DEGC. This issue, referred to as combining loss [89], is examined in Figures 5.9-5.11.

Figures 5.9-5.11, respectively, show the bit error probabilities, average output SNRs, and ergodic capacities versus number of relays for different AF cooperative systems. It is seen that the systems with S-DEGC significantly outperform systems with R-DEGC especially when the number of relays increases, as expected. In particular, as seen in Figure 5.11, the ergodic capacity of a system employing R-DEGC significantly deteriorates by increasing the number of relays. This is mainly due to the repetition-based scheduling protocol used in this system. It is also seen from Figure 5.11 that the upper bound on the ergodic capacity in systems employing R-DEGC is tighter than in systems with S-DEGC schemes especially for larger numbers of relays.

It is seen from Figures 5.9 and 5.10 that when the number of relays increases, the performance does not necessarily improve. In fact, there is an optimum number of relays which either maximizes the average output SNR, N_{\max} , or minimizes the error probability, N_{\min} . As mentioned earlier, this is due to the combining of signals received at the destination with equal weights. Note that the upper bound on the ergodic capacity in systems employing S-DEGC follows the same behavior as the simulated ergodic capacity, as seen in Figure 5.11. Since the upper bound is a logarithm function of the average output SNR and the logarithm function is monotonically increasing with respect to its argument, N_{\max} in systems employing S-DEGC also denotes the optimum number of relays that maximizes the ergodic capacity in these systems. Table 5.1 presents the optimum number of relays N_{\max} and N_{\min} for R-DEGC and S-DEGC schemes under different sets of channel conditions. It is seen from Table 5.1, Figure 5.9 and Figure 5.10 that the R-DEGC scheme is more sensitive to the combining loss than the S-DEGC scheme. This is due to the repetition-based scheduling protocol employed in the R-DEGC scheme, which requires combination

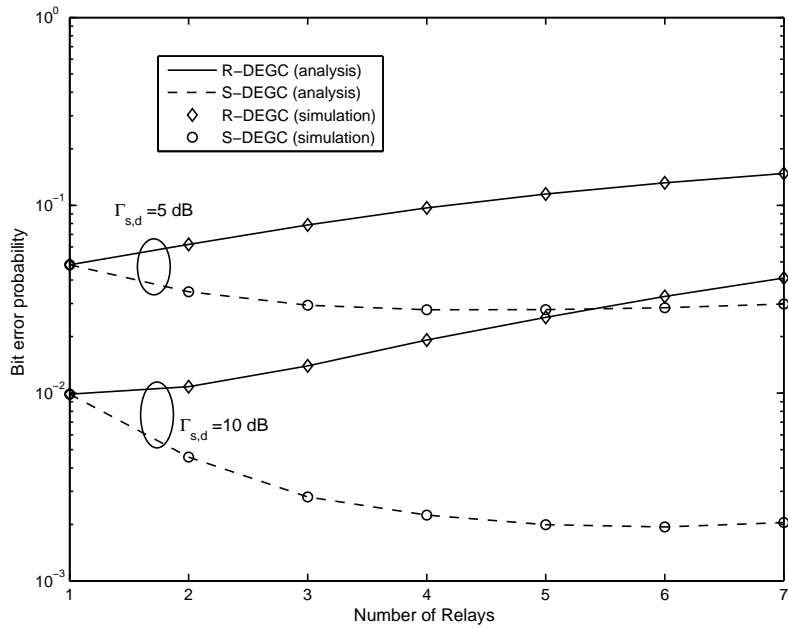


Figure 5.9. Bit error probabilities versus number of relays of different BPSK AF multi-relay systems operating over Rayleigh fading channels with $\delta = 0.5$.

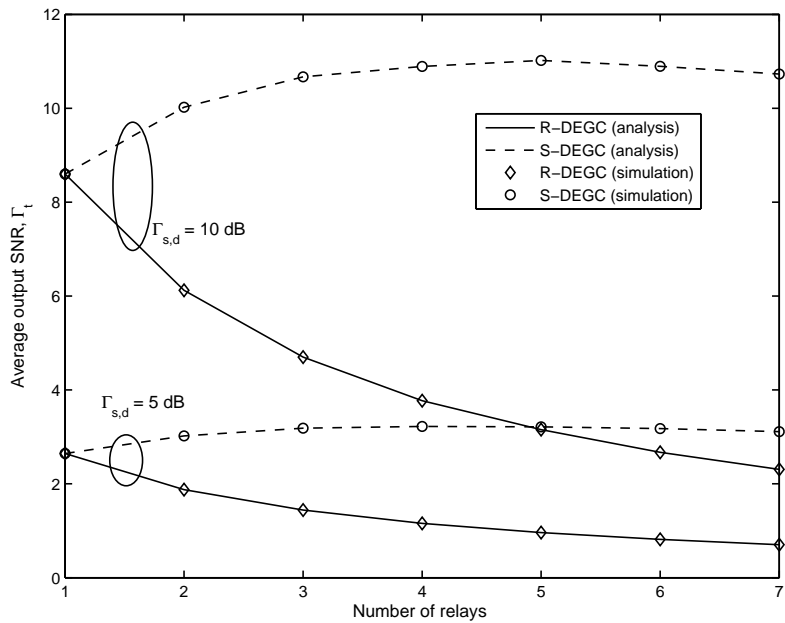


Figure 5.10. Average output SNRs versus number of relays of different AF multi-relay systems operating over Rayleigh fading channels with $\delta = 0.5$.

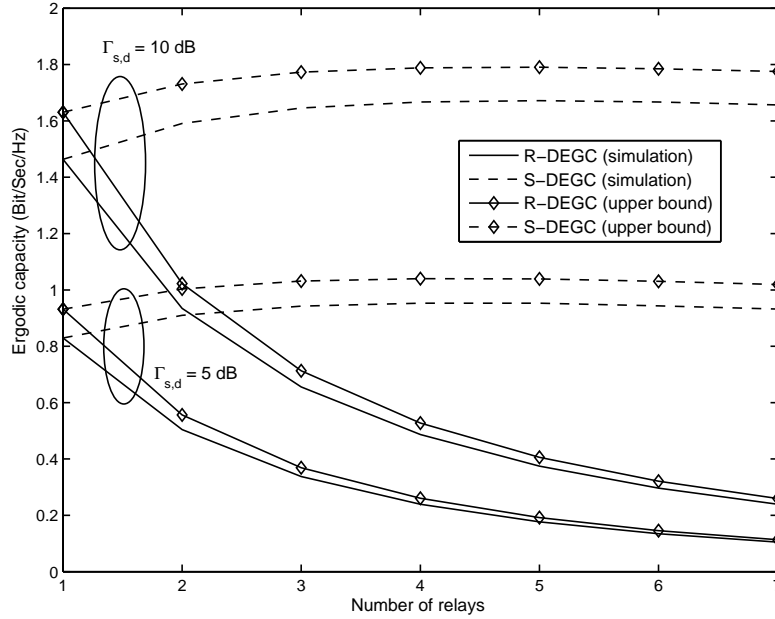


Figure 5.11. Ergodic capacities versus number of relays of different AF multi-relay systems operating over Rayleigh fading channels with $\delta = 0.5$.

of $N + 1$ branches at the destination. Combining more branches in small SNR regions will more probably contribute to the noise rather than signal enhancement and consequently degrades the performance. Therefore, specifying the optimum number of relays is particularly important for the R-DEGC scheme since adding more relays not only degrades the performance but also requires more time slots and hence degrades the spectral efficiency (as seen in Figure 5.11) as well as requiring higher complexity. In addition, it is seen from Table 5.1 and Figures 5.9 and 5.10 that the impact of combining loss on the average output SNR is more severe than on the bit error probability. Note that the expression given in (5.32) for the average output SNR has less computational complexity than the error probability expression given in (5.21), especially as the number of relays increases. Thus, using the expression in (5.32), one can get an estimate for the best number of relays to be used in an AF system employing the proposed DEGC schemes. Note that upon determining the optimal number of relays, a selection algorithm can be employed to select the best relays (based on a given set of criteria) among a pool of potential terminals for cooperating with the source. For example, an algorithmic relay selection method is proposed in [77] which selects the best relays based on the first- and second-order statistics of the individual link SNRs.

Table 5.1. Optimum number of relays for different AF multi-relay systems employing the proposed R-DEGC and S-DEGC schemes

$\Gamma_{s,d}$ (dB)	δ	N_{\max}^{R-DEGC}	N_{\min}^{R-DEGC}	N_{\max}^{S-DEGC}	N_{\min}^{S-DEGC}
1	0.25	1	1	7	8
1	0.3	1	1	6	7
1	0.5	1	1	3	4
5	0.25	1	2	8	9
5	0.3	1	2	7	8
5	0.5	1	1	4	5
10	0.3	1	2	8	10
10	0.4	1	1	6	7
10	0.5	1	1	5	6
15	0.4	1	3	6	9

5.3 Low Complexity Noncoherent Receiver

As mentioned earlier, the general noncoherent ML detection of an AF multi-relay cooperative system is too complex for implementation. In addition, the suboptimal noncoherent receivers proposed for AF cooperative systems either have high complexity or do not achieve full spatial diversity. In this section, we propose employment of a detection scheme in a noncoherent AF system based on square-law envelope (energy) detection [89] at the destination. Note that the relays must re-transmit their received signals over orthogonal time slots⁴. Then, a selection scheme examines the outputs at the square-law detector obtained in all time slots and selects the maximum one for detection. Thus, this scheme is referred to as *maximum energy selection* (MES). We obtain an expression for evaluation of the symbol error probability of the MES scheme when employed in a noncoherent multi-relay AF cooperative system with M -ary FSK signaling. It is also shown that an AF cooperative system employing the MES scheme achieves full spatial diversity.

5.3.1 System Model

Consider a multi-relay cooperative system shown in Figure 2.2. It is assumed that the source transmits the signal x_0 chosen from an M -ary FSK constellation in which all wave-

⁴It can be shown that if the relays transmit simultaneously, only second-order diversity can be achieved regardless of the number of relays.

forms during the symbol interval are equiprobable and have the same energy E_s ⁵.

The source broadcasts the signal x_0 in the first time slot. The relays and the destination receive the signal $y_i^{T_0}$, $i = 1, \dots, N + 1$, given in (5.1). The signal received at the i^{th} relay, $y_i^{T_0}$, $i = 1, \dots, N$, is amplified by a gain \hat{A}_i^F and then forwarded to the destination in a predetermined time slot. The amplification at the i^{th} relay is given by (5.2c) ensuring that a long-term power constraint at the relay is satisfied [41]- [43]. The signal received at the destination through the i^{th} relay is given by .

$$y_{N+1}^{T_i} = \hat{A}_i^F \alpha_{i,N+1} y_i^{T_0} + n_{N+1}^{T_i} = \hat{A}_i^F \alpha_{0,i} \alpha_{i,N+1} x_0 + \hat{A}_i^F \alpha_{i,N+1} n_i^{T_0} + n_{N+1}^{T_i}. \quad (5.39)$$

The destination employs a square-law detector at each branch. Without loss of generality, we can assume that the first symbol from the signal constellation is sent. The square-law detector output for the i^{th} branch is given by

$$V_{i,m} = \begin{cases} \left| 2\alpha_{0,N+1} E_s + U_{N+1}^{T_0} \right|^2, & i = 0 \text{ and } m = 1 \\ \left| 2A_i \alpha_{0,i} \alpha_{i,N+1} E_s + A_i \alpha_{i,N+1} U_{i_1} + U_{N+1}^{T_i} \right|^2, & i = 1, \dots, N \text{ and } m = 1 \\ \left| U_{N+1}^{T_0} \right|^2, & i = 0 \text{ and } m = 2, \dots, M \\ \left| A_i \alpha_{i,N+1} U_{i_m} + U_{N+1}^{T_i} \right|^2, & i = 1, \dots, N \text{ and } m = 2, \dots, M \end{cases} \quad (5.40)$$

where the random variables U_{k_h} , $k = 1, 2, \dots, N + 1$, $h = 1, 2, \dots, M$ are independent complex Gaussian random variables with zero mean and variance $4E_s N_0$ [100].

At the destination, an MES scheme is employed which selects the maximum output from all branches. The destination decision rule is then given by

$$[\hat{i}, \hat{m}] = \arg \max_{\substack{i=0, \dots, N \\ m=1, \dots, M}} \{V_{i,m}\} \quad (5.41)$$

where \hat{i} is the selected branch and \hat{m} is the detected symbol.

5.3.2 Performance Analysis of Noncoherent MES Scheme

5.3.2.1 Error Probability Analysis

The MES scheme in an AF N -relay system selects the maximum outputs of the square-law detector obtained in $N + 1$ time slots. Assuming the first symbol from the signal constellation is sent, then $V_{i,1}$, $i = 0, \dots, N$, contains both signal and noise terms, whereas $V_{i,m}$, $i = 0, \dots, N$, $m = 2, \dots, M$, consists of noise only. Thus, a symbol error occurs if a $V_{i,m}$, $m \neq 1$, $i = 0, \dots, N$, is greater than all $V_{i,1}$, $i = 0, \dots, N$. Therefore, the

⁵Assuming each transmission has a unit duration, the symbol energy can be considered as the transmit power [73].

symbol error probability in a noncoherent M -FSK AF multi-relay system employing the MES scheme is given by

$$P_s^{MES} = Pr \left(\max_{i=0,\dots,N} \{V_{i,1}\} < \max_{\substack{i=0,\dots,N \\ m=2,\dots,M}} \{V_{i,m}\} \right). \quad (5.42)$$

Note that $V_{0,m}$ and $V_{i,m}|\gamma_{i,N+1}$, $i = 1, \dots, N$, and $m = 1, \dots, M$ are exponential random variables with mean $\lambda_{i,m}$ given by

$$\lambda_{i,m} = \begin{cases} 4E_s N_0 (1 + \Gamma_{0,N+1}), & i = 0 \text{ and } m = 1 \\ 4E_s N_0, & i = 0 \text{ and } m = 2, \dots, M \\ 4E_s N_0 (\gamma_{i,N+1} + 1), & i = 1, \dots, N \text{ and } m = 1 \\ 4E_s N_0 \left(\frac{\gamma_{i,N+1}}{\tilde{C}_i} + 1 \right), & i = 1, \dots, N \text{ and } m = 2, \dots, M. \end{cases} \quad (5.43)$$

Now, let $W = \max_{i=0,\dots,N} \{V_{i,1}\}$ and $U = \max_{\substack{i=0,\dots,N \\ m=2,\dots,M}} \{V_{i,m}\}$. Then, the symbol error probability in (5.42) can be written as

$$\begin{aligned} P_s^{MES} &= Pr(W < U) \\ &= \underbrace{\int_0^\infty \dots \int_0^\infty}_{N\text{-fold}} \underbrace{\left\{ \int_0^\infty Pr(W < u|U = u, \boldsymbol{\gamma}_{N+1}) f_{U|\boldsymbol{\gamma}_{N+1}}(u) du \right\}}_{P_{e|\boldsymbol{\gamma}_{N+1}}^{MES}} f_{\boldsymbol{\gamma}_{N+1}}(\boldsymbol{\gamma}_{N+1}) d\boldsymbol{\gamma}_{N+1} \end{aligned} \quad (5.44a)$$

where $\boldsymbol{\gamma}_{N+1} = [\gamma_{1,N+1}, \gamma_{2,N+1}, \dots, \gamma_{N,N+1}]$ is vector of instantaneous received SNRs over the relay-destination links,

$$\begin{aligned} Pr(W < u|U = u, \boldsymbol{\gamma}_{N+1}) &= F_{V_{0,1}}(u) \prod_{i=1}^N F_{V_{i,1}|\gamma_{i,N+1}}(u) \\ &= \prod_{i=0}^N \left(1 - \exp\left(-\frac{u}{\lambda_{i,1}}\right) \right) \\ &= 1 + \sum_{k=1}^N \sum_{i_1=1}^N \sum_{i_2>i_1}^N \dots \sum_{i_k>i_{k-1}}^N (-1)^k \exp\left(-u \sum_{m=1}^k \frac{1}{\lambda_{i_m,1}}\right) \end{aligned} \quad (5.44b)$$

in which $F_{V_{i,j}}(\cdot)$ denotes CDF of an exponential random variable, and

$$\begin{aligned} f_{U|\boldsymbol{\gamma}_{N+1}}(u) &= \sum_{k=2}^M f_{V_{0,k}}(u) \prod_{\substack{l=2 \\ l \neq k}}^M F_{V_{0,l}}(u) \prod_{i=1}^N \prod_{m=2}^M F_{V_{i,m}|\gamma_{i,N+1}}(u) \\ &+ \sum_{k=2}^M \sum_{i=1}^N f_{V_{i,k}|\gamma_{i,N+1}}(u) \prod_{m=2}^M F_{V_{0,m}}(u) \prod_{\substack{h=2 \\ h \neq k}}^M \prod_{\substack{l=1 \\ l \neq i}}^M F_{V_{l,h}|\gamma_{l,N+1}}(u). \end{aligned} \quad (5.44c)$$

The expression in (5.44c) can be simplified because $f_{U|\boldsymbol{\gamma}_{N+1}}(u)$ can be written as a weighted sum of exponential functions as [101, eqs. (8.16) and (8.21)]

$$f_{U|\boldsymbol{\gamma}_{N+1}}(u) = \frac{1}{4E_s N_0} \sum_v \mathcal{W}_v(\tilde{\boldsymbol{\lambda}}) \exp\left(-\frac{u}{4E_s N_0} \mathcal{P}_v(\tilde{\boldsymbol{\lambda}})\right) \quad (5.44d)$$

where $\tilde{\lambda}$ denotes the vector of $\tilde{\lambda}_{i,m} \triangleq \frac{\lambda_{i,m}}{4E_s N_0}$, $i = 0 \dots, N$, $m = 2, \dots, M$, and $\mathcal{W}_v(\cdot)$ and $\mathcal{P}_v(\cdot)$, $v = 1, 2, \dots$ are simple functions in terms of sum of $\frac{1}{\tilde{\lambda}_{i,m}}$, $i \in \{0, 1, \dots, N\}$, $m \in \{2, 3, \dots, M\}$. The functions $\mathcal{W}_v(\cdot)$ and $\mathcal{P}_v(\cdot)$ can be readily obtained by expanding eq. (5.44c). For instance, for the case of a BFSK single-relay system, one has $\mathcal{W}_1 = \mathcal{P}_1 = \frac{1}{\tilde{\lambda}_{0,2}}$, $\mathcal{W}_2 = \mathcal{P}_2 = \frac{1}{\tilde{\lambda}_{1,2}}$, and $\mathcal{W}_3 = \mathcal{P}_3 = \frac{1}{\tilde{\lambda}_{0,2}} + \frac{1}{\tilde{\lambda}_{1,2}}$. Using (5.44b) and (5.44d), the conditional probability of symbol error given γ_{N+1} is obtained as

$$P_{s|\gamma_{N+1}}^{MES}(\gamma_{N+1}) = 1 + \sum_v \sum_{k=1}^N \sum_{i_1=1}^N \sum_{i_2>i_1}^N \dots \sum_{i_k>i_{k-1}}^N (-1)^k \frac{\mathcal{W}_v(\tilde{\lambda})}{\mathcal{P}_v(\tilde{\lambda}) + \sum_{m=1}^k \frac{1}{\tilde{\lambda}_{i_m,1}}}. \quad (5.44e)$$

The symbol error probability in (5.44) can be evaluated using the numerical integration method given in [91, eq. (25.4.45)] as

$$P_s^{MES} \approx \sum_{n_1=1}^{N_p} \dots \sum_{n_N=1}^{N_p} \prod_{i=1}^N \xi_{n_i} P_{e|\gamma_{N+1}}^{MES}(\gamma_{N+1}) \Big|_{\substack{\gamma_{i,N+1} = \xi_{n_i} \Gamma_{i,N+1} \\ i=1, \dots, N}}. \quad (5.45)$$

5.3.2.2 Achievable Diversity Gain

Achievable diversity gain in a noncoherent AF cooperative system employing the proposed MES scheme can be determined from the large SNR behavior of the symbol error probability given in (5.44). The asymptotic symbol error probability for sufficiently large values of SNR can be examined by considering the value of the first nonzero order derivative of the pdf of the random variable $W|\gamma_{N+1}$ at the origin. Note that W is the maximum of $N + 1$ independent random variables, $V_{i,1}$, $i = 0, 1, \dots, N$. Thus, according to [102], the first $N - 1$ order derivatives of the PDF of W at the origin are zero and its N^{th} order derivative at zero is given by [102, eq. (14)]

$$\frac{\partial^N f_W}{\partial w^N}(0) = (N + 1)! \prod_{i=0}^N f_{V_{i,1}}(0). \quad (5.46)$$

Thus, using (3.21), we have

$$Pr(W < u | U = u, \gamma_{N+1}) \rightarrow \frac{u^{N+1}}{(4E_s N_0)^{N+1}} \prod_{i=0}^N \frac{1}{\tilde{\lambda}_{i,1}} \quad (5.47)$$

for large values of SNR. Then, by taking the average of (5.47) with respect to the random variable $U|\gamma_{N+1}$ having the PDF given in (5.44d), an asymptotic expression for the conditional symbol error probability, $P_{s|\gamma_{N+1}}^{MES}$, is obtained as

$$P_{s|\gamma_{N+1}}^{MES} \rightarrow (N + 1)! \prod_{i=0}^N \frac{1}{\tilde{\lambda}_{i,1}} \sum_v \mathcal{W}_v(\tilde{\lambda}) \mathcal{P}_v(\tilde{\lambda})^{-(N+2)} \quad (5.48)$$

using $\int_0^\infty x^n \exp(-\mu x) dx = n! \mu^{-n-1}$ [90, eq. (3.351.3)]. Let $\mathcal{S}^{MES}(n_1, \dots, n_M)$ denote the summand term in the symbol error expression given in eq. (5.45). Note that

$$\begin{aligned} \lim_{SNR \rightarrow \infty} \tilde{\lambda}_{0,1} &= SNR \tilde{\sigma}_{0,N+1}^2 \\ \lim_{SNR \rightarrow \infty} \tilde{\lambda}_{i,1} |_{\gamma_{i,N+1} = \zeta_{n_i} \Gamma_{i,N+1}} &= SNR \zeta_{n_i} \tilde{\sigma}_{i,N+1}^2, \quad i = 1, \dots, N \end{aligned} \quad (5.49)$$

and since

$$\begin{aligned} \lim_{SNR \rightarrow \infty} \tilde{\lambda}_{0,m} &= 1, \quad m = 2, \dots, M \\ \lim_{SNR \rightarrow \infty} \tilde{\lambda}_{i,m} |_{\gamma_{i,N+1} = \zeta_{n_i} \Gamma_{i,N+1}} &= \frac{\zeta_{n_i} \tilde{\sigma}_{i,N+1}^2}{\tilde{\sigma}_{0,i}^2}, \quad i = 1, \dots, N, \quad m = 2, \dots, M \end{aligned} \quad (5.50)$$

then

$$\lim_{SNR \rightarrow \infty} \sum_v \mathcal{W}_v(\tilde{\lambda}) \mathcal{P}_v(\tilde{\lambda})^{-(N+2)} \Big|_{\substack{\gamma_{i,N+1} = \zeta_{n_i} \Gamma_{i,N+1} \\ i=1, \dots, N}} \rightarrow \mathcal{K}^{MES}(n_1, \dots, n_M) \quad (5.51)$$

where $\mathcal{K}^{MES}(n_1, \dots, n_M)$ has a constant value depending on the channel and system parameters. Thus,

$$\lim_{SNR \rightarrow \infty} P_s^{MES} \rightarrow \frac{1}{SNR^{N+1}} \frac{(N+1)!}{\tilde{\sigma}_{0,N+1}^2} \sum_{n_1=1}^{N_p} \dots \sum_{n_N=1}^{N_p} \prod_{i=1}^N \frac{\zeta_{n_i}}{\zeta_{n_i} \tilde{\sigma}_{i,N+1}^2} \mathcal{K}^{MES}(n_1, \dots, n_M) \quad (5.52)$$

which indicates that a noncoherent system with MES scheme achieves full spatial diversity.

5.3.3 Numerical Results

In this section, numerical examples for the performance of different noncoherent AF cooperative systems are presented. We consider systems in Rayleigh fading with both i.i.d links ($\Gamma_{0,i} = \Gamma_{i,N+1} = \Gamma_{s,d}$) and non i.i.d. links assuming $\Gamma_{0,i} = \Gamma_{i,N+1} = \frac{i}{16} \Gamma_{s,d}$ where $\Gamma_{s,d}$ is the average SNR over the direct link. Figures 5.12 and 5.13, respectively, show bit error probabilities for single-relay and double-relay noncoherent BFSK AF cooperative systems employing the proposed MES scheme. Theoretical results were obtained using (5.45) assuming $N_p = 15$. It is clearly seen from both figures that the theoretical results precisely match the simulation results. It is also clearly seen that the slopes of the bit error probability curves steepen from the single-relay systems to the double-relay systems, indicating higher diversity gains achieved in systems with larger numbers of relays, as expected.

For comparison purposes, in Figures 5.12 and 5.13, we have also plotted the bit error probabilities (obtained from Monte Carlo simulation) of the corresponding coherent BFSK AF cooperative systems employing R-MRC or SC [15] as well as noncoherent BFSK systems with SC.

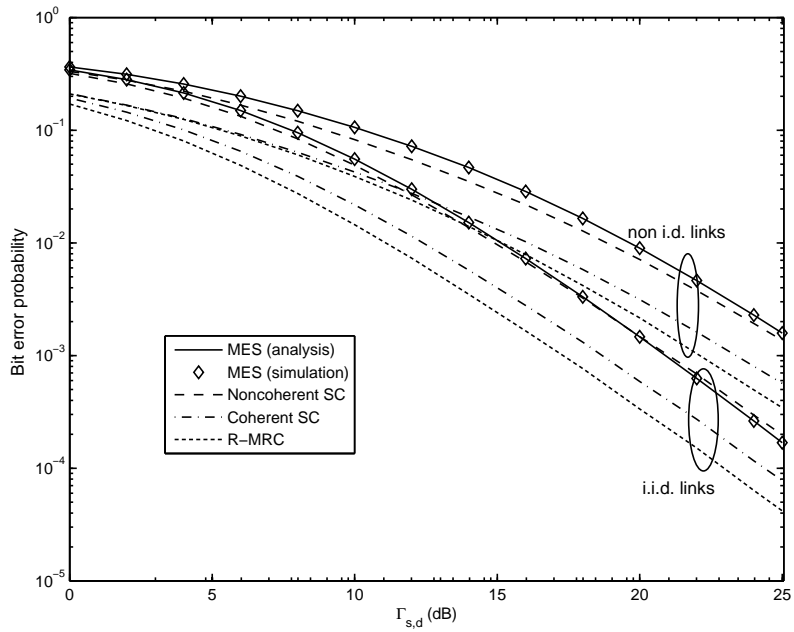


Figure 5.12. Bit error probabilities for different coherent and noncoherent BFSK AF single-relay systems.

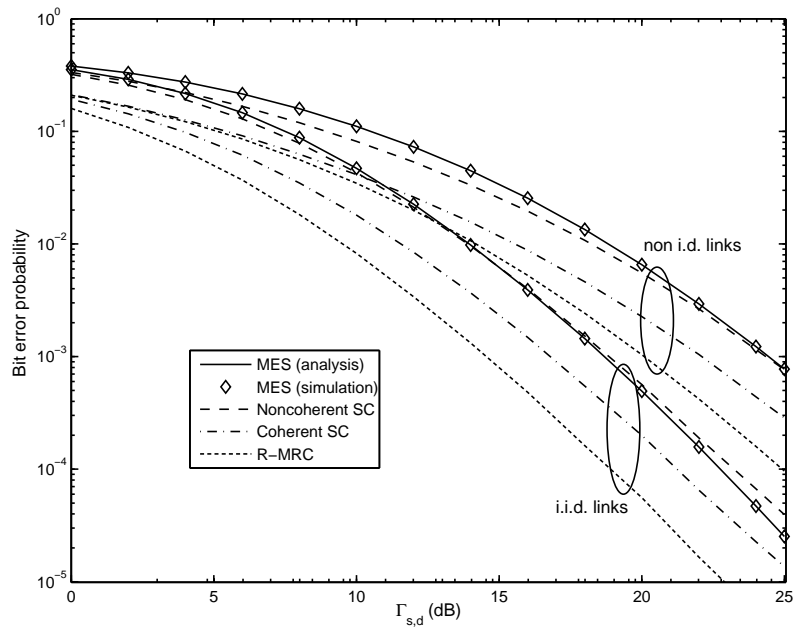


Figure 5.13. Bit error probabilities for different coherent and noncoherent BFSK AF double-relay systems.

It is seen from both figures that the proposed MES scheme performs slightly inferior to the noncoherent SC scheme in small SNR regions and/or in more faded systems, but achieves nearly the same and even slightly better performance as SNR increases. This is because in small SNR regions or in a more faded channel, the branch energy is more likely dominated by the noise term. However, by increasing SNR, the gap between performance of MES and SC decreases. This results can be justified by the fact that the MES scheme selects the branch with the maximum energy taking into account the signs of the real and imaginary components of the noise term. Since the real part of the noise term which is relevant to detection tends to decrease the branch energy [103], the MES scheme is more likely to select the branch with a small real noise component. On the other hand, the SC scheme does not take advantage of the statistical nature of the noise for its operation and selects the branch with the maximum signal to noise power ratio. Therefore, as seen in Figures 5.12 and 5.13, at sufficiently large values of SNR, the MES scheme performs very closely to (or even better than) the SC scheme. Also recall that the conventional SC scheme requires instantaneous amplitude information of all links available at the destination [15]. Thus, the proposed MES scheme is preferred in practice because it offers almost the same performance as the noncoherent SC while requiring no CSI.

It is also seen that the coherent AF systems employing either R-MRC or SC outperform noncoherent systems employing MES, as expected. For instance, the SNR losses in the single-relay system with i.i.d. links employing the MES scheme at the bit error probability 10^{-3} are about 2.2 dB and 3.5 dB comparing to the corresponding coherent systems employing SC and R-MRC, respectively.

Chapter 6

Multi-Hop Diversity Systems

In this chapter we examine performance of multi-hop diversity transmission systems employing either a DF or an AF relaying. While the superior performance of multi-hop diversity transmission systems over multi-hop systems without diversity has been shown in [26], the outage and error probabilities have not been accurately evaluated. Closed-form expressions for evaluation of the outage and bit error probabilities of multi-hop diversity transmission systems employing fixed AF and DF relaying protocols are derived. In addition, as mentioned earlier and as the analysis shows, a multi-hop diversity transmission system with fixed DF relaying does not achieve diversity gain. A selective relaying scheme for multi-hop diversity transmission, which adapts transmissions based on threshold tests on the received SNR at each relay, is proposed and evaluated. It is shown that a multi-hop diversity transmission system employing the proposed selective DF or AF relaying protocol achieves diversity gain equal to the number of hops.

In Section 6.1, system models for various AF and DF multi-hop diversity transmission systems employing either the fixed relaying or the proposed selective relaying are described. Section 6.2 and Section 6.3, respectively, present the outage probability and bit error rate analyses for multi-hop diversity transmission systems employing different types of relaying protocols. Numerical results and discussions are given in Section 6.4.

A version of this chapter has been accepted for publication in IEEE Transactions on Communications and has been published in part in Proceedings of IEEE Global Communications Conference (GLOBECOM), 1:4385-4390 (2007) and Proceedings of IEEE International Conference on Communications (ICC), 1:3748-3754 (2008).

6.1 System Models

Consider a K -hop diversity transmission system as shown in Figure 2.3 operating over independent, not necessarily identical Rayleigh fading channels. The MAC model considered here divides the available bandwidth into orthogonal channels across frequency and these channels are allocated to each source terminal. In addition, due to a half-duplex constraint, each relay node must transmit on separate channels. Hence, the MAC protocol achieves orthogonal relaying by division of each channel into orthogonal subchannels across time (using a time-division scheme) [4]. We also assume that the CSI is only known at the receiving terminals. Thus, the total available power, P_T , is uniformly allocated among the transmitting terminals¹.

In the following subsections, we describe the channel models for two relaying protocols, namely fixed relaying and selective relaying, that can be employed in multi-hop diversity transmission systems. In systems with a fixed relaying scheme, all relays participate in the transmission, while in systems with the proposed selective relaying, particular relays will be selected and then cooperate in the transmission.

6.1.1 Systems With Fixed Relaying

In the first time slot, the source terminal initiates transmission by broadcasting its signal. In general, in the $(k + 1)^{th}$ time slot, $k = 0, 1, \dots, K - 1$, the terminal T_k transmits signal x_k and consequently its following terminals, $T_{k+1}, T_{k+2}, \dots, T_K$, receive the signal

$$y_i^{(T_k)} = \alpha_{k,i} x_k + n_i, \quad i = k + 1, \dots, K \quad (6.1)$$

where $y_i^{T_k}$ denotes the signal received at the i^{th} terminal through the k^{th} terminal. The signals received at the i^{th} terminal through its preceding terminals, $y_i^{T_0}, y_i^{T_1}, \dots, y_i^{T_{i-1}}$, are combined using MRC diversity [26] and then the combiner output is either decoded and re-encoded (in systems with DF relaying) or amplified (in systems with AF relaying) to generate the signal x_k for re-transmission at the $(k + 1)^{th}$ time slot. In systems employing

¹Uniform power allocation policy is employed here due to its simplicity. In practice, more power may be required when the number of combining branches increases (e.g. for relays close to the destination). For example, in [26] approximate optimal power allocations for multi-hop diversity transmissions systems employing fixed DF or AF relaying schemes are given for the case where the noise powers at all terminals are equal. The optimal power corresponding to each terminal obtained in [26] is a portion of the total available power and depends on the inter-terminal distances. Thus, more power is allocated to the terminals closer to the destination. Note that for the case where the terminals are fixed, the optimal powers will be constant portions of the total available power, and hence the analysis presented here is extendable to performance evaluation of such systems.

DF relaying, we focus on the simplest DF relaying protocol, i.e. the un-coded DF [34], in which each relay demodulates its combiner output, re-modulates it and then forwards. In addition, note that the combining scheme at a terminal in DF multi-hop diversity systems requires only the knowledge of CSI of its preceding links. As mentioned in Section 5.2.1.1, this information can be obtained in a decentralized manner using the RTS packet received at a terminal from its preceding terminals. Thus, a multi-hop diversity transmission system with DF relaying is a suitable candidate for application in ad hoc wireless networks.

In systems with AF relaying, the amplification gain used at each relay is the quotient of the transmitted power and the received power at that relay [26]. In addition, the weight factors of the MRC combiner at a terminal in an AF multi-hop diversity system are obtained assuming that the noise components of the signals received at that terminal are uncorrelated [26]². Note that the combining scheme at a terminal in systems with an AF relaying requires the knowledge of CSI of all links between that terminal and all its preceding terminals involved in the cooperation. This implies that there should be a centralized mechanism to provide the required CSI for combining operation at each terminal. Thus, multi-hop diversity transmission systems with AF relaying are suitable for applications in the uplink of cellular multi-hop networks.

6.1.2 Systems With Selective Relaying

The performance of multi-hop diversity transmission systems employing fixed DF relaying strategy is limited by the direct transmission between the source and the first relay terminal [26]. However, the relay terminals can have knowledge of the fading coefficients (e.g. the transmission of RTS packets from the source at the beginning of its transmission allows for the estimation of $\alpha_{0,k}$ at the k^{th} relay terminal). Thus, the relay terminals can decide to cooperate or not with the source terminal in its transmission, based on the quality of their received signals. If the total instantaneous received SNR at the k^{th} , $k = 1, \dots, K-1$, relay terminal is above a certain threshold, that relay will cooperate in the transmission. However, if the received instantaneous SNR at the k^{th} relay falls below the threshold, the source terminal repeats its signal at the $(k+1)^{th}$ time slot. Note that the selective DF relaying scheme for dual-hop diversity transmission as proposed in [4] requires either a channel

²Note that the propagated noise terms received at a terminal from its preceding terminals are not independent, in general [26]. Obtaining the optimal combining scheme that incorporates this correlation is beyond the scope of this thesis. However, the output SNR in an AF multi-hop diversity system employing the combining scheme considered here is a lower bound on the output SNR of the optimal combiner [26].

measurement at the source (e.g. by utilizing the CTS packet received from the relay) or a standard carrier sense scheme to adapt source transmission based on the quality of the received signal at the relay. In our proposed scheme, we assume that a carrier sense scheme is utilized to identify the status of the channel at each time slot and the source adapts its transmission accordingly (i.e. if the channel was sensed idle, the source repeats its signal). The threshold used to examine which relay in a K -hop diversity transmission system is allowed to cooperate can correspond to a certain target rate, R , in the direct transmission scheme transmitting in $\frac{1}{K}$ of the total transmission time, i.e., $\gamma_{th}^{(R)} = 2^{KR} - 1$ [4].

6.2 Outage Probability Analysis

6.2.1 Systems With Fixed Relaying

6.2.1.1 DF Relaying

In a decoded relaying multi-hop diversity system, an outage event occurs when an outage occurs at any intermediate terminal along the multi-hop path [26]³. Thus, the probability of outage is given by [26]

$$P_{out} = 1 - \prod_{k=1}^K (1 - P_{out_k}) \quad (6.2a)$$

where P_{out_k} denotes the probability of outage at the k^{th} terminal. This probability is the probability that the received SNR at the k^{th} terminal falls below a certain threshold, γ_{th} . The instantaneous received SNR at the k^{th} terminal, $k = 1, \dots, K$, is $\tilde{X}_k = \sum_{i=0}^{k-1} \gamma_{i,k}$. Recall that $\gamma_{i,k}$ is an exponential random variable with average $\Gamma_{i,k}$ in Rayleigh fading. Thus, utilizing the MGF of \tilde{X}_k , $M_{\tilde{X}_k}(s)$, P_{out_k} is obtained as

$$\begin{aligned} P_{out_k} &= Pr(\tilde{X}_k \leq \gamma_{th}) = \mathcal{L}^{-1} \left(\frac{M_{\tilde{X}_k}(-s)}{s} \right) \Big|_{\gamma_{th}} = \mathcal{L}^{-1} \left(\frac{1}{s \prod_{i=0}^{k-1} (1 + s\Gamma_{i,k})} \right) \Big|_{\gamma_{th}} \\ &= \begin{cases} 1 - \sum_{i=0}^{k-1} \hat{a}_i \exp\left(-\frac{\gamma_{th}}{\Gamma_{i,k}}\right), & \Gamma_{i,k} \neq \Gamma_{j,k}, i \neq j, i, j = 0, 1, \dots, k-1 \\ \frac{\gamma\left(k, \frac{\gamma_{th}}{\Gamma_{i,k}}\right)}{(k-1)!}, & \Gamma_{i,k} = \Gamma_{j,k}, i \neq j, i, j = 0, 1, \dots, k-1 \end{cases} \end{aligned} \quad (6.2b)$$

³It is assumed that the relay terminals in outage do not back off during the transmission (i.e. the link between the source and that relay does not disconnect). For the case where a relay terminal in outage backs off, transmission can continue with the rest of the non-outage relays that consequently may lead to a better outage probability performance. This case is outside of the scope of this thesis and is not considered here.

where \mathcal{L}^{-1} is the inverse Laplace transform operator, $\gamma(\cdot, \cdot)$ denotes the lower incomplete gamma function [90, eq. (8.350.1)], and

$$\hat{a}_i = \frac{\Gamma_{i,k}^{k-1}}{\prod_{\substack{j=0 \\ j \neq i}}^{k-1} \Gamma_{i,k} - \Gamma_{j,k}}. \quad (6.2c)$$

6.2.1.2 AF Relaying

In an amplified relaying multi-hop diversity transmission system, the outage probability is the probability that the instantaneous received SNR at the destination, γ_t^{MHD} , falls below a threshold, γ_{th} , i.e.,

$$P_{out} = Pr\left(\gamma_t^{MHD} \leq \gamma_{th}\right) \quad (6.3)$$

where the instantaneous received SNR at the destination, γ_t^{MHD} , is given by [26]

$$\gamma_t^{MHD} = \gamma_{0,K} + \sum_{k=1}^{K-1} \tilde{\gamma}_{k,K} \quad (6.4a)$$

where $\tilde{\gamma}_{k,K}$ is the received SNR at the destination over the branch of the diversity combiner corresponding to the received signal from the k^{th} relay and is given by

$$\tilde{\gamma}_{k,K} = \frac{\gamma_{k,K} \hat{\gamma}_k}{\gamma_{k,K} + \hat{\gamma}_k + 1} \quad (6.4b)$$

where

$$\hat{\gamma}_k = \gamma_{0,k} + \sum_{j=1}^{k-1} \tilde{\gamma}_{j,k} \quad (6.4c)$$

where $\tilde{\gamma}_{j,k}$ is the received SNR at the k^{th} terminal over the branch of the diversity combiner corresponding to the received signal from the j^{th} relay given by (6.4b) in which k and K are respectively replaced by j and k .

The instantaneous received SNR at the destination, γ_t^{MHD} , is constituted of dependent summands and the derivation of its PDF which facilitates the analytical evaluation of the outage probability is very involved, if not impossible. Using eq. (3.21), outage probability for sufficiently large values of SNR of an AF multi-hop diversity system can be evaluated by having the value of the first non-zero derivative of the PDF of γ_t^{MHD} at the origin. The following lemmas are used for obtaining the value of derivatives of the PDF of the received SNR (up to the first non-zero one) in a K -hop diversity transmission system employing AF relaying.

Lemma 6.1: Let $V = \sum_{k=0}^{K-1} V_k$ where V_k , $k = 0, 1, \dots, K-1$ denotes a nonnegative random variables. Assume that V_0 is independent of V_k , $\forall k \in \{1, 2, \dots, K-1\}$, but V_i

and $V_j, \forall i, j = \{1, \dots, K-1\}$ ($i \neq j$) are dependent random variables. Then, the first $K-2$ order derivatives of the PDF of V at the origin are zero and its $K-1$ order derivative is given by

$$\frac{\partial^{K-1} f_V}{\partial v^{K-1}}(0) = f_{V_0}(0) f_{V_1, V_2, \dots, V_{K-1}}(0, 0, \dots, 0) \quad (6.5)$$

where $f_{V_1, V_2, \dots, V_{K-1}}(\cdot, \cdot, \dots, \cdot)$ denotes the joint PDF of V_1, V_2, \dots, V_{K-1} .

Proof: A proof of Lemma 6.1 is given in Appendix A.7.

It should be mentioned that for the special case that V_i is independent of $V_j, \forall i, j \in \{1, \dots, K-1\}$ ($i \neq j$), Lemma 6.1 reduces to the Proposition 2 proved in [14].

Now, note that the instantaneous received SNR, γ_t^{MHD} , in (6.4) is the sum of K random variables in which $\gamma_{0,K}$ is independent of $\tilde{\gamma}_{k,K}, k = 1, \dots, K-1$ and $\tilde{\gamma}_{m,K}$ and $\tilde{\gamma}_{n,K}, m \neq n, m, n \in \{1, \dots, K-1\}$ are dependent random variables. Thus, according to Lemma 6.1, the first $K-2$ order derivatives of γ_t^{MHD} at the origin are zero and the value of its $K-1$ order derivative is given by

$$\frac{\partial^{K-1} f_{\gamma_t^{MHD}}}{\partial \gamma^{K-1}}(0) = f_{\gamma_{0,K}}(0) f_{\tilde{\gamma}_{1,K}, \tilde{\gamma}_{2,K}, \dots, \tilde{\gamma}_{K-1,K}}(0, 0, \dots, 0). \quad (6.6a)$$

However, calculation of the joint PDF of $\tilde{\gamma}_{1,K}, \tilde{\gamma}_{2,K}, \dots, \tilde{\gamma}_{K-1,K}$ requires analytic computation of the determinant of a $\frac{K(K+1)}{2} \times \frac{K(K+1)}{2}$ Jacobian matrix and then a $\frac{K(K-1)}{2}$ -fold integration, which are very involved. However, note that the value of this joint PDF at the origin can be evaluated as

$$f_{\tilde{\gamma}_{1,K}, \tilde{\gamma}_{2,K}, \dots, \tilde{\gamma}_{K-1,K}}(0, 0, \dots, 0) = \frac{Pr(\tilde{\gamma}_{1,K} < \epsilon_1, \tilde{\gamma}_{2,K} < \epsilon_2, \dots, \tilde{\gamma}_{K-1,K} < \epsilon_{K-1})}{\epsilon_1, \dots, \epsilon_{K-1}} \quad (6.6b)$$

where $\epsilon_i \rightarrow 0, i = 1, \dots, K-1$. Thus, the value of each instantaneous received SNR at the destination through the k^{th} relay, $\tilde{\gamma}_{k,K}, k = 1, \dots, K-1$, must tend to zero. This means that either $\gamma_{k,K} \rightarrow 0$ or $\hat{\gamma}_k \rightarrow 0$. Except for the first relay terminal, it is more likely that $\gamma_{k,K} \rightarrow 0$. Since $\hat{\gamma}_k$ is the sum of k nonnegative random variables, it is less probable that all of them are near zero, especially for large values of SNR. This implies that $\tilde{\gamma}_{k,K}, k = 2, \dots, K-1$, near zero is more likely only a function of $\gamma_{k,K}$ for sufficiently large values of SNR. Therefore, it can be assumed, as an approximation for sufficiently large values of SNR, that $\tilde{\gamma}_{m,K}$ and $\tilde{\gamma}_{n,K}$ near the origin, for $m \neq n$ and $m, n = 1, \dots, K-1$, are independent, and thus the value of the $K-1$ order derivative of the PDF of γ_t^{MHD} at zero can be approximated by

$$\frac{\partial^{K-1} f_{\gamma_t^{MHD}}}{\partial \gamma^{K-1}}(0) \approx f_{\gamma_{0,K}}(0) \prod_{k=1}^{K-1} f_{\tilde{\gamma}_{k,K}}(0) \quad (6.7a)$$

where $f_{\gamma_{0,K}}(0) = \frac{1}{\Gamma_{0,K}}$ for Rayleigh fading and $f_{\tilde{\gamma}_{k,K}}(0)$, $k = 1, \dots, K-1$ is given by the following lemma.

Lemma 6.2: The value of the PDF of $\tilde{\gamma}_{k,K}$ at zero is given by

$$f_{\tilde{\gamma}_{k,K}}(0) = f_{\gamma_{k,K}}(0) + f_{\hat{\gamma}_k}(0) \quad (6.7b)$$

where $f_{\gamma_{k,K}}(0) = \frac{1}{\Gamma_{k,K}}$ and

$$f_{\hat{\gamma}_k}(0) = \begin{cases} \frac{1}{\Gamma_{0,1}}, & k = 1 \\ 0, & k \neq 1 \end{cases} \quad (6.7c)$$

for Rayleigh fading.

Proof: A proof of Lemma 6.2 is given in Appendix A.8.

Note that eqs. (6.7b) and (6.7c) derived in Lemma 6.2 are consistent with our discussion for the large-SNR approximation used in (6.7a).

Thus, the outage probability of a K -hop diversity transmission system employing fixed AF relaying in Rayleigh fading for sufficiently large values of SNR is obtained from (3.21) with $t = K-1$ and $\frac{\partial^{K-1} f_{\gamma_t}}{\partial \gamma^{K-1}}(0)$ replaced by (6.7).

6.2.2 Systems With Selective Relaying

6.2.2.1 DF Relaying

In a multi-hop diversity transmission system employing fixed DF relaying, occurrence of an outage event at the first relay terminal limits the outage performance. In systems with selective DF relaying, the goal is to exploit the full spatial diversity by avoiding the occurrence of an outage event at the relay terminals. Assuming $\gamma_{th} \leq \gamma_{th}^{(R)}$ guarantees that an outage event does not occur at the intermediate participating relay terminals (if any), as the instantaneous received SNR at each cooperating terminal is already above the threshold, γ_{th} . Thus, in a multi-hop diversity transmission system employing selective DF relaying, the outage event at the destination is equivalent to the event

$$\bigcup_{k=0}^{K-1} (\hat{X}_k \leq \gamma_{th}) \quad (6.8a)$$

where \hat{X}_k denotes the instantaneous received SNR at the destination conditioned on a set of k participating relays in the transmissions and is given by

$$\hat{X}_k = (K-k) \gamma_{0,K} + \sum_{i \in C_k} \gamma_{i,K} \quad (6.8b)$$

where \mathbb{C}_k denotes the set of k specific cooperating terminals. Since the events involved in the union in (6.8a) are mutually independent, the outage probability is obtained as

$$P_{out} = \sum_{k=0}^{K-1} Pr\left(\hat{X}_k \leq \gamma_{th}\right) \quad (6.9a)$$

and since the set of cooperating terminals, \mathbb{C}_k , is a random set,

$$\begin{aligned} Pr\left(\hat{X}_k \leq \gamma_{th}\right) &= \sum_{\mathbb{C}_k} Pr\left((K-k)\gamma_{0,K} + \sum_{i \in \mathbb{C}_k} \gamma_{i,K} \leq \gamma_{th}\right) Pr(\mathbb{C}_k) \\ &= \sum_{\mathbb{C}_k} \left(1 - \hat{b}_{0,k} \exp\left(-\frac{\gamma_{th}}{(K-k)\Gamma_{0,k}}\right) - \sum_{i \in \mathbb{C}_k} \hat{b}_{i,k} \exp\left(-\frac{\gamma_{th}}{\Gamma_{i,k}}\right)\right) Pr(\mathbb{C}_k) \end{aligned} \quad (6.9b)$$

where

$$\begin{aligned} \hat{b}_{0,k} &= \frac{(K-k)^k \Gamma_{0,k}^k}{\prod_{i \in \mathbb{C}_k} ((K-k)\Gamma_{0,k} - \Gamma_{i,k})} \\ \hat{b}_{i,k} &= \frac{\Gamma_{i,k}^k}{(\Gamma_{i,k} - (K-k)\Gamma_{0,k}) \prod_{\substack{j \in \mathbb{C}_k \\ j \neq i}} (\Gamma_{i,k} - \Gamma_{j,k})} \end{aligned} \quad (6.9c)$$

and the probability that k specific relays cooperate in the transmission, $Pr(\mathbb{C}_k)$, is obtained by utilizing a tree diagram illustrating all ways that relays can cooperate in a multi-hop diversity scheme with selective relaying. The tree diagram corresponding to a K -hop diversity scheme consists of K stages with 2^{k-1} branches at the k^{th} stage, $k = 1, \dots, K$, and the total number of branches is $2^K - 1$. For example, Figure 6.1 shows the tree diagram of a triple-hop diversity transmission system employing selective DF relaying. Let q_k denote the path in the tree diagram associated with a particular set of k participating relay terminals, \mathbb{C}_k . The probability of set \mathbb{C}_k , $Pr(\mathbb{C}_k)$, can be then calculated as

$$\prod_{j=2}^K \eta_{q_k, j} \quad (6.9d)$$

where $\eta_{q_k, j}$ denotes the probability associated with the branch in the j^{th} stage, $j = 2, \dots, K$, over the path q_k in the tree diagram given by

$$\eta_{q_k, j} = \kappa_j + (-1)^{\kappa_j} Pr\left(\sum_{i=0}^{j-2} \zeta_i^{(q_k)} \gamma_{i, j-1} < \gamma_{th}^{(R)}\right) \quad (6.9e)$$

where $\zeta_i^{(q_k)} \in \{0, 1\}$, $i = 1, \dots, k-2$, $\zeta_0^{(q_k)} = k-1 - \sum_{i=1}^{k-2} \zeta_i^{(q_k)}$ and

$$\kappa_j = \begin{cases} 0, & T_{j-1} \text{ does not cooperate} \\ 1, & T_{j-1} \text{ cooperates.} \end{cases} \quad (6.9f)$$

⁴The k^{th} stage represents the potential branches deployed at the k^{th} transmission time slot.

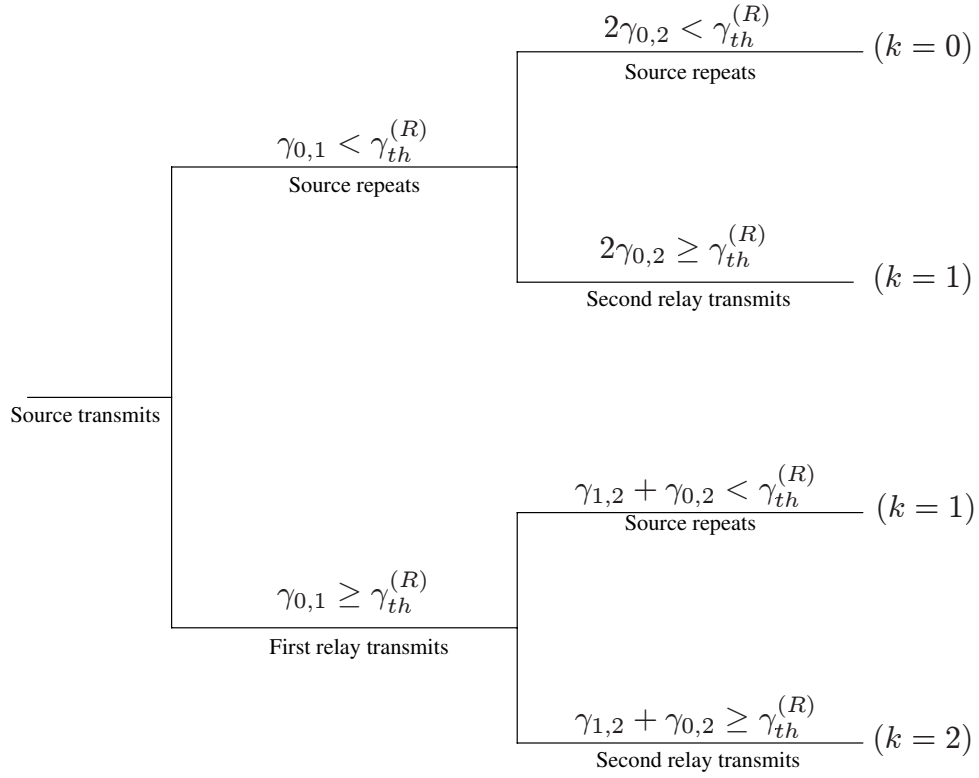


Figure 6.1. Tree diagram for a triple-hop diversity transmission system employing selective DF relaying.

For independent non-identical Rayleigh fading channels, the probability $\eta_{q_k,j}$ can be computed as

$$\eta_{q_k,j} = \kappa_j + (-1)^{\kappa_j} \left(1 - \sum_{i=0}^{j-2} \rho_i^{(q_k)} \exp \left(-\frac{\gamma_{th}^{(R)}}{\zeta_i^{(q_k)} \Gamma_{i,j-1}} \right) \right) \quad (6.9g)$$

where

$$\rho_i^{(q_k)} = \begin{cases} 0, & \zeta_i^{(q_k)} = 0 \\ \frac{(\zeta_i^{(q_k)} \Gamma_{i,j-1})^{N_{j-1}^{(q_k)}}}{\prod_{h=0, h \neq i}^{j-2} \zeta_i^{(q_k)} \Gamma_{i,j-1} - \zeta_h^{(q_k)} \Gamma_{h,j-1}}, & \zeta_i^{(q_k)} \neq 0 \end{cases} \quad (6.9h)$$

where $N_{j-1}^{(q_k)}$ is the number of cooperating relays preceding T_{j-1} over the path q_k .

6.2.2.2 AF Relaying

In a K -hop diversity transmission system employing selective AF relaying, the instantaneous received SNR at the destination conditioned on a set of k particular cooperating

relays, \mathbb{C}_k , is given by⁵

$$\gamma_t^{MHD}|\mathbb{C}_k = (K - k)\gamma_{0,K} + \sum_{i \in \mathbb{C}_k} \tilde{\gamma}_{i,K} \quad (6.10a)$$

where

$$\tilde{\gamma}_{i,K} = \frac{\gamma_{i,K} \hat{\gamma}_i}{\gamma_{i,K} + \hat{\gamma}_i + 1} \quad (6.10b)$$

in which

$$\hat{\gamma}_i = (i - \tilde{N}_i)\gamma_{0,i} + \sum_{\substack{j=1 \\ j \in \mathbb{C}_k}}^{i-1} \tilde{\gamma}_{j,i} \quad (6.10c)$$

where \tilde{N}_i denotes the number of participating relay terminals preceding terminal T_i . The outage probability is then given by

$$P_{out} = Pr\left(\gamma_t^{MHD} \leq \gamma_{th}\right) = \sum_{k=0}^{K-1} \sum_{\mathbb{C}_k} Pr\left(\gamma_t^{MHD} \leq \gamma_{th}|\mathbb{C}_k\right) Pr(\mathbb{C}_k) \quad (6.11a)$$

and since $\gamma_t^{MHD}|\mathbb{C}_k$ is the sum of $k + 1$ random variables in which $\gamma_{0,K}$ is independent of $\tilde{\gamma}_{i,K}$, $\forall i \in \mathbb{C}_k$, and $\tilde{\gamma}_{g,K}$ and $\tilde{\gamma}_{h,K}$ are dependent random variables for $g \neq h$, $g, h \in \mathbb{C}_k$, then according to Lemma 6.1, the first $k - 1$ order derivatives of the PDF of $\gamma_t^{MHD}|\mathbb{C}_k$ at the origin are zero and its k order derivative can be approximated by the product of the values of the PDF of its summands at zero, for sufficiently large values of SNR. Thus, using eq. (3.21) and Lemma 6.2

$$Pr\left(\gamma_t^{MHD} \leq \gamma_{th}|\mathbb{C}_k\right) \approx \frac{\gamma_{th}^{k+1}}{(k+1)!} \frac{1}{(K-k)\Gamma_{0,K}} \prod_{i \in \mathbb{C}_k} \left(\frac{1}{\Gamma_{i,K}} + f_{\hat{\gamma}_i}(0)\right) \quad (6.11b)$$

for sufficiently large values of SNR where

$$f_{\hat{\gamma}_i}(0) = \begin{cases} \frac{1}{(i - \tilde{N}_i)\Gamma_{0,i}}, & k = 1, i = 1, \dots, K - 1 \\ \frac{1}{\Gamma_{0,1}}, & k \neq i, i = 1 \\ 0, & k \neq 1, i > 1 \end{cases} \quad (6.11c)$$

and the probability of a set of k particular cooperating terminals, $Pr(\mathbb{C}_k)$, is given by (6.9d)

in which $\eta_{q_k,j}$ is replaced by

$$\begin{aligned} \eta_{q_k,j} &= \kappa_j + (-1)^{\kappa_j} Pr\left((j-1 - \tilde{N}_{j-1})\gamma_{0,j-1} + \sum_{\substack{h \in \mathbb{C}_k \\ h < j-1}} \tilde{\gamma}_{h,j-1} \leq \gamma_{th}^{(R)}\right) \\ &\approx \kappa_j + (-1)^{\kappa_j} \frac{\gamma_{th}^{(R)\tilde{N}_{j-1}+1}}{(\tilde{N}_{j-1}+1)!} \frac{1}{(j-1 - \tilde{N}_{j-1})\Gamma_{0,j-1}} \prod_{\substack{h \in \mathbb{C}_k \\ h < j-1}} \left(\frac{1}{\Gamma_{h,j-1}} + f_{\hat{\gamma}_h}(0)\right). \end{aligned} \quad (6.11d)$$

⁵Without loss of generality, we can assume that the relays in \mathbb{C}_k are sorted in ascending order.

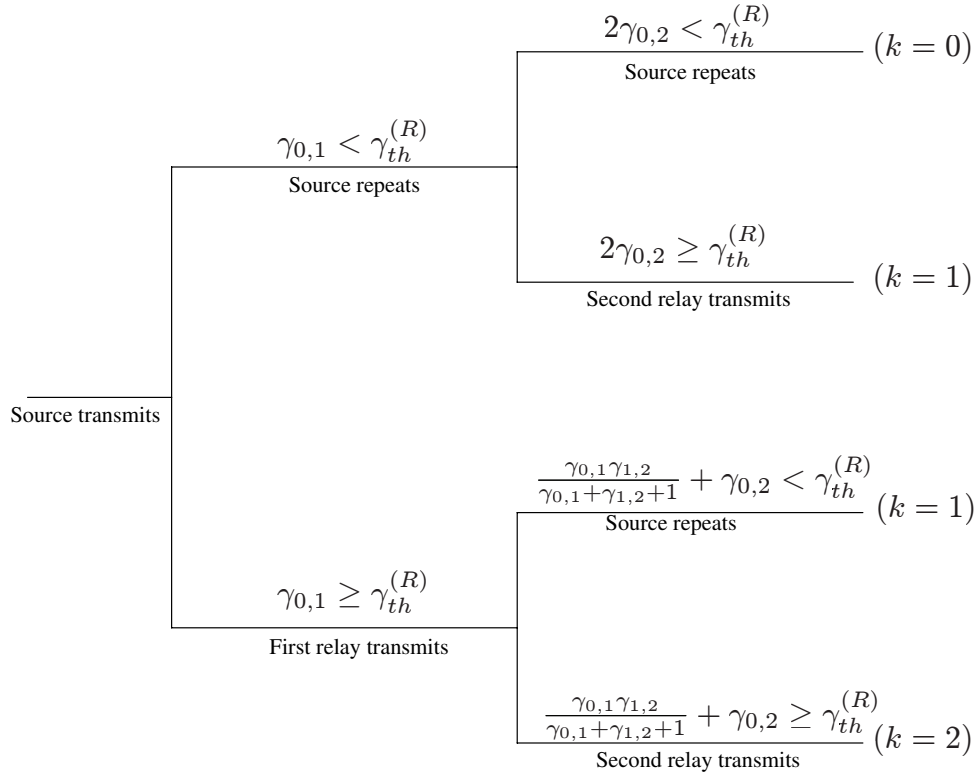


Figure 6.2. Tree diagram for a triple-hop diversity transmission system employing selective AF relaying.

Figure 6.2 shows the tree diagram of a triple-hop diversity transmission system employing selective AF relaying.

6.3 Bit Error Probability Analysis

6.3.1 Systems With Fixed Relaying

6.3.1.1 DF relaying

A tight upper bound for the bit error probability of multi-hop diversity transmission with the fixed DF relaying scheme is obtained in [26] by assuming that any bit error at the relay terminals causes a bit error. For the sake of convenience, this upper bound is given here using the present notation as [26]

$$P_b = 1 - \prod_{k=1}^K (1 - P_{b_k}) \quad (6.12)$$

where P_{b_k} denotes the bit error probability for MRC of k signals at the k^{th} terminal, which can be calculated using the MGF or PDF of $\tilde{X}_k = \sum_{i=0}^{k-1} \gamma_{i,k}$ for a variety of modulation schemes [89]. For instance, for a BPSK multi-hop diversity transmission system with fixed DF relaying operating over independent non-identical Rayleigh fading channels, P_{b_k} is given by

$$P_{b_k} = \sum_{i=0}^{k-1} \hat{a}_i \left(\frac{1 - \mu_i}{2} \right) \quad (6.13a)$$

using [89, eq. (9.6)] where \hat{a}_i is given by (6.2c) and

$$\mu_i = \sqrt{\frac{\Gamma_{i,k}}{\Gamma_{i,k} + 1}}. \quad (6.13b)$$

Recall that the parameter SNR denotes the instantaneous SNR (without fading) defined as $\frac{P_r}{N_0}$. Note that the error probability expression given in (6.12) is simplified as

$$P_b = \sum_{k=1}^K P_{b_k} - \sum_{\substack{k=1 \\ j>k}}^K P_{b_k} P_{b_j} + \dots \quad (6.14)$$

The large SNR behavior of the error probability in (6.12) is then examined by noting that P_{b_k} , $k = 1, \dots, K$ decays as $\frac{1}{SNR^k}$ [89]. Therefore, the error probability when $SNR \rightarrow \infty$ is dominated by its first term, P_{b_1} , and hence

$$\lim_{SNR \rightarrow \infty} P_b \rightarrow \frac{1}{SNR} \quad (6.15)$$

which indicates that the multi-hop diversity transmission scheme with fixed DF relaying does not offer diversity gain.

6.3.1.2 AF Relaying

An expression for the bit error probability of a BPSK multi-hop diversity transmission system employing fixed AF relaying in Rayleigh fading is given in [26]. However, as shown later in Section 6.4, this expression overestimates the bit error rate performance at moderate and large values of SNR. In the following, we present a more accurate, simple, closed-form approximation for calculation of the bit error probability of a multi-hop diversity transmission system employing fixed AF relaying. The bit error probability can be evaluated using (3.13). Exact evaluation of the bit error probability is facilitated by having a closed-form expression for the PDF or MGF of γ_t^{MHD} . However, such expressions are still unknown due to the mathematical form of γ_t^{MHD} . Using eq. (3.22), however, the bit error probability of a K -hop diversity transmission system employing fixed AF relaying can be well

approximated by

$$P_b \approx \frac{\Gamma(b+t+1)}{2\Gamma(b)a^{t+1}(t+1)!} \frac{\partial^{K-1} f_{\gamma_t}^{MHD}}{\partial \gamma^{K-1}}(0) \quad (6.16)$$

for sufficiently large values of SNR where $\frac{\partial^{K-1} f_{\gamma_t}^{MHD}}{\partial \gamma^{K-1}}(0)$ is given in (6.7) and the parameters a and b depend on the type of modulation/detection scheme given in [89, Table 8.1] (e.g. $a = b = 1$ for BPSK systems).

The large SNR behavior of the error probability of a K -hop diversity transmission system with fixed AF relaying is determined by the large SNR behavior of $\frac{\partial^{K-1} f_{\gamma_t}^{MHD}}{\partial \gamma^{K-1}}(0)$. According to eq. (6.7),

$$\lim_{SNR \rightarrow \infty} \frac{\partial^{K-1} f_{\gamma_t}^{MHD}}{\partial \gamma^{K-1}}(0) \rightarrow \frac{1}{SNR^K} \quad (6.17)$$

indicating that a K -hop diversity transmission system with fixed AF relaying achieves diversity order K .

6.3.2 Systems With Selective Relaying

6.3.2.1 DF Relaying

The bit error probability of a multi-hop diversity scheme employing selective DF relaying protocol is given by

$$P_b = \sum_{k=0}^{K-1} \sum_{\mathbb{C}_k} P_{b|\mathbb{C}_k} Pr(\mathbb{C}_k) \quad (6.18)$$

where $Pr(\mathbb{C}_k)$ is calculated using the tree diagram as explained in Section 6.2.2.1. Obtaining exact expressions for the calculation of the conditional error probabilities in (6.18) is very involved, if not impossible. However, in the selective DF relaying, only the relay terminals whose received SNRs are above a certain threshold will cooperate in the transmission. Thus, it can be assumed, as an excellent approximation, that the received signals at the cooperating relays are correctly decoded. Therefore, the conditional probabilities of bit error given a number of specific cooperating relays can be approximated by the corresponding bit error rate at the destination. For instance, the conditional probability of bit error at the destination given k number of cooperating relays in a BPSK multi-hop diversity transmission system with selective DF relaying is obtained as

$$P_{b|\mathbb{C}_k} \approx \sum_{i \in \{0\} \cup \mathbb{C}_k} \hat{\delta}_{i,k} \frac{1 - \mu_{i,K}}{2} \quad (6.19a)$$

where

$$\mu_{0,K} = \sqrt{\frac{(K-k)\Gamma_{0,K}}{(K-k)\Gamma_{0,K} + 1}} \quad (6.19b)$$

$$\mu_{i,K} = \sqrt{\frac{\Gamma_{i,K}}{\Gamma_{i,K} + 1}}, \quad i \in \mathbb{C}_k \quad (6.19c)$$

and $\hat{b}_{i,k}, i \in \{0\} \cup \mathbb{C}_k$, is given in (6.9c). Note that the conditional probabilities of bit error, $P_{b|\mathbb{C}_k}$ can be obtained for a variety of modulation schemes using the MGF or the PDF of the corresponding received SNR at the destination, \hat{X}_k [89].

Note that the large SNR behavior of $Pr(\mathbb{C}_k)$ as $SNR \rightarrow \infty$ is dominated by the case that the received instantaneous SNRs at the first $K - 1 - k$ relays are below the threshold $\gamma_{th}^{(R)}$ and is given by

$$\prod_{i=1}^{K-1-k} Pr(i\gamma_{0,i} < \gamma_{th}^{(R)}) \prod_{j=K-k}^{K-1} Pr\left((K-k)\gamma_{0,j} + \sum_{h=K-k}^{j-1} \gamma_{h,j} \geq \gamma_{th}^{(R)}\right) \quad (6.20)$$

which decays as $\frac{1}{SNR^{K-1-k}}$ for large values of SNR. In addition, the instantaneous received SNR at the destination conditioned on k participating relays, \hat{X}_k , is the sum of $k + 1$ independent exponential random variables. Thus, $P_{b|\mathbb{C}_k}$ is proportional to $\left(\frac{1}{SNR}\right)^{k+1}$ for large values of the SNR [89]. Therefore, the error probability of the proposed selective relaying scheme decays as $\frac{1}{SNR^K}$ as $SNR \rightarrow \infty$, achieving diversity order K .

6.3.2.2 AF Relaying

The bit error probability for a K -hop diversity transmission system employing selective AF relaying is given by (6.18) in which $Pr(\mathbb{C}_k)$ is calculated using the tree diagram as explained in Section 6.2.2.2 and the conditional probability of bit error, $P_{b|\mathbb{C}_k}$, is given by

$$P_{b|\mathbb{C}_k} \approx \frac{\Gamma(b+t+1)}{2\Gamma(b)\alpha^{t+1}(t+1)!} \frac{1}{(K-k)\Gamma_{0,K}} \prod_{i \in \mathbb{C}_k} \left(\frac{1}{\Gamma_{i,K}} + f_{\hat{\gamma}_i}(0) \right) \quad (6.21)$$

for sufficiently large values of SNR utilizing Lemmas 6.1 and 6.2 where $f_{\hat{\gamma}_i}(0)$ is given by (6.11c).

As discussed earlier in Section 6.3.2.1, it can be readily shown that $Pr(\mathbb{C}_k)$ decays as $\frac{1}{SNR^{K-1-k}}$ at large values of SNR. Furthermore, the large SNR behavior of the conditional error probability given in (6.21) is

$$\lim_{SNR \rightarrow \infty} P_{b|\mathbb{C}_k} \rightarrow \frac{1}{SNR^{k+1}} \quad (6.22)$$

indicating diversity order $k + 1$. Thus, a K -hop diversity transmission system employing selective AF relaying achieves diversity order K .

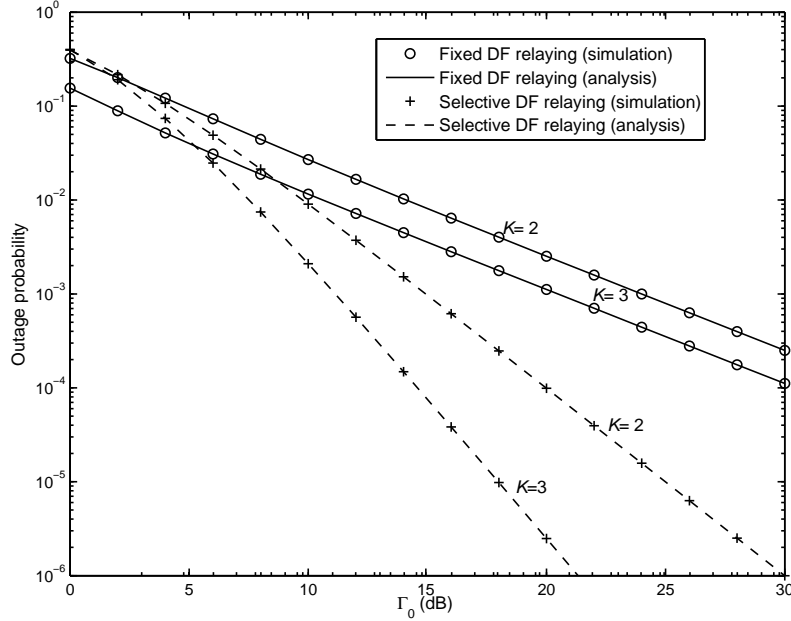


Figure 6.3. Outage probabilities for different multi-hop diversity transmission systems employing DF relaying.

6.4 Results and Discussions

In this section, we compare the performances of the different multi-hop transmission schemes in terms of their outage and bit error probabilities. In the numerical examples, we assume that the terminals are fixed and located in equi-distant points from each other in a straight line. Recall that each transmitting terminal in a K -hop diversity transmission system uses $\frac{1}{K}$ of the total available power, P_T . Thus, using the Friss propagation formula [94], the average link SNR between terminals j and h in a K -hop transmission system is $\Gamma_{j,h} = \frac{1}{K} \left(\frac{K}{h-j} \right)^\epsilon \Gamma_0$, $j = 0, \dots, K-1$, $h = 1, \dots, K$ and $h > j$, where ϵ is the path loss exponent and Γ_0 denotes the average received SNR of the direct link of the single-hop transmission system. In all numerical examples, we assume BPSK modulation, $\epsilon = 3$, $R = 1$ Bit/Sec/Hz (hence $\gamma_{th}^{(R)} = 2^K - 1$), and $\gamma_{th} = 1$. Simulation results for outage probabilities are obtained using the Monte Carlo method, and those for bit error rates are obtained by simulation of the systems described in Section 6.2.

Figures 6.3 and 6.4, respectively, show the outage probabilities and bit error rates versus Γ_0 of various multi-hop diversity transmission systems employing DF relaying. Figure 6.3 shows exact agreement between simulation results and analytical results obtained for the outage probabilities of multi-hop diversity transmission systems with either fixed or selec-

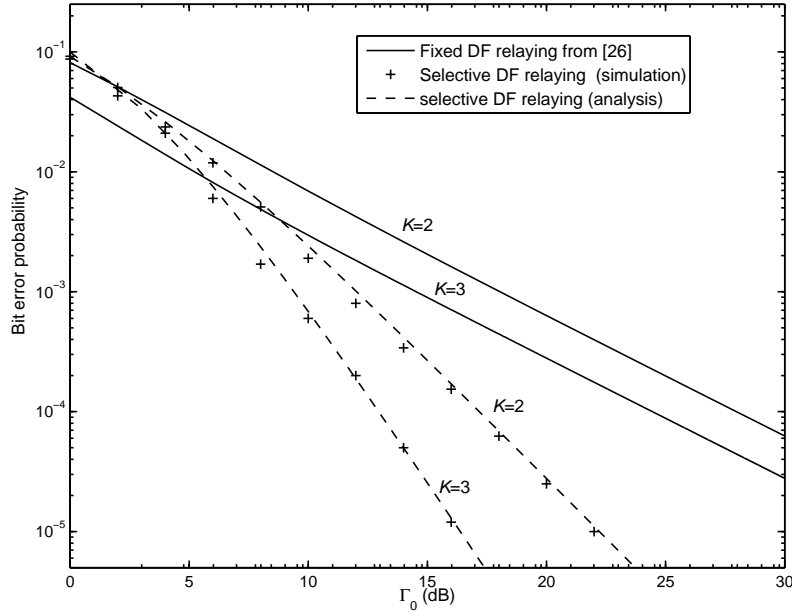


Figure 6.4. Bit error probabilities for different multi-hop diversity transmission systems employing DF relaying.

tive DF relaying. Simulation results presented in Figure 6.4 are also in excellent agreement with the analytical results showing the accuracy of the approximation used to evaluate the bit error rates of multi-hop diversity transmission systems employing selective DF relaying. Although the multi-hop diversity schemes employing a fixed DF scheme perform (in terms of outage probability and bit error rate) better than the corresponding multi-hop schemes without diversity [26], they do not offer diversity gain, as seen in Figure 6.4. It is seen that the system with selective DF relaying scheme significantly outperforms the system with fixed DF relaying achieving diversity order equal to the number of hops. For example, at a probability of bit error of 10^{-5} , the employment of the proposed selective DF relaying in dual-hop and triple-hop diversity systems achieves power gains of 15.72 dB and 18.09 dB, respectively, compared to the corresponding diversity systems employing fixed DF relaying.

Figures 6.5 and 6.6, respectively, show the outage probabilities and bit error rates versus Γ_0 of various multi-hop diversity transmission systems employing an AF relaying. It is seen from these figures that the analytical results for outage probabilities and bit error rates obtained in Sections 6.2.1.2, 6.2.2.2, 6.3.1.2, and 6.3.2.2. are in excellent agreement with the simulation results for medium to large values of SNR. For comparison purposes,

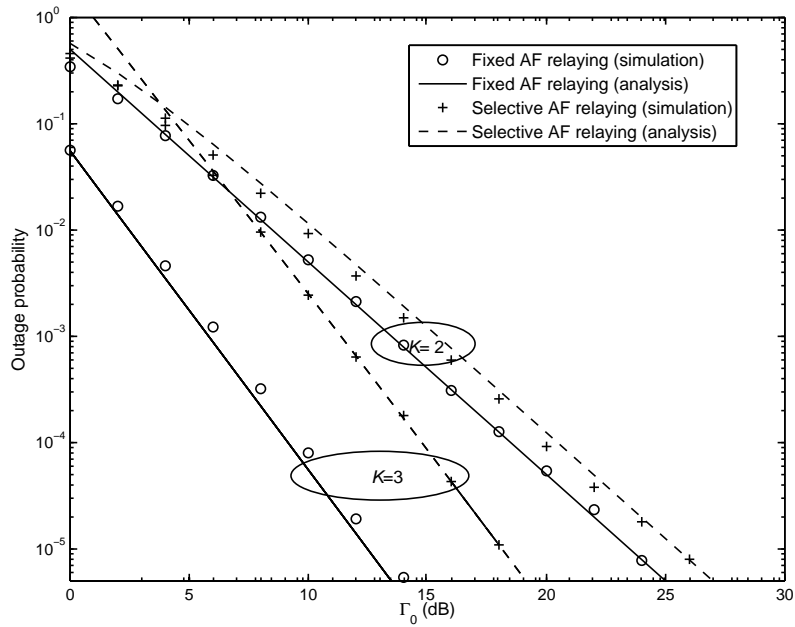


Figure 6.5. Outage probabilities for different multi-hop diversity transmission systems employing AF relaying.

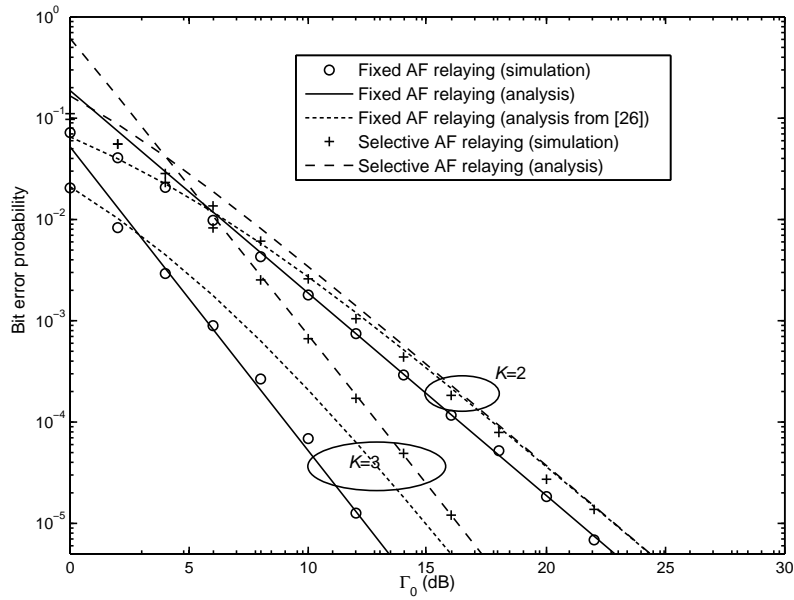


Figure 6.6. Bit error probabilities for different multi-hop diversity transmission systems employing AF relaying.

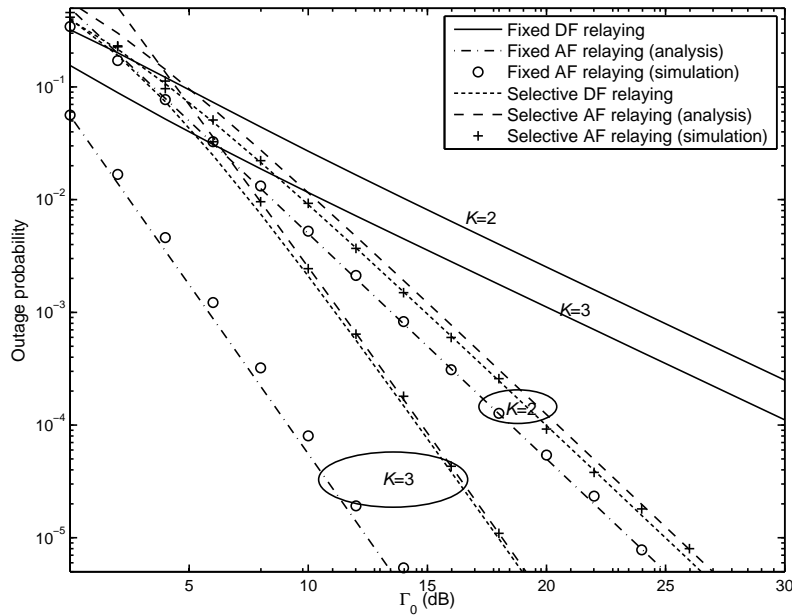


Figure 6.7. Comparison of outage probabilities among different multi-hop diversity transmission systems employing either DF relaying or AF relaying.

the bit error probabilities of multi-hop diversity systems with fixed AF relaying obtained from an expression given in [26] are also included in Figure 6.6. It is clearly seen that the bit error rate analysis in [26] underestimates the bit error rate performance of multi-hop diversity transmission systems with fixed AF relaying at moderate to large values of SNR. As seen in Figures 6.5 and 6.6, both systems with fixed AF and selective AF relaying achieve diversity gain equal to the number of hops. It is also seen that systems with fixed AF relaying perform better than the corresponding systems with selective AF relaying in terms of outage probabilities and bit error rates, despite noise amplification at all relays. For instance, employing fixed AF relaying in dual-hop and triple-hop diversity transmission systems, respectively, attains power gains 1.5 dB and 3.9 dB at probability of bit error 10^{-5} , compared to employment of selective AF relaying in these systems.

Figures 6.7 and 6.8, respectively, compare the outage probabilities and bit error rates of various multi-hop diversity transmission systems employing different relaying protocols. Comparing systems employing selective relaying shows that the systems with selective DF relaying slightly outperform systems employing selective AF relaying. It is seen from Figures 6.7 and 6.8 that multi-hop diversity transmission systems employing fixed AF relaying achieve the best outage and bit error performances compared to the corresponding systems

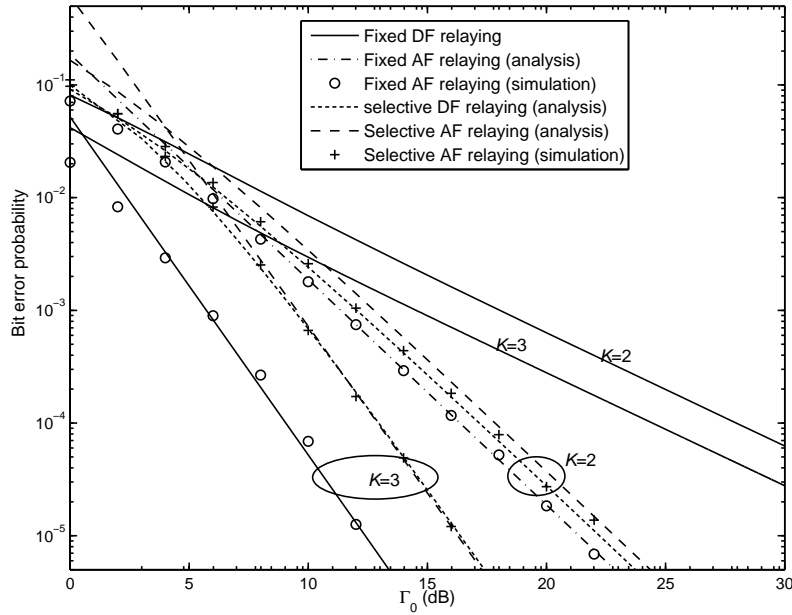


Figure 6.8. Comparison of bit error probabilities among different multi-hop diversity transmission systems employing either DF relaying or AF relaying.

employing fixed DF, selective DF or selective AF relaying protocols. The results shown in Figures 6.7 and 6.8 indicate that the error propagation in multi-hop diversity transmission systems employing DF relaying has more severe effect on the outage probability and bit error rate performances than that of noise amplification in the corresponding system employing AF relaying⁶.

⁶It should be mentioned that combining DF protocols with suitable coding schemes will alleviate the error propagation effect which in turn improves the performance.

Chapter 7

Conclusions and Future Work

This chapter summarizes the contributions of the thesis and suggests some areas for future research.

7.1 Concluding Remarks

In this work, we focused on performance evaluation of a variety of cooperative wireless systems, obtaining new optimal power allocation schemes and development of efficient low complexity receivers. A summary of our contributions is given in the following.

In Chapter 3 of this thesis, we examined performances of multi-hop relaying systems. We first statistically characterized AF multi-hop systems both with variable-gain relays and fixed-gain relays in terms of the MGF (or CHF) of the inverse of the instantaneous received SNR. A closed-form expression for evaluation of the outage probability was then presented using the CHF of the inverse of the reciprocal of the instantaneous received SNR. In addition, we established a general framework for evaluation of the error probabilities in general fading of a variety of modulation schemes using the MGF of the reciprocal of the instantaneous received SNR. This framework was then utilized for performance evaluation of AF multi-hop transmission systems both with variable-gain relays and fixed-gain relays. Asymptotic behaviors of the outages and error probabilities for sufficiently large values of SNR were also examined. In particular, it was shown that if the average link SNRs satisfy a certain criterion, a multi-hop system can achieve better outage and error rate performances than the single-hop system.

In addition, ergodic capacity in Rayleigh fading of multi-hop transmission systems employing AF and DF relaying was investigated assuming CSI is only available at the re-

ceivers. We derived two upper bounds as well as an accurate infinite series expression for the ergodic capacity of AF multi-hop relaying systems. Ergodic capacity of DF multi-hop relaying systems was also obtained. Our analysis showed rigorously that a DF multi-hop relaying system achieves higher ergodic capacity than the corresponding AF multi-hop relaying system.

Furthermore, we derived single integral expressions for evaluation of capacity in general fading of various source-adaptive AF multi-hop relaying systems in terms of the CHF of the inverse of the instantaneous received SNR. It was shown that optimal simultaneous rate and power adaptation achieves the highest capacity, as expected. However, the optimal rate adaption with constant power provides almost the same capacity for large values of SNR while having less complexity. Channel inversion with fixed rate, which is the least complex scheme, slightly outperforms optimal power rate adaptation with constant power technique in small SNR regions but at the cost of increased probability of outage.

In Chapter 4 of this thesis, we obtained optimal power allocation schemes that maximize the instantaneous received SNR in an AF multi-hop transmission system under ST and LT power constraints. The optimal power allocation schemes obtained under both ST and LT power constraints allocate more powers to the terminals with weaker (immediate) forward link. We derived theoretical expressions for evaluation of the outage probability in Rayleigh fading of the proposed power-optimized AF multi-hop transmission systems. In addition, we examined large SNR behavior of the outage probability of these systems. It was shown that at sufficiently large values of SNR, an AF K -hop relaying system employing the optimal power allocation scheme under ST power constraint achieves K times better outage performance than that of the corresponding system employing uniform power allocation. This indicates the importance of employment of the proposed optimal power allocation scheme in AF multi-hop transmission systems subject to a ST power constraint when the number of hops is large. In contrast to the optimal power allocation scheme obtained under ST power constraint that requires a centralized implementation, the optimal strategies obtained under LT power constraints can be implemented in a decentralized manner. In addition, it was shown that a system employing such optimal power allocation schemes offer a significant performance gain by achieving diversity gain 2.

In Chapter 5, we developed low complexity coherent and noncoherent receivers for AF multi-relay cooperative systems. We first reviewed AF multi-relay systems with fixed-gain relays employing R-MRC and S-MRC as benchmarks for performance comparisons. It was shown that these systems offer better error rate performances for larger numbers

of relays and achieve full diversity gain. In addition, the ergodic capacities in Rayleigh fading of these systems were evaluated. It was shown that increasing the number of relays significantly degrades the ergodic capacity of systems with R-MRC due to the employment of the repetition-based scheduling protocol. However, systems with S-MRC achieve larger instantaneous received SNR at the destination for larger numbers of relays, which in turn result in higher ergodic capacities.

We then developed two low complexity receivers, namely, R-DEGC and S-DEGC, for coherent AF cooperative relaying systems. In both schemes, no instantaneous channel amplitude information is needed and the required channel phase information can be acquired in a distributed manner. Theoretical expressions for the evaluation of the error probability and the average output SNR in Rayleigh fading were obtained and it was shown that these schemes achieve full spatial diversity. We also derived upper and lower bounds on the ergodic capacity of the proposed schemes. It was shown that the performance losses of the proposed coherent R-DEGC and S-DEGC systems compared to corresponding systems employing the optimal R-MRC and S-MRC schemes are about 1-1.5 dB for the cases considered. This is a reasonable performance-complexity trade-off considering distributed implementations of the proposed R-DEGC and S-DEGC schemes without requiring fading channel amplitude estimations. In addition, it was shown that S-DEGC scheme achieves larger instantaneous received SNR at the destination and hence better performance than the R-DEGC scheme, especially in terms of ergodic capacity and by increasing the number of relays. In particular, while increasing the number of relays degrades the ergodic capacity of R-DEGC systems, systems employing S-DEGC achieve higher ergodic capacities for larger numbers of relays for sufficiently large values of SNR. Furthermore, it was shown that there is an optimum number of relays that avoids the combining loss (e.g. maximizes the ergodic capacity of a S-DEGC system for a given set of channel parameters) in small SNR regions. This optimum number of relays can be determined using the obtained average output SNR expression.

In the last part of Chapter 5, employment of an MES scheme for noncoherent AF cooperative diversity systems was proposed. An expression for the evaluation of the error probability of this scheme in systems with M -FSK signaling was derived. It was proved that a noncoherent AF cooperative system with MES achieves full diversity. It was also shown that the MES scheme performs slightly inferior to the noncoherent SC scheme in small SNR regions and/or in more faded systems, but achieves almost the same (or even slightly better) performance with increasing SNR. Furthermore, the MES scheme requires

neither knowledge of instantaneous nor statistical fading channel gains at the destination, making it attractive from the practical point of view, especially for application in ad hoc wireless networks.

Chapter 6 studied multi-hop diversity transmission systems. Theoretical expressions for the outage and bit error probabilities of these systems employing either fixed DF relaying or fixed AF relaying were derived. A selective relaying scheme for multi-hop diversity transmission systems was also proposed and evaluated in terms of outage and bit error probabilities. It was shown that multi-hop diversity transmission systems with fixed DF relaying offer no diversity gain, while those employing fixed AF, selective DF or selective AF relaying achieve diversity order equal to the number of hops. In particular, the results showed that multi-hop diversity transmission systems employing fixed AF relaying attain the best outage probability and bit error rate performances, despite noise amplification at the relays, compared to the corresponding systems employing fixed DF, selective DF or selective AF relaying.

7.2 Directions for Future Research

In this thesis, we addressed some issues in the context of cooperative communication systems. On the other hand, the results obtained open some areas for future research.

In this work, we evaluated the capacity of AF multi-hop relaying systems under different source-adaptive schemes. Capacity upper bounds for source-adaptive AF multi-relay systems were recently derived in [104] over Rayleigh fading channels. Capacity of source-adaptive DF multi-hop or multi-relay cooperative systems can be investigated as a future research.

In addition, multi-hop diversity transmission systems have been shown to perform superior to multi-hop systems in terms outage and error probabilities. However, capacity gain of a multi-hop diversity transmission system employing either DF or AF relaying has not been investigated and can be considered as a future research direction.

Furthermore, the results of our study shows that a multi-hop diversity transmission system employing fixed AF relaying achieves the best performance in terms of outage and bit error probabilities. However, the combining scheme employed at each terminal requires a centralized implementation. In practice, it may be highly useful (preferable) to have a combining mechanism that can be implemented by a decentralized structure. The low complexity detection schemes developed in Chapter 5 can be extended for application in

AF multi-hop diversity systems.

The optimal power allocation schemes presented in Chapter 4 were obtained assuming that the source and the relays transmit over equal transmission time slots. However, it may be possible to improve the performance by joint optimization of the transmit power and the channel resources. This requires a new objective function and hence a new optimization problem should be solved.

In addition, in this work as well as most published works in the area of cooperative communications, the functionality of receivers and/or optimal power allocation schemes depend on the perfect channel estimates. It is important to evaluate the robustness of the receivers and optimal power allocations to the noisy estimates of the channel information. However, there have been only a few studies on considering the impact of imperfect channel estimation on the error rate performance of AF dual-hop systems [83], AF single-relay systems [105] as well as on the developing optimal power allocation policies of AF multi-relay systems [106]. Assessing the effects of imperfect channel knowledge on the performance of the systems evaluated and developed in this thesis is an interesting topic for future research.

Bibliography

- [1] A. Sendonaris, E. Erkip, and B. Aazhang, "User cooperation diversity-part I: System description," *IEEE Trans. Commun.*, vol. 51, no. 11, pp. 1927–1938, Nov. 2003.
- [2] A. Sendonaris, E. Erkip, and B. Aazhang, "User cooperation diversity-part II: Implementation aspects and performance analysis," *IEEE Trans. Commun.*, vol. 51, no. 11, pp. 1939–1948, Nov. 2003.
- [3] J. N. Laneman, D. N. C. Tse, and G. W. Wornell, "Cooperative diversity in wireless networks: Efficient protocols and outage behavior," *IEEE Trans. Inform. Theory*, vol. 50, no. 12, pp. 3062–3080, Dec. 2004.
- [4] J. N. Laneman and G. W. Wornell, "Distributed space-time coded protocols for exploiting cooperative diversity in wireless networks," *IEEE Trans. Inform. Theory*, vol. 49, no. 10, pp. 2415–2525, Oct. 2003.
- [5] N. C. Beaulieu and J. Hu, "A closed-form expression for the outage probability of decode-and-forward relaying in dissimilar Rayleigh fading channels," *IEEE Commun. Lett.*, vol. 10, no. 12, pp. 813–815, Dec. 2006.
- [6] I. H. Lee and D. Kim, "BER analysis for decode-and-forward relaying in dissimilar Rayleigh fading channels," *IEEE Commun. Lett.*, vol. 11, no. 1, pp. 52–54, Jan. 2007.
- [7] H. A. Suraweera, P. J. Smith, and J. Armstrong, "Outage probability of cooperative relay networks in Nakagami- m fading channels," *IEEE Commun. Lett.*, vol. 10, no. 12, pp. 834–836, Dec. 2006.
- [8] C. K. Datsikas, N. C. Sagias, F. I. Lazarakis, and G. S. Tombras, "Outage analysis of decode-and-forward relaying over Nakagami- m fading channels," *IEEE Signal Process. Lett.*, vol. 15, pp. 41–44, Jan. 2008.

- [9] A. Müller and J. Speidel, "Exact symbol error probability of M-PSK for multihop transmission with regenerative relays," *IEEE Commun. Lett.*, vol. 11, no. 12, pp. 834–836, Dec. 2007.
- [10] S. Ikki and M. H. Ahmed, "Performance of decode-and-forward cooperative diversity networks over Nakagami- m fading channels," in *Proc. IEEE Global Commun. Conf. (GLOBECOM)*, Washington, DC, Nov. 2007, pp. 4328–4333.
- [11] Y. Lee and M.-H. Tsai, "Performance of decode-and-forward cooperative communications over Nakagami- m fading channels," *IEEE Trans. Veh. Technol.*, vol. 58, no. 3, pp. 1218–1227, Mar. 2009.
- [12] T. A. Tsiftsis, G. K. Karagiannidis, S. A. Kotsopoulos, and F.-N. Pavlidou, "BER analysis of collaborative dual-hop wireless transmissions," *IEE Elect. Lett.*, vol. 40, no. 11, pp. 679–681, May 2004.
- [13] P. A. Anghel and M. Kaveh, "Exact symbol error probability of a cooperative network in a Rayleigh-fading environment," *IEEE Trans. Wireless Commun.*, vol. 3, no. 5, pp. 1416–1421, Sep. 2004.
- [14] A. Riberio, K. Cai, and G. Giannakis, "Symbol error probabilities for general cooperative links," *IEEE Trans. Wireless Commun.*, vol. 4, no. 3, pp. 1264–1273, May 2005.
- [15] T. A. Tsiftsis, G. K. Karagiannidis, P. T. Mathiopoulos, and S. A. Kotsopoulos, "Nonregenerative dual-hop cooperative links with selection diversity," *EURASIP J. Wireless Commun. and Networking*, pp. 1–8, Article ID 17 862, 2006 (2006).
- [16] K. G. Seddik, A. K. Sadek, W. Su, and K. J. R. Liu, "Outage analysis and optimal power allocation for multinode relay networks," *IEEE Signal Process. Lett.*, vol. 14, no. 6, pp. 377–380, Jun. 2007.
- [17] A. Ikki and M. H. Ahmed, "Performance analysis of cooperative diversity wireless networks over Nakagami- m fading channel," *IEEE Commun. Lett.*, vol. 11, no. 4, pp. 334–336, Apr. 2007.
- [18] L. L. Yang and H. H. Chen, "Error probability of digital communications using relay diversity Nakagami- m fading channels," *IEEE Trans. Wireless Commun.*, vol. 7, no. 5, pp. 1806–1811, May 2008.

- [19] M. O. Hasna and M. S. Alouini, "End-to-end performance of transmission systems with relays over Rayleigh fading channels," *IEEE Trans. Wireless Commun.*, vol. 2, no. 6, pp. 1126–1131, Nov. 2003.
- [20] M. O. Hasna and M. S. Alouini, "A performance study of dual-hop transmissions with fixed gain relays," *IEEE Trans. Wireless Commun.*, vol. 3, no. 6, pp. 1963–1968, Nov. 2004.
- [21] T. A. Tsiftsis, G. K. Karagiannidis, and S. A. Kotsopoulos, "Dual-hop wireless communications with combined gain relays (CGR)," *IEE Proc. Commun.*, vol. 152, no. 5, pp. 528–532, Oct. 2005.
- [22] H. A. Suraweera and G. K. Karagiannidis, "Closed-form error analysis of the non-identical Nakagami- m relay fading channel," *IEEE Commun. Lett.*, vol. 12, no. 4, pp. 259–261, Apr. 2008.
- [23] G. K. Karagiannidis, "Performance bounds of multihop wireless communications with blind relays over generalized fading channels," *IEEE Trans. Wireless Commun.*, vol. 5, no. 3, pp. 498–503, Mar. 2006.
- [24] G. K. Karagiannidis, T. Tsiftsis, and R. K. Mallik, "Bounds for multihop relayed communications in Nakagami- m fading," *IEEE Trans. Commun.*, vol. 54, no. 1, pp. 18–22, Jan. 2006.
- [25] M. Di Renzo, F. Graziosi, and F. Santucci, "On the performance of CSI-assisted cooperative communications over generalized fading channels," in *Proc. IEEE Int. Conf. Commun. (ICC)*, May 2008, pp. 1001–1007.
- [26] J. Boyer, D. D. Falconer, and H. Yanikomeroglu, "Multi-hop diversity in wireless relaying channels," *IEEE Trans. Commun.*, vol. 52, pp. 1820–1830, Oct. 2004.
- [27] D. S. Michalopoulos and T. A. Tsiftsis, "Performance analysis of wireless multihop diversity systems," *Int. J. Commun. Sys.*, vol. 21, no. 9, pp. 955–969, Sep. 2008.
- [28] M. O. Hasna and M. S. Alouini, "Outage probability of multi-hop transmission over Nakagami fading channels," *IEEE Commun. Lett.*, vol. 7, pp. 216–218, May 2003.
- [29] M. O. Hasna and M. S. Alouini, "Harmonic mean and end-to-end performance of transmission systems with relays," *IEEE Trans. Commun.*, vol. 52, no. 1, pp. 130–135, Jan. 2004.

- [30] A. Bletsas, A. Khisti, D. P. Reed, and A. Lippman, "A simple cooperative diversity method based on network path selection," *IEEE J. Select. Areas Commun.*, vol. 24, no. 6, pp. 659–672, Mar. 2006.
- [31] Y. Zhao, R. Adve, and T. J. Lim, "Improving amplify-and-forward relay networks: optimal power allocation versus selection," *IEEE Trans. Wireless Commun.*, vol. 6, no. 8, pp. 3114–3123, Aug. 2007.
- [32] A. S. Ibrahim, A. K. Sadek, W. Su, and K. J. R. Liu, "Cooperative communications with relay-selection: When to cooperate and whom to cooperate with?" *IEEE Trans. Wireless Commun.*, vol. 7, no. 7, pp. 2814–2827, Jul. 2008.
- [33] J. N. Laneman and G. W. Wornell, "Energy-efficient antenna sharing and relaying for wireless networks," in *Proc. IEEE Wireless Commun. and Networking Conf. (WCNC)*, Sep. 2000, pp. 7–12.
- [34] D. Chen and J. N. Laneman, "Modulation and demodulation for cooperative diversity in wireless systems," *IEEE Trans. Wireless Commun.*, vol. 5, no. 7, pp. 1785–1794, Jul. 2006.
- [35] T. Wang, A. Cano, G. B. Giannakis, and J. N. Laneman, "High-performance cooperative demodulation with decode-and-forward relays," *IEEE Trans. Commun.*, vol. 55, no. 7, pp. 1427–1438, Jul. 2007.
- [36] Z. Yi and I.-M. Kim, "Diversity order analysis of the decode-and-forward cooperative networks with relay selection," *IEEE Trans. Wireless Commun.*, vol. 7, no. 5, pp. 1792–1799, May 2008.
- [37] T. Q. Duong and V. N. Q. Bao, "Performance analysis of selection decode-and-forward relay networks," *IEE Elect. Lett.*, vol. 44, no. 20, pp. 1206–1207, Sep. 2008.
- [38] D. S. Michalopoulos and G. K. Karagiannidis, "Distributed switch and stay combining (DSSC) with a single decode and forward relay," *IEEE Commun. Lett.*, vol. 11, no. 5, pp. 408–410, May 2007.
- [39] D. S. Michalopoulos and G. K. Karagiannidis, "Two-relay distributed switch and stay combining (DSSC)," *IEEE Trans. Commun.*, vol. 56, no. 11, pp. 1790–1794, Nov. 2008.

- [40] D. Chen and J. N. Laneman, "Cooperative diversity for wireless fading channels without channel state information," in *Proc. Asilomar Conf. Signals, Systems, and Computers*, Nov. 2004, pp. 1307–1312.
- [41] R. Annavajjala, P. C. Cosman, and L. B. Milstein, "On the performance of optimum noncoherent amplify-and-forward reception for cooperative diversity," in *Proc. Military Commun. Conf. (MILCOM)*, Oct. 2005, pp. 3280–3288, vol. 5.
- [42] Y. Zhu, P.-Y. Kam, and Y. Xin, "Non-coherent detection for amplify-and-forward relay systems in a Rayleigh fading environment," in *Proc. IEEE Global Commun. Conf. (GLOBECOM)*, Washington, DC, Nov./Dec. 2007, pp. 1658–1662.
- [43] M. R. Souryal, "Non-coherent amplify-and-forward generalized likelihood ratio test receiver," in *Proc. IEEE Global Commun. Conf. (GLOBECOM)*, New Orleans, LA, Nov./Dec. 2008, pp. 1–6.
- [44] Y.-W. Hong, W.-J. Huang, F.-H. Chiu, and C.-C. J. Kuo, "Cooperative communications in resource-constrained wireless networks," *IEEE Signal Process. Mag.*, vol. 24, no. 3, pp. 47–57, May 2007.
- [45] Q. Zhang, J. Zhang, C. Shao, Y. Wang, P. Zhang, and R. Hu, "Power allocation for regenerative relay channel with Rayleigh fading," in *Proc. IEEE Veh. Technol. Conf.*, May 2004, pp. 1167–1171.
- [46] J. Zhang, Q. Zhang, C. Shao, Y. Wang, P. Zhang, and Z. Zhang, "Adaptive optimal transmit power allocation for two-hop non-regenerative wireless relay system," in *Proc. IEEE Veh. Technol. Conf.*, May 2004, pp. 1213–1217.
- [47] M. O. Hasna and M.-S. Alouini, "Optimal power allocation for relayed transmissions over Rayleigh-fading channels," *IEEE Trans. Wireless Commun.*, vol. 3, no. 6, pp. 1999–2004, Nov. 2004.
- [48] A. P. T. Lau and S. Cui, "Joint power minimization in wireless relay channels," *IEEE Trans. Wireless Commun.*, vol. 6, no. 8, pp. 2820–2824, Aug. 2007.
- [49] I. Maric and R. Yates, "Forwarding strategies for gaussian parallel-relay networks," in *Proc. Int. Symp. Inform. Theory (ISIT)*, Jun./Jul. 2004, p. 269.
- [50] Y. Liang and V. Veeravalli, "Resource allocation for wireless relay channels," in *Proc. Asilomar Conf. Signals, Systems and Computers*, vol. 2, Nov. 2004, pp. 1902–1906.

- [51] N. Ahmed, M. Khojastepour, A. Sabharwal, and B. Aazhang, "Outage minimization with limited feedback for the fading relay channel," *IEEE Trans. Commun.*, vol. 54, no. 4, pp. 659–669, Apr. 2006.
- [52] N. Ahmed and B. Aazhang, "Throughput gains using rate and power control in cooperative relay networks," *IEEE Trans. Commun.*, vol. 55, no. 4, pp. 656–660, Apr. 2007.
- [53] X. Deng and A. M. Haimovich, "Power allocation for cooperative relaying in wireless networks," *IEEE Commun. Lett.*, vol. 9, no. 11, pp. 994–996, Nov. 2005.
- [54] R. Nikjah and N. C. Beaulieu, "On optimal power allocation for source-orthogonal relay-nonorthogonal amplify-and-forward relaying," in *Proc. IEEE Global Commun. Conf. (GLOBECOM)*, Nov./Dec. 2008, pp. 1–6.
- [55] R. Annavajjala, P. C. Cosman, and L. B. Milstein, "Statistical channel knowledge-based optimum power allocation for relaying protocols in the high SNR regime," *IEEE J. Select. Areas Commun.*, vol. 25, no. 2, pp. 292–305, Feb. 2007.
- [56] Y. Li, B. Vucetic, Z. Zhou, and M. Dohler, "Distributed adaptive power allocation for wireless relay networks," *IEEE Trans. Wireless Commun.*, vol. 6, no. 3, pp. 948–958, Mar. 2007.
- [57] J. Luo, R. S. Blum, L. J. Cimini, L. J. Greenstein, and A. M. Haimovich, "Decode-and-forward cooperative diversity with power allocation in wireless networks," *IEEE Trans. Wireless Commun.*, vol. 6, no. 3, pp. 793–799, Mar. 2007.
- [58] M. Chen, S. Serbetli, and A. Yener, "Distributed power allocation strategies for parallel relay networks," *IEEE Trans. Wireless Commun.*, vol. 7, no. 2, pp. 793–799, Feb. 2008.
- [59] E. C. van der Meulen, "Three-terminal communication channels," *Adv. Appl. Prob.*, no. 3, pp. 120–154, 1971.
- [60] T. M. Cover and A. A. El Gamal, "Capacity theorems for relay channels," *IEEE Trans. Inform. Theory*, vol. 25, no. 5, pp. 1463–1474, Sep. 1979.
- [61] A. El Gamal and S. Zahedi, "Capacity of a class of relay channels with orthogonal components," *IEEE Trans. Inform. Theory*, vol. 51, no. 5, pp. 1815–1817, May 2005.

- [62] L. L. Xie and P. R. Kumar, "An achievable rate for the multiple level relay channel," in *Proc. IEEE Symp. Inform. Theory (ISIT)*, Jun./Jul. 2004, p. 3.
- [63] A. Reznik, S. R. Kulkarni, and S. Verdú, "Degraded gaussian multirelay channel: Capacity and optimal power allocation," *IEEE Trans. Inform. Theory*, vol. 50, no. 12, pp. 3037–3046, Dec. 2004.
- [64] G. Kramer, M. Gastpar, and P. Gupta, "Cooperative strategies and capacity theorems for relay networks," *IEEE Trans. Inform. Theory*, vol. 51, no. 9, pp. 3037–3063, Sep. 2005.
- [65] P. Gupta and P. R. Kumar, "The capacity of wireless networks," *IEEE Trans. Inform. Theory*, vol. 46, no. 2, pp. 388–404, Mar. 2000.
- [66] P. Gupta and P. R. Kumar, "Toward an information theory of large networks: an achievable rate region," in *Proc. IEEE Symp. Inform. Theory (ISIT)*, Jun. 2001, p. 159.
- [67] M. Gastpar and M. Vetterli, "On the asymptotic capacity of Gaussian relay channels," in *Proc. IEEE Symp. Inform. Theory*, Jun./Jul. 2002, p. 195.
- [68] A. Høst-Madsen and J. Zhang, "Capacity bounds and power allocation for wireless relay channels," *IEEE Trans. Inform. Theory*, vol. 51, no. 6, pp. 2020–2040, Jun. 2005.
- [69] B. Wang, J. Zhang, and A. Høst-Madsen, "On the capacity of MIMO relay channels," *IEEE Trans. Inform. Theory*, vol. 51, no. 1, pp. 29–43, Jan. 2005.
- [70] R. U. Nabar, H. Bölcskei, and F. W. Kneubühler, "Fading relay channels: Performance limits and space-time signal design," *IEEE J. Select. Areas Commun.*, vol. 22, no. 6, pp. 1099–1109, Aug. 2004.
- [71] I. E. Telatar, "Capacity of multi-antenna gaussian channels," *Eur. Trans. Telecommun.*, vol. 10, no. 6, pp. 585–595, Nov./Dec. 1999.
- [72] M. S. Alouini and A. J. Goldsmith, "Capacity of Rayleigh fading channels under different adaptive transmission and diversity-combining techniques," *IEEE Trans. Veh. Technol.*, vol. 48, no. 6, pp. 1165–1181, Jul. 1999.
- [73] A. Goldsmith, *Wireless Communications*. New York: Cambridge University Press, 2005.

- [74] N. C. Beaulieu, "An infinite series for the computation of the complementary probability distribution function of a sum of independent random variables and its application to the sum of Rayleigh random variables," *IEEE Trans. Commun.*, vol. 38, pp. 1463–1474, Sep. 1990.
- [75] Y. Zhao, R. Adve, and T. J. Lim, "Beamforming with limited feedback in amplify-and-forward cooperative networks," *IEEE Trans. Wireless Commun.*, vol. 7, no. 12, pp. 5145 – 5149, Dec. 2008.
- [76] N. C. Beaulieu and J. Hu, "A noise reduction amplify-and-forward relay protocol for distributed spatial diversity," *IEEE Commun. Lett.*, vol. 10, no. 11, pp. 787–789, Nov. 2006.
- [77] D. S. Michalopoulos, A. S. Lioumpas, and G. K. Karagiannidis, "Low complexity amplify and forward relaying without channel amplitude estimation," in *Proc. IEEE Int. Conf. Commun. (ICC)*, Beijing, China, May 2008, pp. 4295–4299.
- [78] J. G. Proakis, *Digital Communications*, 4th ed. New York: McGraw-Hill, 2000.
- [79] N. Ahmed, M. Khojastepour, and B. Aazhang, "Outage minimization and optimal power control for the fading relay channel," in *Proc. Inform. Theory Workshop (ITW)*, Oct. 2004, pp. 458–462.
- [80] A. Chakrabarti, A. de Baynast, A. Sabharwal, and B. Aazhang, "Half-duplex estimate-and-forward relaying: Bounds and code design," in *Proc. Int. Symp. Inform. Theory (ISIT)*, Jul. 2006, pp. 1239–1241.
- [81] K. S. Gomadam and S. A. Jafar, "On the capacity of memoryless relay networks," in *Proc. Int. Conf. Commun. (ICC)*, Jun. 2006, pp. 1580–1585.
- [82] J. Boyer, D. Falconer, and H. Yanikomeroglu, "Cooperative connectivity models for wireless relay networks," *IEEE Trans. Wireless Commun.*, vol. 6, no. 6, pp. 1992–2000, Jun. 2007.
- [83] C. S. Patel and G. L. Stüber, "Channel estimation for amplify and forward relay based cooperation diversity systems," *IEEE Trans. Wireless Commun.*, vol. 6, no. 6, pp. 2348–2356, Jun. 2007.
- [84] B. Zhao and M. C. Valenti, "Distributed turbo-coded diversity for the relay channel," *IEE Elect. Lett.*, vol. 39, no. 10, pp. 786–787, May 2003.

- [85] R. Liu, P. Sapsiojevic, and E. Soljanin, "User cooperation with punctured turbo codes," in *Proc. Allerton Conf. Commun. Contr. Computing*.
- [86] M. Janani, A. Hedayat, T. E. Hunter, and A. Nosratinia, "Coded cooperation in wireless communications: space-time transmission and iterative decoding," *IEEE Trans. Signal Process.*, vol. 52, no. 2, pp. 362–371, Feb. 2004.
- [87] Z. Wang and G. B. Giannakis, "A simple and general parameterization quantifying performance in fading channels," *IEEE Trans. Commun.*, vol. 51, no. 8, pp. 1389–1398, Aug. 2003.
- [88] H. Shin and J. B. Song, "MRC analysis of cooperative diversity with fixed-gain relays in Nakagami- m fading channels," *IEEE Trans. Wireless Commun.*, vol. 7, no. 6, pp. 2069–2074, Jun. 2008.
- [89] M. K. Simon and M. S. Alouini, *Digital Communications Over Fading Channels*. New York: Wiley-Interscience, 2000.
- [90] I. S. Gradshteyn and I. M. Ryzhik, *Table of Integrals, Series, and Products*, 6th ed. New York: Academic, 2000.
- [91] M. Abramowitz and I. A. Stegun, *Handbook of Mathematical Functions with Formulas, Graphs, and Mathematical Tables*, 7th ed. New York: Dover, 1972.
- [92] K. Cho and D. Yoon, "On the general BER expression of one- and two-dimensional amplitude modulations," *IEEE Trans. Commun.*, vol. 50, no. 7, pp. 1074–1080, Jul. 2002.
- [93] G. M. Dillard, "Recursive computation of the generalized Q-function," *IEEE Trans. Aerosp. Electron. Syst.*, vol. 50, no. AES-9, pp. 614–615, Jul. 1973.
- [94] T. S. Rappaport, *Wireless Communications: Principles and Practice*. New Jersey: Prentice-Hall, 1996.
- [95] E. Biglieri, J. Proakis, and S. Shamai (Shitz), "Fading channels: information-theoretic and communications aspects," *IEEE Trans. Inform. Theory*, vol. 44, no. 6, pp. 2619–2692, Apr. 1998.
- [96] S. Ross, *A First Course in Probability*, 6th ed. New Jersey: Prentice-Hall, 2002.
- [97] S. Boyd and L. Vandenberghe, *Convex Optimization*, 1st ed. New York: Cambridge University Press, 2004.

- [98] R. Negi and J. M. Cioffi, "Delay-constrained capacity with causal feedback," *IEEE Trans. Inform. Theory*, vol. 48, no. 9, pp. 2478–2494, Sep. 2002.
- [99] C. Tellambura, V. K. Bhargava, and A. Annamalai, "A general method for calculating error probabilities over fading channels," *IEEE Trans. Commun.*, vol. 53, no. 5, pp. 841–852, May 2005.
- [100] G.-T. Chyi, J. G. Proakis, and C. M. Keller, "On the symbol error probability of maximum-selection diversity reception schemes over a Rayleigh fading channel," *IEEE Trans. Commun.*, vol. 37, no. 1, pp. 79–83, Jan. 1989.
- [101] M. K. Simon, *Probability Distributions Involving Gaussian Random Variables: A Handbook for Engineers and Scientists*, 1st ed. Massachusetts: Kluwer Academic, 2002.
- [102] Y. Zhao, R. Adve, and T. Lim, "Symbol error rate of selection amplify-and-forward relay systems," *IEEE Commun. Lett.*, vol. 10, no. 11, pp. 757–759, Nov. 2006.
- [103] Y. G. Kim and N. C. Beaulieu, " $S + N$ energy selection combining for BPSK signaling in Rayleigh fading channels," *to appear in IEEE Trans. Commun.*
- [104] T. Nechiporenko, K. T. Phan, C. Tellambura, and H. H. Nguyen, "On the capacity of rayleigh fading cooperative systems under adaptive transmission," *IEEE Trans. Wireless Commun.*, vol. 8, no. 4, pp. 1626–1631, Apr. 2009.
- [105] B. Gedik and M. Uysal, "Impact of imperfect channel estimation on the performance of amplify-and-forward relaying," *IEEE Trans. Wireless Commun.*, vol. 8, no. 3, pp. 1468–1479, Mar. 2009.
- [106] T. Q. S. Quek, H. Shin, and M. Win, "Robust wireless relay networks: Slow power allocation with guaranteed QoS," *IEEE J. Select. Topics Signal Process.*, vol. 1, no. 4, pp. 700–713, Dec. 2007.
- [107] M. R. Spiegel, *Advanced Mathematics for Engineers and Scientists*. New York: McGraw-Hill, 1971.

Appendix A

Proof of Lemmas

A.1 Proof of Lemma 3.1

The proof for the asymptotic symbol error probability in (3.23) is given in [14]. In this section, a proof for the asymptotic bit error probability in (3.22) is first given.

Let $\beta = \gamma_t/\bar{\gamma}$ where $\bar{\gamma}$ denotes the average SNR. Then, using (3.13), the bit error probability is obtained as

$$P_b = \int_0^\infty \frac{\Gamma(b, a\beta\bar{\gamma})}{2\Gamma(b)} f_\beta(\beta) d\beta \quad (\text{A.1})$$

where $f_\beta(\beta) = \bar{\gamma} f_{\gamma_t}(\beta\bar{\gamma})$. For large values of SNR (as $\bar{\gamma} \rightarrow \infty$), the value of $\Gamma(b, a\beta\bar{\gamma})$ tends to zero throughout the integration range except near the origin [91]. Furthermore, for large SNRs, corresponding to values of β close to zero, $f_\beta(\beta)$ is well approximated by the first term of its MacLaurin series, i.e.

$$f_\beta(\beta) \rightarrow \frac{1}{t!} \frac{\partial^t f_{\gamma_t}}{\partial \gamma^t}(0) \bar{\gamma}^{t+1} \beta^t \quad (\text{A.2})$$

where t is the order of the first nonzero derivative of the PDF of γ_t at $\gamma = 0$. Then, one has

$$P_b \rightarrow \int_0^\infty \frac{\Gamma(b, a\gamma)}{2\Gamma(b)} \frac{1}{t!} \frac{\partial^t f_{\gamma_t}}{\partial \gamma^t}(0) \gamma^t d\gamma \quad (\text{A.3})$$

and consequently, eq. (3.22) is obtained by evaluation of the integral in (A.3) using [90, eq. (6.5.37)].

A proof for the asymptotic outage probability in (3.21) was given in [87] by taking integral of the single polynomial term approximation of the PDF of β given in (A.2) from 0 to $\frac{\gamma_{th}}{\bar{\gamma}}$. An alternate proof for (3.21) is given in the following. For large values of SNR,

as $\bar{\gamma} \rightarrow \infty$, the CDF of β , $F_\beta(\beta)$, is well approximated by the first term of its MacLaurin series given by

$$\begin{aligned} F_\beta(\beta) &\approx \frac{\beta^{t+1}}{(t+1)!} \frac{\partial^t f_\beta}{\partial \beta^t}(0) \\ &= \frac{\beta^{t+1} \bar{\gamma}^{t+1}}{(t+1)!} \frac{\partial^t f_{\bar{\gamma}t}}{\partial \gamma^t}(0) \end{aligned} \quad (\text{A.4})$$

using $F_\beta(0) = 0$ and $\frac{\partial F_\beta(\beta)}{\partial \beta} = f_\beta(\beta)$. Now note that

$$P_{out} = F_\beta\left(\frac{\gamma^{th}}{\bar{\gamma}}\right) \quad (\text{A.5})$$

and, consequently, eq. (3.21) is obtained using (A.4) in which β is replaced by $\frac{\gamma^{th}}{\bar{\gamma}}$.

A.2 Proof of Lemma 3.2

The random variable V defined in (3.25) is a multi-dimensional function of independent random variables whose PDF is given by

$$f_V(v) = \int \dots \int_{\{(x_1, \dots, x_{\mathcal{M}}): g(x_1, \dots, x_{\mathcal{M}}) = v\}} \frac{\prod_{h=1}^{\mathcal{M}} f_{X_h}(x_h) dx_h}{|\nabla g(x_1, \dots, x_{\mathcal{M}})|} \quad (\text{A.6})$$

where $f_{X_h}(x_h)$, $h = 1, \dots, \mathcal{M}$, denotes the PDF of X_h and $|\nabla g(x_1, \dots, x_{\mathcal{M}})|$ is the modulus of the gradient of $g(x_1, \dots, x_{\mathcal{M}})$. The integral in (A.6) is taken over an \mathcal{M} -dimensional hyperplane for which $g(x_1, \dots, x_{\mathcal{M}}) = v$. However, calculation of the value of the PDF at zero is equivalent to nullifying one vector component at a time. Thus, to evaluate $f_V(0)$, the integral in (A.6) is taken over the union of \mathcal{M} hyperplanes of dimension $\mathcal{M} - 1$ at which any of x_m is zero. Then, one has

$$f_V(0) = \sum_{m=1}^{\mathcal{M}} f_{X_m}(0) \underbrace{\int \dots \int}_{(\mathcal{M}-1)\text{fold}} \frac{\prod_{\substack{h=1 \\ h \neq m}}^{\mathcal{M}} f_{X_h}(x_h) dx_h}{|\nabla g(x_1, \dots, x_{\mathcal{M}})|_{x_m=0}}. \quad (\text{A.7})$$

It can be shown that the modulus of the gradient at $x_m = 0$, $m = 1, \dots, \mathcal{M}$, is given by

$$|\nabla g(x_1, \dots, x_{\mathcal{M}})|_{x_m=0} = \left(\sum_{j=m-1}^{\mathcal{M}-1} \frac{\prod_{h=0}^j \Psi_h}{\prod_{\substack{h=1 \\ h \neq m}}^{j+1} X_h} \right)^{-1}. \quad (\text{A.8})$$

Thus,

$$f_V(0) = \sum_{m=1}^{\mathcal{M}} f_{X_m}(0) \sum_{j=m-1}^{\mathcal{M}-1} \prod_{h=0}^j \Psi_h$$

$$\begin{aligned}
& \int \cdots \int \frac{\prod_{\substack{h=1 \\ h \neq m}}^{\mathcal{M}} f_{X_h}(x_h) dx_h}{\prod_{\substack{h=1 \\ h \neq m}}^{j+1} X_h} \\
&= \sum_{m=1}^{\mathcal{M}} f_{X_m}(0) \sum_{j=m-1}^{\mathcal{M}-1} \prod_{h=0}^j \Psi_h \mathbb{E} \left(\frac{1}{\prod_{\substack{h=1 \\ h \neq m}}^{j+1} X_h} \right). \tag{A.9}
\end{aligned}$$

Note that (A.9) gives an exact expression for calculation of $f_V(0)$. An exact closed-form formula for $\mathbb{E} \left(\prod_{\substack{h=1 \\ h \neq m}}^{j+1} X_h^{-1} \right)$ required for the evaluation of $f_V(0)$ can not be obtained for our cases of interest in which X_h represent powers of Rayleigh, Ricean, or Hoyt fading envelopes. However, it can be replaced by a simple function of $\mathbb{E}(X_h)$, which is known for a variety of fading channel types to provide valuable insights for performance evaluation of cooperative systems with fixed gain relays. Now let $\mathcal{U}_{j,m} = \prod_{\substack{h=1 \\ h \neq m}}^{j+1} X_h$, then according to Jensen's inequality [96]

$$\mathbb{E} \left(\frac{1}{\mathcal{U}_{j,m}} \right) \geq \frac{1}{\mathbb{E}(\mathcal{U}_{j,m})} = \frac{1}{\prod_{\substack{h=1 \\ h \neq m}}^{j+1} \mathbb{E}(X_h)}. \tag{A.10}$$

Consequently, substituting the inequality (A.10) in (A.9) gives eq. (3.26) and the Lemma is proved.

A.3 Proof of Lemma 3.3

Suppose that the series in (3.38) and (3.39) are truncated, respectively, at $n = M$ and $n = 2M - 1$. Then, the corresponding truncation errors are given by

$$\Delta_1 = 2 \sum_{n=M+1}^{\infty} \frac{1}{2n-1} \left(\frac{x}{x+2} \right)^{2n-1} \tag{A.11}$$

and

$$\Delta_2 = \sum_{n=2M}^{\infty} \frac{1}{n} \left(\frac{x}{x+1} \right)^n \tag{A.12}$$

respectively. Since,

$$\frac{x}{x+2} < \frac{x}{x+1} < 1 \tag{A.13}$$

and

$$\frac{\left(\frac{x}{x+1} \right)^{m+1}}{m+1} < \frac{\left(\frac{x}{x+1} \right)^m}{m} \tag{A.14}$$

for all positive integers m , one has

$$\begin{aligned} \Delta_1 &\stackrel{(A.13)}{<} 2 \sum_{n=M+1}^{\infty} \frac{1}{2n-1} \left(\frac{x}{x+1}\right)^{2n-1} \\ &\stackrel{(A.14)}{<} \sum_{n=2M}^{\infty} \frac{1}{n} \left(\frac{x}{x+1}\right)^n = \Delta_2 \end{aligned} \quad (A.15)$$

and the Lemma is proved.

A.4 Proof of Lemma 3.4

Using (A.13) and (A.14), one has

$$\frac{1}{2n-1} \left(\frac{x}{x+2}\right)^{2n-1} < \frac{1}{n} \left(\frac{x}{x+1}\right)^n. \quad (A.16)$$

Furthermore, recall that the series $\sum_{n=1}^{\infty} \frac{1}{n} \left(\frac{x}{x+1}\right)^n$ converges to the function $\ln(1+x)$ for $x \geq 0$. Therefore, according to the Weierstrass M -test [107], the series in (3.38) converges uniformly for $x \geq 0$.

A.5 Proof of Lemma 3.5

Recall that the function $U(w)$ is a complex function as defined in (3.52). Now note that the complex conjugate of the function $U(w)$ is given by

$$U^*(w) = \Psi_X^*(w) \int_{a_1}^{a_2} g(x) \exp(jwx) dx. \quad (A.17)$$

Using the conjugation property of the Fourier transform for real functions, one has $\Psi_X^*(w) = \Psi_X(-w)$. Furthermore, since $g(x)$ is a real function, one obtains

$$U^*(w) = U(-w). \quad (A.18)$$

Using eq. (A.18), one has

$$\Re(U(w)) = \frac{U(w) + U^*(w)}{2} = \frac{U(w) + U(-w)}{2} \quad (A.19)$$

and

$$\Im(U(w)) = \frac{U(w) - U^*(w)}{2} = \frac{U(w) - U(-w)}{2} \quad (A.20)$$

where $\Im(\cdot)$ denotes the imaginary part of its argument. Eqs. (A.19) and (A.20) show that the real and imaginary parts of $U(w)$ are even and odd functions, respectively. Therefore, one obtains

$$\begin{aligned} \int_{-\infty}^{\infty} U(w)dw &= \int_{-\infty}^{\infty} [\Re(U(w)) + j\Im(U(w))] dw \\ &= 2 \int_0^{\infty} \Re(U(w)) dw = 2 \int_0^{\frac{\pi}{2}} \Re(U(\tan(\theta)))\sec^2(\theta)d\theta \end{aligned} \quad (\text{A.21})$$

using the change of variable $w = \tan(\theta)$ and the Lemma is proved.

A.6 Proof of Lemma 4.1

An asymptotic expression for the outage probability for sufficiently large values of SNR is given by (3.21). According to eq. (3.21), we only need to evaluate the first nonzero order derivative of the PDF of γ_t^{ST} , $f_{\gamma_t^{ST}}(\gamma)$, at the origin. Let \mathbf{u} denote the K -dimensional vector $[\gamma_1, \gamma_2, \dots, \gamma_K]$. According to (4.10), γ_t^{ST} can be rewritten as

$$\gamma_t^{ST} \cong K\hat{\gamma} \quad (\text{A.22a})$$

where

$$\hat{\gamma} = g(\mathbf{u}) = \frac{\prod_{k=1}^K \gamma_k}{\left(\sum_{k=1}^K \prod_{\substack{j=1 \\ j \neq k}}^K \sqrt{\gamma_j}\right)^2}. \quad (\text{A.22b})$$

Then, using (A.7), the value of the PDF of $\hat{\gamma}$ at the origin can be computed as

$$f_{\hat{\gamma}}(0) = \sum_{k=1}^K f_{\gamma_k}(0) \underbrace{\int \dots \int}_{(K-1) \text{ fold}} \frac{\prod_{\substack{h=1 \\ h \neq k}}^K f_{\gamma_h}(\gamma_h)d\gamma_h}{|\nabla g(\mathbf{u})|_{\gamma_k=0}}. \quad (\text{A.23a})$$

It can be shown that the modulus of the gradient at $\gamma_k = 0$, $k = 1, \dots, K$, is equal to unity and then, we have

$$f_{\hat{\gamma}}(0) = \sum_{k=1}^K f_{\gamma_k}(0) \quad (\text{A.23b})$$

where $f_{\gamma_k}(0) = \frac{1}{\Gamma_k}$ in Rayleigh fading. Consequently one has

$$f_{\gamma_t^{ST}}(0) = \frac{1}{K} f_{\hat{\gamma}}(0) = \frac{1}{K} \sum_{k=1}^K \frac{1}{\Gamma_k}. \quad (\text{A.24})$$

Thus, $t = 0$ in eq. (3.21) yielding the asymptotic outage probability as

$$P_{out}^{ST} \rightarrow \gamma_{th} f_{\gamma_t^{ST}}(0) \quad (\text{A.25})$$

and finally substituting (A.24) in (A.25) proves the Lemma.

A.7 Proof of Lemma 6.1

The initial value theorem of Laplace transforms is utilized for calculation of the value of the PDF of the random variable $V = \sum_{k=0}^{K-1} V_k$ at zero in which V_0 is independent of V_k , $k = 1, \dots, K-1$, but all other summands are dependent random variables. Now, let \mathbf{W} be an arbitrary vector of nonnegative random variables such that V_i be independent of $V_j|\mathbf{W}$, $i \neq j$, $i, j \in \{1, 2, \dots, K-1\}$. Then the Laplace transform of $f_V(v)$ can be expressed as

$$L_V(s) = L_{V_0}(s) \int \dots \int_{\mathbf{w}} \prod_{i=1}^{K-1} L_{V_i|\mathbf{w}}(s) f_{\mathbf{w}}(\mathbf{w}) d\mathbf{w} \quad (\text{A.26})$$

where $L_{V_0}(s)$ and $L_{V_i|\mathbf{w}}(s)$, respectively, denote the Laplace transforms of the PDFs of V_0 and $V_i|\mathbf{W}$, $f_{V_0}(z_0)$ and $f_{V_i|\mathbf{w}}(z_i|\mathbf{w})$, $i = 1, \dots, K-1$. According to the initial value theorem, the value of $f_V(v)$ at zero is given by

$$f_V(0) = \lim_{s \rightarrow \infty} s L_V(s) \quad (\text{A.27})$$

which can be rewritten as a product of limits

$$f_V(0) = \lim_{s \rightarrow \infty} s L_{V_0}(s) \int \dots \int_{\mathbf{w}} \prod_{i=1}^{K-1} \lim_{s \rightarrow \infty} L_{V_i|\mathbf{w}}(s) f_{\mathbf{w}}(\mathbf{w}) d\mathbf{w} \quad (\text{A.28})$$

and since $\lim_{s \rightarrow \infty} s L_{V_0}(s) = f_{V_0}(0)$ and $\lim_{s \rightarrow \infty} L_{V_i|\mathbf{w}}(s) = 0$ for $i = 1, \dots, K-1$, thus $f_V(0) = 0$. Then, the first order derivative of $f_V(v)$ at zero is obtained as

$$\frac{\partial f_V}{\partial v}(0) = \lim_{s \rightarrow \infty} s L_{V_0}(s) \int \dots \int_{\mathbf{w}} \lim_{s \rightarrow \infty} s L_{V_i|\mathbf{w}}(s) \prod_{j=2}^{K-1} \lim_{s \rightarrow \infty} L_{V_j|\mathbf{w}}(s) f_{\mathbf{w}}(\mathbf{w}) d\mathbf{w} \quad (\text{A.29})$$

and again since $\lim_{s \rightarrow \infty} L_{V_j|\mathbf{w}}(s) = 0$, then $\frac{\partial f_V}{\partial v}(0) = 0$. Similarly, we can continue this process until the $(K-2)^{nd}$ order derivative of $f_V(v)$ at zero, i.e.,

$$\begin{aligned} \frac{\partial^k f_V}{\partial v^k}(0) &= \lim_{s \rightarrow \infty} s L_{V_0}(s) \int \dots \int_{\mathbf{w}} \prod_{i=1}^k \lim_{s \rightarrow \infty} s L_{V_i|\mathbf{w}}(s) \\ &\quad \prod_{j=k+1}^{K-1} \lim_{s \rightarrow \infty} L_{V_j|\mathbf{w}}(s) f_{\mathbf{w}}(\mathbf{w}) d\mathbf{w} \\ &= 0 \end{aligned} \quad (\text{A.30})$$

for $k = 1, \dots, K-2$, which proves the first part of Lemma 6.1. The $(K-1)^{st}$ order derivative of $f_V(v)$ at zero is then obtained as

$$\frac{\partial^{K-1} f_V}{\partial v^{K-1}}(0) = \lim_{s \rightarrow \infty} s L_{V_0}(s) \int \dots \int_{\mathbf{w}} \prod_{i=1}^{K-1} \lim_{s \rightarrow \infty} s L_{V_i|\mathbf{w}}(s) f_{\mathbf{w}}(\mathbf{w}) d\mathbf{w}$$

$$\begin{aligned}
&= f_{V_0}(0) \int \dots \int_{\mathbf{w}} \prod_{i=1}^{K-1} f_{V_i|\mathbf{w}}(0) f_{\mathbf{w}}(\mathbf{w}) d\mathbf{w} \\
&= f_{V_0}(0) \int \dots \int_{\mathbf{w}} f_{V_1, V_2, \dots, V_{K-1}|\mathbf{w}}(0, 0, \dots, 0) f_{\mathbf{w}}(\mathbf{w}) d\mathbf{w} \\
&= f_{V_0}(0) f_{V_1, V_2, \dots, V_{K-1}}(0, 0, \dots, 0)
\end{aligned} \tag{A.31}$$

proving the second part of Lemma 6.1.

A.8 Proof of Lemma 6.2

Since $\gamma_{k,K}$ and $\hat{\gamma}_k$ given in (6.4c) are nonnegative independent random variables, according to Proposition 4 proved in [14], the value of the PDF of $\tilde{\gamma}_{k,K}$ at the origin is given by eq. (6.7b) as the sum of values of the PDF of $\gamma_{k,K}$ and $\hat{\gamma}_k$ at zero. Now, note that $\hat{\gamma}_1 = \gamma_{0,1}$ and hence $f_{\hat{\gamma}_k}(0) = f_{\gamma_{0,1}}(0)$ which is equal to $\frac{1}{\Gamma_{0,1}}$ in Rayleigh fading. Furthermore, $\hat{\gamma}_k$ for $k \neq 1$, is the sum of k random variables in which $\gamma_{0,k}$ is independent of $\tilde{\gamma}_{j,k}$, $j = 1, \dots, k-1$ and $\tilde{\gamma}_{g,k}$ and $\tilde{\gamma}_{h,k}$ are dependent random variables for $g \neq h$, $g, h \in \{1, \dots, k-1\}$. Thus, according to the Lemma 6.1, the value of the PDF of $\hat{\gamma}_k$ for $k \neq 1$ is zero at the origin.